

THE  
LONDON, EDINBURGH, AND DUBLIN  
PHILOSOPHICAL MAGAZINE  
AND  
JOURNAL OF SCIENCE.

---

[SEVENTH SERIES.]

---

MARCH 1927.

---

LIII. *Application of an Integral Equation to the Whirling Speeds of Shafts.* By R. C. J. HOWLAND, M.A., M.Sc.,  
*University College, London* \*.

*Summary.*

THE squares of the whirling speeds of a shaft are exhibited as the characteristic numbers of a homogeneous integral equation. Approximate solutions are sought by applying approximation formulæ to the integral and the whirling speeds are found as the roots of a determinantal equation. The method is shown to be closely related to that of Jeffcott and Hahn, who gave a determinantal equation for the whirling speeds of shafts carrying concentrated masses. The examples worked out show that considerable accuracy may be attained. An important advantage is that the data for the calculation may be obtained experimentally when a theoretical method is not available.

1. *The Integral Equation* †.

It will be assumed

- (1) that the deflexion of any point of the shaft due to a force acting at any other point is proportional to the force;
- (2) that the deflexions due to different forces are additive.

These conditions follow from the linearity of the differential

\* Communicated by the Author.

† Cf Kneser, *Integralgleichungen*, § 12, pp. 47 *et seq.* Lovett, 'Linear Integral Equations,' Chaps. IV. and VI.

*Phil. Mag.* S. 7. Vol. 3. No. 15. March 1927. 2 L

equation in the ordinary theory, but must be made explicit assumptions if the present theory is to be independent.

Consider any non-uniform shaft and let

- $l$  = length of shaft,  
 $x$  = distance from one end,  
 $y$  = deflexion perpendicular to axis of  $x$ ,  
 $m$  = mass per unit length.

In general  $m$  will be a function of  $x$ .

A unit force acting at the point whose coordinate is  $x$  will produce at a point whose abscissa is  $\alpha$  a deflexion whose magnitude, being a function of both  $x$  and  $\alpha$ , will be denoted by  $K(x, \alpha)$ . This function is of the class known as Green's functions. It is, by a well-known reciprocal theorem, symmetrical in the two variables; it is continuous in each variable in the range  $0 < \frac{x}{\alpha} < l$ ; the differential coefficient with respect to either variable has a single, finite discontinuity at  $x = \alpha$ .

During whirling let the deflexion be

$$y = f(x).$$

Then the force perpendicular to the shaft at the point  $\alpha$  on a length  $\delta\alpha$  is

$$m\omega^2 f(\alpha)\delta\alpha,$$

and the deflexion due to this at the point  $x$  is

$$\omega^2 m K(x, \alpha) f(\alpha) \delta\alpha.$$

The integral of this along the shaft must give the whole deflexion at  $x$ . Hence

$$f(x) = \omega^2 \int_0^l m K(x, \alpha) f(\alpha) d\alpha \quad . \quad . \quad . \quad (1)$$

The theory of this type of integral equation is well known\*. The equation has a unique non-zero solution when  $\omega^2$  has any one of an infinite sequence of values. These values are called the characteristic numbers of the equation. For other values of  $\omega^2$  the equation has no solution except  $f(x) = 0$ . The transcendental equation of which the characteristic numbers are the roots† was obtained by Fredholm from a limiting case of the process to be used in the next section.

\* See for example, Whittaker and Watson, 'Modern Analysis,' 3rd ed. (1920).

Extensive references to the original papers are given by Bateman—'Report on the Theory of Integral Equations,' British Association Reports, 1910.

† See section 5, below.

It is to be noted that the method now to be given for the determination of the whirling speeds applies to all cases in which the function  $K(x, \alpha)$  is known, either in an analytical form, or by means of numerical values. It applies to shafts of any form, with any end conditions. In addition, there may be an end-thrust or tension and this may vary along the length of the shaft. These conditions will affect the form of  $K(x, \alpha)$  but not the method of calculation.

## 2. Approximate Solutions.

If the value of the integral in (1) is written down approximately for selected values  $x_1, x_2, \dots$  of  $x$  by means of a formula involving the values  $y_1, y_2, \dots$  of the unknown function  $f(\alpha)$  corresponding to  $x_1, x_2, \dots$ , a series of linear equations in  $y_1, y_2, \dots$  is obtained. The number of equations is equal to the number of unknowns and the ratios of these may be determined. The elimination of  $y_1, y_2, \dots$  from the equations gives an equation for  $\omega$ .

For example, let the trapezoidal rule with  $n$  equal intervals be applied. Then

$$\frac{1}{\omega^2} f(x) = \frac{l}{n} \left\{ \frac{1}{2} m_0 K(x, \alpha_0) f(\alpha_0) + \frac{1}{2} m_n K(x, \alpha_n) f(\alpha_n) + \sum_{r=1}^{n-1} m_r K(x, \alpha_r) f(\alpha_r) \right\},$$

whence

$$\frac{n}{l\omega^2} y_s = \frac{1}{2} m_0 k_{os} y_0 + \frac{1}{2} m_n k_{ns} y_n + \sum_{r=1}^{n-1} m_r k_{rs} y_r, \quad \dots \quad (2)$$

where

$$k_{rs} = K\left(\frac{rl}{n}, \frac{sl}{n}\right). \quad \dots \quad (3)$$

The elimination of the deflexions from (2) gives the equation for  $\omega$ :

$$\begin{vmatrix} \frac{1}{2}k_{00} - \frac{n}{lm_0\omega^2} & k_{01} & k_{02} & \dots & \frac{1}{2}k_{0n} \\ \frac{1}{2}k_{10} & k_{11} - \frac{n}{lm_1\omega^2} & k_{12} & \dots & \frac{1}{2}k_{1n} \\ \frac{1}{2}k_{20} & k_{12} & k_{22} - \frac{n}{lm_2\omega^2} & \dots & \frac{1}{2}k_{2n} \\ \dots & \dots & \dots & \dots & \dots \\ k_{n0} & k_{n1} & k_{nz} & \dots & \frac{1}{2}k_{nn} - \frac{n}{lm_n\omega^2} \end{vmatrix} = 0 \quad \dots \quad (4)$$



A similar equation will result from the use of any other integration formula of this type. The only difference will be that the terms in  $\omega^2$  will contain additional constant factors.

### 3. *Application to a Uniform Shaft.*

For a uniform shaft with short bearings at the two ends, the usual method gives

$$\left. \begin{aligned} \underline{x \leq \alpha}, K(x, \alpha) &= \frac{(l-\alpha)(2\alpha l - \alpha^2 - x^2)x}{6lEI} \\ \underline{x \geq \alpha}, K(x, \alpha) &= \frac{(l-x)(2xl - x^2 - \alpha^2)\alpha}{6lEI} \end{aligned} \right\} \quad \dots (5)$$

in which, as usual

E denotes Young's Modulus,

I ,, the second moment of the cross-section.

With six intervals the values of  $k_{rs}$  are as follows :—

$$\left. \begin{aligned} k_{0s} &= k_{ns} = 0 \text{ for all values of } s; \\ k_{11} &= k_{55} = \frac{25l^3}{3 \times 6^4 EI}, & k_{22} &= k_{44} = \frac{64l^3}{3 \times 6^4 EI}, \\ k_{12} &= k_{45} = \frac{38l^3}{3 \times 6^4 EI}, & k_{13} &= k_{35} = \frac{39l^3}{3 \times 6^4 EI}, \\ k_{14} &= k_{25} = \frac{31l^3}{3 \times 6^4 EI}, & k_{23} &= k_{34} = \frac{69l^3}{3 \times 6^4 EI}, \\ k_{15} &= \frac{17l^3}{3 \times 6^4 EI}, & k_{24} &= \frac{56l^3}{3 \times 6^4 EI}, & k_{33} &= \frac{81l^3}{3 \times 6^4 EI}. \end{aligned} \right\} \quad \dots (6)$$

Hence, if

$$\lambda = \frac{3 \times 6^5 EI}{ml^4 \omega^2}, \quad \dots \dots \dots (7)$$

the equation for  $\lambda$  is

$$\left| \begin{array}{ccccc} 25-\lambda & 38 & 39 & 31 & 17 \\ 38 & 64-\lambda & 69 & 56 & 31 \\ 39 & 69 & 81-\lambda & 69 & 39 \\ 31 & 56 & 69 & 64-\lambda & 38 \\ 17 & 31 & 39 & 38 & 25-\lambda \end{array} \right| = 0 \quad \dots \dots \dots (8)$$

The minors in this determinant reduce very easily and the equation is, without much labour, reduced to the form

$$\lambda^5 - 259\lambda^4 + 4705\lambda^3 - 17827\lambda^2 + 15501\lambda - 3465 = 0. \quad (9)$$



The values of  $\lambda$  given by this are

240 nearly, 14.55, 3.65, 0.79, 0.355,

from which  $\left(\frac{m}{EI}\right)^{\frac{1}{2}} l^2 \omega$  has the values

9.86, 40.0, 80.0, 171.8, 256.

The correct values are

9.87, 39.48, 88.83, 157.9, 247,

so that the approximate method gives the first five whirling speeds with errors of

0.1 %, 1.3 %, 10 %, 9 %, 4 %,

respectively.

The first two are thus obtained with considerable accuracy. The comparative accuracy of the fifth is probably accidental.

It might be anticipated that greater accuracy would be obtained by using integration formulæ such as Simpson's, which are known to be, as a rule, more accurate than the trapezoidal rule with the same number of ordinates. This expectation is not in all cases realized.

Thus, Simpson's Rule with six intervals gives errors of 0.1 per cent. and 2 per cent. in the first two whirling speeds and errors of over 20 per cent. in the next three. The three-eighths rule \* gives errors of

0 %, 2.9 %, 0 %, 8.8 %, 10 %.

while Weddle's rule † gives errors of

0 %, 3.5 %, 21 %, 39 %, 24 %.

The success of the trapezoidal formula is, at first sight strange. An examination of the curves

$$y = mK(x, \alpha)f(x),$$

to which approximations are being made, shows, however, that for the higher modes of whirling they are highly inflected and are thus very likely to be better represented by a series of straight line segments than by a smaller number of parabolic arcs or polynomial curves of higher order. A physical reason for the comparative failure of the other integration rules will appear in Section 6.

\* Whittaker and Robinson, 'Calculus of Observations,' p. 157.

† *Ibid.* p. 151.

4. *Some Simplifications.*

When the shaft is symmetrical about its middle point a great simplification can be made by treating the symmetrical and asymmetrical modes separately.

Thus the assumption of symmetry gives in equation (2)

$$y_0 = y_n, \quad y_1 = y_{n-1}, \quad \text{and so on.}$$

The number of unknowns is reduced to  $\frac{1}{2}n + 1$ , if  $n$  is even, or to  $\frac{n+1}{2}$  if  $n$  is odd. The degree of the equation in  $\omega^2$  is reduced in the same way, with a further reduction of one degree if, as is generally the case,

$$y_0 = y_n = 0.$$

The trapezoidal rule with six intervals gives the equations

$$\left(k_{11} + k_{15} - \frac{6}{lm_1\omega^2}\right)y_1 + (k_{12} + k_{14})y_2 + k_{13}y_3 = 0,$$

$$(k_{21} + k_{25})y_1 + \left(k_{22} + k_{24} - \frac{6}{lm_2\omega^2}\right)y_2 + k_{23}y_3 = 0,$$

$$(k_{31} + k_{35})y_1 + (k_{32} + k_{34})y_2 + \left(k_{33} - \frac{6}{lm_3\omega^2}\right)y_3 = 0,$$

from which

$$\begin{vmatrix} k_{11} + k_{15} - \frac{6}{lm_1\omega^2} & k_{12} + k_{14} & k_{13} \\ k_{21} + k_{25} & k_{22} + k_{24} - \frac{6}{lm_2\omega^2} & k_{23} \\ k_{31} + k_{35} & k_{32} + k_{34} & k_{33} - \frac{6}{lm_3\omega^2} \end{vmatrix} = 0 \quad (10)$$

Similarly, the assumption of asymmetry gives

$$y_5 = -y_1, \quad y_4 = -y_2, \quad y_3 = 0,$$

and  $\omega^2$  satisfies the equation

$$\begin{vmatrix} k_{11} - k_{15} - \frac{6}{lm_1\omega^2} & k_{12} + k_{14} \\ k_{21} - k_{25} & k_{22} - k_{24} - \frac{6}{lm_2\omega^2} \end{vmatrix} = 0 \quad (11)$$

The fifth degree equation is thus broken up into a cubic and a quadratic which may be solved separately.

A further great simplification results from the fact that the third and fifth whirling speeds are so much higher than the first that only a small error is made by taking the sum of the roots in (10) in place of the highest root and writing for the lowest whirling speed

$$\frac{6}{l\omega_1^2} = m_1(k_{11} + k_{15}) + m_2(k_{22} + k_{24}) + m_3k_{33}. \quad (12)$$

A similar approximation in (11) gives for the second whirling speed

$$\frac{6}{l\omega_2^2} = m_1(k_{11} - k_{15}) + m_2(k_{22} - k_{24}). \quad (13)$$

For the uniform shaft these formulæ give the first two whirling speeds with errors of 0.7 per cent. and 3.3 per cent. respectively.

The values of  $\omega_1, \omega_2$  given by (12) and (13) will always be too low.

When the shaft is not symmetrical the above simplifications cannot be used. The calculations need not, however, be very long if only the first whirling speed is required.

Consider, for example, a conical shaft with its thick end in a long bearing and free at the tip. If

$a$  = radius at thick end,

$l$  = length of shaft,

it is easy to verify that for  $x \leq a$

$$\frac{E\pi a^4}{4l^4} K(x, \alpha) = \frac{(l-\alpha)^2}{6\alpha^2 l^3} \{3\alpha l - (l+2\alpha)x\}.$$

Writing

$$p_{rs} = \frac{3 \times 6^3 E\pi a^2}{2l^5} K\left(\frac{rl}{6}, \frac{sl}{6}\right) \quad (14)$$

we have the following values of  $p_{rs}$  :—

$$p_{11} = 250, \quad p_{22} = 64, \quad p_{33} = 18, \quad p_{44} = 4, \quad p_{55} = \frac{2}{5},$$

$$p_{12} = 104, \quad p_{13} = 42, \quad p_{14} = \frac{29}{2}, \quad p_{15} = \frac{74}{25}, \quad p_{23} = 30.$$

$$p_{24} = 11, \quad p_{25} = \frac{58}{25}, \quad p_{34} = \frac{15}{2}, \quad p_{35} = \frac{42}{25}, \quad p_{45} = \frac{26}{25}.$$

Also, if  $m_r$  denote the mass per unit length at a distance  $\frac{rl}{6}$  from the tip,

$$m_r = \frac{\rho\pi a^2}{6^2} r^2. \quad (15)$$



Thus, using (4) with 6 intervals and putting

$$\lambda = \frac{3 \times 6^5}{2} \frac{Ea^2}{\rho l^4 \omega^2}, \quad \dots \quad (16)$$

the equation for  $\lambda$  becomes

$$\begin{vmatrix} 250-\lambda & 104 & 42 & \frac{29}{2} & \frac{74}{25} \\ 416 & 256-\lambda & 120 & 44 & \frac{232}{25} \\ 378 & 270 & 162-\lambda & \frac{135}{2} & \frac{378}{25} \\ 232 & 176 & 120 & 64-\lambda & \frac{416}{25} \\ 74 & 58 & 42 & 26 & 2-\lambda \end{vmatrix} = 0 \quad \dots \quad (17)$$

Since  $y$  is not zero at the origin the equation would be of the sixth degree, but the zero value of  $m_0$  removes the first column of the determinant.

The first two terms in the equation are evidently

$$-\lambda^5 + 734\lambda^4.$$

The coefficient of  $\lambda^3$  is the sum of 10 second order determinants. When these are evaluated we find

$$\lambda^5 - 734\lambda^4 + 77609\lambda^3 - \text{etc.} = 0.$$

Truncating the equation at this point, the value of  $\lambda$  may be found by successive approximation from

$$\lambda = 734 - \frac{77609}{\lambda},$$

whence

$$\lambda = 606,$$

and

$$\omega = 4.39 \sqrt{\frac{E}{\rho} \cdot \frac{a}{l^2}} \quad \dots \quad (18)$$

This result may be tested by comparing it with Kirchhoff's exact solution of the equivalent vibration problem\*. In the notation here used, Kirchhoff's analysis gives

$$\omega = 4.359 \sqrt{\frac{E}{\rho} \cdot \frac{a}{l^2}} \quad \dots \quad (19)$$

\* Kirchhoff, "Ueber die Transversalschwingungen eines Stabes von veränderlichen Querschnitt." *Sitz. der Akad. zu Berlin*, 1897, p. 815, or *Gesammelte Abhandlungen*, p. 339.

The error in the approximate method is thus considerably less than 1 per cent.

If the second whirling speed is required, the coefficient of  $\lambda^2$  must be calculated. This is obtained as the sum of 10 determinants of the third order.

### 5. Integral Formulæ.

With  $n$  intervals, the approximate formula (12) becomes

$$\frac{n}{l\omega_1^2} = \sum_{r=1}^p m_r k_{rr} + \sum_{r=1}^{p-1} m_r k_{r,n-r}^*,$$

where, if  $n$  is even,  $p = \frac{n}{2}$ ;  
if  $n$  is odd,  $p = \frac{n+1}{2}$ .

When  $n$  tends to infinity the formula becomes

$$\frac{1}{\omega_1^2} = \int_0^{\frac{l}{2}} m_x \{K(x, x) + K(x, l-x)\} dx. \quad (20)$$

This formula, which gives accurately the sum of the squared reciprocals of the odd whirling speeds, may be used for the first only without much error.

Similarly the second whirling speed will be given with tolerable accuracy by

$$\frac{1}{\omega_2^2} = \int_0^{\frac{l}{2}} m_x \{K(x, x) - K(x, l-x)\} dx, \quad (21)$$

which gives accurately the sum of the squared reciprocals of the even whirling speeds.

These formulæ, like (12) and (13), apply only to a symmetrical shaft. In the general case the corresponding formula is

$$\sum_{r=1}^{\infty} \frac{1}{\omega_r^2} = \int_0^l m_x K(x, x) dx. \quad (22)$$

If the higher whirling speeds are neglected, this gives

$$\frac{1}{\omega_1^2} = \int_0^l m_x K(x, x) dx, \quad (23)$$

a formula which is equivalent to Dunkerley's †.

\* It may be taken that in practice symmetry will imply that there are bearings at the two ends. Otherwise terms in  $k_{00}$  and  $k_{nn}$  must be added.

† See section 6, below.

In the case of a uniform shaft (23) gives  $\omega_1$  with an error of about 4 per cent. The other formulæ (20) and (21) are more accurate. When the shaft is uniform they give

$$\omega_1^2 = 96c^2, \quad \omega_2^2 = 1440c^2, \\ i. e. \quad \omega_1 = 9.8c, \quad \omega_2 = 38.0c \text{ approx.},$$

$$\text{where} \quad c^2 = \frac{EI}{\rho A l^4}.$$

The correct values are  $9.87c$  and  $39.5c$ , so that the errors are 0.7 per cent. and 3.8 per cent. respectively.

It is, of course, not obvious that the above limiting processes are justified. A rigorous proof of (23) follows from Fredholm's theory of the homogeneous integral equation\*. If, in the determinantal equation (4),  $n$  is allowed to tend to  $\infty$ , the result is

$$0 = f(\omega^2) \equiv 1 - \omega^2 \int_0^l K(x, x) m_x dx \\ + \frac{\omega^4}{2} \int_0^l \int_0^l \begin{vmatrix} K(x, x) & K(x, y) \\ K(x, y) & K(y, y) \end{vmatrix} m_x m_y dx dy \\ - \frac{\omega^6}{3} \int_0^l \int_0^l \int_0^l \begin{vmatrix} K(x, x) & K(x, y) & K(x, z) \\ K(x, y) & K(y, y) & K(y, z) \\ K(x, z) & K(y, z) & K(z, z) \end{vmatrix} m_x m_y m_z dx dy dz \\ + \text{etc.} \quad \dots \dots \dots (24)$$

This series converges absolutely for all values of  $\omega^2$ †, and  $f(\omega^2)$  is thus an integral function of  $\omega^2$  and the roots of the equation (24) satisfy the relations

$$\sum_{r=1}^{\infty} \frac{1}{\omega_r^2} = \int_0^l K(x, x) m_x dx \\ \sum_{r,s=1}^{\infty} \frac{1}{\omega_r^2 \omega_s^2} = \frac{1}{2} \int_0^l \int_0^l \begin{vmatrix} K(x, x) & K(x, y) \\ K(x, y) & K(y, y) \end{vmatrix} m_x m_y dx dy, \\ \text{and so on.} \quad \dots \dots \dots (25)$$

The value of  $\frac{1}{\omega_1^2}$  will usually be large compared with that of  $\frac{1}{\omega_2^2}$ , which will itself be large compared with the succeeding

\* Whittaker and Watson, 'Modern Analysis,' 3rd ed., Cambridge, pp. 213 *et seq.* (1920).

† *Ibid.* p. 215.



values. If these are regarded as negligible, the formulæ become

$$\frac{1}{\omega_1^2} + \frac{1}{\omega_2^2} = \int_0^l K(x, x) m_x dx$$

$$\frac{1}{\omega_1^2 \omega_2^2} = \frac{1}{2} \int_0^l \int_0^l \begin{vmatrix} K(x, x) & K(x, y) \\ K(x, y) & K(y, y) \end{vmatrix} m_x m_y dx dy$$

. . . . . (26)

The further neglect of  $\frac{1}{\omega_2^2}$  leads to equation (23). If this value of  $\frac{1}{\omega_1^2}$  is substituted in the second equation of (26) and the resulting value of  $\frac{1}{\omega_2^2}$  used in the first equation of (26), a second approximation is obtained in the form

$$\frac{1}{\omega_1^2} = \int_0^l K(x, x) m_x dx - \frac{\frac{1}{2} \int_0^l \int_0^l \begin{vmatrix} K(x, x) & K(x, y) \\ K(x, y) & K(y, y) \end{vmatrix} m_x m_y dx dy}{\int_0^l K(x, x) m_x dx}.$$

Since

$$\left\{ \int_0^l K(x, x) m_x dx \right\}^2 = \int_0^l K(x, x) m_x dx \int_0^l K(y, y) m_y dy,$$

the equation may be written

$$\frac{1}{\omega_1^2} = \frac{\frac{1}{2} \int_0^l \int_0^l [K(x, x) K(y, y) + \{K(x, y)\}^2] m_x m_y dx dy}{\int_0^l K(x, x) m_x dx}$$

or

$$\frac{1}{\omega_1^2} = \frac{\int_0^l m_x dx \int_0^x [K(x, x) K(y, y) + \{K(x, y)\}^2] m_y dy}{\int_0^l K(x, x) m_x dx}$$

. . . . . (27)

The last is the more convenient form because  $K(x, y)$  is expressed by different formulæ for  $x > y$  and for  $x < y$ . In (27) only the form for  $x > y$  is required.

For a uniform shaft

$$\begin{aligned}\int_0^l m_x dx \int_0^x K(x, x) K(y, y) m_y dy &= \frac{1}{16200} \frac{m^2 l^8}{E^2 I^2}, \\ \int_0^l m_x dx \int_0^x \{K(x, y)\}^2 m_y dy &= \frac{1}{18900} \frac{m^2 l^8}{E^2 I^2}, \\ \int_0^l K(x, x) m_x dx &= \frac{1}{90} \frac{m l^4}{EI}.\end{aligned}$$

The substitution of these values in (27) gives

$$\omega_1 = 9.85 \sqrt{\frac{EI}{m} \cdot \frac{1}{l^2}},$$

the correct value being  $9.87 \sqrt{\frac{EI}{m} \cdot \frac{1}{l^2}}$ .

For the conical shaft considered in § 4,

$$\begin{aligned}\int_0^l K(x, x) m_x dx \int_0^x K(y, y) m_y dy &= \frac{1}{800} \cdot \frac{16 \rho^2 l^8}{9 E^2 a^4}, \\ \int_0^l m_x dx \int_0^x \{K(x, y)\}^2 m_y dy &= \frac{9}{2800} \cdot \frac{4 \rho^2 l^8}{9 E^2 a^4}, \\ \int_0^l K(x, x) m_x dx &= \frac{1}{20} \cdot \frac{4 \rho l^4}{3 E a^2},\end{aligned}$$

whence

$$\omega_1^2 = 4.26 \frac{\rho l^4}{E a^2},$$

the true value being  $4.35 \frac{\rho l^4}{E a^2}$ .

The simplicity of these integral formulæ is only apparent. Except when  $K(x, y)$  is a very simple type of function the integrals can be evaluated only by the use of approximate formulæ. The calculations involved will be as considerable and the accuracy obtainable less than in the methods illustrated in the previous sections.

## 6. Shafts Carrying Concentrated Masses.

In equation (1) let  $m$  be zero except at the points whose abscissæ are  $x_1, x_2, x_3, \dots, x_k$ . At these points let there be infinities of the type

$$\lim_{\epsilon \rightarrow 0} \int_{x_i - \epsilon}^{x_i + \epsilon} m dx = M_i. \quad . \quad . \quad . \quad (28)$$

Then the equation becomes

$$f(x) = \omega^2 \sum_{i=1}^k M_i K(x, x_i) f(x_i). \quad . \quad . \quad . \quad (29)$$

In this equation give  $x$  successively the values  $x_1, x_2, \dots x_k$  and write

$$K(x_i, x_j) = k_{ij}$$

$$f(x_i) = y_i.$$

The  $k$  equations obtained are

$$\left(M_1 k_{11} - \frac{1}{\omega^2}\right)y_1 + M_2 k_{12}y_2 + \dots + M_n k_{1n}y_n = 0,$$

$$M_1 k_{21}y_1 + \left(M_2 k_{22} - \frac{1}{\omega^2}\right)y_2 + \dots + M_n k_{2n}y_n = 0,$$

$$\dots \dots \dots$$

$$M_1 k_{n1}y_1 + M_2 k_{n2}y_2 + \dots + \left(M_n k_{nn} - \frac{1}{\omega^2}\right)y_n = 0.$$

The elimination of the  $y$ 's gives

$$\begin{vmatrix} k_{11} - \frac{1}{M_1 \omega^2} & k_{12} & \dots & k_{1n} \\ k_{21} & k_{22} - \frac{1}{M_2 \omega^2} & \dots & k_{2n} \\ \dots & \dots & \dots & \dots \\ k_{n1} & k_{n2} & \dots & k_{nn} - \frac{1}{M_n \omega^2} \end{vmatrix} = 0$$

(30)

This is the formula of Jeffcott\* and Hahn†. It gives for the sum of the squared reciprocals of the whirling speeds the formula

$$\sum_{r=1}^k \frac{1}{\omega_r^2} = \sum_{r=1}^n M_r k_{rr}. \quad (31)$$

If all the masses except the  $r$ th are removed the single remaining whirling speed  $\Omega_r$  is given by

$$\frac{1}{\Omega_r^2} = M_r k_{rr},$$

\* Jeffcott, "The Periods of Lateral Vibration of Loaded Shafts," Proc. Roy. Soc. (A), vol. xcv. (1918).

† Hahn, "Note sur la Vitesse Critique des Arbres et la Formule de Dunkerley," *Schweizerische Bauzeitung*, Nov. 1918.



526 Mr. R. C. J. Howland: *Application of an*  
and (31) may therefore be written

$$\sum_{r=1}^k \frac{1}{\omega_r^2} = \sum_{r=1}^k \frac{1}{\Omega_r^2}. \quad \dots \quad (32)$$

The neglect of all the terms on the left-hand side after the first gives

$$\frac{1}{\omega_1^2} = \sum_{r=1}^k \frac{1}{\Omega_r^2}, \quad \dots \quad (33)$$

which is Dunkerley's approximate formula \*. When the number of masses tends to infinity the integral formula (23) results. The errors in Dunkerley's formula have been studied by Hahn † and by the present writer ‡.

It is now evident that the method of section 2 is equivalent to replacing the continuous mass of the shaft by a number of isolated masses and then applying the formula (30) of Jeffcott and Hahn. The arrangement of the concentrated masses will be different according to which integration formula is used. The use of the trapezoidal formula with  $n$  intervals is equivalent to placing at each point of division a mass equal to that of a shaft of length  $\frac{l}{n}$  and of uniform section and density equal to those at the point, while at the ends are placed masses equal to those of shafts of length  $\frac{l}{2n}$  and with sections and densities identical with those at the ends of the original shaft.

The other formulae are equivalent to local redistributions of the mass relatively greater than those given by the trapezoidal formula. Their failure to give the higher whirling speeds with any accuracy is, from this point of view, intelligible; for the higher whirling speeds depend on local displacements of the shaft and are likely to be greatly changed by any considerable local disturbance of the mass distribution.

When, in addition to carrying concentrated masses, the shaft has a distributed mass which cannot be neglected,

\* Phil. Trans. A, clxxv. (1894).

† *Loc. cit.*

‡ "The Whirling Speeds of Shafts Carrying Concentrated Masses," Phil. Mag. xlix. pp. 1131-1145 (1925). "The Vibrations of Rods and Shafts with Tension or End-Thrust," *ibid.* March 1926.

equation (29) must be written

$$f(x) = \omega^2 \left[ \sum_{i=1}^k M K(x, x_i) f(x_i) + \int_0^l m K(x, \alpha) f(\alpha) d\alpha \right]. \quad (34)$$

The approximate method of § 2 may be applied to this equation in several different ways.

First, the integral may be evaluated by means of an approximate formula involving only ordinates corresponding to  $x_1, x_2 \dots x_k$ . If  $x$  is then given these values in the resulting equation, we obtain  $k$  equations from which the  $k$  ordinates may be eliminated, leaving an equation for  $\omega^2$ . This method can only be used if the concentrated masses are sufficiently numerous and sufficiently well spaced for the integration formula to be reasonably accurate.

A second method is to use an integration formula in terms of  $n+1$  equally spaced ordinates and, in the resulting equation, give  $x$  the corresponding  $n+1$  values and also the  $k$  values  $x_1, x_2 \dots x_k$ . From the resulting  $k+n+1$  equations the ordinates may be eliminated and an equation for  $\omega^2$  found. This method is likely to be more accurate than either the first or the third but leads to an equation of higher degree in  $\omega^2$  unless the added masses happen to fall at the division points of the integration formula.

A third method which is always applicable but leads to a simpler equation for  $\omega^2$  consists in using an integration formula with equally spaced ordinates while replacing each added mass by two, situated at the nearest division points and having their mass-centre at the position of the original mass. This local redistribution of mass is likely to have but a slight effect on the first whirling speed while changing some of the higher whirling speeds considerably.

Consider, for example, a shaft of uniform section, in short bearings at its two ends and carrying at a distance  $\frac{7}{18}l$  from one end a mass equal to half the mass of the shaft. The first method is here not applicable. The second, using the trapezoidal rule with six equal intervals, leads to an equation of the 6th degree in  $\omega^2$  which is identical with (8) except for an additional row and column. It gives

$$\lambda = 478.6 - \frac{10846.5}{\lambda},$$

whence

$$\lambda = 454.8$$

and

$$\omega_1 = 7.16 \sqrt{\frac{EI}{m}} \cdot \frac{1}{l^2}.$$

The third method would replace the mass by two masses as follows :—

$$\frac{ml}{3} \text{ at the point } x = \frac{1}{6}l,$$

$$\frac{ml}{6} \quad \text{,,} \quad \text{,,} \quad x = \frac{1}{3}l.$$

The equation for  $\lambda$  follows immediately from (8). It is only necessary to replace  $\lambda$  by  $\frac{1}{3}\lambda$  in the second column and by  $\frac{1}{2}\lambda$  in the third. The equation then gives

$$\lambda = 468 - \frac{11796}{\lambda},$$

which gives  $\lambda = 441.2$ ,

$$\omega_1 = 7.27 \sqrt{\frac{EI}{m} \cdot \frac{1}{l^2}}.$$

The exact solution of the differential equation leads to the equation

$$\begin{aligned} & \left( \cot \frac{7}{18} \theta + \cot \frac{11}{18} \theta \right) \left( \coth \frac{7}{18} \theta + \coth \frac{11}{18} \theta \right) \\ &= \frac{1}{4} \theta \left( \cot \frac{7}{18} \theta + \cot \frac{11}{18} \theta - \coth \frac{7}{18} \theta - \coth \frac{11}{18} \theta \right), \end{aligned}$$

where

$$\theta^4 = \frac{\rho A \omega^2 l^4}{EI}.$$

This has a root a little greater than 2.66 and gives

$$\omega_1 = 7.1 \sqrt{\frac{EI}{m} \cdot \frac{1}{l^2}} \text{ nearly.}$$

The first of the approximate methods is thus nearly accurate. The error in the other is not large. In this case the concentrated mass is large. When the added masses are relatively smaller it is likely that their redistribution will have an even smaller effect on the value of  $\omega_1$ . If, in addition, they are numerous the last method will have the important advantage of reducing the degree of the equation in  $\omega^2$  considerably, the calculation of  $\omega$  being correspondingly simplified.



LIV. *The Annual Periodicity of Earthquakes.*By CHARLES DAVISON, *Sc.D., F.G.S.\**

IN a paper read before the Royal Society in 1893 †, I considered the annual periodicity of earthquakes in various districts of both hemispheres. Since that year, much new material has become available, and, in the present paper, I propose to make use of it with regard to two points of some interest—(i.) the relations between the annual periodicity and intensity, and (ii.) the small amplitude of the annual period in some insular regions ‡.

*Relations between Annual Periodicity and  
Intensity of Earthquakes.*

In the paper referred to above, it was shown that the amplitude of the annual period is usually greater with weak, than with strong, earthquakes; and that, in some cases, the epoch is reversed. In the following Table (I.), the districts mentioned fall into two classes—(i.) composite districts, consisting of some or many sub-regions in which the epoch occurs in various months; (ii.) simple districts, in which the epoch seems to occur throughout in the same month.

\* Communicated by the Author.

† *Phil. Trans.*, 1893 A, pp. 1107–1169.

‡ The catalogues used are given in the following list, the numbers prefixed being inserted in the Tables after the name of the district:—

1. Barbiani, D. G., and B. A. Dijon, *Ac. Sci. Mém.* vol. xi. pp. 1–112 (1863).
2. Cavasino, A., *Ital. Soc. Sism. Boll.* vol. xxv. p. 80 (1924–25).
3. Eginitis, D. Athènes, *Obs. Nat. Ann.* vol. ii. 1900, pp. 29–346; vol. iii. 1901, pp. 336–375; vol. iv. 1906, pp. 489–578; vol. v. 1910, pp. 560–592; vol. vi. 1912, pp. 304–332; vol. vii. 1916, pp. 338–360.
4. Früh, J., *Schweiz. Natf. Ges. Verh.* 1911, 24 pp.
5. Fuchs, C. W. C., *Wien. Ak. Sitzber.* vol. xcii. pt. i. pp. 13–37, 404–408 (1886).
6. Hector, Sir J., *Austral. Assoc. Trans.* vol. iii. pp. 505–532 (1891).
7. Hogben, G., *Ibid.* vol. iv. pp. 8–27 (1892).
8. Holden, E. S., ‘List of Recorded Earthquakes in California, etc.’ Sacramento, 1887, 78 pp.
9. Masó, M. Saderra, *Manila Weather Bur. Bull.* 1910–1922.
10. Milne, J., *Seism. Jl. Japan*, vol. iv. pp. 1–367 (1895).
11. Milne, J., *Brit. Assoc. Rep.* 1911, pp. 649–740.
12. Omori, F., *Earthq. Inv. Com. For. Publ.* no. 8, 1902, pp. 9–30.
13. Omori, F., *Earthq. Inv. Com. Bull.* vol. ii. pp. 56–88 (1908).
14. Quervain, A. de, “Jahresbericht des Schweiz. Erdbebendienstes, 1913–1923” (in *Schweiz. Meteorol. Zentralanstalt Ann.*).
15. Sekiya, S., *Tokyo Coll. Sci. Jl.* vol. xi. pt. iv. pp. 319–388 (1889).

*Phil. Mag.* S. 7. Vol. 3. No. 15. March 1927.

2 M

According to Milne's scale of intensity for destructive earthquakes, shocks of intensity 1 are strong enough to crack walls, break chimneys or shatter old buildings; by those of intensity 2, buildings may be unroofed or shattered and some may fall; earthquakes of intensity 3 are those which destroy towns and devastate districts. The disturbed area of Japanese earthquakes is measured in square ri, one square ri being equal to 5.96 square miles. The scale of intensity used in Switzerland, Greece, and the Philippines is the Rossi-Forel scale. The different numbers of earthquakes for Zante and California depend on the definitions adopted for the unit earthquake. The larger number in each case is of course due to the inclusion of slighter shocks. The maximum epoch of the annual period falls about the end of the month mentioned in the penultimate column. In estimating the amplitude, the mean monthly number of earthquakes is taken as unity.

TABLE I.—Periodicity and Intensity.

		Duration of record.	No. of Earth- quakes.	Epoch.	Ampli- tude.
(i.)	Destructive earthquakes—				
	N. hemisphere, intensity 3 (11).....	7-1899	770	July	·13
	"      "      2 .....	"	983	July	·05
	"      "      1 .....	"	1779	Dec.	·17
	S. hemisphere, "      3 (11).....	"	74	Jan.	·51
	"      "      2 .....	"	74	Apr.	·30
	"      "      1 .....	"	192	July	·32
	Japan, disturbed area >1000 sq. ri (10) ..	1885-90	176	Mar.	·16
	"      "      100-1000 " .....	"	565	Feb.- Mar.	·17
	"      "      < 100 " .....	"	2256	Sep.- Oct.	
	"      "      >1000 " (13) ..	1902-07	621	Apr.	·19
	"      "      <1000 " .....	"	170	Aug.	·17
	Philippines, intensity >3 (9) .....	1910-22	964	Aug.	·11
	"      "      2, 3 .....	"	1192	July	·08
	Italy, " intensity >4 (2) .....	1891-1900	2084	June	·13
(ii.)	"      "      1-4 ..	"	11,447	Aug.	·08
	Switzerland, principal earthquakes (4)...	1880-1909	195	Jan.	·41
	"      "      minor shocks.....	"	767	Jan.	·64
	"      "      intensity >3 (14) ..	1913-23	209	Jan.	·21
	"      "      2, 3 .....	"	281	Jan.	·62
	Greece (without Zante), intensity >3 (3) ..	1904-13	591	Mar.	·52
	"      "      "      2, 3 ..	"	286	Mar.	·60
	Zante (1) .....	1825-63	1326	Aug.	·10
	"      "      "      " .....	"	1663	Aug.	·29
	California (8) .....	1850-86	768	Oct.	·19
	"      "      "      " .....	"	949	Oct.	·30

Thus, it will be seen from this Table that :

(i.) In composite districts, the amplitude varies but slightly for different intensities, but the epoch is reversed for the destructive earthquakes of intensities 3 and 1 in both hemispheres, and, though less distinctly, for those of Japan.

(ii.) In simple districts, the amplitude is greater for slight, than for strong, earthquakes, but the epochs of both occur in the same months.

*Annual Periodicity of Earthquakes in Insular Districts.*

From the periodicity point of view, islands may be divided into two classes. (i.) In the first, we have the large insular districts—composite districts, it will be seen—of Japan, the Philippines, and New Zealand, and, with these, the Italian peninsula may be included, as it shows similar features. (ii.) The second class includes small insular districts, such as Zante and Hawaii. In Table II., the maximum epoch and the amplitude of the annual seismic period are given for these districts and for adjacent continental areas. The two classes differ greatly in area.

TABLE II.—Insular Districts.

	Duration of record.	No. of Earth- quakes.	Epoch.	Ampl.
Japan (10) .....	416-1867	1869	May	·08
Philippines (9) .....	1903-21	2863	July	·08
New Zealand (6) .....	1868-90	641	May	·06
N.S. Wales, Victoria, and S. Australia (5) .....	1865-84	159	May	·48
Italy (2) .....	1891-1920	13,531	June	·08
Switzerland (4) .....	1880-1909	998	Jan.	·59
Austria (5) .....	1865-84	461	Jan.	·37
Zante (3) .....	1893-1913	3248	Apr.	·30
Greece (without Zante) (3) ...	"	3440	Mar.	·38
Hawaii (5) .....	1865-84	245	June	·33

Of the first group, Japan contains 155,000 sq. miles, the Philippines 116,000, New Zealand 106,240, and Italy 110,623 sq. miles. In the second group, the total area of the Ionian Islands is 1010 sq. miles, and of the Hawaiian Archipelago 6564 sq. miles.

Table II. thus shows that :

(i.) The amplitude of the annual period is small (·06 to ·08) in the first group of islands, and four times as great (·30 and ·33) in the second group.

(ii.) In Japan, the Philippines, Italy, and Hawaii, the maximum epoch occurs in the summer months. In the continental areas of both hemispheres, it usually occurs in the winter months.

In the remaining Tables, the districts of the first group and their various sub-regions are considered separately. In Table III., the catalogues used are those of earthquakes registered at various stations scattered over Japan.

TABLE III.—Japan.

	Duration of record.	No. of Earth- quakes.	Epoch.	Ampl.
Japan (15) .....	416-1867	1869	May	·08
Tokyo (12) .....	1876-99	2208	Mar.- Apr.	·08
Hikone (13) .....	1895-1907	351	May	·27
Sapporo (12) .....	1877-99	134	Dec.	·24
Nagano .....	1890-99	307	Feb.	·37
Oita .....	1887-99	264	Dec.- Jan.	·22
Hakodate.....	1873-99	305	Dec.	·17
Niigata .....	1887-99	214	June	·51
Wakayama .....	1888-99	403	May	·17
Hiroshima .....	1893-99	101	Dec.	·17
Nemuro .....	1887-93	352	Sep.	·16
Yamagata .....	1890-99	186	June	·76
Ishinomaki .....	1886-99	1034	Aug.	·38
Fukushima .....	1890-99	767	Apr.	·29
Utsunomiya .....	1891-92 1894-99	466	July	·08
Numazu .....	1885-99	160	Dec.	·24
Hamamatsu.....	1885-99	99	Dec.	·75

In the northeast of Japan, where the earthquakes are chiefly of submarine origin, the maximum epoch occurs from May to July; in other parts, most frequently in December or January. In the former region, the amplitude rises as high as ·76 with an average of ·36; in the latter, as high as ·75 with an average of ·30. If we group together the earthquakes at all the 16 stations (reducing them to their equivalent monthly numbers for equal durations of records), the resulting amplitude is only ·11 while the maximum epoch falls in May, results which agree closely with those obtained for the whole of Japan from 416 to 1867.



TABLE IV.—Philippines.

	Duration of record.	No. of Earth- quakes.	Epoch.	Ampl.
Philippines (9) .....	1903-21	2863	July	·08
Luzon, E. side .....	1910-22	326	Dec.	·16
„ W. side .....	„	241	Jnly	·30
Mindanao, E. side .....	„	363	July	·17
„ W. side .....	„	86	Dec.	·44

TABLE V.—New Zealand.

	Duration of record.	No. of Earth- quakes.	Epoch.	Ampl.
New Zealand (6) .....	1868-90	641	May	·06
North Island, E. side .....	„	188	May	·11
„ „ W. side .....	„	186	Apr.	·19
South Island, E. side .....	„	98	Oct.	·10
„ „ W. side .....	„	118	Sep.	·22

Thus, in the Philippines, the epochs of the east and west sides of the two main islands of Luzon and Mindanao are very nearly reversed, and this is also the case with corresponding sides in both islands. In New Zealand, the epochs on the east and west sides of the North and South Islands are nearly the same, while those in the two islands separately are reversed.

The results for four Italian provinces—Venetia, the Marches, Apulia, and Calabria—are doubtful, owing chiefly to the large number of after-shocks felt in certain months. Omitting these provinces, the maximum epoch occurs in November and December in the north and continental portion, and in the spring or summer in the peninsular portion.

TABLE VI.—Italy.

	Duration of record.	No. of Earth- quakes.	Epoch.	Ampl.
Italy (2) .....	1891-1920	13,531	June	·08
Piedmont.....	"	231	Dec.	·33
Lombardy .....	"	158	Nov.	·60
Venetia .....	"	703	May	·49
Liguria .....	"	124	Mar.	·29
Emilia .....	"	659	Apr.	·33
Tuscany .....	"	1234	Aug.	·16
Marches .....	"	1101	Oct.	·60
Umbria .....	"	1626	Apr.	·33
Latium.....	"	470	Mar.	·49
Abruzzo and Molise .....	"	1037	Jan.- Feb.	} ·40
Campania .....	"	956	Mar.- Apr.	
Basilicata .....	"	116	Mar.	·35
Apulia .....	"	660	June	·79
Calabria .....	"	955	Oct.- Nov.	} ·45
Sicily .....	"	3199	July	

Thus, in each of the large insular districts of the first class, there are sub-regions marked by high amplitudes of the annual period, but by maximum epochs which may differ by five or six months; and it is to this opposition of epoch in the sub-regions that the small amplitude for the whole district must be attributed. In the smaller island districts of Hawaii and Zante there is no such opposition, and the amplitudes are as high as in adjoining continental regions.

LV. *The Vapour Pressures of the Alkali Metals.* By H. ROWE, B.Sc., Demonstrator in Physics, University College of the South-West of England, Exeter\*.

### 1. Introduction.

METHODS of producing high vacua have developed to such an extent during the last ten years that it is now possible easily to attain pressures that previously could not be reached, and, moreover, apparatus and means have been devised whereby these pressures can be measured

\* Communicated by Prof. F. H. Newman, D.Sc., A.R.C.S.

accurately. Much attention has been paid to the measurement of these pressures, especially in the case of those elements whose vapour tension in the solid state was presumed so small as to be negligible. Comparatively few measurements, however, have been made of the vapour pressures of the alkali metals and, in general, the data concerning them have been obtained at high temperatures; there are very few published results for these vapour pressures at low temperatures, and these are contradictory.

In this paper experimental data for all the alkali metals have been compared with results obtained by extrapolating various formulæ which have been proposed to represent the pressure at different temperatures, but it must be noted that this extrapolation is only justifiable over a comparatively small temperature range.

On the basis of the Clausius-Clapeyron relations the following formula represents the variation of vapour pressure of a solid with temperature, the vapour being monatomic :

$$\log p = -\frac{\lambda_0}{RT} + \int_0^T \frac{dT}{RT^2} \int_0^T [C_p^g - C_p^s] dT + i,$$

where

$\lambda_0$  = molecular latent heat of the solid at  $0^\circ$  Abs.,

$C_p^g$  = molecular heat of vapour (constant) =  $4.963$ ,

$C_p^s$  = " " " " solid at constant pressure,

$C_v^s$  = " " " " " " " " volume.

Also

$$C_p^s = C_v^s + aT^{3/2}.$$

It has been shown by Egerton \* that this formula may be condensed to the form  $\log p = -\frac{A}{T} + B$ , and that this new type closely represents the variation of vapour pressure of a solid with temperature; also, since  $B$  can be calculated from the thermal constants of the element, a vapour-pressure determination at one temperature should suffice to determine the course of the whole temperature-vapour-pressure curve. While it is probably true that the vapour-pressure equation for a metal can be deduced from a single measurement and this type of equation, yet the extrapolation necessary will involve considerable error. The constant  $B$  is not a true constant since it depends upon the variation of specific heat

\* Phil. Mag. xlviii. p. 1048 (1924).

with temperature, and the equation will only hold good over a short range of temperature near the point where the vapour pressure was measured experimentally.

The variation of the specific heat of a metal at constant volume needs an accurate knowledge of the characteristic temperature ( $\beta v$ ) of the element considered and, unfortunately, the characteristic temperatures of the alkali metals are not known to a sufficient degree of accuracy to give a decisive value to  $B$ . Their thermal constants have been collected together by Egerton\*, and it will be noted that there is a considerable difference between the values of  $\beta v$  computed from Lindemann's melting-point formula and those from formulæ based on the coefficient of expansion of the metal. It is therefore impossible to determine theoretically a value of  $B$  with the necessary degree of accuracy and to compare the actually determined vapour pressures with those calculated from thermodynamic values.

## 2. Vapour Pressure of Sodium.

A number of determinations of the vapour pressure of sodium have been made at high temperatures. Gebhardt† determined the vapour pressure by the boiling-point method, but his results do not agree with those of Haber and Zisch‡, who used temperatures from 40°–50° C. higher than Gebhardt. The latter worked with a temperature range 360°–860° C., but Haber only made four determinations between 470°–570° C. Heycock and Lamplough§ have determined the boiling-point of sodium at atmospheric pressure to be 883° C. The great objection to the boiling-point method is that true thermal equilibrium may not exist between the vapour and the liquid and, in addition, the slightest trace of impurity affects the boiling-point. It has been shown by Bridgman|| that the metallic oxide, and this applies to all the alkali metals, is capable of dissolving within the molten metal, thus elevating the boiling-point.

Hackspill¶ by a very unsatisfactory method obtained four readings of the vapour pressure between 350°–400° C.

\* Proc. Phys. Soc. xxxvii. part 2, p. 75 (1925).

† Dissertation, Erlangen 1903, and Kroner, *Ann. Physik*, xl. p. 438 (1913).

‡ *Zeits. Physik*, ix. p. 325 (1922).

§ Journ. Chem. Soc. xxviii. p. 3 (1912).

|| Phys. Rev. xxvii. p. 68 (1926).

¶ *Comp. Rend.* cliv. p. 877 (1912).



At the present time the most reliable data are those published by Rodebush and de Vries \*, who used Knudsen's † method, modified to suit the conditions, and obtained five readings between 180°–260° C., and five between 520°–600° C. These investigators found that the results could be represented accurately by the formula

$$\log p \text{ (mms.)} = -\frac{5922}{T} - 1.6184 \log T + 12.9605, \quad (1)$$

or by a simpler and more approximate formula

$$\log p = -\frac{5370}{T} + 7.4925. \quad . \quad . \quad . \quad (2)$$

Rodebush and de Vries assumed 883° C. as the boiling-point of sodium at atmospheric pressure.

Millar ‡ from considerations of the entropy of sodium has shown that Gebhardt's results conform to the equations

$$\log p = -\frac{5135}{T} - 1.2 \log T + 11.071 \quad . \quad . \quad (3)$$

for liquid sodium, and

$$\log p = -\frac{7091.9}{T} + 15.056 \log T - 2.7136 (\log T)^2 - 4.605 \quad . \quad . \quad (4)$$

for solid sodium.

In work on the line absorption spectra of the alkali metals Sowerby and Barratt § quote a formula obtained from A. C. Egerton,

$$\log p = -\frac{5420}{T} + 7.566. \quad . \quad . \quad . \quad (5)$$

Using these various equations, values of the vapour pressure have been extrapolated and are compared with the experimental results in Table I.

Equation (2) gives approximate values of the vapour pressure between 100°–250° C., but outside this range, more especially at the higher temperatures, there is a considerable discrepancy between the calculated and experimental values. The values at the higher temperatures are far too low, and hence it must be assumed that there is a proportional increase in the values of the pressure at the lower temperatures, the calculated values from equation (2) being too high.

\* Journ. Amer. Chem. Soc. *xlvi*, p. 2488 (1925).

† *Ann. Physik*, *xlvi*, p. 697 (1915).

‡ Journ. Amer. Chem. Soc. *xl*, p. 2323 (1923).

§ Proc. Roy. Soc. A. *cx*, p. 190 (1926).

TABLE I.—Vapour Pressure of Sodium.

Temperature in ° C.	Pressures deduced from formula (1) in mms.	Pressures deduced from formula (2) in mms.	Pressures deduced from formulae (3) (4) in mms.	Pressures deduced from formula (5) in mms.	Experimental values of pressures in mms.
0.....	$2.154 \times 10^{-13}$	$6.64 \times 10^{-13}$		$5.16 \times 10^{-13}$	
20.....	$5.794 \times 10^{-12}$	$1.46 \times 10^{-11}$		$1.17 \times 10^{-11}$	
40.....	$1.017 \times 10^{-10}$	$2.17 \times 10^{-10}$		$1.78 \times 10^{-10}$	
60.....	$1.258 \times 10^{-9}$	$2.32 \times 10^{-9}$		$1.95 \times 10^{-9}$	
80.....	$1.163 \times 10^{-8}$	$1.90 \times 10^{-8}$		$1.63 \times 10^{-8}$	
97.9 (M.Pt.)	$6.915 \times 10^{-8}$	$1.04 \times 10^{-7}$	$1.4 \times 10^{-6}$	$9.06 \times 10^{-8}$	
140.....	$2.461 \times 10^{-6}$	$3.09 \times 10^{-6}$	$3.2 \times 10^{-5}$	$2.76 \times 10^{-6}$	
181.8 .....	$4.372 \times 10^{-5}$	$4.87 \times 10^{-5}$	$3.9 \times 10^{-4}$	$4.48 \times 10^{-5}$	$4.926 \times 10^{-5}$
200.3 .....	$1.323 \times 10^{-4}$	$1.41 \times 10^{-4}$	$1.0 \times 10^{-3}$	$1.31 \times 10^{-4}$	$1.412 \times 10^{-4}$
219.8 .....	$3.872 \times 10^{-4}$	$3.96 \times 10^{-4}$	$2.6 \times 10^{-3}$	$3.71 \times 10^{-4}$	$3.880 \times 10^{-4}$
239.9 .....	$1.073 \times 10^{-3}$	$1.06 \times 10^{-3}$	$6.5 \times 10^{-3}$	$1.00 \times 10^{-3}$	$1.030 \times 10^{-3}$
261.2 .....	$2.898 \times 10^{-3}$	$2.77 \times 10^{-3}$	$1.5 \times 10^{-2}$	$2.64 \times 10^{-3}$	$2.852 \times 10^{-3}$
300.....	$1.485 \times 10^{-2}$	$1.35 \times 10^{-2}$	$6.3 \times 10^{-2}$	$1.28 \times 10^{-2}$	
350.....	$9.824 \times 10^{-2}$	$7.46 \times 10^{-2}$	0.3	$7.35 \times 10^{-2}$	0.21
395.....	0.33	0.28	1.0	0.28	0.47
514.....	5.61	4.88	12.6	4.98	5.56
536.....	85.9	7.16	18.1	7.35	8.42
548.....	10.78	8.95	20.9	9.21	10.98
550.....	11.13	9.30	21.6	9.50	11.05
579.....	24.91	20.89	43.8	21.68	24.92
B.Pt. (calc.).	883° C.	892° C.	861° C.	884° C.	

\* Rodebush and de Vries.

† Hackspill.

On the other hand, the values of the pressures at low temperatures calculated from equation (1) are probably too low since the theoretical values are considerably lower than the experimental values.

Formula (5) also gives values which are too high at the low temperatures and too low at the high temperatures, but the differences are not so great as in the case of formula (2).

Equations (3) and (4) have been obtained from results

which are far from reliable, and the extrapolated values from these formulæ are therefore of no great value for purposes of comparison.

The most probable value of the vapour pressure of sodium at 0° C. is  $4 \times 10^{-13}$  mm.

### 3. Vapour Pressure of Potassium.

There are few published experimental data on the vapour pressure of potassium. Hackspill \*, using the same method for this metal as he had employed with sodium, measured the pressures at temperatures between 270°–400° C. Unfortunately the method adopted is very unsatisfactory, and the results cannot therefore be taken as reliable. Kroner † determined the vapour pressure of potassium by measuring the pressure of an inactive gas, nitrogen, in the apparatus at a constant temperature, introducing the metal, and measuring the increase in pressure thereby caused. His temperature range was from 250°–400° C.

Killian ‡ has used the thermionic effects produced by vapours of the alkali metals to make quantitative measurements of the vapour pressure of potassium. At high filament temperatures the positive ion emission becomes limited by the rate at which the vapour comes in contact with the filament, all atoms striking the filament being converted into ions, and this property is utilized to calculate the vapour pressure. The following formula is given by Killian as representing the variation of pressure with temperature between 80°–130° C. :

$$\log p = -\frac{4964}{T} + 8.71. \quad . \quad . \quad . \quad (6)$$

Sowerby and Barratt § quote an equation obtained from Egerton which is

$$\log p = -\frac{4438}{T} + 7.232 \quad . \quad . \quad . \quad (7)$$

The values of the vapour pressure have been extrapolated from these formulæ and compared with the experimental data in Table II.

Hackspill's results are far higher than those obtained by Kroner, especially at the lower end of their temperature

\* *Comp. Rend.* cliv. p. 877 (1912).

† *Ann. Physik*, xl. p. 438 (1913).

‡ *Phys. Rev.* xxvii. p. 578 (1926).

§ *Proc. Roy. Soc. A.* cx. p. 190 (1926).

range, and for purposes of reference it is therefore necessary to consider the theoretical values in the light of Kroner's experimental values.

TABLE II.—Vapour Pressure of Potassium.

Temperature in °C.	Pressures deduced from formula (6) in mms.	Pressures deduced from formula (7) in mms.	Pressures deduced from formula (8) in mms.	Experimental values of pressures in mms. (Kroner).	Experimental values of pressures in mms. (Hackspill).	
0 .....	$3.36 \times 10^{-10}$	$9.46 \times 10^{-10}$	$5.46 \times 10^{-10}$			
20 .....	$5.86 \times 10^{-9}$	$1.22 \times 10^{-8}$	$7.53 \times 10^{-9}$			
40 .....	$7.10 \times 10^{-8}$	$1.22 \times 10^{-7}$	$7.45 \times 10^{-8}$			
63.6 (M.Pt.)	$9.17 \times 10^{-7}$	$1.11 \times 10^{-6}$	$7.83 \times 10^{-7}$			
80 .....	$4.45 \times 10^{-6}$	$4.57 \times 10^{-6}$	$3.33 \times 10^{-6}$			
100 .....	$2.52 \times 10^{-5}$	$2.29 \times 10^{-5}$	$1.65 \times 10^{-5}$			
120 .....	$1.23 \times 10^{-4}$	$8.70 \times 10^{-5}$	$6.90 \times 10^{-5}$			
140 .....	$4.91 \times 10^{-4}$	$3.06 \times 10^{-4}$	$2.52 \times 10^{-4}$			
160 .....	$1.76 \times 10^{-3}$	$9.61 \times 10^{-4}$	$8.15 \times 10^{-4}$			
180 .....	$5.65 \times 10^{-3}$	$2.72 \times 10^{-3}$	$2.38 \times 10^{-3}$			
200 .....	$1.64 \times 10^{-2}$	$7.04 \times 10^{-3}$	$6.31 \times 10^{-3}$			
249.5 .....	0.16	$3.59 \times 10^{-2}$	$5.18 \times 10^{-2}$	0.05		
268.8 .....	0.35	0.11	0.106	0.11	272°	0.2
288.0 .....	0.72	0.21	0.204	0.21		
307.5 .....	1.44	0.39	0.386	0.43	315°	0.8
327.2 .....	2.75	0.69	0.700	0.73	332°	1.2
346.5 .....	5.01	1.17	1.21	1.17	340°	1.5
364.0 .....	8.32	1.84	1.92	1.86	360°	2.3
381.5 .....	13.4	2.82	2.99	2.85	380°	3.3
398.6 .....	20.9	4.21	4.51	4.01	400°	4.7
B.Pt. (calc.).	578° C.	747° C.	726° C.			

The values of the vapour pressure extrapolated from formula (6) are not comparable with those of Kroner at the high temperatures, being many times too high. Killian's temperature range was from 80°–130° C., *i.e.* over 50° C., and any slight error over such a small range becomes highly magnified when the calculations are extended to the full range.

Formula (7) gives values which are comparable to those



obtained by Kroner, and a formula obtained by applying the theory of least squares to Kroner's results approximates closely to formula (7), viz.:

$$\log p = -\frac{4564}{T} + 7.449. \quad . \quad . \quad . \quad (8)$$

It is unfortunate that no experimental results are available of vapour pressure determinations within the range 60°–200° C.

#### 4. Vapour Pressure of Rubidium.

Hackspill\*, measured the vapour pressure of rubidium over a temperature range 250°–365° C., using the same methods as previously described.

A direct measurement has been made by Scott†, who used a modified form of Haber's vibrating quartz-fibre manometer. The temperature range used was from 90°–130° C., and over this range it was found that the relation between  $\log p$  and  $\frac{1}{T}$  was approximately linear and the results could be represented by the formula

$$\log p = -\frac{4209}{T} + 7.331. \quad . \quad . \quad . \quad (9)$$

Killian‡ has applied the thermionic effects of alkali metals to rubidium and found that the formula

$$\log p = -\frac{4132}{T} + 7.43. \quad . \quad . \quad . \quad (10)$$

represents the relation between vapour pressure and temperature over the range 40°–110° C.

Sowerby and Barratt§ quote the following equation from Egerton:

$$\log p = -\frac{3571}{T} + 6.356. \quad . \quad . \quad . \quad (11)$$

In Table III. are collected the extrapolated and experimental values of the vapour pressure of rubidium.

\* *Comp. Rend.* cliv. p. 877 (1912).

† *Phil. Mag.* xlvii. p. 32 (1924).

‡ *Phys. Rev.* xxyii. p. 578 (1926).

§ *Proc. Roy. Soc. A.* cx. p. 190 (1926).

TABLE III.—Vapour Pressure of Rubidium.

Temperature in °C.	Pressures deduced from formula (9) in mms.	Pressures deduced from formula (10) in mms.	Pressures deduced from formula (11) in mms.	Experimental values of pressures in mms.
0 .....	$9.036 \times 10^{-9}$	$2.00 \times 10^{-8}$	$1.90 \times 10^{-7}$	
20 .....	$9.354 \times 10^{-8}$	$2.14 \times 10^{-7}$	$1.49 \times 10^{-6}$	
39 M.(Pt.)	$7.534 \times 10^{-7}$	$1.50 \times 10^{-6}$	$8.22 \times 10^{-6}$	
60 .....	$4.920 \times 10^{-6}$	$1.07 \times 10^{-5}$	$4.32 \times 10^{-5}$	
80 .....	$2.541 \times 10^{-5}$	$5.36 \times 10^{-5}$	$1.75 \times 10^{-4}$	
91.4 .....	$6.077 \times 10^{-5}$	$1.24 \times 10^{-4}$	$3.61 \times 10^{-4}$	$5.61 \times 10^{-5}$ } $1.10 \times 10^{-4}$ } $1.69 \times 10^{-4}$ } $2.24 \times 10^{-4}$ } $3.00 \times 10^{-4}$ } $5.04 \times 10^{-4}$ } $5.50 \times 10^{-4}$ } $6.45 \times 10^{-4}$ }
98.2 .....	$9.895 \times 10^{-5}$	$2.01 \times 10^{-4}$	$5.48 \times 10^{-4}$	
104.9 .....	$1.571 \times 10^{-4}$	$3.18 \times 10^{-4}$	$8.61 \times 10^{-4}$	
111.6 .....	$2.456 \times 10^{-4}$	$4.90 \times 10^{-4}$	$1.18 \times 10^{-3}$	
115.0 .....	$3.063 \times 10^{-4}$	$6.08 \times 10^{-4}$	$1.43 \times 10^{-3}$	
122.1 .....	$4.796 \times 10^{-4}$	$9.46 \times 10^{-4}$	$2.09 \times 10^{-3}$	
124.7 .....	$5.631 \times 10^{-4}$	$1.11 \times 10^{-3}$	$2.39 \times 10^{-3}$	
126.9 .....	$6.437 \times 10^{-4}$	$1.26 \times 10^{-3}$	$2.70 \times 10^{-3}$	
150 .....	$2.404 \times 10^{-3}$	$4.65 \times 10^{-3}$	$8.20 \times 10^{-3}$	
200 .....	$2.844 \times 10^{-2}$	$4.95 \times 10^{-2}$	$5.09 \times 10^{-2}$	
250 .....	0.200	0.34	0.34	0.1
305.5 .....	1.135	1.95	1.52	1.6
330 .....	2.244	3.80	2.72	2.8
352 .....	3.954	6.61	4.39	4.4
364 .....	5.297	8.71	5.62	5.7
B.Pt.(calc.).	673° C.	635° C.	755° C.	

\* Scott.

† Hackspill.

The results obtained by Hackspill are, owing to the method he adopted, far too high and cannot be used for comparison purposes. The extrapolated values from formula (11) give results which at the high temperatures agree with Hackspill's data but do not agree with the others; at low temperatures they are too high, giving a correspondingly high value to the boiling-point of rubidium at atmospheric pressure.

The values calculated from formula (9) agree well with the experimental values over the range 90°–130° C., and the results at low temperatures are probably of the right order. Comparison of the results obtained from Killian's formula

with those from Scott's formula show that over the range considered, 0°–350° C., Killian's results have approximately twice the value of Scott's. This seems to indicate a systematic error in one or other of these experimenters' work.

Scott's method may be dismissed for the time being, as his was the direct determination and the error, if any, probably lies in Killian's indirect method. As stated previously, he used the positive ion emission from a heated tungsten filament in the presence of the alkali vapour. Under these conditions the maximum positive ion emission is given by

$$i_+ = \frac{ep}{\sqrt{2\pi mkT}} \text{ amps. per sq. cm.,}$$

where

$e$  = electronic charge,

$p$  = pressure,

$m$  = mass of atom,

$k$  = Boltzmann's constant,

$T$  = Absolute temperature,

provided that the mass of the positive carrier is that of a single atom and that it carries unit charge. The single atom theory has been investigated by Ives\*, who claims that under certain conditions the carriers are atomic aggregates positively charged. Also under the strong electric fields used in the experiments it is probable that an atom would lose two electrons and hence acquire twice its previous charge, and the calculated values of the vapour pressure would then be double their true value.

Assuming this to be the case, the calculated value of the boiling-point of rubidium at atmospheric pressure becomes 700° C., which is closer to the recognized boiling-point than the values obtained from formulæ (10) and (11). As far as can be ascertained at the present time, the values obtained by extrapolation from formula (9) or the values divided by two obtained from formula (10) give an approximate value of the vapour pressure of rubidium.

### 5. Vapour Pressure of Cæsium.

Hackspill† and Kroner‡ have both measured the vapour pressure of cæsium at high temperatures, the former over

\* *Frank. Inst. Journ.* cci. p. 47 (1926).

† *Loc. cit.*

‡ *Loc. cit.*

the range  $230^{\circ}$ – $400^{\circ}$  C. and the latter from  $250^{\circ}$ – $350^{\circ}$  C. Their experimental results are given in Table IV.

Using the same method for caesium as he had used for rubidium, Scott\* measured the vapour pressure from  $50^{\circ}$ – $115^{\circ}$  C., and the equation he deduces from the result is

$$\log p = -\frac{3753}{T} + 7.256. \quad . \quad . \quad . \quad (12)$$

From a measurement of the positive ion emission of a heated tungsten filament in caesium vapour the following formula was obtained by Langmuir and Kingdom†

$$\log p = -\frac{3992}{T} + 7.53. \quad . \quad . \quad . \quad (13)$$

The temperature range used was presumably from  $0^{\circ}$ – $80^{\circ}$  C.

In Table IV. are shown the extrapolated values from these formulæ.

The boiling-points at atmospheric pressure calculated from formulæ (12) and (13) are far too low, and the pressures at the high temperatures are far greater than those obtained by Hackspill. There is no justification for assuming that Hackspill's pressures are too low, as in his work with the other alkali metals by the same method the vapour pressures have all erred on the high side. In considering Scott's results it must therefore be assumed that the experimental values obtained for caesium are too high, and this may be due to hydrogen occluded by the metal.

Applying the same reasoning to Langmuir and Kingdom's values as was used in the case of rubidium, *i. e.* that the values of the vapour pressure calculated from the positive ion emission are double their true value owing to the atom having lost two electrons in the intense electric field, then values of the vapour pressure of caesium are obtained which are considerably less than any of the others at low temperatures but comparable with Kroner's experimental values at high temperatures, and the new value of the boiling-point, *viz.*  $645^{\circ}$  C., approaches more closely the recognized boiling-point of caesium.

Kroner's experimental values over the range  $250^{\circ}$ – $350^{\circ}$  C. are slightly less than those obtained by Hackspill and appear to be more reliable. Applying the theory of least squares to Kroner's results it is found that the most probable formula connecting  $\log p$  and  $\frac{1}{T}$  is

$$\log p = -\frac{3965.5}{T} + 7.1650. \quad . \quad . \quad . \quad (14)$$

\* *Loc. cit.*

† Proc. Roy. Soc. A. cvii. p. 61 (1925).



TABLE IV.—Vapour Pressure of Cæsium.

Temperature in °C.	Pressures deduced from formula (12) in mms.	Pressures deduced from formula (13) in mms.	Pressures deduced from formula (14) in mms.	Experimental values of pressures in mms.	
0 .....	$3.266 \times 10^{-7}$	$8.2 \times 10^{-8}$	$4.42 \times 10^{-8}$		
20 .....	$2.825 \times 10^{-6}$	$8.1 \times 10^{-7}$	$4.32 \times 10^{-7}$		
28.5 (M.Pt.)	$6.501 \times 10^{-6}$	$2.0 \times 10^{-6}$	$1.04 \times 10^{-6}$		
48.3 .....	$3.793 \times 10^{-5}$	$1.3 \times 10^{-5}$	$6.38 \times 10^{-6}$	$3.85 \times 10^{-5}$	}
56.9 .....	$7.638 \times 10^{-5}$	$2.7 \times 10^{-5}$	$1.41 \times 10^{-5}$	$7.07 \times 10^{-5}$	
68.0 .....	$1.795 \times 10^{-4}$	$6.7 \times 10^{-5}$	$3.46 \times 10^{-5}$	$1.79 \times 10^{-4}$	
75.4 .....	$3.069 \times 10^{-4}$	$1.2 \times 10^{-4}$	$6.11 \times 10^{-5}$	$3.08 \times 10^{-4}$	
79.4 .....	$4.064 \times 10^{-4}$	$1.6 \times 10^{-4}$	$8.24 \times 10^{-5}$	$4.30 \times 10^{-4}$	}
89.1 .....	$7.834 \times 10^{-4}$	$3.2 \times 10^{-4}$	$1.65 \times 10^{-4}$	$7.86 \times 10^{-4}$	
101.9 .....	$1.663 \times 10^{-3}$	$7.2 \times 10^{-4}$	$3.90 \times 10^{-4}$	$1.81 \times 10^{-3}$	}
113.5 .....	$3.532 \times 10^{-3}$	$1.6 \times 10^{-3}$	$8.09 \times 10^{-4}$	$3.23 \times 10^{-3}$	
150 .....	$2.421 \times 10^{-2}$	$1.2 \times 10^{-2}$	$6.17 \times 10^{-3}$		
200 .....	0.21	0.12	$7.06 \times 10^{-2}$		
249.5 .....	1.18	0.78	0.38	0.31	245° 0.4
268.8 .....	2.13	1.44	0.70	0.74	272° 1.0
288.0 .....	3.68	2.59	1.25	1.34	
307.5 .....	6.18	4.50	2.19	2.26	308° 2.7
327.2 .....	10.07	7.59	3.61	3.61	330° 5
346.5 .....	15.78	12.2	5.81	5.45	
355.5 .....	19.28	15.1	7.18	6.65	350° 6.8
B.Pt. (calc.)	585° C.	585° C.	652° C.		

\* Scott.

† Kroner.

† Hackspill.

For purposes of comparison values have been extrapolated from this formula and are given in Table IV. It will be noted that they are considerably less than the others and in all cases about one-half of the values obtained by Langmuir and Kingdom.

It is evident from this work that the vapour pressures of the alkali metals are not known with any great degree of accuracy.

### 6. Summary.

1. Formulæ representing the vapour pressures of the alkali metals have been compared with experimental values.

*Phil. Mag.* S. 7. Vol. 3. No. 15. March 1927. 2 N

2. The vapour pressures have been extrapolated at various temperatures for purposes of comparison and many variations are shown in the pressures obtained by different methods.

3. No single formula represents the variation of pressure with temperature for any given metal, but from a comparison of all the results for any one metal it is possible to get an approximate evaluation of the pressure at various temperatures.

In conclusion the author wishes to thank Prof. F. H. Newman for suggesting the subject of this paper.

LVI. *The Magnetic Rotary Dispersion of Water, Alcohol, and Alcohol-Water Mixtures.* By D. J. STEPHENS, M.Sc., and E. J. EVANS, D.Sc., *Physics Department, University College of Swansea* \*.

#### INTRODUCTION.

THE magnetic rotation of a large number of substances for sodium light has been examined by Perkin and others, but a great deal of work remains to be done on the problem of the magnetic rotary dispersion of substances in other regions of the spectrum. The present research was commenced with the intention of examining the magnetic rotation of several substances in the ultra-violet, but as water and alcohol are often used as solvents, it was considered desirable, in the first place, to examine the magnetic rotation produced by them. The magnetic rotary dispersion is intimately connected with the natural dispersion, and experiments on both for a particular substance, when examined in the light of theory, give information as to the position of the absorption bands.

The natural dispersion in regions of the spectrum not too close to an absorption band is given by an equation of the Ketteler-Helmholtz type †.

$$n^2 - 1 = b_0 + \frac{b_1}{\lambda^2 - \lambda_1^2} + \frac{b_2}{\lambda^2 - \lambda_2^2} + \dots \quad (1)$$

Flatow determined the refractive index of water for wave-lengths ranging from  $\cdot 5893 \mu$  to  $\cdot 214 \mu$  and found that

\* Communicated by Prof. E. J. Evans, D.Sc.

† The notation used in this paper is the same as that given by S. S. Richardson, *Phil. Mag.* xxxi. p. 232.

the dispersion could be represented by an equation of the type

$$n^2 - 1 = a_0 + \frac{a_1 \lambda^2}{\lambda_1 - \lambda_1^2} - c \lambda^2. \quad . \quad . \quad . \quad (2)$$

In this equation  $a_0$  is the contribution of electrons of very high frequency, and  $-c \lambda^2$  is the small effect in the visible and ultra-violet of the infra red vibrators. The values of the various constants in the above equation for water at 20° C. are :—

$$a_0 = .37512 ; c = .013414 ; a_1 = .38850, \text{ and } \lambda_1 = .12604 \mu.$$

It has been shown by Larmor \* that the magnetic rotation  $\delta$  can be expressed in the form

$$\delta = \frac{e}{2mC^2} \lambda \frac{dn}{d\lambda}, \quad . \quad . \quad . \quad (3)$$

where  $C$  is the velocity of light and  $e/m$  is the ratio of charge to mass for all the resonators.

If the value of  $\frac{dn}{d\lambda}$  from equation (1) is substituted in (3) and if  $n\delta\lambda^2$  is put equal to  $\phi$ , it can be shown † that

$$\phi = K_1 \left( \frac{\lambda^2}{\lambda^2 - \lambda_1^2} \right)^2 + K_2 \left( \frac{\lambda^2}{\lambda^2 - \lambda_2^2} \right)^2 + \dots, \quad . \quad . \quad (4)$$

where  $K_1, K_2$ , etc., are constants and  $\lambda_1, \lambda_2$ , etc. are wave-lengths corresponding to the free periods of the vibrators.

For substances which are transparent in the visible and infra red,  $\lambda_1$  and  $\lambda_2$  will represent wave-lengths corresponding to ultra-violet free periods. If the substance has only one free period in the ultra-violet, the equation reduces to the form

$$\phi = K_1 \left( \frac{\lambda^2}{\lambda^2 - \lambda_1^2} \right)^2 \quad . \quad . \quad . \quad (5)$$

From two values of  $\phi$  corresponding to two values of  $\lambda$ , it is therefore possible to determine values of  $K_1$  and  $\lambda_1$  for that region of the spectrum. If it be found that the experimental results lead to different values of  $\lambda_1$  depending on the wave-lengths chosen, and if the values change progressively when the chosen wave-lengths are taken in regions of shorter and shorter wave-lengths, it is presumed that the substance has more than one free period.

\* 'Æther and Matter,' Appendix F, p. 352.

† Richardson, *loc. cit.*

In such a case an attempt is made to represent the results by the equation

$$\phi = K_1 \left( \frac{\lambda_2}{\lambda^2 - \lambda_1^2} \right)^2 + K_2 \left( \frac{\lambda^2}{\lambda^2 - \lambda_2^2} \right)^2, \quad \dots \quad (6)$$

where  $K_1$ ,  $K_2$ , and  $\lambda_1$ ,  $\lambda_2$ , can be determined from values of  $\phi$  corresponding to four known wave-lengths.

When the substance has more than one absorption band, an equation which represents the experimental results with greater accuracy than equation (4) can be obtained by neglecting the dispersional part of  $K^2 \left( \frac{\lambda^2}{\lambda^2 - \lambda_2^2} \right)^2$  whilst retaining its constant part.

Equation (5) then assumes the form

$$\phi = K_1 \left( \frac{\lambda^2}{\lambda^2 - \lambda_1^2} \right)^2 + K_2, \quad \dots \quad (7)$$

where  $K_1$ ,  $K_2$ , and  $\lambda_1$  can be deduced from three values of  $\phi$ .

#### EXPERIMENTAL ARRANGEMENT.

A parallel beam of light was obtained by placing a nickel-steel spark or a tungsten arc at the focus of a quartz lens. This lens together with the modified Jellett prism immediately behind it formed the polarizing unit of the Bellingham-Stanley polarimeter\*. The lens and prism were supported in a brass tube and mounted on a metal base. The beam of light on emerging from the lens passes through the Jellett prism, giving a beam on the other side, the two semi-circular portions of which are polarized at a small angle to each other. The beam then traversed the liquid contained in a tube, which was placed inside a solenoid. The magnetic field produced at various points of the axis of the solenoid for a given current had been previously determined. The temperature of the liquid during an experiment was kept approximately constant (within about a degree on the average) by means of water-cooling, and the temperature measured. The polarized beam after traversing the tube falls on the analyser, and is brought to a focus on the slit of a quartz spectrograph by a quartz-fluorite lens, which forms a part of the Bellingham-Stanley analyser-unit. The analyser, which may be rotated, has a vernier scale fixed to it, and the rotation can be measured on a fixed circular scale to 1' of arc.

\* 'Dictionary of Applied Physics,' iv. p. 476.



*The Solenoid.*

The coil consists of 22 layers of insulated wire wound on a brass tube 47.2 cm. long and 4.75 cm. radius, and each layer contains 357 turns of wire. The resistance of the coil has remained constant during the experiments, as shown by the constant value of the field at the centre of the solenoid when a current of 2 amperes is passing through it. The magnetic field at various points along the axis of the solenoid due to a current of 2 amperes (the current used in all the present experiments) was carefully determined, and consequently the value of  $\Sigma Hl$ , where  $H$  is the magnetic field at a given point of the polarimeter tube and " $l$ " the length of tube over which  $H$  is approximately constant, could be determined for each tube employed in the present experiments. The current was measured by a sensitive Weston volt-ammeter with 30 divisions to the ampere, and the scale readings were certified to be correct to within  $\frac{1}{4}$  of 1 per cent. The observed and calculated values of the field agreed to about 1 part in 300. An error in the determination of the magnetic field will not affect the relative values of Verdet's constant for different wave-lengths, and it is important to note that the position of the absorption bands can be determined from these relative values. The rotation produced in the present experiments by conductivity water for sodium light was too small for standardising the field, and the values given for Verdet's constant for lines in the ultra-violet seemed rather uncertain.

*Polarimeter Tubes.*

In the case of water three glass tubes of lengths 40.09, 31, and 5 cm. were employed. They were closed by pairs of right- and left-handed quartz disks of almost equal thicknesses, and consequently the natural rotation of each pair was comparatively small. The magnetic field was almost constant over the whole length of the tube 31 cm. long, and for that reason it was used in preference to the longer tube. The shortest tube, of length 5 cm., was employed in a few experiments in the neighbourhood of  $2300\mu$ . In experiments on the magnetic rotation of alcohol and alcohol-water mixtures, a quartz tube 30.5 cm. long closed by two plates of polished fused quartz was employed. The end plates were carefully fused round the edges to the ends of the tube, and the central portions of the plates did not distort the beam of light. The values of  $\Sigma Hl$  for the glass tube 31 cm. long and the quartz tube were 12644 and 12445 gauss cm. respectively.

*Sources of Light and Spectrograph.*

The two sources of light chiefly used in these investigations were the Nickel-steel spark and the Tungsten arc. Both sources gave a spectrum containing a very large number of lines well distributed over the region of the spectrum chiefly investigated, *i.e.*, between  $5000\mu$  and  $2300\mu$ . A very intense nickel-steel spark could readily be obtained by connecting up flat strips of nickel steel at a distance apart of about 6 mm. to the secondary terminals of a 16-inch induction coil with a large capacity in parallel. In these experiments it was found that the spark was a more reliable source of light than the arc, and in most cases was employed in preference to it. The most satisfactory source, from the point of view of intensity, was the Tungsten arc, and it was employed in pushing the experimental work to the furthest limit in the ultra-violet. It was found impossible with the apparatus used to push the investigation below the wave-length  $2383\mu$ , and when the light from a Tungsten arc was passed through only the polarizing and analysing units, no spectrum lines were photographed below  $2200\mu$ , and the lines between this wave-length and  $2390\mu$  were weak. This is probably due to the absorption of light by Iceland spar, and to a much lesser extent by the thin film of glycerine employed in assembling the analyser of the Bellingham-Stanley polarimeter. According to the experiments of Pflüger\*, a piece of Iceland spar 1 cm. thick absorbs 15 per cent. of the light at wave-length  $2800\mu$  and 97 per cent. at  $2140\mu$ . Glycerine also absorbs on the more refrangible side of  $2300\mu$ . These substances therefore absorb to a greater degree than water, which, according to Kreusler†, absorbs only 14.2 per cent. at  $2\mu$  for a thickness of about 2 cm.

The spectrograph employed was of the usual type consisting of a Cornu quartz prism and two quartz lenses. The instrument, which was constructed in the Laboratory, gave a spectrum approximately 14 cm. long, extending from  $7000\mu$  to  $2000\mu$ . The dispersion at  $2300\mu$  was approximately  $0.010\mu$  per mm., at  $2800\mu$  about  $0.0176\mu$  per mm., and at  $4000\mu$  about  $0.0050\mu$  per mm.

*Mode of Experiment.*

As previously explained, the two semi-circular half-fields consisting of two beams of plane-polarized light vibrating in directions making a small angle with one another, are

\* Lyman, 'The Spectroscopy of the Extreme Ultra-Violet,' p. 13.

† *Loc. cit.* p. 60.

focussed on the slit of the spectrograph by the quartz-fluorite lens. The line of demarcation between the half-fields is horizontal, and two spectra, one on top of the other, are produced by the Cornu prism. These spectra are, in general, of different intensity, but if the quartz disks closing the polarimeter tubes are of exactly the same thickness, and also if no current passes through the solenoid, it is possible, by rotating the analyser, to make the two semi-circular halves of the same intensity, and the two contiguous spectra have the same intensity throughout their length. The reading of the analyser when this occurs is noted, and called the zero-reading of the polarimeter. There are two positions of the analyser, inclined at  $90^\circ$  to one another, which will give equality of fields; but in all measurements described here the most sensitive position was used, and the intensity of the light falling on the spectrograph slit was small. The analyser is now rotated through a known angle, the polarimeter tube filled with liquid, the magnetic field excited, and a photograph is taken. When the photographic plate is examined, it is found that, although the two spectra are of very different intensity, there is a definite line in each of same intensity. The rotation of the analyser then measures the rotation produced by the liquid due to a magnetic field of known strength for light of a known wave-length.

The method of experimenting was, however, not quite as simple as the one described, since it was found that each pair of quartz disks closing the polarimeter tubes was not exactly compensated for natural rotation, and, in addition, a correction must be applied for the magnetic rotation produced by the disks. These corrections increase rapidly as the wave-length diminishes. The zero position of the analyser was carefully determined with no polarimeter tube inside the solenoid and without the magnetic field. A magnetic field corresponding to 2 amperes in the solenoid was then applied, the polarimeter tube placed in the solenoid, and spectra corresponding to various small rotations of the analyser were taken. The wave-lengths of the points of equality in the spectrum were then determined and a correction curve drawn. In these experiments the direction of the magnetic field was such as to produce a rotation in the quartz disks in the same direction as the uncompensated natural rotation. The results were also verified by determining experimentally for the pair of disks the values of the uncompensated natural rotation for different wave-lengths, and adding the values calculated \* for the magnetic rotation

\* Landolt and Börnstein, ii. p. 1012.

of crystalline quartz of the same thickness as the two disks. It is considered that the corrections to be applied were determined with an accuracy of about 1' to 2' at any point of the wave-length scale. The magnetic rotation produced by a liquid is, therefore, the difference between two readings. If for a given reading of the analyser the point of equality is found at a wave-length  $\lambda$ , the rotation produced by the liquid for that wave-length is obtained by subtracting from the reading of the analyser the reading for equality at that point of the spectrum with no liquid in the tube and all other conditions remaining the same.

The temperature of the liquids in the tubes was kept constant within about half a degree on either side of the mean given in the Tables, which will be discussed later. In the case of water the effect of temperature on the value of Verdet's constant was determined by Rodger and Watson for sodium light and is given by the following equation:—

$$w_t^D = \cdot 01311(1 - \cdot 0000305t - \cdot 00000305t^2)3 < t < 98^*.$$

It is considered that, for the experiments here described, it is not worth while reducing all the values of the rotation to one temperature, as the temperature correction is certainly smaller than the experimental error, especially in the visible region of the spectrum. These experiments were carried out to determine the values of Verdet's constant for the ultra-violet region of the spectrum, and great accuracy is not possible in the visible, especially near  $\cdot 6 \mu$ , as the rotation produced is comparatively small. The rotations actually measured with a tube about 31 cm. long, containing water with a current of 2 amps. passing through the solenoid, varied from about 160' at  $\cdot 5893 \mu$  to  $\cdot 1568'$  at  $\cdot 2383 \mu$ . In good photographs, especially in the region about  $\cdot 2700 \mu$ , the point of equality could be determined with an accuracy of about  $\cdot 0005 \mu$ , and in the region about  $\cdot 4800 \mu$  it is estimated that on the average the point of equality could be fixed with an accuracy of about  $\cdot 0020 \mu$ .

The exposures required with the nickel-steel spark employing panchromatic plates for the yellow and red regions of the spectrum, and imperial plates for the ultra-violet, varied from about 15 minutes to 45 minutes for various regions of the spectrum. During these exposures the current passing through the solenoid was kept constant to 1 part in 600. The values of Verdet's constant for water were determined with conductivity-water prepared in the

\* *Loc. cit.* p. 1011.



Chemical Department; but it is not known to what extent, if any, the results are affected by the small solubility of the glass of the polarimeter-tube in the water. The water in the tube was changed from time to time, but the values obtained were the same within experimental error. The same values were also obtained with conductivity-water contained in a quartz tube. It is estimated that the values of Verdet's constant given in the tables and those obtained from an accurately drawn curve representing the experimental results are correct to about  $\frac{1}{2}$  per cent. on the average, except possibly in the visible portion of the spectrum. It seems \* that a possible source of error in polarimetric work is the inequality of the intensity of illumination in the two halves of an ordinary Lippich polarizer. This produces a systematic error in the measurement of a rotation if the substance under examination is slightly birefringent, or if a small amount of accidental double-refraction is introduced into the path after the zero reading of the polarimeter has been taken. These considerations, however, do not apply to the polarizer used in the present experiments. The experiments with alcohol and alcohol-water mixtures were carried out in quartz tubes closed with polished fused quartz plates. The rotation produced by the fused quartz ends when in the magnetic field were determined experimentally. The rotations produced by alcohol for several wave-lengths and alcohol-water mixtures at  $2753\mu$  and  $3363\mu$  were determined, and compared with the rotations produced by water under the same conditions.

#### EXPERIMENTAL RESULTS.

The magnetic rotary dispersion of water has been examined by Siersteina †, Landau ‡, U. Meyer §, S. S. Richardson ||, R. W. Roberts ¶. Siersteina's and Meyer's results are given in Landolt and Börnstein \*\*, and S. S. Richardson †† gives a table comparing his results over the range  $4958\mu$  to  $3100\mu$  with those obtained by Landau with an electromagnet of small power. Roberts ‡‡ gives a table of the values of

\* 'Dictionary of Applied Physics,' iv. p. 479.

† *Arch. Naerl.* (2) vi. p. 830 (1901).

‡ *Phys. Zeit.* (9) p. 417 (1908).

§ *Ann. d. Phys.* (4) xxx. p. 629 (1909).

|| *Phil. Mag.* xxxi. p. 232 (1916).

¶ *Loc. cit.* xlix, p. 397 (1925).

\*\* Landolt and Börnstein, ii. p. 104.

†† *Loc. cit.*

‡‡ *Loc. cit.*

Verdet's constant for eight different wave-lengths from  $\cdot 5193\mu$  to  $\cdot 3100\mu$ . In the tables given below the values of Verdet's constant are given for a large number of wave-lengths, and the determination has been extended to the wave-length  $\cdot 2383\mu$ . The values of Verdet's constant obtained in the present work are about 4 per cent. higher in the ultra-violet than those due to Meyer, and about 1 per cent. to 2 per cent. higher than those given by Roberts. Richardson calculated the position of the absorption band of water from the values of the rotation for eight different wave-lengths ranging from  $\cdot 5893\mu$  to  $\cdot 303\mu$ , and found that the value of  $\lambda_1$  varied from  $\cdot 109\mu$  to  $\cdot 114\mu$ . There was a progressive increase in the value of  $\lambda_1$  as the two wave-lengths chosen for the calculation of the constant were shifted towards the ultra-violet. Richardson therefore came to the conclusion that there were at least two frequencies responsible for the magnetic dispersion in water, and that the smallness of the progression was probably due to the value of  $\lambda_1$  being small compared with the shortest waves used in the experimental work. He therefore calculated the values of the constants  $K_1$ ,  $K_2$ , and  $\lambda_1$  of the formula

$$\phi = K_1 \left( \frac{\lambda^2}{\lambda^2 - \lambda_1^2} \right) + K_2 \dots, \quad ,$$

which would fit his experimental results, and found them to be approximately  $\cdot 1375\mu$ ,  $K_1 = \cdot 9499$ , and  $K_2 = \cdot 7012$ . Lowry\* has determined the dispersion ratio of the magnetic rotations of water for the mercury lines  $\cdot 5461\mu$  and  $\cdot 4359\mu$  and found  $\frac{\delta(\cdot 4359\mu)}{\delta(\cdot 5461\mu)} = 1\cdot 645$ . On the assumption that water has one

absorption band in the ultra-violet, Richardson† has calculated its position to be at  $\cdot 113\mu$ . The values obtained in the present experiments of Verdet's constant for water for wave-lengths ranging from  $\cdot 5997\mu$  to  $\cdot 2383\mu$  are given in Tables I. and II. and are plotted in Curve I. The values of the function  $\phi$  are calculated in Table III.

In the last column of Table III. are calculated the values of the function  $\phi$ , which is equal to  $n\delta\lambda^2$  for different lines in the spectrum. The values of the refractive index of water are calculated from the equation given by Flatow‡, and corrected to  $15^\circ\text{C}$ ., which is about the mean temperature used in the present experiments.

\* Journ. Chem. Soc., Jan. 1914.

† *Loc. cit.*

‡ *Loc. cit.*

TABLE I.

Conductivity-water contained in glass polarimeter tubes with right and left-handed crystalline quartz ends.

Temperature in degrees centigrade.	Wave-length in microns ( $10^{-4}$ cm.).	Verdet's Constant.	Temperature in degrees centigrade.	Wave-length in microns ( $10^{-4}$ cm.).	Verdet's Constant.
19	·5997	·0127	16·4	·3352	·0478
20	·5893	·0130	16·6	·3220	·0525 <sub>s</sub>
13·2	·4920	·0191	16·6	·3132	·0573
17·0	·4880	·0194	19·6	·3118	·0575
15·0	·4845	·0197	13·8	·3045	·0615
15·0	·4610	·0222	17·0	·2992	·0655
21·3	·4500	·0237	15·8	·2940	·0684
15·5	·4315	·0261	20·0	·2890	·0709
13·5	·4190	·0278	17·7	·2828	·0756
21·1	·4100	·0285	14·5	·2740	·0825
20·6	·4022	·0308	15·8	·2734	·0829
18·9	·3880	·0333	16·6	·2673	·0883
14·6	·3745	·0365	18·2	·2593	·0974
15·0	·3618	·0396	13·0	·2533	·1048
16·5	·3598	·0401	17·9	·2495	·1100
15·0	·3520	·0420	18·7	·2431	·1179
18·9	·3480	·0429	16·3	·2414	·1202
17·4	·3415	·0455	15·7	·2383	·1240
19·8	·3363	0473			

TABLE II.

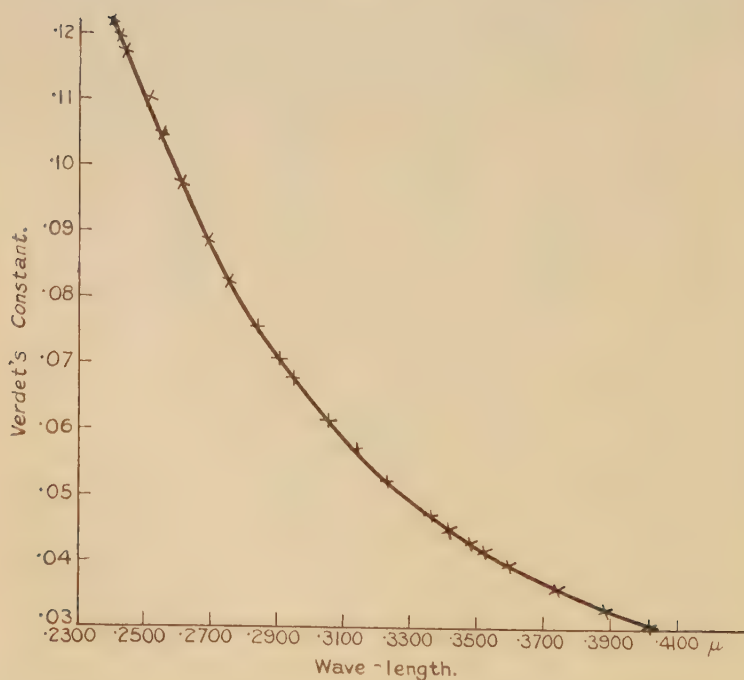
Verdet's Constant for Conductivity-Water contained in a quartz tube with polished fused quartz ends.

Temperature in degree centigrade.	Wave-length in microns.	Verdet's Constant.	Temperature in degrees centigrade.	Wave-length in microns.	Verdet's Constant.
12·1	·4441	·0244	14·6	·3363	·0475
11·3	·4056	·0301	14·4	·3113	·0579
11·7	·4036	·0306	11·4	·3100	·0585
11·6	·3792	·0353	12·2	·2742	·0819

TABLE III.

Wave-length in microns.	Refractive index at 15° C. $\eta$ .	Verdet's Constant in minutes per cm. gauss.	Verdet's Constant in circular measure $\times 10^6$ , i. e. $8 \times 10^6$ .	$\phi \times 10^{14}$ ( $\phi = n\delta\lambda^2$ ).
(a) .5893	1.3332	.0131	3.81064	1.76269
(b) .3618	1.3475	.0396	11.51917	2.03183
(c) .3045	1.3577	.0615	17.88962	2.25135
(d) .2734	1.3669	.0829	24.11463	2.46385
(e) .2428	1.3814	.1184	34.44116	2.80475

Curve I.



The value of  $\phi$  for sodium light (.5893  $\mu$ ) has been calculated on the assumption that Verdet's constant for that wave-length is .0131, and the value at .2428  $\mu$  has been deduced



from Verdet's constant read off from a large scale magnetic rotary dispersion curve constructed from the experimental data. The values of  $\phi$  for other wave-lengths have been calculated from the values of Verdet's constants actually determined at those wave-lengths.

The values of  $\lambda_1$ , the wave-length of the absorption band determined from the above observations on the assumption that

$$\phi = K_1 \left( \frac{\lambda^2}{\lambda^2 - \lambda_1^2} \right)^2,$$

are from

(b) and (d)	$\lambda_1 = .1194 \mu$ ,
(b) and (e)	$\lambda_1 = .1193 \mu$ ,
(d) and (e)	$\lambda_1 = .1191 \mu$ ,
(c) and (e)	$\lambda_1 = .1194 \mu$ ,
(a) and (e)	$\lambda_1 = .1188 \mu$ .

The mean value of  $\lambda_1$  is approximately  $.1192 \mu$ . The magnitude of  $K_1$  in the above formula can be calculated from the value of  $\phi$  corresponding to a known value of  $\lambda$ .

The expression deduced for the variation of  $\phi$  with wave-length in the ultra-violet, visible, and near infra-red regions of the spectrum is given by:—

$$\phi = 1.61567 \left( \frac{\lambda^2}{\lambda^2 - (.1192)^2} \right)^2 \cdot \cdot \cdot \cdot (8)$$

This equation was employed to calculate the values of  $\phi$  corresponding to different wave-lengths in the visible and ultra-violet regions of the spectrum, and from the calculated values of  $\phi$  the magnitudes of Verdet's constants were deduced. The results of the calculation are given in Table IV.

The equation

$$\phi = 1.61567 \frac{(\lambda^2)^2}{[(\lambda^2) - (.1192)^2]^2}$$

therefore represents the experimental returns with the degree of accuracy to be expected, and the magnetic rotations in the region of the spectrum investigated (about  $.6 \mu$  to  $.238 \mu$ ) can be explained on the assumption that there is only one absorption band situated at  $.1192 \mu$ . There may be other absorption bands, but their contribution to the magnetic rotation is negligible in the region of the spectrum investigated.

TABLE IV.

Wave-length in microns.	Verdet's Constant calculated from equation (8).	Verdet's Constant observed.	Remarks.
·5893	·01306		
·4610	·0224	·0222	
·4416	·0247	·0247	→ Calculated from observed value at 4441 $\mu$ on assumption that rotation $\propto \frac{1}{\lambda^2}$ .
·4190	·0279	·0278	
·4060	·0300 <sub>4</sub>	·0300 <sub>4</sub>	→ Calculated from observed value at 4056 $\mu$ .
·3790	·0353 <sub>8</sub>	·0353 <sub>4</sub>	
·3415	·0457	·0455	
·3363	·0475	·0475	
·2593	·0970	·0974	

THE EXPERIMENTAL RESULTS FOR ALCOHOL AND  
ALCOHOL-WATER MIXTURES.

*Magnetic Rotation of Ethyl Alcohol.*

The magnetic rotation of ethyl alcohol relative to water for sodium light ( $\lambda = \cdot 5893 \mu$ ) was determined by Perkin\*, who obtained the value ·8637. S. Landau† investigated the rotation produced by the liquid for various wave-lengths in the visible and ultra-violet regions of the spectrum, and found the following values for Verdet's constant at the specified wave-lengths at 16° C. :—

Wave-length in microns.	Verdet's Constant at 16° C.
0·2563	0·0777
0·3100	0·0469
0·3609	0·0330
0·3886	0·0277
0·4046	0·0250
0·4529	0·0195

\* Kaye & Laby's Tables of Physical and Chemical Constants, p. 10.

† *Loc. cit.* p. 427 (1908).

In the present experiments the absolute alcohol was placed in a flask provided with a fractionating column and distilled. The middle portion, which distilled over at the boiling-point of ethyl alcohol, was retained, and employed in the determination of Verdet's constant for eight of different wave-lengths. It was found, however, that fractional distillation made no appreciable difference in the results obtained. The alcohol contains a small amount of water, and on the assumption that water is the only impurity, density determinations showed that the percentage of alcohol in the liquid was 99.4. The alcohol was introduced into a quartz tube provided with polished fused quartz ends \*, so as to avoid contamination with substances soluble in the liquid. Special experiments were carried out to determine the correction for the quartz ends at different wave-lengths, when a current of 2 amperes was passed through the solenoid. The temperature of the alcohol was kept constant within .3° C. during a particular experiment. Several experiments were carried out at each wave-length, and the results were found to be consistent. The presence of a small amount of dissolved impurity can seriously affect the experimental results, and great trouble was experienced from this cause when the ordinary glass polarimeter tubes with rubber bands at the ends were employed. The experimental results obtained for ethyl alcohol are given in Table V.

TABLE V.

Verdet's Constant for 99.4 per cent. alcohol.

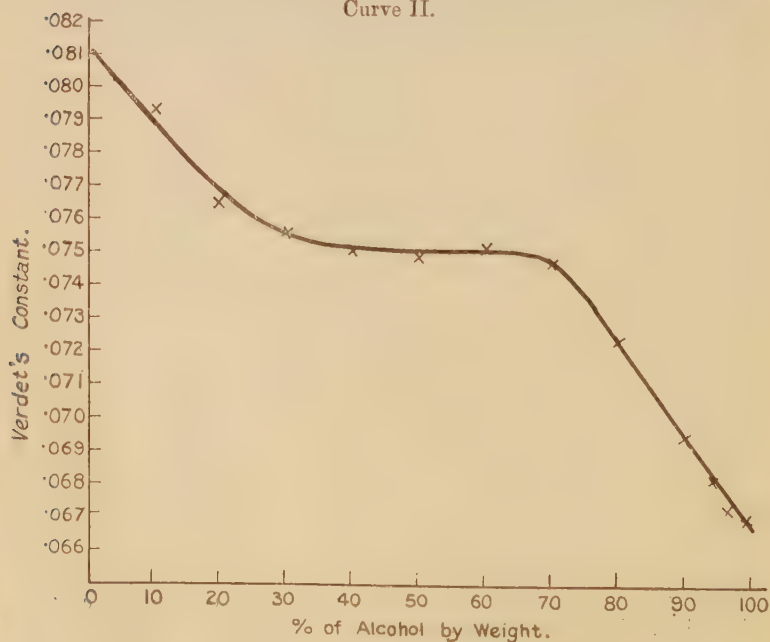
Temperature in degrees centigrade.	Wave-lengths in microns.	Verdet's Constant.
12.6	.4390	.0214 <sub>5</sub>
12.7	.4136	.0246
12.3	.4060	.0255
13.0	.3803	.0297
12.2	.3363	.0400 <sub>5</sub>
12.4	.3090	.0494
12.8	.2985	.0541
12.9	.2753	.0670
12.3	.2600	.0785

\* This tube gave the same results for water as the glass tube closed by pairs of right- and left-handed quartz disks.

TABLE VI.—Verdet's Constant for Alcohol-Water Mixtures at  $\cdot 2753 \mu$  and  $\cdot 3363 \mu$ .

Percentage of alcohol by weight.	Temperature in degrees centigrade.	Verdet's Constant at $\cdot 2753 \mu$ .	Verdet's Constant at $\cdot 3363 \mu$ .
0	12.2	$\cdot 0812$	$\cdot 0475$
10	12.3	$\cdot 0793$	$\cdot 0465$
20	12.3	$\cdot 0765$	$\cdot 0463$
30	13.4	$\cdot 0756$	$\cdot 0461$
40	11.9	$\cdot 0751$	$\cdot 0459$
50	12.3	$\cdot 0749$	$\cdot 0460$
60	12.3	$\cdot 0752$	$\cdot 0458$
70	13.0	$\cdot 0747$	$\cdot 0456$
80	12.5	$\cdot 0724$	$\cdot 0437$
90	12.5	$\cdot 0695$	$\cdot 0415$
94.4	12.5	$\cdot 0682_5$	$\cdot 0406$
96.7	11.8	$\cdot 0673$	$\cdot 0403$
99.4	12.5	$\cdot 0670$	$\cdot 0400_5$

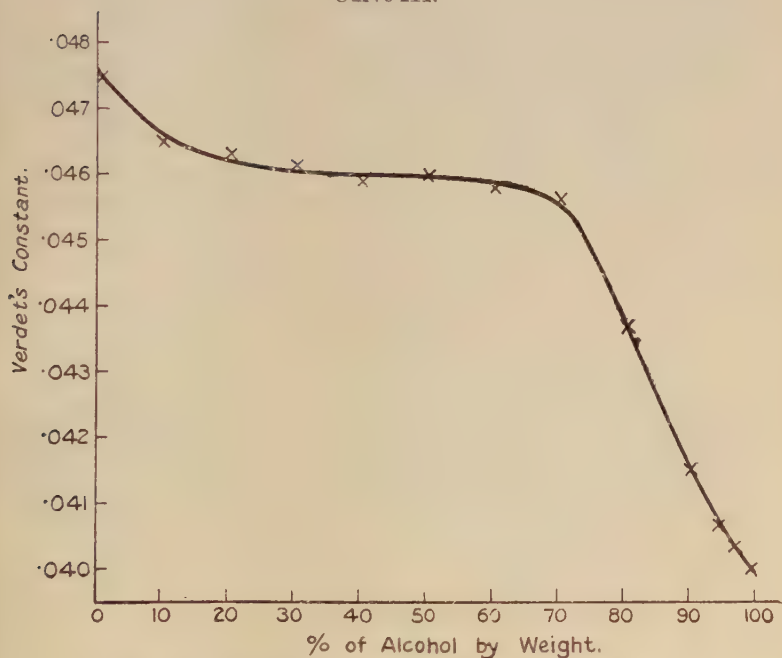
Curve II.

Magnetic Rotation of Alcohol-Water Mixtures at  $\cdot 2753 \mu$ .



Experiments were also carried out on the magnetic rotation of various alcohol-water mixtures at  $\cdot 2753\mu$  and  $\cdot 3363\mu$ . These mixtures were also placed in the quartz tube, and the determinations carried out in the same way as for 99.4 per cent. alcohol. The experimental results are given in Table VI. and plotted in Curves II. and III.

Curve III.



Magnetic Rotation of Alcohol-Water Mixtures at  $\cdot 3363\mu$ .

The experimental results show that the magnetic rotation of ethyl alcohol relative to water diminishes with decrease of wave-length. It can be calculated from the results given in the preceding tables that the ratio of Verdet's constant for alcohol relative to water assumes the values  $\cdot 861$ ,  $\cdot 850$ ,  $\cdot 843$ ,  $\cdot 825$ , and  $\cdot 813$  at  $\cdot 4390\mu$ ,  $\cdot 4060\mu$ ,  $\cdot 3363\mu$ ,  $\cdot 2753\mu$ , and  $\cdot 2600\mu$  respectively. These results suggest that the absorption band controlling the magnetic rotation in the case of ethyl alcohol is situated further in the ultra-violet than in

the case of water. The values of the function  $\phi$  for 99.4 per cent. alcohol are given in Table VII.

TABLE VII.

Wave-length in microns.	Refractive index. $\eta$ .	Verdet's Constant in minutes per cm. gauss.	Verdet's Constant in circular measure $\times 10^6$ , <i>i. e.</i> $\delta \times 10^6$ .	$\phi \times 10^{14}$ ( $\phi = n\delta\lambda^2$ ).
(a) .4390	1.372	.02145	6.2396	1.64983
(b) .3363	1.382	.04005	11.6500	1.82091
(c) .3090	1.388	.0494	14.3699	1.90441
(d) .2985	1.391	.0541	15.7371	1.95048
(e) .2753	1.398	.0670	19.4895	2.06500
(f) .2600	1.403	.0785	22.8347	2.16571

The values of the refractive indices of alcohol at different wave-lengths given in column 2 are not as accurate as the corresponding values for water, and were deduced from results given in Landolt and Börnstein's tables\*.

The values of  $\lambda_1$ , the wave-length of the absorption band determined from the above observations on the assumption that  $\phi = K_1 \frac{(\lambda^2)^2}{(\lambda^2 - \lambda_1^2)^2}$ , are from

$$(a) \text{ and } (b) \quad \lambda_1 = .1110_6 \mu,$$

$$(b) \text{ and } (e) \quad \lambda_1 = .1115 \mu,$$

$$(c) \text{ and } (f) \quad \lambda_1 = .1119 \mu,$$

$$(d) \text{ and } (f) \quad \lambda_1 = .1110 \mu.$$

The mean value of  $\lambda_1$  is approximately .1114  $\mu$ , and the value of  $K_1$  is calculated to be 1.4441.

The expression giving the variation of  $\phi$  with wave-length is given by:—

$$\phi = 1.4441 \frac{(\lambda^2)^2}{\{\lambda^2 - (.1114)^2\}^2} \cdot \cdot \cdot \cdot (9)$$

This equation was used to calculate the values of Verdet's constant at .5193  $\mu$ , .4136  $\mu$ , .4060  $\mu$ , .3803  $\mu$ , and the

\* Landolt & Bornstein, vol. ii. p. 969.

results obtained were  $\cdot 01127$ ,  $\cdot 0246$ ,  $\cdot 0256$ ,  $\cdot 0298$ . The experimental results are  $\cdot 01130$ ,  $\cdot 0246$ ,  $\cdot 0255$ ,  $\cdot 0297$ , and it is concluded that equation (9) represents the results within the limits of experimental error. The magnetic rotations produced by ethyl alcohol in the visible and ultra-violet regions of the spectrum can be explained on the assumption that there is only one absorption band situated at  $\cdot 1114\mu$ .

There is evidence\* in the case of ethyl alcohol for the existence of a faint absorption band at  $\cdot 2231\mu$ ; but the present experiments seem to indicate that this band does not contribute appreciably to the magnetic rotation. It is interesting, however, to point out that the frequency of the faint band is very nearly one-half that of the band responsible for the magnetic rotation†. The experimental results given in Table V., and analysed in Table VII., were obtained with 99·4 per cent. alcohol; but it seems reasonable to assume from the results obtained with alcohol-water mixtures of various compositions that the values for absolute alcohol would not be appreciably different.

The experimental results for various alcohol-water mixtures which are plotted in Curves II. and III. reveal some points of interest. The two curves corresponding to wave-lengths of  $\cdot 2753\mu$  and  $\cdot 3363\mu$  are of the same type, and show three stages in the variation of Verdet's constant as the percentage of alcohol in the mixture is increased. The rotation at first diminishes, then becomes constant, and finally diminishes still more rapidly. The initial diminution in the rotation is greater for the lower wave-length; but in each case the rotation remains approximately constant as the percentage of alcohol is increased from about 30 to 70.

An examination of the results shows that the values of Verdet's constant for the various mixtures cannot be calculated by adding the effects due to each constituent of the mixture. If the values of Verdet's constant for  $\lambda = \cdot 2753\mu$  are calculated in this manner, it is found that the results are greater than the observed values for mixtures ranging from 10 per cent. to 40 per cent. alcohol, and smaller than the observed values for mixtures ranging from 50 per cent. to 94·4 per cent. alcohol. In the same way it is found for  $\lambda = \cdot 3363\mu$  that the calculated value of Verdet's constant for 10 per cent. alcohol is greater than the observed value, and that the results obtained for all other mixtures up to

\* Victor Henry, 'Etudes de Photochimie,' p. 56.

† *Loc. cit.* p. 62.

94.4 per cent. alcohol are less than the observed values. The experimental results, however, seem to indicate that the values of Verdet's constant for mixtures containing a small percentage of either constituent could be calculated without appreciable error by simply adding the effects due to each constituent. If the ratio of Verdet's constant at  $2753 \mu$  to that at  $3363 \mu$  be calculated for the various alcohol-water mixtures, the following results are obtained :—

Percentage of alcohol by weight.	$\frac{\delta \cdot 2753}{\delta \cdot 3363}$	Percentage of alcohol by weight.	$\frac{\delta \cdot 2753}{\delta \cdot 3363}$
0	1.709	60	1.641
10	1.706	70	1.638
20	1.652	80	1.655
30	1.640	90	1.675
40	1.636	100	1.675
50	1.628		

The above values show that the ratio  $\frac{\delta \cdot 2753}{\delta \cdot 3363}$  diminishes at first, then remains fairly constant, and finally increases. It is difficult to account for the above results and also the results given in Table VI. without further experimental data, as both may depend upon complex changes taking place on mixing the two liquids. Further light may be thrown on the problem by determining the values of Verdet's constant of each mixture for several different wave-lengths, and also the corresponding refractive indices. It may then be possible to represent the experimental results for the mixtures by a formula of the type

$$\phi = n\delta\lambda^2 = K_1 \frac{(\lambda^2)^2}{(\lambda^2 - \lambda_1^2)^2} + K_2 \frac{(\lambda^2)^2}{(\lambda^2 - \lambda_2^2)^2} \dots,$$

where  $n$ ,  $K_1$ ,  $K_2$ ,  $\lambda_1$ , and  $\lambda_2$  will probably vary from mixture to mixture.

#### SUMMARY OF RESULTS.

1. The magneto-optical rotation of water has been examined from wave-length  $5997 \mu$  to  $2383 \mu$ . The experimental results lead to the conclusion that, in the region of the spectrum investigated, the only absorption band contributing materially to the magnetic rotation is situated at  $1192 \mu$ .

2. The magneto-optical rotation of 99·4 per cent. alcohol has also been investigated in the region of the spectrum extending from  $4390\mu$  to  $2600\mu$ . In this region the experimental results could be explained on the assumption that the absorption band contributing to the rotation is situated at  $1114\mu$ .

3. The magneto-optical rotation of various alcohol-water mixtures was examined at  $\lambda = 2753\mu$  and  $\lambda = 3363\mu$ . The value of Verdet's constant was found to diminish initially with increasing percentage of alcohol, then to become almost constant (30 per cent. to 70 per cent. alcohol), and finally to decrease as the percentage of alcohol in the mixture was further increased.

We wish to thank the Department of Scientific and Industrial Research for a grant, which made the Research possible.

---

LVII. *The Torsion of Circular and Elliptical Cylinders of Homogeneous Æolotropic Material.* By S. J. WRIGHT, B.A.\*

(From The National Physical Laboratory.)

SUMMARY.

(a) *Purpose of Investigation.*—In a recent report† it was assumed, for the purpose of comparison with experimental results, that the stress system existing in a circular bar, consisting of a single cubic crystal of arbitrary orientation, when twisted about its axis by terminal couples was the same as that which would exist if the material were isotropic. The present work was undertaken in order to justify this assumption analytically.

(b) *Range of Investigation.*—Since the assumption of cubic symmetry about arbitrary axes did not simplify the general problem, the stress system due to the torsion of circular and elliptical cylinders of homogeneous but completely æolotropic material has been worked out.

(c) *Conclusions.*—The stress system in each of the above cases is precisely the same as that which would exist if the material were isotropic; the assumption of the previous report is therefore justified.

---

IN a recent report† by the author and two of his colleagues, a comparison was made between the slip

\* Communicated by Sir J. E. Petavel, K.B.E.

† "Some Further Experiments on the Behaviour of Single Crystals of Aluminium under Reversed Torsional Stresses," by Gough, Wright, and Hanson. *Journal Inst. of Metals*, September 1926 (Liège Meeting).



phenomena observed in a single crystal specimen of aluminium tested under alternating torsion and the stress system due to the torque, this stress system being assumed to be the same as that which would exist in the isotropic medium. The agreement between the arrangement of slip bands on the specimen and the assumed stress distribution was so close that an attempt was made to justify the above assumption by an analytical investigation of the stress system when the material possessed the type of elastic symmetry associated with a cubic crystal.

When the axes of reference are the three cubic axes of the crystal, the strain-energy function, and therefore the stress-strain relations, can be expressed in terms of three "elastic constants" \*; in fact, the only difference between this case and the case of perfect isotropy is that a certain relation between these three constants which exists in an isotropic material does not hold in the case of a cubic crystal. When the axis of torsion is one of these cubic axes, and also when it is normal to a 110 plane, the solution of the general torsion problem presents no great difficulty. Both are particular cases of the solution given by Love† for the case of an *aeolotropic* prism possessing a plane of symmetry perpendicular to its axis.

For the present purpose, a solution is required for a circular cylinder when the orientation of the crystal with respect to the axis of the cylinder is entirely arbitrary. When the strain-energy function is transformed in the ordinary way to three arbitrary axes, it will have 21 coefficients or "elastic constants" analogous to those which are necessary in the case of complete *aeolotropy*. Whilst in general these coefficients will be all different from one another, they will not be all independent, being functions of the three primitive constants and the direction cosines which fix the arbitrary axes. The relations which exist between them, however, are not such as will simplify the solution of the problem under consideration. The Torsion problem has therefore been worked out for a circular cylinder of *aeolotropic* material possessing no planes of symmetry whatever, and the case of an elliptical cross-section has been deduced from it. *In both cases the stress distribution is exactly the same as that which would exist if the material were isotropic.* These results are not surprising, since they will follow from a more general principle that

\* See Love, 'Mathematical Theory of Elasticity,' 3rd edition, Chapter VI.

† *Op. cit.* p. 329.

can be established — namely, that a constant or linear stress distribution which constitutes the solution of any problem in elasticity in which the boundary conditions relate to stresses alone, and in which the material possesses any given type of elastic symmetry, will apply equally well when any other type of elastic symmetry prevails; for the stress distribution will obviously still satisfy the boundary conditions when the type of elastic symmetry is changed, and, furthermore, the strains calculated from a constant or linear stress distribution will necessarily be themselves constant or linear, and consequently will satisfy the equations of compatibility identically.

In what follows, however, the solutions have been deduced from assumed displacements in the ordinary way.

Referred to rectangular axes  $ox$ ,  $oy$ ,  $oz$ , the stress-strain relations for an æolotropic material may be written in the ordinary notation :

$$\widehat{x}x = C_{11}e_{xx} + C_{12}e_{yy} + C_{13}e_{zz} + C_{14}e_{yz} + C_{15}e_{zx} + C_{16}e_{xy}, \quad (1)$$

$$\widehat{y}y = C_{12}e_{xx} + C_{22}e_{yy} + C_{23}e_{zz} + C_{24}e_{yz} + C_{25}e_{zx} + C_{26}e_{xy}, \quad (2)$$

$$\widehat{z}z = C_{13}e_{xx} + C_{23}e_{yy} + C_{33}e_{zz} + C_{34}e_{yz} + C_{35}e_{zx} + C_{36}e_{xy}, \quad (3)$$

$$\widehat{y}z = C_{14}e_{xx} + C_{24}e_{yy} + C_{34}e_{zz} + C_{44}e_{yz} + C_{45}e_{zx} + C_{46}e_{xy}, \quad (4)$$

$$\widehat{z}x = C_{15}e_{xx} + C_{25}e_{yy} + C_{35}e_{zz} + C_{45}e_{yz} + C_{55}e_{zx} + C_{56}e_{xy}, \quad (5)$$

$$\widehat{x}y = C_{16}e_{xx} + C_{26}e_{yy} + C_{36}e_{zz} + C_{46}e_{yz} + C_{56}e_{zx} + C_{66}e_{xy}, \quad (6)$$

Let the axis  $oz$  be the axis of the cylinder. Then we require the stress distribution due to terminal couples about  $oz$ .

Considerations of symmetry indicate that

$$\widehat{x}x = \widehat{y}y = \widehat{x}y = 0.$$

The equations of equilibrium then reduce to

$$\frac{\partial \widehat{z}x}{\partial z} = \frac{\partial \widehat{y}z}{\partial z} = 0, \quad . \quad . \quad . \quad . \quad . \quad (7)$$

$$\frac{\partial \widehat{x}z}{\partial x} + \frac{\partial \widehat{y}z}{\partial y} + \frac{\partial \widehat{z}z}{\partial z} = 0; \quad . \quad . \quad . \quad . \quad . \quad (8)$$

while in the case of a circular cylinder, the condition that the cylindrical surface shall be free from stress becomes

$$\widehat{z}x \cdot x + \widehat{y}z \cdot y = 0. \quad . \quad . \quad . \quad . \quad . \quad (9)$$

We shall assume that the displacements are homogeneous

functions of the 2nd degree in  $x, y, z$ . Then, since there must be no resultant force on a cross-section, and no resultant couple about any axis perpendicular to that of the cylinder,  $\widehat{z}z$  must vanish, and therefore the whole distribution of stress and strain will be independent of  $z$ .

With these conditions we can write the displacements  $(u, v, w)$  in their most general form :

$$\left. \begin{aligned} u &= A_1x^2 + B_1y^2 + G_1z^2 + 2D_1yz & + 2F_1xy, \\ v &= A_2x^2 + B_2y^2 + G_2z^2 & - 2D_1zx + 2F_2xy, \\ w &= A_3x^2 + B_3y^2 & - 2G_2yz + 2G_1zx - 2F_3xy. \end{aligned} \right\} \quad (10)$$

The strain components are then

$$\left. \begin{aligned} e_{xx} &= 2A_1x + 2F_1y, \\ e_{yy} &= 2B_2y + 2F_2x, \\ e_{zz} &= -2G_1x - 2G_2y, \\ e_{yz} &= -2(D_1 - F_3)x + 2B_3y, \\ e_{zx} &= 2A_3x + 2(D_1 + F_3)y, \\ e_{xy} &= 2(A_2 + F_1)x + 2(B_1 + F_2)y. \end{aligned} \right\} \quad \cdot \quad \cdot \quad \cdot \quad (11)$$

Substituting these values in equations (1), (2), (3), and (6), and putting

$$\widehat{xx} = \widehat{yy} = \widehat{zz} = \widehat{xy} = 0,$$

we have four equations of the type :

$$\begin{aligned} 2C_{11}(A_1x + F_1y) + 2C_{12}(B_2y + F_2x) - 2C_{13}(G_1x + G_2y) \\ - 2C_{14}\{(D_1 - F_3)x - B_3y\} + 2C_{15}\{A_3x + (D_1 + F_3)y\} \\ + 2C_{16}\{(A_2 + F_1)x + (B_1 + F_2)y\} = 0, \quad \cdot \quad \cdot \quad \cdot \quad (12) \end{aligned}$$

Also, from the boundary condition (9),

$$\begin{aligned} x[2C_{15}(A_1x + F_1y) + 2C_{25}(B_2y + F_2x) - 2C_{35}(G_1x + G_2y) \\ - 2C_{45}\{(D_1 - F_3)x - B_3y\} + 2C_{55}\{A_3x + (D_1 + F_3)y\} \\ + 2C_{56}\{(A_2 + F_1)x + (B_1 + F_2)y\}] + y[2C_{16}(A_1x + F_1y) \\ + 2C_{26}(B_2y + F_2x) - 2C_{36}(G_1x + G_2y) - 2C_{46}\{(D_1 - F_3)x - B_3y\} \\ + 2C_{56}\{A_3x + (D_1 + F_3)y\} + 2C_{66}\{(A_2 + F_1)x + (B_1 + F_2)y\}] \\ = 0. \quad \cdot \quad \cdot \quad \cdot \quad (13) \end{aligned}$$

Equations (12) and (13) must hold for all values of  $x$  and  $y$ . If, then, we equate separately to zero the coefficients of  $x$  and  $y$  in equations (12) and the coefficients

of  $x^2$ ,  $y^2$ , and  $xy$  in (13), we shall have eleven equations between the twelve coefficients  $A_1, A_2, \dots$ , etc.\*

After appropriate rearrangement of these equations, their solution can at once be written down as

$$\begin{aligned} \frac{A_1}{\Delta_{14}} &= -\frac{F_2}{\Delta_{24}} = -\frac{G_1}{\Delta_{34}} = -\frac{A_3}{\Delta_{45}} = -\frac{(A_2 + F_1)}{\Delta_{46}} = -\frac{F_1}{\Delta_{15}} \\ &= -\frac{B_2}{\Delta_{25}} = -\frac{G_2}{\Delta_{35}} = -\frac{B_3}{\Delta_{45}} = -\frac{(B + F_2)}{\Delta_{56}} \\ &= \frac{2F_3}{(\Delta_{55} - \Delta_{44})} = \frac{2D_1}{(\Delta_{55} + \Delta_{44})} = K, \text{ say,} \end{aligned}$$

where  $\Delta_{14}, \Delta_{24}, \dots$ , etc. are the minors of  $C_{14}, C_{24}, \dots$ , etc. in the determinant :

$$\Delta = \begin{vmatrix} C_{11} & C_{12} & C_{13} & C_{14} & C_{15} & C_{16} \\ C_{12} & C_{22} & C_{23} & & & \\ C_{13} & C_{23} & & & & \\ C_{14} & \text{etc.} & & & & \\ C_{15} & & & & & \\ C_{16} & & & & & \end{vmatrix}.$$

We have finally the stress system

$$\begin{aligned} \widehat{xx} &= \widehat{yy} = \widehat{zz} = \widehat{xy} = 0, \\ \widehat{yz} &= Kx[C_{14}\Delta_{14} - C_{24}\Delta_{24} + C_{34}\Delta_{34} - C_{44}\Delta_{44} + C_{45}\Delta_{45} \\ &\quad - C_{46}\Delta_{46}] = K\Delta x, \\ \widehat{zx} &= Ky[C_{15}\Delta_{15} - C_{25}\Delta_{25} + C_{35}\Delta_{35} - C_{45}\Delta_{45} + C_{55}\Delta_{55} \\ &\quad - C_{56}\Delta_{56}] = -K\Delta y, \end{aligned}$$

and it is obvious that this system can be maintained by terminal couples about  $oz$  only.

If we transform to cylindrical polar coordinates and integrate over the cross-section, we have

$$\begin{aligned} \widehat{rr} &= \widehat{\theta\theta} = \widehat{zz} = \widehat{zr} = \widehat{r\theta} = 0, \\ \widehat{\theta z} &= \frac{2T}{\pi a^4} \cdot r, \end{aligned}$$

where  $T$  is the applied torque and  $a$  is the radius of the cross-section.

\* A similar substitution in the Equation of Equilibrium (8) gives rise to an equation which is the sum of two of those obtained above.

This, of course, is the stress-distribution assumed in E.F. 169. If the cross-section of the cylinder is an ellipse of semi-axes  $a$  and  $b$ , the only change necessary is in the boundary condition (9), which becomes

$$\widehat{zx} \cdot b^2x + \widehat{yz} \cdot a^2y = 0,$$

with a corresponding change in (13). The solution of the equations for  $A_1, B_1$ , etc., then becomes

$$\begin{aligned} \frac{A_1}{b^2\Delta_{14}} &= -\frac{F_2}{b^2\Delta_{24}} = \text{etc.} = \frac{F_1}{a^2\Delta_{15}} = -\frac{B_2}{a^2\Delta_{25}} \\ &= \text{etc.} = \frac{2F_3}{(a^2\Delta_{55} - b^2\Delta_{44})} \\ &= \frac{2D_1}{(a^2\Delta_{55} + b^2\Delta_{44})}; \end{aligned}$$

giving finally

$$\widehat{xx} = \widehat{yy} = \widehat{zz} = \widehat{xy} = 0,$$

$$\widehat{yz} = \frac{2T}{\pi a^3 b} \cdot x,$$

$$\widehat{zx} = -\frac{2T}{\pi ab^3} y,$$

where  $T$  is the torque, as before.

It will be seen from the form of the displacements that the distribution of shear stress gives rise to a bending of the cylinder in a plane containing the axis, in addition to a twist about the axis involving a buckling of the cross-section. When comparatively large distortion tends to occur, as is no doubt the case in the early stages of a single crystal test in the Stromeyer machine, the ordinary means of gripping the ends of the specimen will impose a considerable secondary stress system. This may account for the confused "settling down" slipbands which have always been recorded in such tests.



LVIII. *Molecular Association and Mechanism of Separation into Two Phases.* By G. N. ANTONOFF, D.Sc. (Manch.)\*.

*Introduction.*

**I**N my previous papers I tried to disregard as much as possible all that has been written about association of liquids, in order to work out a theory without having any preconceived ideas on the subject.

However, in my paper of July 1925 I made some concessions to the conventional views by force of habit. Thus, on pp. 287 and 288 I made suggestions that the process of association may take place in two different ways, according as to whether the liquids are normal or associated.

Since then I had the opportunity of investigating the matter more fully in the light of my own theory, and I came to the conclusion that all liquids behave in a similar manner, and that if there are sometimes certain individual differences, there is no justification for dividing them into "normal" and "associated," because they undergo changes according to the same laws in all cases. All liquids are alike in the sense that their properties vary with temperature in a discontinuous manner. As stated in my paper (Phil. Mag., July 1925), the discontinuity can be noticed:—

- (1) By direct observation, although the effect is sometimes very small.
- (2) By plotting  $\delta$  against temperatures ( $\delta = \delta_l - \delta_v$ , where  $\delta_l$  is density of liquid and  $\delta_v$  that of vapour), whereby the effect is magnified.
- (3) By plotting latent heats of vaporization, calculated on a basis of density measurements by the formula of J. E. Mills. Thereby the effect is magnified still more.
- (4) By plotting  $\frac{\delta_l + \delta_v}{2}$  against temperatures. By so doing the curve between two kinks becomes in most cases rectilinear, and the so-called rectilinear diameter is a zigzag line.

These effects are small as a rule, and are smaller in some cases than in others. In some cases they only just exceed the limits of experimental errors, and in some cases may be even within. But in any case this character appears quite systematically. It is therefore important

\* Communicated by the Author.

to consider whether this effect is not due to some impurities present or formed as a result of temperature changes, or whether it is not due to some systematical error in the experiments.

In this sense a great interest is presented by the publications of Leiden Laboratories, on the rectilinear diameter of various elementary substances, such as hydrogen, nitrogen, argon, helium, neon, etc. The absolute purity and stability of substances and the accuracy of experimental methods are beyond all doubts. The authors, E. Mathias, C. A. Crommelin, and H. Kamerlingh Onnes noticed an irregularity in the diameter of hydrogen, but they infer that it may be due to some systematic error.

In comm. No. 172 on helium they say:—"The deviations, which are all smaller than  $\frac{1}{2}$  per cent., are somewhat larger than possible experimental errors; moreover, the systematic character of the deviations cannot be denied. In comm. No. 162, p. 16 . . . in the case of neon they (the deviations) show an absolutely systematic character." In the case of nitrogen these deviations having systematic character amount to nearly 2 per cent. (comm. No. 145, p. 24); and they are quite distinct and systematic in the case of argon (comm. No. 131). *In these communications the zigzag character of the rectilinear diameter is quite obvious.* The experimental data, however, do not contain enough figures to establish the exact position and number of kinks.

In figures of Young these phenomena show also quite systematic character. As his figures contain often 5-6 figures between two kinks, their position can be often determined without difficulty.

If I add that similar kinks can be observed in systems liquid-liquid and much more distinctly (personally I observed them in the system aniline-amylene), it appears highly improbable that such a phenomenon can appear always and invariably as a result of experimental errors.

I therefore believe that in this case I deal with a law of nature general for all substances, and intimately connected with the liquid state.

I will try to show that the so-called normal and associated liquids are both subject to the above law.

Before substantiating the above statement in the light of my theory, I want to say a few words about the literature of the subject.

*Literary Data.*

The subject dealing with association of liquids is not very advanced. In most cases one cannot see even any attempt at treating it rationally, and most of the authors were content with finding purely empirical rules which were said to hold true for a small number of liquids and not for others. The rules laid down by different authors, in most cases, do not agree with one another, and thus liquids described by one author as normal are often regarded as abnormal by others. The literature on the subject is fairly extensive, but it can be found summarized up to 1915 in the monograph by W. E. S. Turner—'Molecular Association'—whereby a lot of time and trouble can be saved.

The state of the subject up to 1915 is made very clear on pp. 87-88. There the above-mentioned author shows how much the usually-accepted views were influenced by van der Waals's formula. Owing to it some authors held the view that the liquid on condensation must have the same molecular weight as in the gaseous state, in the case of normal liquids. A number of empirical rules seemed to corroborate the above view. Thus Ramsay and Shields assumed that the temperature coefficient of molecular surface energy throws some light on the molecular state of liquids (Trans. Chem. Soc. lxiii. p. 1089, 1893; Phil. Trans. 184 A, p. 647, 1893).

Some other authors (Kistiakowsky \*, Walden †, Dutoit and Moijou ‡) assumed that the ratio between the specific cohesion and latent heat of vaporization is a constant for normal liquids.

Apart from the purely empirical rules as above, there is a distinct tendency in more recent years to recognize the change in the molecular state on condensation. Van der Waals himself began to doubt in his more recent work whether the molecular weight of normal liquid is that of gas. Amongst authors definitely believing in formation of complex molecules in liquids, Garver §, Drucker ||, and Schames ¶ should be mentioned in the first place. Drucker assumes that all liquids contain complex molecules, but he believes that the so-called "normal" liquids are little affected by temperature changes compared with associated.

\* *Zeit. electrochemie*, xii. p. 513 (1906).

† *Zeit. phys. Chem.* lxv. p. 129 (1909).

‡ *Journ. Chem. Phys.* vii. p. 169 (1909).

§ *Journ. Phys. Chem.* xvi. (1912); xvii. (1913).

|| *Zeit. phys. Chem.* lxxviii. (1908); lxxvi. (1911).

¶ *Ann. Phys.* xxxviii. (1912).

However, the above theories have not received general recognition, and according to W. E. S. Turner have only reached the suggestion stage. He concludes Chapter VII. by saying:—"In view of the great influence which van der Waals's equation and its applications have had and still have on our conception of condensation and allied phenomena, it is certain that the newer views mentioned will receive the closest scrutiny before being accepted. Undoubtedly before any real advance can be made in our knowledge of the liquid state, we must have first a clear conception of the phenomenon of condensation, particularly in regard to any molecular change that occurs. To accumulate empirical methods of testing liquids is fruitless."

#### *Method of Treating the Problem.*

I very often myself used such expressions as normal liquids, or associated, simply because it is customary to do so, and I did it without really understanding the reason for such classification.

As indicated above, some authors were inclined to see a connexion between surface tension and molecular state in the liquid state. I myself never could understand their reasoning, and do not understand it now. It is partly for this reason that I began to work out a theory of surface tension some years ago. I wanted to see whether one could arrive at a simple relation between surface tension and molecular state, on theoretical grounds.

My theory, published in Phil. Mag. 1918, shows that such relation can, indeed, be derived, but unfortunately it involves a number of indefinite factors which cannot be determined in the present state of our knowledge. Thus the expression for surface tension, deduced under the assumption that molecules behave like doublets (electric, magnetic, or both) small compared with the intermolecular distance, was shown to be as follows:—

$$\alpha = Kl^2 \frac{(\delta_1)^{5/3}}{M}, \quad . \quad . \quad . \quad . \quad (1)$$

where  $\alpha$  is surface tension,

$K$  a constant,

$l$  the length of a doublet,

$\delta_1$  the density of liquid, and

$M$  the molecular weight in the liquid state,

$M$  being  $= mx$ , where  $m$  is the lowest molecular weight known and  $x$  is the association factor.

In this expression the power  $5/3$  is not certain, because the law of molecular attraction may be different from what it was assumed to be. The constant  $K$  is unknown, and there is no way of determining  $l$ .

Thus, although the formula indicates the relation between surface tension and molecular weight, it is of no practical use as such in the present state of knowledge.

However, it was shown in my previous papers that all these indefinite factors can be eliminated under special conditions.

In this sense the law of difference (Phil. Mag., May 1926, p. 1138) renders invaluable service. First of all, the uncertainty with regard to the law of molecular attraction is eliminated. It was shown in my paper (Phil. Mag. xxxviii. p. 417, 1919), that the same result is obtained under any law of molecular attraction. Both  $K$  and  $l$  are also eliminated, and in special conditions (corresponding to a state of equilibrium between two coexisting phases) we get the relation

$$\frac{\delta_l}{mx} = \frac{\delta_v}{my}, \quad . . . . . (2)$$

where  $\delta_l$  is density of liquid,

$\delta_v$  is that of vapour,

$m$  the molecular weight lowest known,

$x$  = association factor of liquid, and

$y$  = association factor of vapour.

In some cases the association factor of vapour may be assumed to be  $=1$ . Then the above formula gives all the necessary data for  $x$ , the association factor of liquids, at all temperatures.

By plotting

$$x = \frac{\delta_l}{\delta_v} \quad . . . . . (3)$$

against  $\delta_l$ , or  $\delta$  ( $\delta = \delta_l - \delta_v$ ), or against  $L$  (latent heat of vaporization), one can find the values of  $x$  corresponding to the kinks in the above properties. The kinks in the  $\delta_l$  curve correspond well to the kinks in the  $\delta$  and  $L$  curves. In my paper of July 1925 I preferred, however, to deal with  $\delta$  curves, because, as explained on pp. 280 and 281, their kinks are more easily perceptible to the eye. Another reason why I preferred them is that the quantity  $\delta$  is generally used in calculating the surface tension in the capillary method. Finding the accurate position of the kinks is not easy, but it can be done, all the same, with a certain amount of patience.

In my paper of July 1925 I expressed the view, in the



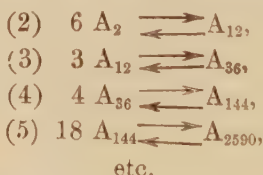
form of a suggestion, that the association may take place in two different ways, viz. :



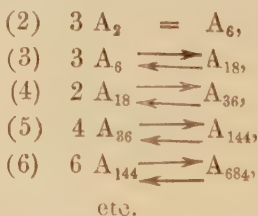
This was nothing else but a concession to the conventional views.

Now, on the basis of the considerations just outlined, I can show that the process of association consists of a number of definite stages. To illustrate the above I shall choose ethyl acetate, which is believed to be a normal liquid, and propyl alcohol; the latter is an example of an "associated" liquid containing OH. For the lower alcohols I found a difference in figures by different authors; this is apparently due to the fact that it is very difficult to dry them, and they very easily attract moisture again. Their general behaviour, however, is just the same.

Thus for propyl alcohol I find the following stages, leaving out for the moment the change immediately following after the critical point; the figures in brackets indicate the number of the change from the critical point :



And for ethyl acetate :



Comparing the two schemes, one can see only one difference—viz. in the case of propyl alcohol there is one change with a comparatively high numerical coefficient 18. I have no reason to suspect that this is due to a mistake in experimental data. Assuming this, I can only say that it is a peculiarity due probably to the size and shape of the molecules in question. But the general character is substantially the same in both cases.

Thus I see no justification whatever for the conventional

view, according to which OH-containing substances are regarded as abnormal.

The above schemes were outlined under the assumption that vapour is mono-molecular. I believe this is a reasonable assumption on the whole, but I cannot help recognizing *special conditions in the critical region*.

In my paper of July 1925 it was mentioned that in changes immediately following the critical point the equation  $Ae^{\lambda\delta} = T + B$  becomes simplified—viz. constants A and B must be the same. This is a necessary condition in order to bring  $\delta$  to zero, when the critical point is reached. The simplified form of the equation is

$$Ae^{\lambda\delta} = T + A. \quad . \quad . \quad . \quad . \quad . \quad (4)$$

The evidence suggests that in this case the nature of the change is also somewhat different.

The latter equation holds true within about 3° C. from the critical point, as a rule \*. It is just within these limits that the *meniscus at the interface between two phases remains flat*. This and similar facts led me to the conclusion (see my paper, Journ. Chem. Phys. (Genève), v. p. 364, 1907) that the separation into two phases in the critical region takes place *without expenditure of energy*. It was stated there that the surface tension in the critical region (*i. e.* also a few degrees above the critical point) must be independent on concentration. This, according to the formula (1) on p. 574 of the present paper, must mean the formation of complex molecules above critical point.

The molecules thus formed apparently are  $A_{2y}$ . Just above the critical point about one-third of the molecules must combine with another one-third. Thus the number of complex molecules must be equal to the remaining number of simple ones. Above the critical point these molecules are distributed at random. When the critical point is reached, the complex molecules suffer a diminution of kinetic energy, so that they begin to settle down and replace the simple molecules, driving them away into the upper layer. The nature of the process is such (see formula (4)) that the separation takes place very rapidly with small changes of temperature, and we can observe just below the critical point the formation of two phases of *equal volume*. Both phases must contain an equal number of molecules in accordance with the law of difference. The complex molecules must have the same length of doublet, and therefore their

\* It suggests that the accurate position of the critical point may be thereby determined.

concentration in one layer may take place without an appreciable expenditure of energy.

The above-mentioned process of separation must take place *without involving any molecular changes*, and comes to an end about 2-3 degrees below the critical point. Just there the existing experimental data indicate the presence of a kink. The critical region has not been investigated fully, and

owing to the nature of the relationship  $\left(\frac{d\delta}{dT} = \infty\right)$  the experimenting in this region is extremely difficult. All the same, the calculations in my paper of July 1925 make me believe that the kink in  $\delta$  curves nearest the critical point corresponds to the value of  $x=2y$ . At this point if  $y=1$  the liquid must be bi-molecular.

Starting from this point, the molecules of liquid must begin to associate with one another and form new kinds of molecules with a higher molecular weight.

In the case of ethyl acetate, the second change ends when  $x=6$ . It thus appears that the second change is  $3 A_2 \rightleftharpoons A_6$ . It should be pointed out that the experimental data, such as they exist now, do not always indicate the accurate position of kinks to exclude the possibility of alternative schemes, especially at high temperatures. Thus some individual changes may have to be modified when more accurate experimental data are available. There is some doubt as to the actual number of the above changes at higher temperatures, but mistakes of this kind do not affect further results, and what is important,  $x$  can be always calculated with accuracy.

The second change of propyl alcohol, according to my estimate, must be



When molecules associate with one another their number decreases. Similarly, in the gaseous phase the molecules associate with the decrease of temperature, leave the gaseous phase, and increase the volume of the liquid, if their density exceeds that of the saturated vapour at that temperature, so as to maintain equilibrium in accordance with the law of difference.

It should be pointed out that my present view is not quite identical with the one I accepted in my paper of July 1925 on pp. 267-268. It was a matter of convenience to deal with  $\delta$  and not  $\delta_1$  and  $\delta_r$ , because it made the kinks more apparent to the eye.

The equations for  $\delta$ , however, require a somewhat different

interpretation. From equation (2) it follows that

$$\frac{x-y}{y} = \frac{\delta_1 - \delta_v}{\delta_v} = \frac{\delta}{\delta_v},$$

i. e.

$$\frac{x}{y} - 1 = \frac{\delta}{\delta_v},$$

or, assuming,  $y=1$ ,

$$x-1 = \frac{\delta}{\delta_v}.$$

Thus, if the expression

$$\delta_1 = x \delta_v$$

enables us to calculate  $x$  (the association factor), the expression

$$\delta = (x-1) \delta_v$$

gives the value of it diminished by 1.

Similar molecular changes can be shown to take place in systems liquid-liquid. In fact, all those molecular changes which take place in a tube filled with individual substance are precisely reproduced in systems liquid-liquid. The substantial difference is that in the latter case the space is filled with a dissolvent, in which the reactions take place. In systems liquid-gas the dissolvent is absent. This explains also another difference between the two systems. It is well known that in systems liquid-gas, unstable conditions, such as over-saturation of vapours, are often observed. These phenomena, however, are not known in systems liquid-liquid. The over-saturated conditions can be done away with by introducing a drop of liquid into the system, or by some other catalytic agency. In systems liquid-liquid the liquid is always present, and therefore the unstable conditions never occur.

I have examined more fully the system water-phenol. The figures used were those by Rothmund, taken from Landoldt-Börnstein Tables. The difference of concentrations ( $c=c_1-c_2$ ) of both layers plotted against temperatures from the critical point in degrees C. was shown in the diagram on p. 1129.

The kinks in this curve, beginning from the critical point, correspond, as far as one can see, to the values of the ratio  $\frac{c_1}{c}$

$$2, \quad 4, \quad 8.$$

In this case this ratio is a measure of  $\frac{x}{y}$ , and not the ratio

between the densities, because the latter quantities may undergo expansions or contractions due to the influence of the dissolvent.

### Conclusion.

The above relations are based on theory, outlined in a number of papers recently published.

My method is entirely different from the ones used by previous authors.

The conclusions arrived at also differ from the usually-accepted views. The difference is more of the quantitative character. Thus Aston and Ramsay (Trans. Chem. Soc. lxvi. p. 167, 1894) long ago expressed the view that the low vapour pressure must be a sign of association taking place in the liquid. Such conclusion seems to be quite in agreement with common sense. Only, most of the authors assume that the associated molecules consist of a few simple molecules only, and that the degree of association remains very nearly the same at different temperatures; whereas, according to my theory, *the association factor varies with temperature*, and may reach such values as 10,000 at low temperatures. Assuming that the number of simple molecules in 1 c.c. of liquid is of the order  $10^{21}$ , the number of associated molecules as above would be  $10^{17}$ .

As material for my work I used chiefly the figures from the experimental work of Sydney Young. I cannot say anything definite about water; I can only say that its behaviour at about  $4^{\circ}\text{C}$ . is the only example of an abnormal behaviour I have come across so far. All liquids in the paper of the above author behave in exactly the same way whether they contain OH or not, and I therefore came to the conclusion that *all liquids are normal*. It goes without saying that throughout my work I regarded the van der Waals's formula as invalid. The discontinuous character of temperature changes and the peculiar characteristic of critical region below and above the critical point convinced me that *the change of state is intimately connected with the change of molecular aggregation*.

6 Featherstone Buildings,  
High Holborn.  
London, W.C. 1.



LIX. *The Formation of Pendant Drops.*By L. I. A. MICHELI, *Ph.D.*\*

IN some recent work on the adsorption of vapours at a liquid-gas interface the author has had occasion to employ the "drop-weight" method for the determination of surface-tension, and has thus been led to a consideration of pendant drops in general.

The problems associated with the formation of pendant drops have attracted considerable attention during the last fifty years. Two main lines of attack have been followed. First, the symmetry of drops in a condition of equilibrium has been discussed, and, secondly, attempts have been made to obtain a relationship between the weights of drops which fall and the capillary constants of the liquids.

*The Symmetry of Drops.*

One of the earliest discussions of the shape which drops hanging, in equilibrium, from a tube will assume is found in a book by Dupré ('*Théorie Mécanique de la Chaleur*,' p. 329). Dupré shows that it is impossible for a given liquid to form drops of the same shape hanging from tubes of different diameters.

Worthington (*Proc. Roy. Soc.* xxxii. p. 365, 1881) follows Dupré's method of discussion, and shows that if two drops of different liquids, hanging from two tubes of radius  $r_1$  and  $r_2$  respectively, be similar in shape, then

$$\frac{r_1}{r_2} = \sqrt{\frac{\sigma_1 \rho_2}{\sigma_2 \rho_1}}, \quad \dots \dots \dots (1)$$

where  $\sigma_1 \sigma_2$  are the respective surface-tensions and  $\rho_1$  and  $\rho_2$  the respective densities. Worthington takes the case where the part of the surface of the drop which meets the tube is plane and vertical. It will subsequently be seen that this condition is seldom satisfied, even when the angle of contact between the liquid and the tube is zero.

Other discussions of interest are those of Bashford and Adams in '*An Attempt to test the Theory of Capillarity*' (*Camb. Univ. Press*, 1883), Guye and Perrot (*Arch. des Sc. Phys.* xi. p. 225, 1901), and L. Perrot (*Jour. Chim. Phys.* xv. p. 164, 1917).

*The Weights of Detaching Drops.*

The first attempt to find a relation between the weight of a falling drop and the surface-tension of a liquid is due to

\* Communicated by Prof. F. G. Donnan, F.R.S.

Tate (Phil. Mag. xxvii. p. 176, 1864). We may state Tate's results by the equation

$$W = Kr\sigma, \quad . . . . . (2)$$

where  $W$  is the weight of the drop;  $K$  is a constant.

Rayleigh (Phil. Mag. xlviii. p. 321, 1899) repeated Tate's work and found that equation (2) is not strictly true; as a rough approximation, he found that he could summarize his results for water drops by the equation

$$W = 3.8r.$$

Lohnstein (*Ann. der Phys.* xx. p. 237, 1906; xxi. pp. 1030 *t seq.*) has developed a theory of drop detachment, which it is impossible here to discuss in detail. Assuming that the angle of contact of the liquid with the tube just before and just after detachment is the same, he has arrived at the equation

$$W = 2\pi r\sigma f\left(\frac{r}{a}\right), \quad . . . . . (3)$$

where  $a^2$  is the capillary constant of the liquid.

Harkins (*Journ. Am. Chem. Soc.* xxxviii. p. 227, 1916; xli. p. 449, 1919; xlii. p. 2534, 1920) has investigated equation (3) experimentally, and has found that it is only an approximation. He has set out to find an empirical relationship between the weight of a detaching drop and the quantity  $2\pi r\sigma$ , which he has called an "ideal drop." His method is roughly as follows:—The surface-tensions of water, benzene, ethylene dibromide, and carbon tetrachloride were determined by the capillary-rise method. The weights of the drops of these liquids which detach from tubes of different size are determined, and hence the ratio of  $W$  to  $2\pi r\sigma$  can be obtained for the several liquids for different values of  $r$ . Harkins finds that when  $2\pi r\sigma/W$  is plotted against  $V^{1/3}/r$  (where  $V$  is the volume of the detached drop) the four curves obtained are coincident: that is, in the case of the liquids investigated the quantity  $V^{1/3}/r$  uniquely determines the value of  $2\pi r\sigma/W$ . If, now, a liquid of unknown surface-tension be taken,  $V^{1/3}/r$  can be determined experimentally, and hence from the original curve  $2\pi r\sigma/W$ , an expression in which all the quantities except  $\sigma$  are known, can be obtained.

Much adverse criticism has been directed against Harkins's work. His method is, however, perfectly sound. The term "ideal" drop for the quantity  $2\pi r\sigma$  appears to have caused most of the trouble. The particular name given to this

quantity appears to the author to be a matter of minor importance. It certainly supplies a useful quantity with which to compare the actual weight of the detached drop. The only point which appears to the author open to discussion is the extension of the use of the curve to other liquids, though this extension will be probably justified unless the viscosity of the liquids is high.

Iredale (Phil. Mag. xlv. p. 1088, 1923) assumes that  $V^{\frac{1}{3}}/r$  (or, as he has actually stated,  $r'/r$ , where  $r'$  is the radius of the detached drop considered as a sphere) determines completely the shape of a drop, and hence assumes that the Worthington equation can be applied to any two drops for which  $V^{\frac{1}{3}}/r$  has the same value. The procedure seems somewhat arbitrary, especially as the assumptions involved in the Worthington equation require careful consideration. It can, however, be shown from Harkins's experimental results that the Worthington equation holds for drops of the type considered by Iredale.

Let us consider two drops of two different liquids (using the suffixes <sub>1</sub> and <sub>2</sub> to distinguish the two cases) such that

$$\frac{r_1}{V_1^{\frac{1}{3}}} = \frac{r_2}{V_2^{\frac{1}{3}}}, \quad \left( \frac{r_1}{r_1'} = \frac{r_2}{r_2'} \right). \quad \dots \quad (4)$$

From Harkins's curves it will be seen that in this case

$$\frac{2\pi r_1 \sigma_1}{W_1} = \frac{2\pi r_2 \sigma_2}{W_2}; \quad \dots \quad (5)$$

from (5)

$$\frac{r_1 \sigma_1}{V_1 \rho_1} = \frac{r_2 \sigma_2}{V_2 \rho_2}, \quad \dots \quad (6)$$

from (4) and (6)

$$\frac{V_1}{V_2} = \frac{r_1 \sigma_1 \rho_2}{r_2 \sigma_2 \rho_1} = \left( \frac{r_1}{r_2} \right)^3.$$

$$\therefore \left( \frac{r_1}{r_2} \right)^2 = \frac{\sigma_1 \rho_2}{\sigma_2 \rho_1}. \quad \dots \quad (7)$$

It is thus seen that the application of equation (7) to two drops for which  $V^{\frac{1}{3}}/r$  is the same, has Harkins's experimental work as a basis; so that its use in the following manner seems justified.

From the data of Harkins and Brown for the weights of drops of water which fall from different radii a curve is drawn plotting  $r_1$  as ordinates, and ratio  $r_1/r_1'$  as abscissæ. (Here the suffix <sub>1</sub> distinguishes water.) To determine the surface-tension of a second liquid, the ratio  $r_2/r_2'$  is obtained

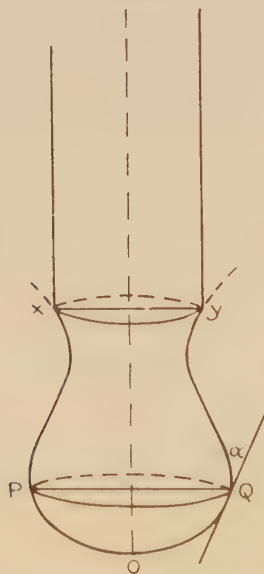
in a particular case ; then from the reference curve for water the value of  $r_1$  is found such that  $\frac{r_1}{r_1'} = \frac{r_2}{r_2'}$ . Substitution can now be made in equation (7).

There is little to choose between this method and that of Harkins. The fact, however, that the relation between  $r$  and  $r'/r$  is almost linear is a point in favour of Iredale's method.

### *The Equilibrium of Pendant Drops.*

The "correct" expression for the maximum weight of a pendant drop of liquid has given rise to so much discussion that it seems desirable to consider what is involved in this problem.

Fig. 1.



Let XOY (fig. 1) represent a section through the axis of symmetry of a drop hanging in equilibrium from a tube of radius  $r$ . Let PQ be any plane section of the drop perpendicular to the axis of symmetry. Let  $\alpha$  be the angle between the surface of the drop and PQ,  $a$  the area of PQ, and  $c$  the perimeter.

Let us consider the equilibrium of the mass POQ resolving

in vertical direction and taking the downward direction as positive; the forces acting are:—

- (1)  $+Mg$  (weight);
- (2)  $-c \cos \alpha \sigma$  (due to surface-tension);
- (3)  $-aP$  (the resultant upward force due to a uniform external hydrostatic pressure  $P$ );
- (4)  $+aP'$  (where  $P'$  is the pressure exerted from above on the plane  $PQ$ ).

For equilibrium we have:

$$Mg - c \cos \alpha \cdot \sigma - aP + aP' = 0. \quad . \quad . \quad (8)$$

From hydrostatic principles we have:

$$*P' = P + \sigma \left( \frac{1}{R_1} + \frac{1}{R_2} \right), \quad . \quad . \quad . \quad (9)$$

where  $R_1$  and  $R_2$  are a pair of principal radii of curvature at the point  $P$ .

Equation (8) becomes

$$Mg - c \cos \alpha \sigma + a\sigma \left( \frac{1}{R_1} + \frac{1}{R_2} \right) = 0. \quad . \quad . \quad (10)$$

Let us now consider a drop enlarged in stages by allowing successive amounts of the liquid to enter the drop. If the plane  $PQ$  be fixed, the mass of  $POQ$  will increase; yet it will be seen from equation (10) that equilibrium may still be possible.

For the plane  $XY$ , equation (10) will become (using  $M$  and  $R$  to apply now to part  $X$ )

$$Mg = 2\pi r \sigma \cos \alpha - \pi r^2 \sigma \left( \frac{1}{R_1} + \frac{1}{R_2} \right). \quad . \quad . \quad (11)$$

Here  $\alpha$  becomes the angle of contact between the liquid and the tube. In equation (11) there are two variables  $Mg$  and  $\left( \frac{1}{R_1} + \frac{1}{R_2} \right)$ . The maximum value of  $Mg$  will be determined by the minimum value of  $\left( \frac{1}{R_1} + \frac{1}{R_2} \right)$  subject to the stability of the whole drop.

If the angle of contact  $\alpha$  be zero,  $\cos \alpha = 1$ , and one of the principal radii of curvature becomes  $r$  the radius of the tube; so that equation (11) becomes

$$Mg = \pi r \sigma - \pi r^2 \sigma \left( \frac{1}{R_2} \right). \quad . \quad . \quad . \quad (12)$$

\* From equation (9) it can be seen that when  $P$  is low for certain values of  $R_1$  and  $R_2$ ,  $P'$  becomes negative: that is, the tensile strength of the liquid is brought into play.



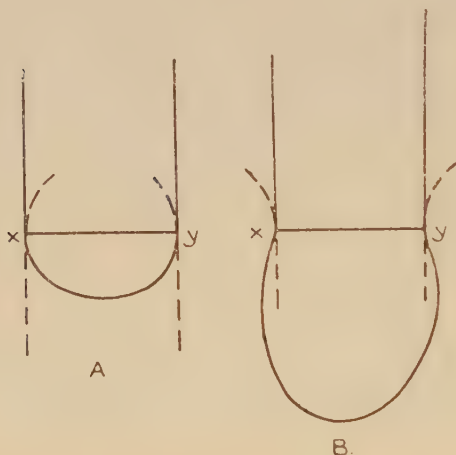
Fig. 2 represents two drops of different size of a liquid which wets the tube, both of which are in a state of equilibrium. In fig. 2 (A)  $R_2$  is positive, so that

$$Mg < \pi r \sigma.$$

In fig. 2 (B)  $R_2$  has become negative, so that

$$Mg > \pi r \sigma.$$

Fig. 2.



Under most experimental conditions the weight of the drop which detaches, which is only part of the pendant mass, is greater than  $\pi r \sigma$ . For certain of Harkins's drops the weight is as high as  $1.74 (\pi r \sigma)$ : that is, the drop must become concave outwards at X before detachment takes place.

In this brief survey the author has attempted to draw attention to some of the main features of drop formation, and to methods which may be used to correlate the "drop weight" with surface-tension.

The Sir William Ramsay Laboratories of  
Physical and Inorganic Chemistry,  
University College, London.

LX. *The Conductivity of Clouds dispersed from an Arc.*—II.  
By H. P. WALMSLEY, M.Sc.\*

*Introduction and Summary.*

IN a previous paper † it has been shown that the type of ionization currents obtained from the cloud of particles produced from an arc between cadmium electrodes depends upon the mass of material dispersed. For sparse clouds a curve is obtained which approximates to that which is given by ions disappearing according to the ordinary law of recombination, but, as the concentration of the cloud increases, a rise appears in the ionization curve, usually within the first half hour, and produces a marked minimum. With increasing concentration, the minimum approaches the origin of time and becomes less marked. These are illustrated in fig. 1, which shows the ionization currents from positive charges, taken under approximately the same experimental conditions for three different clouds. In each case the rate of flow of cloud through the ionization chamber was the same, and the field was such that the saturation current was obtained for all ions of mobility greater than  $1.0 \times 10^{-4}$  cm./sec./volt./cm. The mass of material dispersed was least for curve I. and greatest for curve III. With still further increasing mass, the minimum may disappear altogether, so that the ionization curve begins to rise almost as soon as measurements can be taken.

The curves in fig. 1 represent the saturation currents from the clouds, provided no ions are present of mobility lower than  $1 \times 10^{-4}$ . As it has been shown previously that both the average mobility of the ions and the mobility of the slowest ions diminish as the cloud ages, there is no certainty that ions of less mobility are totally absent throughout the life of the cloud. It is believed, however, that the currents measured were approximately saturation currents. The point is not easy to establish practically, for it is found with ionization currents from clouds that a change in field strength produces transient effects which take some time to disappear. An increase in field strength is usually followed by a temporary rise in the current and a decrease by a temporary fall—effects which seem due to alterations in the distribution of the ions in motion within the electric field.

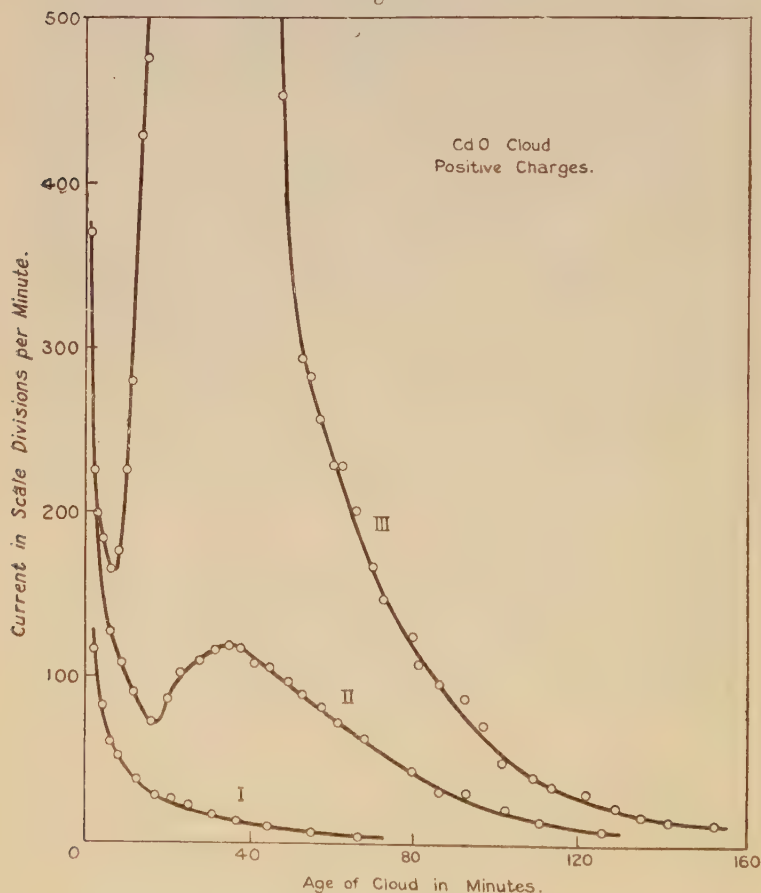
The initial fall in current strength has already been attributed mainly to recombination. In the present paper

\* Communicated by Prof. W. L. Bragg.

† Walmsley, *Phil. Mag.* (7) i. p. 1266 (1926).

it is shown that the subsequent rise is due either to the production of new charges within the cloud as it ages, or to an increase in the mobility of existing ions. In either case it follows that during the process of coalescence the cloud particles form unstable aggregates which subsequently

Fig. 1.



disrupt and give rise to the observed effect. As a result of the disruptive process the particulate number curve does not decrease indefinitely as the cloud ages, but flattens and tends to approach an equilibrium value.

If it be granted that the increase in current strength occurring at some time after the dispersal process is completed arises from the same cause in all cases, increasing

the mass of material dispersed merely augments the effect. It can be shown that in most cases mobility changes are insufficient to account for the magnitude of the whole effect. Thus there must be a production of ions as the cloud ages under the conditions of the experiments. This result is independent of whether the currents measured are saturation currents or not, for the initial currents may be considerably less than the maximum current subsequently attained. If this were due to mobility changes only, the average mobility initially would have to be lower than that when the maximum current was attained. Apart from being improbable, this would be contrary to the fact previously established that the current during a rise is carried mainly by (the larger) ions in the cloud.

The intensity of the ionization due to the disruption of unstable aggregates in the cloud and the total number of complex particles are assumed to change with age in a similar way. The intensity is thus zero initially. It rises to a maximum and afterwards diminishes as the cloud ages. The cloud is ionized on formation. The total ionization at any subsequent time is thus the resultant of two factors. The effect of the former relative to the latter increases as the number of particles per unit volume increases. When this is small the ionization current disappears mainly by recombination according to the ordinary law; but as the number of particles increases, the ionization curve develops a maximum which may grow until the ionization current actually appears to increase in magnitude immediately after dispersion has taken place.

The ionization current due to the disruptive process is oscillatory. Lines drawn through the actual observations in the curves of fig. 1 will be found to oscillate about those drawn in the sketch. The effect is more prominently drawn in fig. 1 of the previous paper. This seems to indicate that the unstable aggregates form groups which disrupt in succession as the cloud ages.

#### *The Distribution of the Initial Charges on the Particles.*

The demonstration in the previous paper that there is a production of charges in the cloud as it ages, rests on the assumption that the ions enter the electric field with the gas stream. The assumption was introduced to avoid having to consider effects due to possible changes in the mobilities of the ions. It is natural to inquire whether the assumption is necessary from this standpoint. The discussion would be

simplified if we knew the initial distribution and number of the charges in the cloud and the number and mode of formation of the particles. As this information is lacking, perhaps we can obtain some evidence bearing on the subject from other data. Experiments on the evaporation of liquids from charged insulated vessels have shown that the molecules of vapour which leave the surface are uncharged \*. Further, from experiments on water vapour it is known that the condensation of supersaturated vapours can occur in the absence of charged nuclei †. Hence it appears possible to obtain a cloud of particles initially uncharged by the condensation of a supersaturated vapour, even though the substance dispersed is volatilized from an electrically-charged vessel. If we consider the production of clouds in these experiments as analogous, the function of the arc would be merely to produce a sufficiently high temperature to volatilize the metal, which presumably oxidizes immediately to form a supersaturated vapour. The condensation of this vapour in the cold-air stream forced by the fan between the electrodes of the arc would produce uncharged primary particles. The oxidation of the metallic vapour is unlikely of itself to give rise to charged molecules and thereby charged particles on condensation. In general, chemical action does not give rise to ionization. If it did, it would be at once indicated by an increase in conductivity. The oxidation of nitric oxide ‡ and the oxidation of ether vapour, both of which occur at low temperatures, have little or no effect on the conductivity, so no ionization is produced by these reactions. The case is different, however, if the oxidation is sufficiently vigorous to produce a high temperature as in the combustion of hydrogen and oxygen in the oxyhydrogen flame. Here considerable ionization occurs, but it is attributed to the high temperatures produced by the reaction and not to the reaction itself. The electrical charges which are found initially on the primary particles of the clouds produced by the electric arc may therefore be considered as adventitious to the formation of the particles. They originate from the thermoelectrical effects inseparable from the working of an arc.

This view is supported to some extent by the experiments of Tyndall and Grindley § on the ionization from a heated

\* Pellat, *C. R.* cxxviii. p. 169 (1899).

† Wilson, *Phil. Trans. A*, clxxxix. p. 265 (1897); *A*, excii. p. 403 (1899). Lenard, *Sitz. d. Heidelburger Akad.* no. 29 (1914).

‡ Bloch, *Ann. d. Chemie et de Physique*, xxii. pp. 370, 441; xxiii. p. 28.

§ Tyndall & Grindley, *Phil. Mag.* xlvii. p. 689 (1924).



platinum wire. In this case they have shown that electrons, positive charges (probably charged atoms), and neutral particles in large numbers are independently produced, although combination occurs afterwards between the charges and the particles.

Consider only clouds in which the initial number of particles per unit volume is considerably greater than the number of charges. Collisions will occur between the charges and the particles, and after an exceedingly short time the charges will be distributed over the surfaces of the particles. Since the particles greatly outnumber the charges, it is clear that the chance of finding particles carrying multiple charges initially is very small. Hence we may assume that the cloud contains  $n_1$  particles carrying unit positive charges,  $n_2$  particles on which there are unit negative charges, and  $n_3$  neutral particles,  $n_3$  being considerably greater than  $n_1 + n_2$ . It is desirable to show that the subsequent production of particles carrying multiple charges is not very probable.

If the effects of the electrical forces between the particles were neglected, the collision frequencies between the various categories would be proportional to the products of their concentrations. The electrical forces modify the frequencies. In the case of a collision between a positively-charged particle and a neutral one, the induction effect will facilitate the occurrence of a collision, although its actual magnitude is small compared with the effect of the charges in a collision between particles carrying unlike charges. For simplicity we will neglect the increased frequency caused by the induction effect. The ratio of the collision frequencies between positively-charged and negatively-charged particles, positively-charged and neutral particles, positively-charged particles alone and between the neutral particles may be written

$$\kappa n_1 n_2 : n_1 n_3 : n_1^2 / \kappa_1 : n_3^2,$$

where  $\kappa_1$  is never less than unity. The actual values of  $\kappa$  and  $\kappa_1$  depend upon the size of the particles. For ions produced in dry air by X-rays,  $\kappa$  is of the order of  $10^4$ , but with increasing size of particles its magnitude diminishes\*, the minimum value being of course unity. Assuming that the particles always unite on collision, the ratio of the number of singly-charged positive particles to the number of particles carrying a double charge after one collision is  $\kappa_1 n_3 / n_1$ , and since  $n_3 > n_1$ , the probability of a collision

\* Townsend, 'Electricity in Gases,' p. 215 (Oxford, 1915).

producing a doubly-charged complex particle is always less than the probability of producing a singly-charged one, and it diminishes with diminishing size of the primary particles.

Similarly, the ratio of the number of collisions which result in the production of an uncharged system, or possibly an electrical doublet, to the number of those forming a singly-charged system, is  $\kappa n_2/n_3$ , which can only become less than unity when  $\kappa$  is small, *i. e.* when the primary particles are relatively large. It therefore appears that if the size of the cloud particles is such that the electric forces exert an appreciable influence on the collision frequency, the original charges tend to disappear mainly by recombination. A small number of the charged particles unite with neutral particles, and this number is always greater than the number which unite to form doubly-charged particles. The same process must continue subsequently, so that even in the unfavourable case of  $n_1 \neq n_2$  the probability of finding multiple charges on particles is always less than the probability of finding singly-charged particles.

The conditions necessary to make the number of particles carrying multiple charges due to coalescence relatively small are therefore :—

1. The initial number of uncharged particles should be great compared with the number of charged particles.
2. The number of positively-charged particles should equal the number of negatively-charged particles.
3. The electric forces due to the charges should exert an appreciable influence on the collision frequency.

To determine whether the first two conditions hold with the types of cloud described in this paper would require special experiments. A direct count of the number of charged and uncharged particles, using an ultramicroscope, would give some information concerning the first condition. The second can only be satisfactorily settled by measuring the total charge per unit volume of the cloud. Alternately, a duplicated apparatus might be employed measuring the current due to positive charges on one stream and that due to negative charges on the other. The currents, however, are so weak that the steady deflexion method of measuring currents is not accurate, and the alternative method of measuring the rate of charging-up of the needle requires two observers, on account of the rapid initial fall in current strength. The experimental evidence which is available on these points, although not conclusive, indicates that both conditions are approximately satisfied for the clouds under

discussion. The third condition must be satisfied for the ions which contribute to the currents actually measured. The electric force at the surface of a sphere of radius  $a$ , carrying a unit electronic charge, is equal to  $e/a^2$ . The value of this force for certain values of  $a$  is tabulated below, with the mobility of the particle calculated from the Stokes-Cunningham formula.

Radius $a$ .		Field at surface.	Mobility.
10 $\mu$ .....	$10^{-6}$ cm.	$1.4 \times 10^5$ volts/cm.	$4 \times 10^{-3}$ cm./sec./volt/cm.
100 $\mu$ .....	$10^{-5}$ "	$1.4 \times 10^3$ "	$7 \times 10^{-5}$ " "
1 $\mu$ .....	$10^{-4}$ "	1.4 "	$5 \times 10^{-6}$ " "

If the particles are so large that their electric fields are negligible, it appears that their mobilities will be so small that they will pass uninfluenced through the fields employed in the ionization chamber in these experiments. It seems, therefore, legitimate to neglect the consideration of the presence of multiple charges on the particles in these clouds. Even if such particles do result from coalescence, the effects of the charge would facilitate recombination later with an oppositely-charged particle, so that their average life as such would be probably short.

#### *Mobility Changes due to Coalescence and Disruption.*

With particles carrying only single electronic charges, it is quite easy to follow the effects of coalescence upon the mobilities of the particles. If two oppositely-charged particles coalesce, we obtain either a charged doublet or an uncharged neutral particle. In the latter case the mobility in an electric field vanishes altogether, and although with the doublet there is still a residual field, the mobility is zero in a uniform electric field and very small in a radial field of force. Where coalescence occurs between a neutral and a charged particle, we have an increase in mass, which in general will cause an increase in the resistance of the medium to the motion of the new particle, and thereby reduce its mobility. Thus in all cases of coalescence the mass of the resulting complex is increased and its mobility decreased.

If subdivision of a complex occurs, the reverse processes take place. We may have uncharged particles separating with the production of new charges. There is the possibility of the separation of a doublet into two new particles carrying

opposite charges. If neither effect occur, then the subdivision of a complex carrying a single charge will produce a charged particle with reduced mass and increased mobility. Thus subdivision of a complex will result in the production of particles of less mass, which, if charged, will show increased mobility. In addition, doublets, if present, may separate into particles carrying single charges, and there remains the possibility that uncharged complexes may give rise to new ionization on disruption.

Changes in the mobilities of the ions affect the currents obtained from our apparatus. The rearrangement of the ions in motion in the electric field resulting from such changes causes a temporary additional current to be received by the electrode if their mobilities increase, and a corresponding temporary drop if their mobilities decrease. Hence, if an ionization current rises, we must be obtaining either new particles with increased mobilities, or we must have a production of new charges. If the ionization current decreases, either the rate of production of charges is decreasing or coalescence is taking place, producing either neutral systems or particles with decreased mobility.

The ionization current from the clouds is oscillatory. Hence there must be either a successive production of new charges or of particles showing increased mobilities throughout the life-history of the clouds. In the early part of the curve of fig. 3 of the previous paper, the total loss of charge due to coalescence preponderates over the effects due to disruption and (or) the production of charges, but after the minimum the reverse occurs. For this cloud, it is easy to show that change of mobility caused by disruption is not sufficient to account for the magnitude of the effect which occurs after the minimum. For simplicity we will assume that a parallel plate ionization chamber is employed and that in all cases the saturation current is obtained. The current due to a class of ions of given mobility is  $\rho Qe$ , where  $\rho$  is their volume density,  $e$  their charge, and  $Q$  the flux through the ionization chamber. If  $\rho_0$  be their initial density in the cloud, the ionization current when the time  $t=0$  is  $i_0 = \Sigma \rho_0 Qe$ . The number of ions which are in motion in the electric field after the steady state is attained is  $\Sigma \frac{1}{2} \rho Q T$ , where  $T$  is the time required for the ion to cross the electric field. Since we are measuring the saturation current,  $T$  cannot be greater than  $\tau$ , the mean time taken by an uncharged particle moving with the gas stream to pass through the ionization chamber. It may be considerably less. The maximum possible change in the number of ions



in the field is  $\Sigma \frac{1}{2} \rho Q T$ . Hence, if  $i$  be the current resulting from this change,

$$\int i dt = \Sigma \frac{1}{2} \rho Q e T,$$

which is less than  $\Sigma \frac{1}{2} \rho Q e \tau$ . Even in the most favourable case, where none of the original charges disappears altogether by the production of uncharged systems,

$$\int i dt \gtrless \frac{1}{2} \tau \Sigma \rho_0 Q e,$$

$$i. e. \quad \int i dt \gtrless \frac{1}{2} \tau i_0.$$

The integral is the area between the rise curve and the axis of time, and this cannot be greater than the area of a rectangle of height  $i_0$  and base  $\frac{1}{2} \tau$ . To make the two areas equal for this cloud, it would be necessary for  $\tau$  to have a value of the order of a few hours, whereas its actual value during the experiment was about 20 seconds. It is evident, therefore, that the majority of the ions giving rise to the increase in current after the minimum are new ones. As the experimental value of 20 seconds for  $\tau$  gives a much overestimated value for the effect of the disruption of particles carrying single charges prior to disruption and to the effect, if any, due to the separation of doublets, it is clear that we may neglect the effects of change of mobility as a possible explanation of the origin of the oscillatory current. Hence all our previous deductions on the assumption that the ions enter the electric field are now independent of that assumption. It has been replaced by the assumption that the ions are produced within the cloud. They may enter the field with the gas stream, or be produced in that portion of the cloud which is in motion in the ionization chamber.

### *Origin of the Ions produced after Dispersal.*

It has been shown previously that the new ions are associated with the larger particles in the cloud. Further, since the ionization currents are oscillatory, groups of ions are produced successively. The two facts seem to indicate their origin. There are no external ionizing sources acting on the cloud, so the charged particles must be produced by a direct process from the uncharged. The new ions are clearly not caused by chemical action occurring at this stage in the cloud, for ionization does not usually accompany chemical action, particularly at low temperatures. Moreover, from the conditions of the experiment there are no obvious chemical actions which can occur, and if they did



occur, there seems no reason why the larger particles should be affected and not the smaller: in fact, the reverse would be expected. The ionization being associated mainly with the larger particles rules out the possibility that it is due to a frictional effect between the medium and the particles, as in Rudge's\* experiments, and this is confirmed by the fact that the negative and positive ionization currents are similar, showing that both negatively- and positively-charged particles are produced. If, further, we were to assume that all collisions do not result in coalescence and that non-coalescing particles may acquire charges by collision, one would expect the ionization to be associated with the smaller particles and not the larger, since their Brownian motion is more violent. This is contrary to fact.

From dynamical considerations, the production of charges within a cloud must be ascribed to disruption of some kind, since it is necessary to perform work to separate the charges, and it is in consequence a forced and not a spontaneous process. Further, since the new ions are large ones, it follows, on the assumption that they arise in the cloud, that each must consist of a charged particle or complex of particles which has dissociated or disrupted from a larger complex. The production of ions shows, therefore, that the complex particles produced by the coagulation of the primary particles are not all stable. Some of them subsequently break up, and in doing so give rise to charged particles. Since the current due to these is oscillatory, the unstable complex particles form groups which break up in succession. Without further experiments it is not obvious whether the unstable particles break up throughout the cloud or only when they come under the influence of an electric field. For the purposes of this paper this is immaterial. Actually, the results of unpublished experiments which have been carried out on the intensity of the light scattered from the Tyndall beam in clouds produced by the arc from cadmium electrodes, indicate that the complexes break up in the absence of an electric field.

*Effects due to the Instability of Certain Complex Particles.*

The formation of ions by the disruption of unstable complex particles in the cloud leads to a simple qualitative explanation of all the ionization curves which have been obtained. From dynamical considerations, coagulation of the particles in the cloud must be the dominating process,

\* Rudge, Phil. Mag. xxiii. p. 852 (1912); xxv. p. 481 (1913).

as is shown by the gradual decrease in the mobilities of the slowest moving ions. The primary particles disappear by uniting with one another to produce complex particles, and these in turn disappear by coagulation with one another, although some are unstable and ultimately break up. The problem of determining the number of complex particles present in the cloud at a given time bears some resemblance to that of determining the amount of radioactive substance B which is present at a given time when it is produced by the disintegration of a primary substance A, the latter only being present initially. The solutions will be analogous, so that in general the number of complexes, initially zero, will increase with time to a maximum and subsequently diminish. Smoluchowski \* has solved the problem mathematically on the assumption that coagulation is due to collisions produced by the Brownian motion of the particles and that it is an irreversible process. If every collision is effective in producing coalescence, and the cloud contains initially  $n_0$  homogeneous primary particles, the number of particles at any subsequent time  $t$  is given by

$$\Sigma n = \frac{n_0}{1 + \alpha n_0 t},$$

where  $\alpha$  is a constant. The number of primary particles left is

$$n_1 = \frac{n_0}{(1 + \alpha n_0 t)^2}.$$

Hence the number of complexes, *i. e.* particles resulting from the coagulation of two, three, etc. primary particles, is the difference  $\alpha n_0 t / (1 + \alpha n_0 t)$  between these quantities. The number of complex particles is zero when  $t=0$ ; it increases to a maximum at  $t=1/2\alpha n_0$ , and then decreases, becoming very small for large values of  $t$ . This formula cannot give the number of complexes in the clouds described, for disruption of unstable complexes occurs during the process of coagulation. It, however, gives a curve of the shape to be expected on general grounds.

The current due to the ions from the unstable complex particles depends upon their number and the charges on the dismembered particles. If the number of electronic charges produced when a given complex breaks up is independent of the time at which disruption occurs, the ionization curve resulting from the disruption of complexes in the cloud will have zero value when  $t=0$ , will rise to a maximum and afterwards slowly fall as the cloud ages. The

\* Smolucnowski, *Zeit. Physikal. Chem.* xcii. p. 129 (1918).

rise curve of fig. 1 (II.) is due to the slowly-moving ions\* (complex particles) and is of this shape.

The ionization curves obtained from clouds of cadmium-oxide particles may therefore be considered to consist of two parts. The first is due to the effect of recombination of the charges initially present on the formation of the cloud, and the second is due to ions formed by the disintegration of unstable complexes formed during the process of coagulation. The initial charged particles disappear by recombination and by combination with uncharged particles which form less mobile ions. For the positive current the ratio of the number recombining to the number losing mobility is  $\kappa n_2 : n_3$ , using the previous notation. Hence for a given initial ionization the current disappears more slowly as the initial concentration of particles in the cloud increases and as their age increases (decrease in  $\kappa$ ). The production of ions due to disruption increases with the number of complex particles, and therefore with increasing initial concentration. Thus, if we have a cloud containing relatively few particles, we obtain an ionization curve which very nearly obeys the ordinary law of recombination. With increasing density the ionization current falls more slowly and, with the increase in magnitude of the current due to disruption, the type of curve of fig. 1 (II.) develops, producing a minimum. With a still greater initial volume density of particles the minimum begins to disappear and move nearer to the origin until it finally disappears, giving a curve showing an initial rise.

Qualitatively, at least, this agrees with experiment. If we wish to increase the effect due to the complexes, we must increase their number. This can be done by increasing the time of sparking with the arc: probably without much alteration in their average size, since the fan replaces the vapour-laden air surrounding the poles of the arc by air comparatively free from particles, provided the time of sparking is not too long. At the same time the electrification produced by the arc probably increases too. On the other hand, if we keep the time of sparking constant and alter the distance between the pole-pieces, the arc changes from the "silent" arc to the "hissing arc," and there results a great increase in the mass of the material dispersed. In this case the average size of the particles probably increases also, but perhaps without a corresponding increase in the electrification. In practice a combination of the two methods has to be employed, since the electrodes must be pulled apart to strike the arc. With care a series of clouds can be obtained in which there is a gradual increase in the initial concen-

\* Walmsley, *Phil. Mag.* (7) i. p. 1266 (1926).

tration of the primary particles, and it is found that the series show the changes in type for the currents which have been described above.

The presence of unstable particles in the clouds will prevent coagulation proceeding indefinitely. Their disruption increases the number of particles per unit volume, so that when the loss of number by coagulation has diminished until it is equal to the gain from disruption, the number of particles will become stationary. The curve showing the variation in the number of particles per unit volume with the age of the cloud—the particulate number curve—will, of course, be rapidly oscillatory like the ionization curve. If, however, we consider only the mean smoothed curve, coagulation will cause an initial rapid fall, but later the disruption of the unstable particles must tend to flatten out the curve until the stationary value is reached.

This is the general shape of the number curves recorded by Whytlaw Gray\*. They are described as falling into three periods:—(a) an unstable period in which the decrease in number with time is very rapid; (b) a stable period, reached only after five hours or longer, in which the change is very slow (it often lasts for 24 hours or longer in a chamber of one cubic metre capacity); and (c), an intermediate period where the fall in number is the resultant of the factors operative in (a) and (b). Obviously the second period (b) is at least partially accounted for by disruption. The slow change in number is not altogether due to aggregation ceasing in the cloud as the paper suggests, but must in part result from an equilibrium between the rate of coagulation and the rate at which particles are produced from unstable aggregates.

Since the number of particles in the cloud tends to assume an equilibrium value, the particles will not obey the Boyle-van't Hoff law. Let  $n$  be the number of particles in unit volume of a cloud at any time  $t$ ,  $-\frac{\partial n}{\partial t}$  be the rate at which they disappear by coalescence, and  $\frac{\partial \nu}{\partial t}$  be the rate at which new particles are formed by disruption. Then

$$\frac{dn}{dt} = \frac{\partial \nu}{\partial t} - \frac{\partial n}{\partial t}.$$

If  $n_x$  be the number of complex particles per unit volume each of which contains  $x$  primary particles, and  $n_y$  the corresponding quantity for complexes containing  $y$  particles, the rate of coalescence between these classes is  $\zeta n_x n_y$ , where

\* Whytlaw Gray, Proc. Roy. Soc. A, cii. p. 600 (1923).

$\zeta$  is an appropriate coefficient. Thus we may write

$$\frac{\partial n}{\partial t} = \sum \zeta n_x n_y,$$

the summation extending over every possible combination. If we take a given volume of cloud at time  $t$  and suddenly expand it until it occupies  $p$  volumes of the medium, the rates will change. The values immediately after expansion become

$$\frac{\partial n'}{\partial t} = \sum \zeta \frac{n_x}{p} \cdot \frac{n_y}{p} = \frac{1}{p^2} \frac{\partial n}{\partial t},$$

and since  $\nu$  depends only upon the number of unstable complex particles at expansion

$$\frac{\partial \nu'}{\partial t} = \frac{1}{p} \frac{\partial \nu}{\partial t}.$$

Thus

$$\frac{dn'}{dt} = \frac{1}{p} \left( \frac{\partial \nu}{\partial t} - \frac{1}{p} \frac{\partial n}{\partial t} \right).$$

If  $n$  were at the equilibrium value prior to expansion

$$\frac{\partial \nu}{\partial t} - \frac{\partial n}{\partial t} = 0,$$

so  $\frac{dn'}{dt}$  immediately after expansion is positive or negative,

according as  $p$  is greater or less than unity. Thus, if we dilute a cloud, we shall obtain a new equilibrium value of  $n'$  greater than would be expected from the Boyle-van't Hoff law, and if we concentrate it, the new equilibrium value will be less.

This restricts the methods available for the enumeration of particles in clouds of this type. Thus the classical method of Aitken \*, which depends upon dilution, and to a less extent that of Owens †, where a pressure gradient is introduced into the cloud to make the particles impinge on the glass slide on which they are counted, cannot be used. Apart from probable effects of the water vapour present in these methods upon the degree of dispersion of the clouds, the results obtained from them will require correction by what is as yet an undetermined factor.

My thanks are due to Professor W. L. Bragg, F.R.S., for the interest he has taken in the preparation of this paper.

The Physical Laboratories,  
The University, Manchester.

\* Aitken, Trans. Roy. Soc. Edin. xxxv. p. 1 (1888).

† Owens, Proc. Roy. Soc. A, ci. p. 18 (1922).



LXI. *The Molecular Scattering of Light in a Binary Liquid Mixture.* By Dr. KULESH CHANDRA KAR, D.Sc.\*

A.

IN a paper published in the Philosophical Magazine for Jan. 1923, Drs. Raman and Ramanathan have made an attempt to improve Einstein's equation for molecular scattering of light in a binary liquid mixture by a method essentially the same as that of Einstein †. More recently Gans ‡ and the present writer § have arrived at Einstein's expression for scattering by different methods.

The immediate object of the present paper is to show that the additional improvement-term obtained by Raman and Ramanathan is wrong, and that the corrected term is vanishingly small, so that Einstein's equation holds quite good.

In Section B a brief account is given of Einstein's derivation of his own formula ; and in order to make the mistake quite clear, we shall derive the complete equation in Section C, following Drs. Raman and Ramanathan's somewhat cumbrous thermodynamical method.

B.

In deducing the equation of scattering in a mixture, the first thing to be done is to obtain an expression for the work done in bringing about a small change of concentration.

According to Einstein, this work is

$$d\psi = \frac{dk}{M_2} \cdot RT \cdot \log \frac{p_2}{p_{2.0}}, \quad . \quad . \quad . \quad (1)$$

where  $M_2$  is the molecular weight of the second component and  $p_2$ ,  $p_{2.0}$  are its vapour-pressures at concentrations  $k$  and  $k_0$ .

We may note that in deriving the above equation Einstein has made the following simplifying assumptions: (1) That the liquid is incompressible ; (2) that the specific volume of the liquid is negligible compared with the specific volume of its vapour ; and (3) that the saturated vapour obeys the ideal gas equation  $pr=RT$ . If, however, we disregard the first assumption and take the mixture to be compressible, then it is easily seen that along with the concentration

\* Communicated by the Author.

† Einstein, *Ann. d. Phys.* xxxix. 1908.

‡ Gans, *Zs. f. Phys.* xvii. p. 371.

§ Kar, *Phys. Zeit.* xxiv. 1923, p. 429.

fluctuation there will be going on also fluctuation of density, so that the resultant scattering will be due to the combined effect of the two variations.

Now the total work done in changing the concentration by  $dk$  can be divided into three parts :

$$E_1 = -\frac{dk}{M_2} \cdot p_{2.0} v_{2.0}, \quad . \quad . \quad . \quad . \quad (2)$$

which is the work done in taking out the second component from the larger volume in the state of vapour,  $M_2$  being the molecular weight,

$$E_2 = +\frac{dk}{M_2} \cdot RT \cdot \log \frac{p_2}{p_{2.0}}, \quad . \quad . \quad . \quad . \quad (3)$$

being the work done in compressing the vapour from  $p_{2.0}$  to  $p_2$ , the pressure of saturated vapour of the second component in the smaller volume separated by a semi-permeable membrane from the larger volume, and

$$E_3 = +\frac{dk}{M_2} \cdot p_2 v_2, \quad . \quad . \quad . \quad . \quad (4)$$

being the work done in forcing the vapour into the smaller volume.

It can be easily seen that the sum of all these works is equal to the work  $d\psi$  given by Einstein's equation (1).

### C.

Raman and Ramanathan have considered a small volume in equilibrium with a large volume, both being initially at the same concentration, and they have calculated the work done in bringing both the liquids from the larger to the smaller volume. This being superfluous so far as the concentration variation is concerned, we shall simplify their thermodynamical operations by considering only the work done in bringing  $(\Delta m_2 - k\Delta m_1)$  gms. of the second liquid from the larger to the smaller volume. This work can be divided into two parts: the first part is obtained by adding the equations (1) and (2) ,

$$E_1 = -p_{2.0} v_{2.0} (\Delta m_2 - k\Delta m_1) + S_{2.0} (\Delta m_2 - k\Delta m_1) \phi_0, \quad (5)$$

and the second part is, according to them,

$$E_3 = v^{2.0} (\Delta m_2 - k\Delta m_1) (p_{2.0} + \frac{1}{2} \Delta p_{2.0}) - S_{2.0} (\Delta m_2 - k\Delta m_1) (\phi_0 + \frac{1}{2} \Delta \phi_0), \quad . \quad . \quad (6)$$

where  $p_{2.0}$  is the vapour-pressure of the second liquid in the

mixture,  $v_{2.0}$ ,  $S_{2.0}$  its specific volumes in the state of vapour and liquid,  $k \left( = \frac{m_2}{m_1} \right)$  the concentration, and  $\phi_0$  the 'total vapour-pressure' (sic).

The equation (5) represents the work done in taking out in the state of vapour  $(\Delta m_2 - k\Delta m_1)$  gms. of the second liquid from the larger volume, and when  $S_{2.0} = 0$ , it agrees with Einstein's equation (2). But equation (6), giving the work done in forcing this vapour into the smaller volume, is wrong, as it neglects the changes of specific volumes during the process.

Thus the corrected equation is

$$E_3' = (v_{2.0} + \frac{1}{2}\Delta v_{2.0})(\Delta m_2 - k\Delta m_1)(p_{2.0} + \frac{1}{2}\Delta p_{2.0}) \\ - (S_{2.0} + \frac{1}{2}\Delta S_{2.0})(\Delta m_2 - k\Delta m_1)(\phi_0 + \frac{1}{2}\Delta\phi_0). \quad (7)$$

It is evident that this equation corresponds to Einstein's equation (4) when  $S_{2.0} = 0$ . Thus the total work done according to Raman and Ramanathan should be

$$E_1 + E_3' = \frac{1}{2} [\Delta(p_{2.0}v_{2.0}) - \Delta(S_{2.0}\phi_0)] (\Delta m_2 - k\Delta m_1), \quad (8)$$

neglecting second order small quantities.

It is clear from the above discussions that Drs. Raman and Ramanathan have left out of their consideration the work done in compressing the vapour from  $p_{2.0}$  to  $p_{2.0} + \frac{1}{2}\Delta p_{2.0}$ , which is

$$E_2 = \frac{\Delta m_2 - k\Delta m_1}{M_2} \cdot RT \log \frac{p_{2.0} + \frac{1}{2}\Delta p_{2.0}}{p_{2.0}} \\ = \frac{1}{2} \cdot \frac{\Delta m_2 - k\Delta m_1}{M_2} \cdot RT \cdot \frac{\Delta p_{2.0}}{p_{2.0}}. \quad (9)$$

Thus the total work done in bringing  $(\Delta m_2 - k\Delta m_1)$  or  $m_1\Delta k$  grms. of the second component from the larger to the smaller volume is

$$w = \frac{1}{2} m_1 \Delta k \left[ \frac{RT}{M_2} \cdot \frac{\Delta p_{2.0}}{p_{2.0}} + \Delta(p_{2.0}v_{2.0}) - \Delta(S_{2.0}\phi_0) \right]. \quad (10)$$

We shall now consider the following simple case showing that  $\phi_0$  cannot be the total pressure as conceived by Raman and Ramanathan. If we consider a very large volume of, say, water containing a small quantity of alcohol, and force into it 1 gm. of alcohol vapour at the saturation pressure of alcohol in the mixture, then the work done is

$$E = p_2 v_2 - S_2 \phi. \quad (11)$$

The first term in the above equation is finite, while the

second term is infinite,  $S_2$  being infinitely large and  $\phi$  finite. We see, then, that  $\phi$  cannot be the total pressure when the liquids are miscible; in fact, it is the osmotic pressure (P) \*. In the case of immiscible liquids, however,  $\phi$  will be  $p_2$ , the vapour-pressure of the second liquid; so in the first case the equation (11) becomes

$$w_1 = \frac{1}{2} m_1 \Delta k \left[ \frac{RT}{M_2} \cdot \frac{\Delta p_{2.0}}{p_{2.0}} + \Delta(p_{2.0} v_{2.0}) - \Delta(S_{2.0} P_0) \right]. \quad (12)$$

If the vapour and the osmotic pressures are supposed to obey perfect gas laws, (12) becomes

$$w_1' = \frac{1}{2} m_1 \Delta k \cdot \frac{RT}{M_2} \cdot \frac{\Delta p_{2.0}}{p_{2.0}}. \quad . \quad . \quad . \quad (13)$$

In the case of mixtures of immiscible liquids

$$w_2 = \frac{1}{2} m_1 \Delta k \left[ \frac{RT}{M_2} \cdot \frac{\Delta p_{2.0}}{p_{2.0}} + \Delta\{p_{2.0}(v_{2.0} - S_{2.0})\} \right], \quad (14)$$

and it is evident that, neglecting  $S_2$  compared with  $v_2$ , and supposing the ideal gas equation to hold, Eq. (14) reduces to Eq. (13). Thus the additional term is zero both in the case of miscible and immiscible liquid mixtures.

Calcutta,  
July 20, 1926.

LXII. *Mean Free Paths in a Gas whose Molecules are attracting Rigid Elastic Spheres.* By EDWARD CONDON and E. V. VAN AMRINGE †.

THE beautiful results which the founders of the kinetic theory of gases were able to attain by regarding gas molecules simply as rigid elastic spheres have been considerably refined in several directions by theorists who have imagined a gas molecule which exerts a weak attractive force on its fellows. This concept of attracting molecules lies at the basis of van der Waals' pioneer work on the equation of state, and enabled Sutherland to give a theoretical basis to his remarkably accurate equation for the variation of the coefficient of viscosity with the temperature.

In spite of the success of the attracting elastic sphere molecule in explaining gas behaviour, an evaluation of the

\* Nernst, 'Theoretische Chemie,' 1921, p. 150.

† Communicated by Prof. L. B. Loeb, Ph.D.

mean free path of such molecules which proceeds along classical lines does not seem to have been given. In view of the importance of the free path concept in kinetic theory, it was thought worth while to supply this deficiency. The results are presented in this paper.

On the historical side it may be noted that Sutherland \* carried his approximate analysis merely to the point of indicating how the free path should vary with the absolute temperature. Chapman †, in two papers, has approached the problem from the point of view of finding the solution for the law of distribution of velocities in a gas presenting small deviations from the steady state. James ‡ has made certain corrections and extensions in Chapman's work.

1. *Effective Collision Area*.—Let us suppose a gas made up of molecules of diameter  $\sigma$ , the density of which is such that the mean distance apart of the molecules is large compared with their size. Suppose that the molecules interact in collision as do rigid elastic spheres. Let it be further supposed that they attract each other through symmetrical fields of force such that the work required to separate them to infinity when their centres are initially at a distance  $r$  is  $E(r)$ . If  $m$  is the mass of each molecule, then the equations of motion of the second with respect to the first are

$$m\ddot{r} = + \frac{2x}{r} \frac{\partial E}{\partial r}, \quad m\ddot{\theta} = + \frac{2y}{r} \frac{\partial E}{\partial r}. \quad (1)$$

Since the forces are central, these possess an integral of angular momentum. If  $V$  is the relative velocity when the molecules are widely separated, and if  $B$  is the perpendicular from the origin (centre of first molecule) on the initial line of motion of the second, the angular momentum is equal to  $VB$ , i. e.,

$$r^2 \frac{d\theta}{dt} = VB. \quad (2)$$

Similarly the energy integral is

$$\frac{1}{2}mV^2 - \frac{1}{2}mv^2 = -2E(r). \quad (3)$$

Eliminating the time between these integrals we have

$$\frac{1}{2}m \left[ \left( \frac{dr}{dt} \right)^2 + \frac{V^2 B^2}{r^2} \right] = \frac{1}{2}mV^2 + 2E(r). \quad (4)$$

\* Sutherland, Phil. Mag. [5] xxxvi. p. 507 (1893).

† Chapman, Phil. Trans. Roy. Soc. A, ccxvi. p. 326 (1915).

‡ James, Cambr. Phil. Soc. Proc. xx. p. 447 (1920).



We are interested in the distance  $r_0$  of minimum approach between the two molecules. This is the value of  $r$  in the preceding equation, which corresponds to the condition  $dr/dt=0$ . A collision will occur if this value,  $r_0$ , is equal to or less than  $\sigma$ . That is, a collision will occur if  $B$  is less than the critical value of  $B$  given in this equation :

$$B^2 = \sigma^2 \left[ 1 + \frac{2E(\sigma)}{\frac{1}{2}mV^2} \right] \dots \dots \dots (5)$$

This is the result obtained by Sutherland, who obtains his viscosity formula by writing this value of  $B$  for  $\sigma$  in the classical free path formulæ, and observing that  $V^2$  is proportional to the absolute temperature  $T$ .

2. *Maxwell Free Path.*—In this section the expression obtained in the preceding section for the effective collision area of the molecules will be employed for the computation of the mean free path according to Clerk Maxwell. In Maxwell's method the mean free path is defined to be the ratio of the mean speed of the molecules,  $\bar{c}$ , to the mean number of collisions per second,  $Z$ . In this section the correction to Maxwell's mean path which arises from the attractions of the molecules is evaluated. The method follows closely that used by Jeans \* in his treatise on kinetic theory. If  $f(u, v, w)$  be written for the distribution function of velocities,  $\nu$  for the number of molecules in unit volume,  $\theta$  for the angle between the relative velocity and the line of centres when at distance  $B$  apart, then the mean number of collisions in unit time occurring between molecules of speed components  $u, v, w$  and  $u', v', w'$  under the conditions described by Jeans as a collision of class  $\alpha$  is given by his expression (48) :

$$\nu^2 f(u, v, w) f(u', v', w') V B^2 \cos \theta \, du \, dv \, dw \, du' \, dv' \, dw', \quad (6)$$

where  $B^2$  has been written for  $\sigma^2$  to take into account the increased number of collisions arising from the molecular attractions. The evaluation of the total number of collisions per second is effected by integrating over all the variables with appropriate limits.

If in (6) the value of  $B$  given by (5) be substituted, it is evident that the unity term in brackets will contribute exactly the same number of collisions as in the classical elastic sphere theory, and that the correction to this number

\* Jeans, 'The Dynamical Theory of Gases,' 3rd ed. (1921).

is given by study of the second term. Thus the analysis may be carried parallel to that in Jeans's book as far as his expression (52), which gives the total number of collisions per second in which the relative velocity lies between  $V$  and  $V+dV$ . Writing in  $B^2$  for  $\sigma^2$  in this, one has

$$\sqrt{\frac{\pi h^3 m^3}{2}} v^2 \sigma^2 \left[ 1 + \frac{4E}{mV^2} \right] e^{-\frac{1}{2}hmV^2} V^3 dV. \quad (7)$$

The total number of collisions per second is obtained on integrating this expression from  $\theta$  to  $\infty$ . The definite integrals involved are well known, and the result is

$$v^2 \sigma^2 \sqrt{\frac{2\pi}{hm}} (1 + 2hE) \quad (8)$$

as the corrected mean number of collisions per second experienced by each molecule. If  $R$  is the gas-constant for a single molecule, we have the well-known relation  $RT = \frac{1}{2}h$ , so that finally the modified form of the mean free path according to Maxwell becomes

$$l = \frac{1}{\sqrt{2}\pi v \sigma^2 \left( 1 + \frac{E}{RT} \right)},$$

in which  $E$  stands for  $E(\sigma)$  and represents the work required to separate from contact two molecules to an infinite distance.

Letting  $z = E/RT$ , this can be written

$$l = \frac{1}{\pi v \sigma^2} \cdot H(z), \text{ where } H(z) = \frac{1}{\sqrt{2}(1+z)}. \quad (9)$$

3. *Collision Frequency for Molecules of Specified Speed.*—As was first pointed out by Tait, the mean collision frequency of the molecules in an assemblage whose speeds are distributed according to Maxwell's law depends on the speed of the particular group of molecules under consideration. Tait\* showed that, as a result, there is a mean free path proper to molecules of each speed, and then computed a mean free path which was the mean of those peculiar to a given speed, weighted according to the Maxwell distribution law for the speeds.

In this section the computation of the correction to this branch of the theory arising from the attractions of the molecules is undertaken. Here again, for brevity, the presentation may be conveniently made to parallel that of

\* Tait, Edin. Trans. xxx. p. 74 (1886).

the classical work given in Jeans's book. His treatment is contained in Sect. 341 of the third edition. His notation is somewhat encumbered by the fact that it is for the case of a mixture of various kinds of molecules. The reader will find no difficulty in extending a simple treatment for a single kind of molecule to this gas, and so the more concise notation will be used here.

Jeans's expression (706) is applicable to our needs if we write in  $B^2$  in place of  $S_{12}^2$ . The transformation yielding his (707) is also directly applicable, so that we have

$$2\nu B^2 \sqrt{\pi h^3 m^3} e^{-hmc'^2} \frac{c'}{c} dc' V^2 dV \dots (10)$$

for the number of collisions experienced by molecules of speed  $c$  with molecules of speeds between  $c'$  and  $c' + dc'$ , when the relative velocity is contained between the limits  $V$  and  $V + dV$ .

Now, as before, substitution of the expression for  $B$  given in (5) will contribute a term to which the classical treatment is applicable, and a correction term. The total number of collisions per second experienced by a molecule of speed  $c$  is obtained by integrating  $V$  from the difference of the speeds to the sum of the speeds, and then integrating  $c'$  from 0 to  $\infty$ . Let  $Z$  be the mean number of collisions on the uncorrected theory and  $\Delta Z$  the correction arising from the attractions of the molecules. For  $Z$  we can quote directly the result given by Jeans:

$$Z = \frac{\sqrt{\pi\nu\sigma^2}}{hmc} \psi(c\sqrt{hm}), \dots (11)$$

in which  $\psi(x)$  is the following function of its argument:

$$\psi(x) = xe^{-x^2} + (2x^2 + 1) \int_0^x e^{-y^2} dy. \dots (12)$$

Proceeding now to the evaluation of  $\Delta Z$ , we observe that it is given by

$$\Delta Z = \int_0^\infty \int_{c-c'}^{c+c'} 2\nu\sigma^2 \sqrt{\pi h^3 m^3} e^{-hmc'^2} \frac{c'}{c} dc' \cdot \frac{4E}{m} dV. (13)$$

The integration with respect to  $V$  yields a factor

$$\begin{aligned} 2c' & \text{ when } c' < c, \\ 2c & \text{ when } c' > c. \end{aligned}$$

The correction term  $\Delta Z$  is therefore given by

$$\Delta Z = \frac{16\nu\sigma^2 E}{m} \sqrt{\pi h^3 m^3} \left[ \frac{1}{c} \int_0^c e^{-hmc'^2} c'^2 dc' + \int_0^\infty e^{-hmc'^2} c' dc' \right]. (14)$$

The first integral may be made to depend on the probability integral by integration by parts, the second integral may be calculated directly. If these reductions be carried out, the correction term assumes the form

$$\Delta Z = \frac{8\nu\sigma^2 E \sqrt{\pi}}{mc} \int_0^{c\sqrt{hm}} e^{-y^2} dy. \quad (15)$$

The correction arising from the attraction is more clearly exhibited when it is expressed as a fractional amount of the total number of collisions. If this be done we arrive at the following expression for the mean number of collisions per second experienced by those molecules which are travelling with a speed  $c$ :

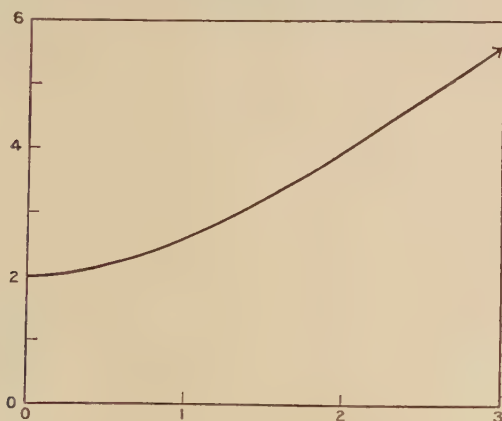
$$Z + \Delta Z = \sqrt{\frac{\pi}{hm}} \nu \sigma^2 \frac{\psi(x)}{x} \left[ 1 + z \frac{2\sqrt{\pi} \text{Erf } x}{\psi(x)} \right], \quad (16)$$

in which  $\text{Erf } (x)$  is the error-function,

$$\text{Erf } x = \frac{2}{\sqrt{\pi}} \int_0^x e^{-y^2} dy,$$

and the argument  $x$  is written for  $c\sqrt{hm}$ .

Fig. 1.— $\frac{\psi(x)}{x}$  plotted as a function of  $x$ .



The manner in which the mean number of collisions per second varies with the speed of the particular molecules under consideration, and the manner in which this is affected by the attractions, are so complicated that a pair of graphs have been made to clarify the situation. In fig. 1 the

uncorrected  $Z$  is plotted against  $x$  on the supposition that  $\sqrt{\frac{\pi}{hm}} v \sigma^2$  is equal to unity. In fig. 2 the coefficient of  $z$  in the correction term has been plotted against  $x$ . Values of the error-function are available in many places, while those of  $\psi(x)$  are from Tait.

Fig. 2.— $\frac{\Delta Z}{Z}$  plotted as a function of  $x$ .

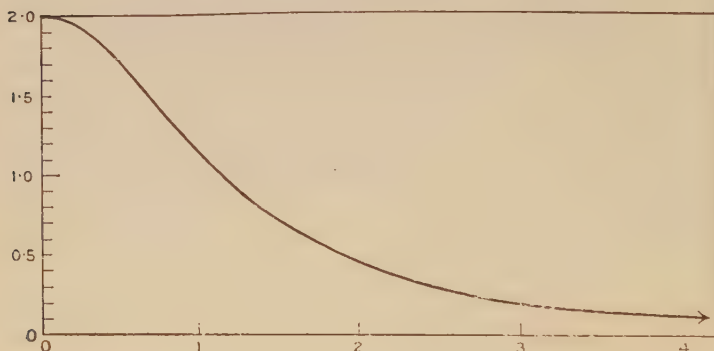
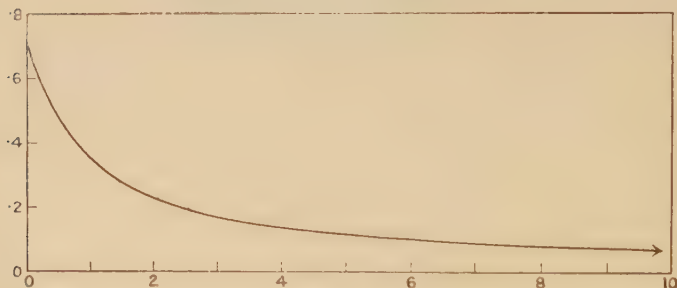


Fig. 3.— $H(z)$  plotted against  $z$ .



4. *The Tait Free Path.*—With the results of the preceding section at hand we are prepared to calculate the modification in the value of the Tait free path which results from molecular attraction. The mean free path of molecules moving with speed  $c$  is simply the ratio of the distance gone in a second,  $c$ , to the mean number of collisions in a second, that is,

$$\lambda_c = \frac{c}{\sqrt{hm}(Z + \Delta Z)} \cdot \cdot \cdot \cdot (17)$$

Tait's free path is obtained by computing the average of  $\lambda_c$  when the various  $\lambda_c$  are weighted according to the number



of molecules whose speeds lie between  $c$  and  $c+dc$ , as given by the Maxwell distribution formula. The corrected Tait free path, therefore, is given by

$$\lambda = \frac{1}{\pi\nu\sigma^2} \int_0^\infty \frac{4x^4 e^{-x^2} dx}{\psi(x) \left(1 + z \frac{2\sqrt{\pi} \operatorname{Erf} x}{\psi(x)}\right)} \dots \quad (18)$$

This expression is comparable with Jeans's equation (78), where attractive forces are not considered. It is evident at once that, while the Maxwell free path was a simple function of the absolute temperature, the manner in which  $\lambda$  varies with the temperature is extremely complicated.

For the convenient discussion of the variation of  $\lambda$  one may write

$$\lambda = \frac{1}{\pi\nu\sigma^2} F(z), \text{ where } F(z) = \int_0^\infty \frac{4x^4 e^{-x^2} dx}{\psi(x) \left[1 + z \frac{2\sqrt{\pi} \operatorname{Erf} x}{\psi(x)}\right]} \quad (19)$$

The exact evaluation of the Tait free path therefore requires a study of the complicated function  $F(z)$ . The evaluation of this function can only be effected by quadratures. This has been done in an approximate way which yields values sufficiently accurate for the needs of kinetic theory.

We have at once that  $F(0)$  is the integral occurring in Tait's work, the value of which is 0.677, and that  $F(\infty) = 0$ . Other values of  $F(z)$  are contained in Table I.

TABLE I.  
Values of  $F(z)$ ,  $G(z)$ , and  $H(z)$ .

$z$ .	$F(z)$ .	$G(z)$ .	$H(z)$ .
0.0	.677	.744	.707
.2	.572	.638	.589
.5	.464	.532	.471
1.0	.354	.418	.353
2.0	.245	.295	.236
3.0	.187	.231	.177
10.0	.0696	.0897	.0643

5. *Transfer Theory of Viscosity*.—Neither the Maxwell nor the Tait free path is the proper one to use in the development of the kinetic theory of the viscosity coefficient by the method of transfer of momentum, as is well known. Again, it is convenient to parallel the treatment of the subject as given by Jeans in order to avoid lengthy repetitions. The discussion of his Sect. 364–369 is applicable here.

What we require for the transfer theory in the case of attracting elastic sphere molecules \* is an exact calculation of the integral (*cf.* Jeans's expression (766))

$$\int_0^{\infty} f(c) \lambda_c c \, dc, \quad . \quad . \quad . \quad . \quad (20)$$

In the case of attracting spheres, the evaluation of this integral requires the use of our equation (17) for the value of the mean free path of a molecule of speed  $x/\sqrt{hm}$ . The viscosity coefficient  $\eta$ , by the transfer theory, is then given by

$$\eta = \frac{1}{3} \rho \bar{c} l, \quad \text{where } l = \frac{2 \sqrt{2\pi}}{\sqrt{2\pi\nu\sigma^2}} \int_0^{\infty} \frac{x^5 e^{-x^2} dx}{\psi(x) \left[ 1 + \frac{E}{RT} \frac{2 \sqrt{\pi} \operatorname{Erf} x}{\psi(x)} \right]}. \quad (21)$$

This, again, is a new kind of mean free path, differing from both the Maxwellian free path and the Tait free path. It is also a very complicated function of the temperature. Inasmuch as it is this latter free path which is appropriate to the theory of viscosity, we see that the Sutherland formula is not a rigorous consequence of the physical assumptions from which it was deduced.

To see how this free path depends on the temperature, one may define the function  $G(z)$  to be that part of the free path which is independent of  $1/\pi\nu\sigma^2$ :

$$\lambda_v = \frac{1}{\pi\nu\sigma^2} G(z),$$

$$\text{where } G(z) = 2 \sqrt{\pi} \int_0^{\infty} \frac{x^5 e^{-x^2} dx}{\psi(x) \left[ 1 + z \frac{2 \sqrt{\pi} \operatorname{Erf} x}{\psi(x)} \right]}. \quad (22)$$

Several values of this function have been computed by quadratures. These are included in Table I. along with  $H(z)$  and  $F(z)$ .

6. *Discussion of Results.*--In fig. 4 are plotted the ratios  $F(z)/H(z)$  and  $G(z)/H(z)$ . If these ratios remained constant, or fairly constant, this would indicate that the functions  $F$  and  $G$  could be fairly well represented by a Sutherland formula of the form

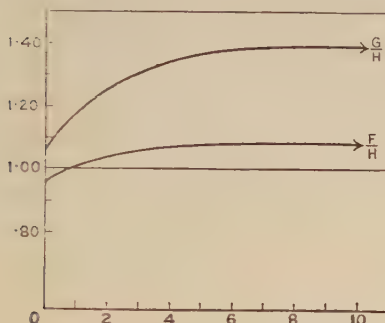
$$F(z) = F(0) \cdot \frac{1}{1+z}; \quad G(z) = G(0) \cdot \frac{1}{1+z}.$$

\* Here, as in Sutherland's theory, we neglect the momentum transfer due to deflexions of paths, without collisions.

However, in the important case of  $G(z)$ , the ratio shows a 35 per cent. variation. One may try to fit a Sutherland form to  $G(z)$ , introducing another constant  $c$ :

$$G(z) = G(0) \cdot \frac{1}{1 + cz} \quad \dots \quad (23)$$

Fig. 4.— $\frac{F}{H}$  and  $\frac{G}{H}$  plotted as functions of  $z$ .



If  $c$  be computed from the values of  $G$ , it is found that  $c$  is not constant, but takes these values:

$z$ .	$c$ .
0.2	0.810
.5	.802
1.0	.774
2.0	.756
3.0	.740
10.0	.728

For rough numerical work this analysis indicates that one may take  $c=0.75$  as representing the correct function over the range of values important in the theory of viscosity. Remembering the definition of  $z$ , this means that the Sutherland constant in the formula for temperature coefficient of viscosity is approximately three-fourths of the ratio of the energy of two molecules at contact to the gas-constant per molecule.

To summarize, one may say:

1. The Maxwell mean free path is accurately represented by a formula of the Sutherland type, in which Sutherland's constant  $C$  is to be interpreted as the ratio of the energy of two molecules in contact to the gas-constant per molecule.

2. The mean free path appropriate to the transfer theory of viscosity is *approximately* represented by a formula of the Sutherland type, in which  $C$  is interpreted as about three-fourths of the above ratio.

The results here given lead to a direct method of evaluating the energy of two molecules in contact by means of the published experimental data on temperature coefficient of viscosity. The results so obtained should be of use in the study of other properties of gases. In closing it is desirable to mention a wide discrepancy between this analysis and that given by James\*, where he concludes that the Sutherland constant  $C$  depends on the form of the law of force, and varies from 0.31 to 0.15 of the ratio of the energy of contact to the gas-constant. James's approach to the problem is an entirely different one, but it is surprising that such a discrepancy should appear. This will require explanation before the results can be used to estimate the energy of the molecules at contact.

University of California,  
Department of Physics,  
September 3, 1925.

---

LXIII. *On Spectral Notation.* By W. M. Hicks, F.R.S.†

**I**N a subject such as that of spectral analysis, with ever growing complexity, the provision of a uniform and suitable notation is a matter of the first importance. Yet the present state is almost chaotic. The following remarks may therefore not be out of place and will it is hoped at least draw attention to the problem. General assent will probably be given to the following conditions for any satisfactory scheme.

1. It should be unambiguous and at the same time clear. Degree of clearness is to be measured by the quickness with which the eye and mind recognize the indication. For instance in dealing with series lines, the mind instantaneously grasps the full meaning of say  $D_{12}(2)$ , whilst it takes a considerable fraction of a second to decipher  $p_1(1)-d_2(2)$ . The time taken measures the mental effort called for.

2. Attention should be paid to difficulties of type-setting.

\* James, Cambr. Phil. Soc. Proc. xx. p. 447 (1920).

† Communicated by the Author.

A notation which may be excellent for writing, may require so much building up of type as to increase by many times the cost of printing. Too little attention is paid to this in general. In any case there must be some compromise between what is best for writing and best for printing. *E. g.* in Landé and Heisenberg's notation for multiplets of higher order, we find  $n$  with subscripts such as  $21a$  and an index 1335 with dashes over the 13 or 35—admirable for writing and reading, but extremely costly for printing. It might for example be written  $n-13(35)-21a$ , admirable for printing but requiring time to decipher. So again in recent papers we find whole pages of capital letters adorned all round with subscripts, dashes, powers, and overlines.

3. Where an original investigator has used a notation to describe his discoveries, or where any notation has been in general use, no change should be made by an individual writer without exceptionally good reason.

4. Notation for new advances should be as far as possible a development of the old.

5. Names and letters should not be chosen to connote the first hypothetical views of writers. For instance, Rydberg gave the names principal, sharp, and diffuse series, writing P, S, D. We now know sharpness and diffuseness are not their necessary distinctions, and that the series corresponding to his principal in other elements than the alkalies are not the most important. Kayser called them principal and associated. The association is real, but his notation was too cumbersome to be generally adopted. Now we use the letters P, S, ... as denoting the series without thinking of the words principal, etc.\*

6. As far as possible details of notation should be easily understood by physicists whose activities lie in other branches of the science.

In the early days of Kayser and Rydberg the only series recognized were the P, S, D, and doublet and triplet series, which latter were only known in separate elements. Later to these were added the F series and certain singlets. Rydberg's notations were generally adopted. Here capital letters indicated lines, small letters the terms, the small letters referring to the current terms in the series. Thus  $P(m) = s-p(m)$ ,  $D(m) = p-d(m)$ , such combinations as  $d-p(m)$  not then being known. With his discovery of complex

\* P, S, D, F may be regarded as standing for prima, seconde, dritte, fourth. The writer must confess to being a worse offender in the above respect in having called the fourth, the fundamental.



triplets Rydberg introduced his well-known subscript notation. It admirably met rule 1 as to definiteness and clearness. Then later came the recognition of associated singlet and triplet series, and of doublet series in the same element, chiefly by the work of Saunders and Paschen. It was necessary to distinguish these, and, unfortunately as I think, Paschen introduced a completely new system, indicating the multiplicity by separate type—Roman capitals for singlets, German type for doublets, and small Roman for triplets: *e.g.* P, p, p. This necessitated a change in the term notation, to that now in general use of placing the variable before the functional sign. Its general adoption is a striking testimony to the pre-eminence of Paschen and his Tübingen school in spectroscopic investigation. I believe I have been alone in keeping loyally to the old Rydberg notation, denoting multiplicity by dashes; *e.g.* triplet  $p$  as  $p'''$ . Then a few years ago came a new outburst of activity following the discovery of multiplets in Mn and Cr by Catalán, and the classification and rules of their formation by Sommerfeld and Landé. Clearly it was out of the question to introduce new letters for new multiplets, and there are indications of a return to Rydberg's methods. It is here that chaos reigns. To get definiteness I offer for consideration the following scheme.

1. *Term sequences*.—Small type to be used  $s, p, d, f, g \dots$ . In any sequence, say  $s(m)$ , the order  $m$  is always to be the observed or "effective" value of  $m$ . If Bohr's theoretical value is to be indicated, the notation  $n_{k_j}^r$  or perhaps  $n.r.k_j$  to be used.

2. *Series lines*.—Capitals to be used when the wave number is given by the difference between the ground term of one sequence and a current term of the next succeeding term (S excepted), the capital being that of the current sequence. When, however, the current term belongs to the preceding sequence—a much less frequent occurrence—the two terms should be expressed. *E.g.*  $d-f(m) = F(m)$  but  $f-d(m)$  in full. Whether the order  $m$  is placed before or after the functional symbol does not affect clearness and may be left to individual taste. Personally I can never bring myself to write  $x \cos$  for  $\cos x$ .

3. *Complex terms*.—To be indicated by subscripts. But the question now arises as to whether these should be on Rydberg's basis of 1, 2, 3, ... for descending orders of importance (probability of orbit occupation) or according to their  $j$  values. At first sight the latter might appear the preferable method for obvious reasons. But there are at

least two good reasons for keeping to the old basis. (a) Most spectroscopists in dealing with multiplets will form a vivid mental picture of the arrangement of the lines as ordinarily represented in a frame. This is indicated at once by the Rydberg notation—*e. g.*  $D_{23} = p_2 - d_3$  is placed at once in its framework. (b) If the lowest—or highest— $j$  value of all terms had the same value, the corresponding  $j$  subscripts would serve the same purpose as the old. As this is not the case, a reader must carry in his mind the  $j$  arrangement of all the term-types before he can place a given symbol. Even so, an interval of time and calculation are required to place it. A physicist whose ordinary activities lie in other regions, and probably many spectroscopists themselves, would have to look up references. Even very few of the latter could place off-hand say the term  $f_4^4 = f_2^4$  (Rydberg). On this scheme Rydberg's subscript  $i$  denotes the  $i$ th  $j$ -value counting from the highest  $j$ —the  $i$  running up as the  $j$  run down. There will be many instances where a  $j$ -subscript arrangement may be convenient. In such a case, for the particular purpose a writer might definitely state that the  $j$  were used. But even here the notation ( $rkj$ ) might be more convenient. Tuhs  $f_2^4 = (444)$ ,  $f_1^4 = (445)$ .

4. *Related terms*.—The sets of terms relating to the same  $kj$  and independent of the ordinary direct terms require special notation. It has been common to represent these by dashes and overlines. Some writers indicate them by attaching letters  $a, b, \dots$  before the term symbol. The latter method conforms to rule 2 above and would appear to be far more elastic. On the first method further additional term-types would call for multiple dashing or overlining or even underlining.

5. *Multiplicity*.—To be entered as a power index in accordance with the usage of all the first investigators in this region: Catalán, Sommerfeld, Landé, Back, Gieseler, Grotrian, etc. Some recent writers have put the multiplicity index on the left of the symbol. To express new ideas by upsetting all previous notations instead of inventing new ones for the special purpose is to make havoc of clear and definite exposition.

6. *Multiplet schemes*.—It would be convenient if multiplets were always represented as framed on the same system. If this system follows that of the familiar diffuse triplet of Rydberg, the rule would run—the columns indicate the first term type (the greater  $k$ ), with  $j$  decreasing to the right (increasing subscripts). The horizontal lines would represent the second sequent (the smaller  $k$ ) with  $j$

decreasing upwards (the same way round in both cases).  
For example :

		$F^4$ .			
$j$	$d$	4	3	2	1
2			$F_{24}$	$F_{34}$	$F_{44}$
3		$F_{13}$	$F_{23}$	$F_{33}$	
4		$F_{12}$	$F_{22}$		
5		$F_{11}$			

7. *A minor matter.*—The letter  $\nu$  has always been used to denote frequency, or number of waves per second. May one express regret at the confusion of ideas shown by the increasing use of the same symbol to denote number of waves per cm. The evil is that the same symbol is used for two allied but different quantities. To use  $\nu$  also for a doublet separation—a different conception—as Rydberg did, can never cause confusion.

LXIV. *The Infra-red Oscillation Spectrum of Water Molecules and its Variation with State.* By JOSEPH W. ELLIS \*.

AN extensive investigation of the absorption spectrum of water vapour in the infra-red to a wave-length value as great as  $34\mu$  has been made by Hettner † by employing spectrographs equipped with gratings and quartz, fluorite, rock-salt, and sylvite prisms. He has shown ‡ that all of the oscillation bands below  $7\mu$  which characterize this vapour may be interpreted as harmonics and simple additive combinations of two fundamental frequencies existing at wave-length values of  $6\cdot26\mu$  and  $2\cdot66\mu$  respectively. Table I. gives the summarized results of his observations and calculations.

Paschen § observed in the emission spectrum of the Bunsen flame bands at  $6\cdot04\mu$ ,  $2\cdot51\mu$ ,  $1\cdot83\mu$ , and  $1\cdot38\mu$ , and identified these with water vapour. The writer || has

\* Communicated by the Author.

† Hettner, *Ann. der Physik*, lv. p. 476 (1918).

‡ Hettner, *Zeits. für Physik*, i. p. 345 (1920).

§ Paschen, *Ann. der Physik*, lii. p. 209 (1894).

|| Ellis, *Phys. Rev.* xxvi. p. 469 (1925).

TABLE I.

Designation.	Obs. $\lambda$ .	Calc. $\lambda$ .
$\nu_1$ .....	6.26 $\mu$	—
$2\nu_1$ .....	3.15	3.13 $\mu$ .
$3\nu_1$ .....	2.09	2.09
$\nu_2$ .....	2.66	—
$2\nu_2$ .....	1.37	1.33
$3\nu_2$ .....	—	0.89
$4\nu_2$ .....	0.69	0.67
$\nu_1 + \nu_2$ .....	1.87	1.87
$\nu_1 + 2\nu_2$ .....	1.13	1.10
$\nu_1 + 3\nu_2$ .....	0.77	0.78
$2\nu_1 + \nu_2$ .....	1.46	1.44
$2\nu_1 + 2\nu_2$ .....	0.94	0.93
$3\nu_1 + \nu_2$ .....	1.16	1.17

made observations on the last three bands, using quartz prisms for dispersion, and has found them at 2.58  $\mu$ , 1.79  $\mu$ , and 1.40  $\mu$ . Table II. represents an attempt to identify the 1.79  $\mu$  and 1.40  $\mu$  bands as combinations of those at 6.04  $\mu$  and 2.58  $\mu$ .

TABLE II.

	Obs. $\lambda$ .	Calc. $\lambda$ .
$\nu_1$ .....	6.04 $\mu$	—
$\nu_2$ .....	2.58	—
$\nu_1 + \nu_2$ .....	1.79	1.81 $\mu$
$2\nu_1 + \nu_2$ .....	1.40	1.39

The absorption spectrum of water, recorded by numerous observers, is characterized by a number of bands which form essentially a linear series\* starting at 6.1  $\mu$ . Using the average of the most accurate determinations the wave-length values of these bands are: 6.1  $\mu$ , 2.97  $\mu$ , 1.98  $\mu$ , 1.46  $\mu$ , 1.18  $\mu$ , 0.98  $\mu$ , 0.85  $\mu$ , 0.75  $\mu$ . We are led to look among these bands for values corresponding to  $\nu_1$  and  $\nu_2$  of Tables I. and II. The association of the 6.1  $\mu$  band with  $\nu_1$  seems self-evident. There is considerable evidence that absorption at 2.97  $\mu$  is composed of two superposed bands, one corresponding to  $\nu_2$  and the other one to the first harmonic of  $\nu_1$ . Such a superposition would account for the abnormal intensity of this latter band. Kemble† has stated that

\* Ellis, J. O. S. A. and R. S. I. viii. p. 1 (1924).

† Kemble, Phys. Rev. viii. p. 707 (1916).

"water shows a weak band at  $1.50\ \mu$ , a strong one at  $2.97\ \mu$ , and one of medium intensity at  $5.99\ \mu$ . The harmonic ratio between the last two bands must be regarded as accidental since the band corresponding to the greater wave-length is the less intense."

It is probable that the wave-length corresponding to  $\nu_2$  is slightly less than that corresponding to  $2\nu_1$ , thus accounting for the lack of an exact multiple relationship. Assuming both  $\nu_2$  and  $\nu_1$  to have a series of overtones, the slight deviations from multiple relationship among the shorter wave-length bands may be accounted for on this basis and on the basis of superpositions of combination bands of the type  $m\nu_1 + n\nu_2$ , where  $m$  and  $n$  are integers. This superposition of bands is shown in Table III., a value of  $2.9\ \mu$  having been assigned arbitrarily to the  $\nu_2$  band. By the assignment of such a value we can account, in particular, for the low wave-length position of the  $1.46\ \mu$  maximum.

Assuming that the overtone bands are in general more intense than the combination bands\*, it now becomes easy to account for the abnormal intensities of alternate bands in the water absorption spectrum. These abnormal intensities are brought out in Table IV. by comparing the ratios of the absorption coefficients for four of the bands as measured by Aschkinass† and also by Collins‡. The column marked "ratio" gives the absorption coefficient for that band divided by that for the band next preceding.

TABLE III.

$m$ .	$n$ .	Obs. $\lambda$ .	$m\nu_1$ .	$n\nu_2$ .	Combinations.
1		$6.1\ \mu$	—		
2	1	2.97	$3.05\ \mu$	$2.9\ \mu$	
3		1.98	2.03		$1.96\ \mu$ $\nu_1 + \nu_2$
4	2	1.46	1.52	1.45	$1.48$ $2\nu_1 + \nu_2$
5		1.18	1.22		$1.17$ $\nu_1 + 2\nu_2$
6	3	0.98	1.015	0.97	$0.98$ $2\nu_1 + 2\nu_2$
7		0.85	0.875		$0.84$ $3\nu_1 + 2\nu_2$
8	4	0.75	0.765	0.725	$0.73$ $2\nu_1 + 3\nu_2$
9		} 0.63	0.675	} 0.58	
10	5		0.61		
11		0.55	0.555		

\* This assumption is consistent with the writer's observations on the infra-red absorption by organic liquids. Phys. Rev. xxvii. p. 297 (1926); xxviii. p. 25 (1926).

† Aschkinass, *Ann. der Physik*, lv. p. 406 (1895).

‡ Collins, Phys. Rev. xx. p. 486 (1922).



TABLE IV.

Band.	ASCHEINASS.		COLLINS.	
	Coeff.	Ratio.	Coeff.	Ratio.
0.98 $\mu$ .....	0.416		0.448	
1.18 .....	1.221	2.92	1.220	2.72
1.46 .....	38.4	31.4	29.4	24.1
1.98 .....	123.2	3.24	103.0	3.50

The water transmission curves of Abney and Festing\* show bands of absorption at 0.63  $\mu$  and 0.55  $\mu$ . The first of these may be interpreted as an overlapping of  $5\nu_2$ ,  $9\nu_1$ , and  $10\nu_1$ , while the latter satisfies the value of  $11\nu_1$ . Russell and Lapraik †, observing visually the absorption produced by a six-foot cell of water, recorded a band between 0.605  $\mu$  and 0.655  $\mu$ , sharp on the short wave-length side and shading off toward longer wave-lengths. Their observation is consistent with the above identification of the band. These bands in the visible spectrum have been included in Table III.

A band at 4.7  $\mu$ , which cannot be interpreted in terms of  $\nu_1$  and  $\nu_2$ , is generally observed in the absorption spectrum of water. The writer's earlier suggestion ‡ that this band may arise due to polymerization in the liquid state is further strengthened by the fact that Hettner's curves show no corresponding band in water-vapour absorption. It is also interesting to note that Bode § found the analogue to this band at 4.5  $\mu$  in the absorption spectrum of ice, in which polymerization reaches a maximum. The works of Bode and of Plyler || show bands of absorption in ice analogous to all of the near infra-red bands characteristic of water.

\* Abney & Festing, Proc. Roy. Soc. xxxv. p. 328 (1883).

† Russell & Lapraik, Journ. Chem. Soc. xxxix. p. 168 (1881).

‡ Ellis, J. O. S. A. and R. S. I. viii. p. 1 (1924).

§ Bode, Ann. der Physik, xxx. p. 326 (1909).

|| Plyler, J. O. S. A. and R. S. I. ix. p. 545 (1924).

LXV. *The Variable Mass of the Electron.**By* L. T. JONES\*.

THE work of J. J. Thomson first showed that an electric charge in motion possessed mass, independent of the nature of the charge or the manner in which it is set in motion. Abraham was the first to point out the increase in mass that occurs at velocities comparable with that of light. His expressions for the longitudinal and transverse masses were based on the assumption of a spherical electron whose form is unchanged during its motion. It is now well known that in general the distinction between longitudinal and transverse mass is entirely artificial. Lorentz's theory of the variability of the mass was based on the deformable electron, the electron surface remaining an equipotential surface.

The theory of relativity leads to an expression for the mass of any moving body which, for the electron, is identical with that of Lorentz, the well-known Lorentz-Einstein expression for the mass being

$$m = m_0(1 - \beta^2)^{-\frac{1}{2}}.$$

This expression for the variable mass has been repeatedly verified experimentally. Its validity is accepted.

If an electron is permitted to fall through a large difference of potential,  $V$ , the kinetic energy acquired may be expressed by

$$Ve = e^2(m - m_0),$$

where  $m$  is the mass at the velocity acquired.

This may be written in the form

$$Ve = \frac{1}{2} m_0 v^2 (1 + \frac{3}{4} \beta^2 + \dots). \quad . \quad . \quad . \quad (1)$$

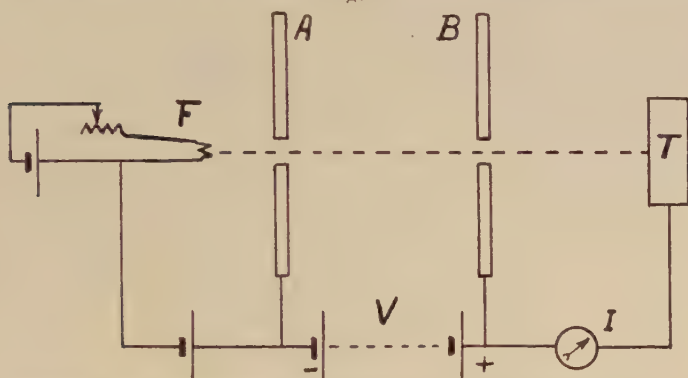
This expression is experimentally correct.

Suppose an electron emitted by the filament F (fig. 1) to fall through the potential  $V$  maintained between two perforated metal disks, A and B, and to strike the target T, giving up both charge and kinetic energy to the target. The charge of the electron now resides on T. During its fall through the field formed by A B it caused a slight change in the potentials of A and B. It thereby acquired and later gave up an amount of energy represented by either term of equation (1). The electron, now left to its own

\* Communicated by the Author.

devices, will return to the filament F. During its return to the filament it constitutes a current,  $I$ . The energy expended by the source of potential during its return (assume unit time) is  $VI$ . The whole system has now returned to the original condition, except that the source of

Fig. 1.



potential has expended an amount of energy which may be represented by any one of the four expressions:

$$Ve, \quad VI, \quad c^2(m-m_0), \quad HJ, \quad . . . . \quad (2)$$

where  $H$  is in calories and  $J$  the mechanical equivalent. An equation formed of any two of these expressions will satisfy the conditions for the experimentally verified variable mass.

Using two of the above expressions, form the equation

$$VI = c^2(m-m_0),$$

and write it in the form

$$\frac{VI}{1 + \frac{3}{4}\beta^2 + \dots} = \frac{1}{2}m_0v^2.$$

This will in no wise affect its experimental validity. The first term of this equation will now represent the energy acquired by the electron in its fall through the potential  $V$  on the assumption that the mass of the electron is a constant, and that the force driving the electron is a function of its velocity relative to the driving field.

If the first term correctly represents the energy expended on the electron, the equation

$$\frac{VI}{1 + \frac{3}{4}\beta^2 + \dots} = HJ$$

should be experimentally verified. White and Ham (Phys.

Rev. xxiii. p. 777, 1924) have, however, reported a verification of the equality

$$VI = HJ.$$

The experiment was carried out with an accuracy of .1 per cent. and with voltages up to 23 kv. Any departure from equality that might have been expected on the supposition of a variable driving force would have been easily detected. If, now, a continuous beam of electrons be emitted by the filament F and pass through AB to the target T, there will be a continuous current supplied by V, none of which passes to AB, and the potentials of A and B will not be altered during the passage of the beam. Since these potentials are not altered, the field AB is incapable of giving energy to the electron, but the field nevertheless constitutes a region wherein the energy of the electron changes from potential to kinetic without altering in magnitude. Changes in mass must then occur in two places: loss of mass at the target T and gain of mass during the passage of the electron up through the source of potential to the filament F.

The mass of the electron is then not a function of the velocity alone, but also a function of the potential.

The mass of the electron is always measured at the potential of the observer, and the slow-velocity mass inherently can never be measured by deflexion methods while at a high potential relative to him.

If the mass of only the negative charge is a fraction of its potential, this should be evidenced by the greater gravitational attraction of a metal mass at potential V. This would be independent of intermediate screening. If, however, the masses of both the proton and electron are a function of their potential, the effect will be *nil*.

Many years ago Prof. Nipher sought for an increased gravitational effect due to potential. He used a hollow metal container instead of a solid. The results did not convince him that such an effect exists.

The equivalence of energy and mass has not been verified except through the variable mass of the electron. If kinetic energy alone is mass, then every tree that grows and falls contributes its mite toward maintaining the temperature of the earth; and should any of the resulting radiation condense into matter (radiation should not always condense into matter "out in space"), the mass of the earth will *per se* increase.

Department of Physics,  
University of California.

LXVI. *A new Loss-measuring Device and its Application to High-Frequency Measurements.* By P. A. COOPER, *Research Department, Woolwich* \*.

**D**URING the last thirty or forty years quite a number of methods have been developed for the measurement of dielectric losses in condensers, usually at frequencies within the audible range. In most of these methods a variable resistance in series with a condenser has been used as the loss-measuring device, and has proved entirely satisfactory. For use at radio frequencies, however, the difficulties associated with the design and construction of an entirely satisfactory variable resistance are very considerable. They can be largely avoided by using a suitable fixed resistance in series with a variable condenser. Hitherto there has been one serious objection to the use of such an arrangement, and that has been the fact that it involves a change in the natural frequency of the circuit with which it is associated. This objection does not apply to the device the description of which is the main object of this paper.

The fixed resistance, to which reference has already been made, consists of a single straight wire about 10 cm. long. By using resistance wire of the smallest available gauge the distributed inductance for a particular value of resistance is reduced to a minimum, and at the same time the skin effect, which is a frequent source of error at high frequencies, is entirely avoided. That actually used is No. 48 S.W.G. bare manganin wire, and its resistance at  $3 \times 10^6$  cycles/sec., calculated from the formulæ of Kelvin, Maxwell, and Rayleigh as modified by Brylinski, is less than 0.01 per cent. greater than its direct-current resistance. The maximum oscillation current passed through it is never more than 0.003 ampere, and in order to make certain that currents of this magnitude do not heat the wire sufficiently to alter its resistance, a long piece of the same wire was tested in a Wheatstone bridge fed with direct current which could be varied by means of an external rheostat; for currents ranging up to 0.61 ampere the resistance was always between 235.65 and 235.70 ohms.

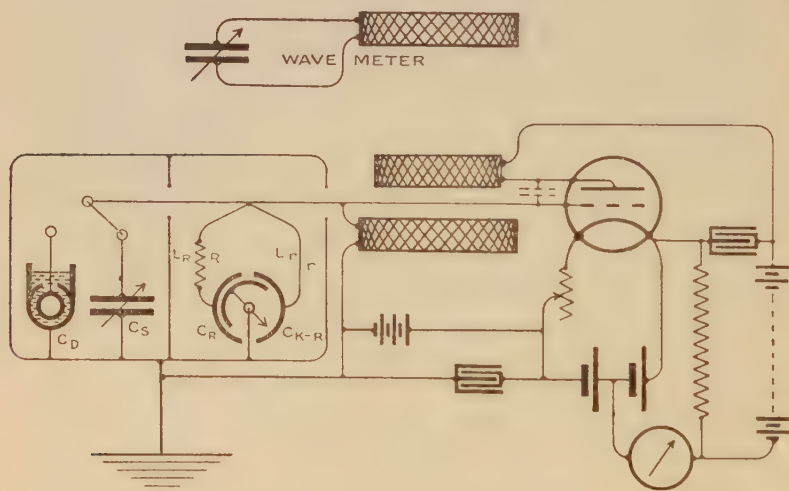
The change in frequency accompanying the use of a variable condenser in series with such a fixed resistance can be compensated by connecting a second condenser in parallel with the series arrangement. With sharply-tuned circuits,

\* Communicated by the Author.



however, the manipulation of two separate condensers to give the required effect is very tedious, though it is capable of giving good results. The method is much more easily applied if the two condensers are mounted on a common shaft as is shown diagrammatically in fig. 1, in such a way that, as the shaft is turned, the capacity of one condenser,  $C_R$ , increases at exactly the same rate as the capacity of the other,  $C_{K-R}$ , decreases. The arrangement is very similar to the well-known double condenser used for tuning two separate circuits at the same time, the only difference being that one set of movable plates is turned round

Fig. 1.



through  $180^\circ$  with respect to the other set; alternatively, of course, the moving plates can be built up as usual and one set of fixed plates turned round through  $180^\circ$ , though the former construction is preferable since it gives a balanced rotor. Using two supplementary condensers in this manner, a constant capacity is maintained over a considerable range of setting amounting to about  $160^\circ$ , so avoiding any change in the frequency of the circuit in which the device is used. Also, as will be seen later, this construction makes possible the measurement of the distributed inductance associated with resistance  $R$ , as well as the effective series resistances of the condensers themselves.  $R$  is connected in series with one condenser, and a low-resistance lead  $r$  goes to the other. Although in the figure

this resistance  $R$  and lead  $r$  are shown directly below the main lead or bus-bar running from the valve-grid to the condensers  $C_D$  and  $C_S$ , actually they are arranged so that this main lead is perpendicular to the plane containing them. This also applies to the leads to condensers  $C_D$  and  $C_S$ . The indicating instrument is a short-period critically-damped galvanometer in the anode circuit of the valve, compensation for the steady e.m.f. across it being made in the manner indicated. The galvanometer is used as a null instrument, the conditions which existed before switching out the condenser  $C_D$  containing the dielectric under investigation being simulated exactly by the use of the variable standard condenser  $C_S$  and the loss-measuring device. The wave-meter, which is used without its own local detector\*, serves two purposes—it fulfils its normal function of measuring frequency, and at the same time it shows exactly what capacity has to be taken from  $C_S$  to compensate for switching out  $C_D$ . The load which it throws on the oscillator when the two are in tune lessens the amplitude of the oscillations generated and, consequently, the deflexion given by the galvanometer.

In what follows we need only consider those parts of the circuit which are subject to change. The inductance of the grid-coil and bus-bar is constant, and is in series with the same total capacity after switching over as it was before. If care is taken to see that the distributed inductances of the branches containing  $C_D$  and  $C_S$  are matched they may be ignored completely. The inductances inherent in  $R$  and  $r$  are quite another matter, and their individual effects on the accuracy of the measurements will be considered later.

*Notation:—*

Leakage in ohms <sup>-1</sup> associated with condenser $C_D$ .....	$H$ .
Capacity from standard condenser needed to replace $C_D$ .....	$C_S$ .
Initial and final values of capacities in series with resistance $R$ .....	$C_{R_1}$ and $C_{R_2}$ .
Initial and final values of capacity in series with lead $r$ .....	$C_{K-R_1}$ and $C_{K-R_2}$ .
Values of distributed inductance of $R$ and $r$ .....	$L_R$ and $L_r$ .

\* See P. A. Cooper in Journ. Sc. Instruments, Aug. 1925.

With condenser  $C_D$  in circuit, then, the total admittance in ohms<sup>-1</sup> of the network concerned is

$$H + j\omega C_D + \frac{R + j\left(\frac{1}{\omega C_{R_1}} - \omega L_R\right)}{R^2 + \left(\frac{1}{\omega C_{R_1}} - \omega L_R\right)^2} + \frac{r + j\left(\frac{1}{\omega C_{K-R_1}} - \omega L_r\right)}{r^2 + \left(\frac{1}{\omega C_{K-R_1}} - \omega L_r\right)^2}.$$

With  $C_D$  replaced by  $C_s$ , and  $H$  transferred to the less-measuring device, we have

$$j\omega C_s + \frac{R + j\left(\frac{1}{\omega C_{R_2}} - \omega L_R\right)}{R^2 + \left(\frac{1}{\omega C_{R_2}} - \omega L_R\right)^2} + \frac{r + j\left(\frac{1}{\omega C_{K-R_2}} - \omega L_r\right)}{r^2 + \left(\frac{1}{\omega C_{K-R_2}} - \omega L_r\right)^2}.$$

Now  $R=15.75$  ohms, and the lowest likely value of  $\left(\frac{1}{\omega C_{R_2}} - \omega L_R\right)$  is about 600 ohms,  $C_{R_2}$  having the value  $75 \times 10^{-12}$  farad and  $\omega = 2\pi \times 3 \times 10^6$  /sec.  $\omega L_r$ , as will be seen later, is quite small compared with  $\frac{1}{\omega C_{R_2}}$ .  $(15.75)^2$  then, for experimental purposes, is negligible compared with  $(600)^2$ .

Omitting  $R^2$  and  $r^2$ , rearranging the expressions, and equating real and imaginary parts,

$$H = \omega^2 R \left[ \frac{C_{R_2}^2}{(1 - \omega^2 C_{R_2} L_R)^2} - \frac{C_{R_1}^2}{(1 - \omega^2 C_{R_1} L_R)^2} \right] + \omega^2 r \left[ \frac{C_{K-R_2}^2}{(1 - \omega^2 C_{K-R_2} L_r)^2} - \frac{C_{K-R_1}^2}{(1 - \omega^2 C_{K-R_1} L_r)^2} \right], \quad (1)$$

and

$$C_D = C_s + \left[ \frac{C_{R_2}}{1 - \omega^2 C_{R_2} L_R} - \frac{C_{R_1}}{1 - \omega^2 C_{R_1} L_R} + \frac{C_{K-R_2}}{1 - \omega^2 C_{K-R_2} L_r} - \frac{C_{K-R_1}}{1 - \omega^2 C_{K-R_1} L_r} \right]. \quad (2)$$

Some of the terms in the above expressions are probably negligibly small compared with others, and in this connexion it is important to find values for  $r$  and  $L_R$  and  $L_r$ . It will be convenient to examine the expression for the change in capacity first, since this does not contain  $r$ , whereas that for the leakage contains all three.

Each of the terms of the form  $\frac{\omega CR}{1-\omega^2 CL}$  in the expression for the capacity change represents the admittance of a residual inductance of fixed value, either  $L_R$  or  $L_r$ , in series with a condenser of variable capacity. In the writer's case, when the supplementary condensers were in the mean position, each had a capacity of  $49.4 \times 10^{-12}$  farad, the admittance of the system then being

$$\frac{\omega \times 49.4 \times 10^{-12}}{1 - \omega^2 L_R \times 49.4 \times 10^{-12}} + \frac{\omega \times 49.4 \times 10^{-12}}{1 - \omega^2 L_r \times 49.4 \times 10^{-12}} \text{ ohms}^{-1}.$$

With the setting such that one condenser had a capacity equal to half the mean value, and the other half as much again, the total admittance was

$$\frac{\omega \times 24.7 \times 10^{-12}}{1 - \omega^2 L_R \times 24.7 \times 10^{-12}} + \frac{\omega \times 74.1 \times 10^{-12}}{1 - \omega^2 L_r \times 74.1 \times 10^{-12}} \text{ ohms}.$$

It will be clear, then, that however carefully the condensers are matched the admittance is not independent of the dial-setting. If  $L_R$  and  $L_r$  were equal the total apparent capacity would have a minimum value with the dial in the mean position, increasing as it was moved in either direction, the rate of increase depending upon the values of the residual inductances and upon the square of the frequency. The values of  $L_R$  and  $L_r$  cannot very well be calculated, since the (well) known formulæ for the inductance of straight wires are not strictly applicable to wires as short as 10 cm. in proximity to condenser plates and metal screens. They can, however, be determined from experimentally obtained values of apparent capacity corresponding to particular dial-settings. Although both  $L_R$  and  $L_r$  can be obtained concurrently from such measurements, this was not done, because it was anticipated that the changes in apparent capacity would be quite small and would be noticeable only when the dial was turned as far as possible from the main position; moreover, from the point of view of loss-measurement it is only  $L_R$  which is of importance. Even at frequencies as high as  $3 \times 10^6 \sim$  sec. the inductance of a No. 48 S.W.G. wire is independent of its resistance, since the current which it carries is distributed evenly throughout the cross-section. As far as the inductance  $L_R$  is concerned, there is no change introduced by temporarily replacing resistance  $R$  by a copper wire of the same diameter, while measurements are facilitated by avoiding the large changes in the amplitude of the generated oscillations which would

otherwise occur when the setting of the condensers was changed. By replacing lead  $r$  by a similar thin wire, the number of unknown quantities is reduced to one, the inductance of the lead to each condenser now being  $L_R$ . With the object of determining  $L_R$ , measurements of the apparent capacity of the system were made first with the dial in the mean position and then in either of the extreme positions when, as has already been stated, the capacities of the condensers were  $24.7$  and  $74.1 \times 10^{-12}$  farad. It was necessary to make slight adjustments to condenser  $C_s$  in order to compensate for small irregularities in the sum of  $C_R$  and  $C_{K-R}$ , but these adjustments were precisely the same for oscillation frequencies of  $0.3$  and  $0.5 \times 10^6 \sim/\text{sec.}$ , showing that  $L_R$  was having an entirely negligible effect. At  $2.72 \times 10^6 \sim/\text{sec.}$ , however, with the dial of the device in either of the extreme positions, the apparent capacity was  $0.3 \times 10^{-12}$  farad greater than the corresponding value for the mean position.

We have, if we let  $\alpha = \omega \times 24.7 \times 10^{-12}$ ,

$$\frac{\alpha}{1 - \alpha\omega L_R} + \frac{3\alpha}{1 - 3\alpha\omega L_R} - \frac{4\alpha}{1 - 2\alpha\omega L_R} = \omega\delta C = 0.5 \times 10^{-6} \text{ ohm}^{-1}.$$

This reduces to

$$\frac{2\alpha^2\omega L_R}{1 - 6\alpha\omega L_R + 11\alpha^2\omega^2 L_R - 6\alpha^3\omega^2 L_R} = 0.5 \times 10^{-6} \text{ ohm}^{-1}.$$

For values of  $L_R$  less than, say, one microhenry the value of the denominator is sensibly unity, so that we can put

$$L_R = \frac{0.5 \times 10^{-6}}{2\alpha^2\omega}, \text{ i. e. } L_R < 0.1 \times 10^{-6} \text{ henry.}$$

The outcome of this is that the rather clumsy expression for the value of  $C_D$  reduces to  $C_D = C_s$  for most purposes; even at  $3 \times 10^6 \sim/\text{sec.}$  the maximum error that can be introduced by neglecting the contents of the bracket is only  $0.05 \times 10^{-12}$  farad.

Knowing  $L_R$ , we are in a position to examine the expression for the leakage  $H$ . It will be clear that any resistance which is in series with the loss-measuring device as a whole will have no influence at all on the accuracy of the measurements, since the capacity in series with the resistance is the same after as before changing the setting of the dial. This applies to the external leads and to the resistance at the rotor bearings, where electrical contact is



made with the moving plates. As far as the accuracy of loss-measurements is concerned, then, the effective series resistance of each of the supplementary condensers is just the resistance involved in making contact through the spacer washers with each set of fixed plates, together with the eddy-current losses in the aluminium plates in the neighbourhood of the washers. The resistance  $R$  and lead  $r$  were connected to these plates by clamping between copper washers, the points being hermetically sealed by painting them with paraffin wax; as long as the metal parts are kept cool the wax does not interfere with the electrical contacts.

Concurrently with the experiments just described, observations were also made on the galvanometer deflexions, from which, and from the behaviour of the device with resistance  $R$  in use, the value of the effective series resistance of each condenser could be obtained. At the highest frequency at which measurements were made, that is at  $2.72 \times 10^7$  ~/sec., the change in effective series resistance of the device as a whole, when the dial was moved from the mean position to either of the positions in which the capacity of one was  $\alpha/\omega$  and the other  $3\alpha/\omega$ , was 0.17 ohm. At the two lower frequencies there was no measurable change in the magnitude of the galvanometer deflexion. While this is partly due to the fact that the inductances used for these lower frequencies were of higher resistance, the effect of which would be to mask the small resistance we are out to measure, at the same time this small effective resistance would itself be less, since the eddy-current loss would be diminished. Applying equation (1) to the observations made at the highest frequency

$$r \left[ \frac{\alpha^2}{(1 - \alpha\omega L_R)^2} + \frac{(3\alpha)^2}{(1 - 3\alpha\omega L_R)^2} - \frac{2(2\alpha)^2}{(1 - 2\alpha\omega L_R)^2} \right] \\ = 0.17 \text{ ohm} \times \frac{(4\alpha)^2}{(1 - 4\alpha\omega L_R)^2},$$

$\alpha$  having the same value as before, that is  $\omega \times 24.7 \times 10^{-12}$ .

Now  $r$  will be a quantity which, from the experimental figures obtained, we shall not be justified in expressing to more than two significant figures. For this degree of precision the denominators of the fractions are sensibly unity, and we have immediately

$$r = 8 \times 0.17 \text{ ohm} = 1.4 \text{ ohms.}$$

For the purpose of the experiments just described  $r$  is, as

has already been stated, the resistance of each of the No. 48 S.W.G. copper leads temporarily replacing  $R$  and  $r$  added to the effective series resistance of the condenser. The d.c. resistance—and *ipso facto* the high-frequency resistance—of each of the wires was 1.3 ohms, leaving less than 0.1 ohm as the effective series resistance of each condenser at  $2.72 \times 10^6 \sim/\text{sec}$ . Were it not for the fact that these condenser resistances tend to neutralize each other and to produce on the circuit an aggregate effect less than that of either of them considered separately, this could hardly be considered negligible compared with 15.73 ohms, the value of  $R$ . The condensers under consideration were built up from standard aluminium plates separated by brass washers, admittedly not the best low-loss construction. Returning now to the loss-measuring device in the form in which it is actually used, we have a resistance  $R$  of self-inductance  $L_R$  in series with one condenser, and a lead of thin copper strip  $r$ —a No. 26 S.W.G. wire rolled out—of negligible resistance and of self-inductance  $L_r$  in series with the other.  $L_R$  has been determined and shown to have for practical purposes a negligible effect on the terms in the expression for capacity (2).  $L_r$  certainly has a smaller value than  $L_R$ , and will tend to compensate it as far as equation (2) is concerned. With regard to the expression for the leakage  $H$ , the resistance of the copper strip  $r$  being negligible compared with  $R$ , equation (1) becomes

$$H = \omega^2 R \left[ \frac{C_{R_2}^2}{(1 - \omega^2 C_{R_2} L_R)^2} - \frac{C_{R_1}^2}{(1 - \omega^2 C_{R_1} L_R)^2} \right] \quad (4)$$

or

$$H = \omega^2 R \left[ \frac{C_{R_2}^2}{1 - 2\omega^2 C_{R_2} L_R} - \frac{C_{R_1}^2}{1 - 2\omega^2 C_{R_1} L_R} \right] \quad (5)$$

The effect of neglecting the  $2\omega^2 C_R L_R$  terms and putting

$$H = \omega^2 R [C_{R_2}^n - C_{R_1}^n] \quad (6)$$

is, of course, to introduce an error which is most noticeable at the highest frequency at which measurements are made. Thus with  $C_{R_1}$  and  $C_{R_2}$  having the limiting values of 22.5 and  $76.3 \times 10^{-12}$  farad respectively, and  $L_R$  the experimentally found value  $0.1 \times 10^{-6}$  henry, the maximum possible error that can be so caused is about 0.5 per cent., at  $3 \times 10^6 \sim/\text{sec}$ ., while at  $2 \times 10^6$  it is about 0.2 per cent. and at one million less than 0.1 per cent. For all ordinary purposes, then, and for wave-lengths ranging down to 100 metres, the simplified expressions (3) and (6) can be employed. The power-factor

for small angles of loss and the angle of loss itself are given by

$$\frac{H}{\omega C_D} = \frac{\omega R [C_{R_2}^2 - C_{R_1}^2]}{C_S} . . . . . (7)$$

The loss-measuring device as it has been described is, at the higher radio frequencies, quite adequate to deal with losses of the magnitude usually encountered in measurements on dielectrics. Since, however,  $\omega^2$  occurs in the expression for the loss (6), it is clear that it becomes less effective as the frequency at which measurements are made is lowered. This effect is best counteracted by making available a larger range of capacity variation for measurements at frequencies, say, below  $3.5 \times 10^6 \sim/\text{sec}$ . This is readily achieved by the use of a small fixed condenser, which initially is connected in parallel with the compensating condenser and finally in parallel with the loss-measuring condenser. The constant capacity principle is still maintained, and any loss which the condenser may have does not affect the accuracy of the measurements in any way.

When measuring losses or power-factors it is convenient to use loose coupling between the oscillator and the wave-meter; there is no point in making the apparatus extremely sensitive to capacity change, since it is the loss component which is the more difficult to measure accurately. For special purposes, however, such as the measurement of small changes in capacity or the measurement of dielectric constants of insulators having low losses, closer coupling can be very usefully employed. Fig. 2 shows a set of curves which demonstrate the effect of coupling between the oscillator and the wave-trap on the sensitivity to capacity change. These changes were produced in the grid-circuit of the oscillator by the use of the fine adjustment condenser employed in the determination of  $L_R$ . Curve A was obtained with fairly loose coupling, and C with the coupling as tight as is practicable; if it is increased much more, oscillation hysteresis sets in. It will be seen, though, that the available sensitivity is ample for the purposes for which it is intended. The capacity in the wavemeter circuit was about  $60 \times 10^{-12}$  farad.

The use of a sensitive galvanometer in the plate-circuit of a valve is not always advisable, since it might easily be damaged, say, by forgetting to break the galvanometer circuit before changing the plug-in coils or by switching on the filament-heating current before connecting up the high-tension battery. From this point of view the circuit shown

Fig. 2.

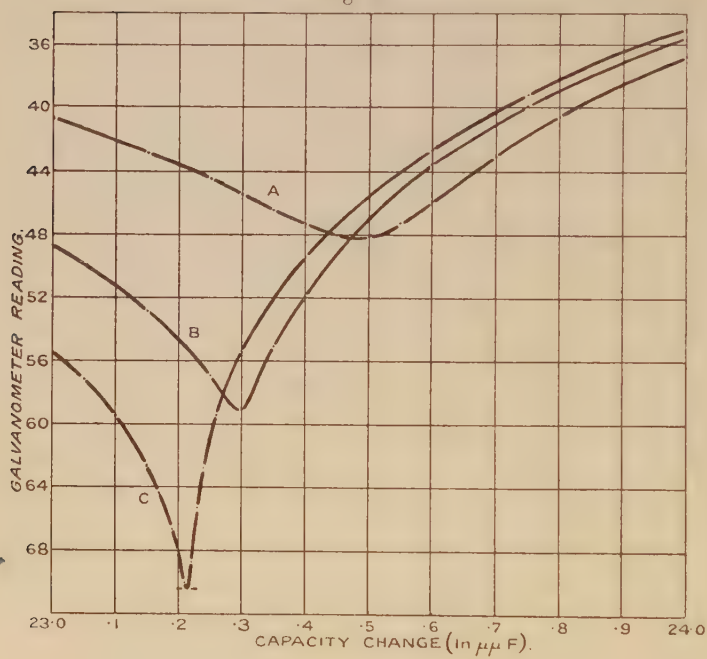
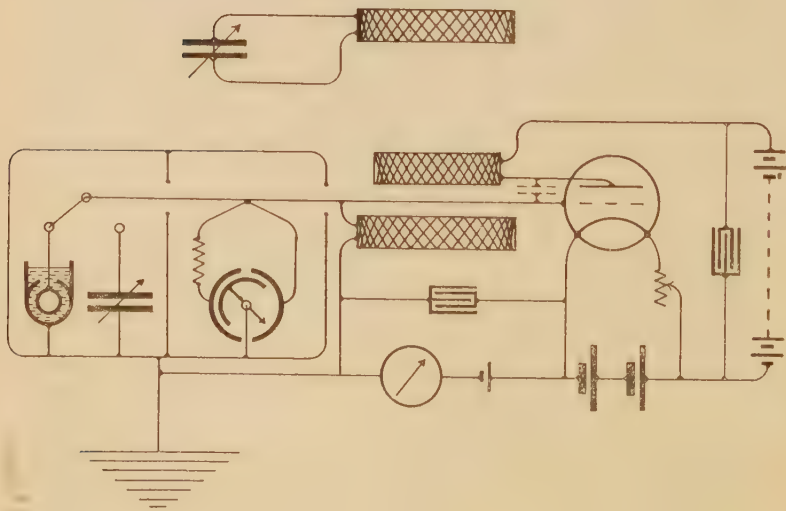
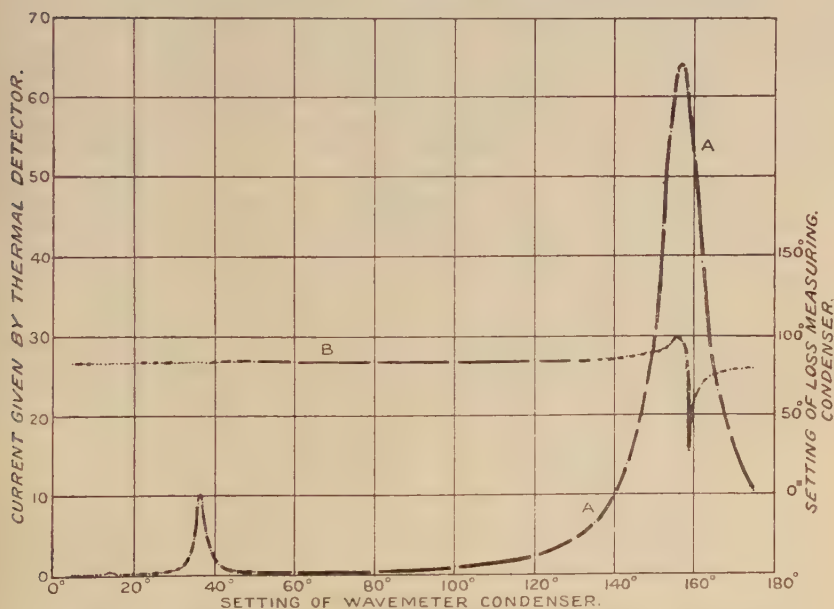


Fig. 3.



in fig. 3 is preferable. Here the galvanometer is in the path between the filament and the grid. The e.m.f. given by a single-grid biasing cell is sufficient to prevent any current from passing through the galvanometer when the circuit is not oscillating. When oscillations of sufficient amplitude are generated, however, the grid begins to rectify, and the galvanometer deflexion then is a measure of the amplitude of these oscillations. The use of a rectifying grid does, of course, entail a certain amount of distortion of wave-form, but, provided that the rectified current does not

Fig. 4.



exceed twenty to thirty microamperes, it is small compared with that already present. This question of distortion and its probable effect on measurements was investigated by including in the wavemeter circuit a vacuum-type thermojunction heated by the oscillation current, a second galvanometer being used to measure the thermoelectric current produced. Throughout this series of measurements it was necessary to keep the losses constant, and this was accomplished by adjusting the loss-measuring device to compensate for the variable load thrown on the oscillator by the wave meter circuit. Curve A in fig. 4 shows the thermal current plotted against the setting of the wavemeter condenser. Without



going actually into figures, it is evident that the harmonic of twice the fundamental frequency is quite strong, while the third harmonic is feeble. Curve B in the same figure was obtained by plotting the setting of the loss-measuring device also against the setting of the wavemeter condenser. The striking point about it is that it almost entirely ignores the second harmonic, and, this being the case, its presence does not affect the accuracy of the measurements. The reason for this is evident when it is realized that the area included between a sine curve and the time axis from 0 to  $\pi$  is the same as that included between such a curve distorted by the presence of an even harmonic, say the second, and the time axis, over the same time interval. Although the areas are the same, however, the effect of the second half-wave of the harmonic does not entirely cancel that of the first. The extent to which it does depends on the form of the grid voltage-grid current characteristics, and becomes more complete as the ratio between the negative-grid biasing e.m.f. and the grid-swing e.m.f. becomes less. It is also influenced by the amount of capacity in the grid circuit and by the frequency of the oscillations generated.

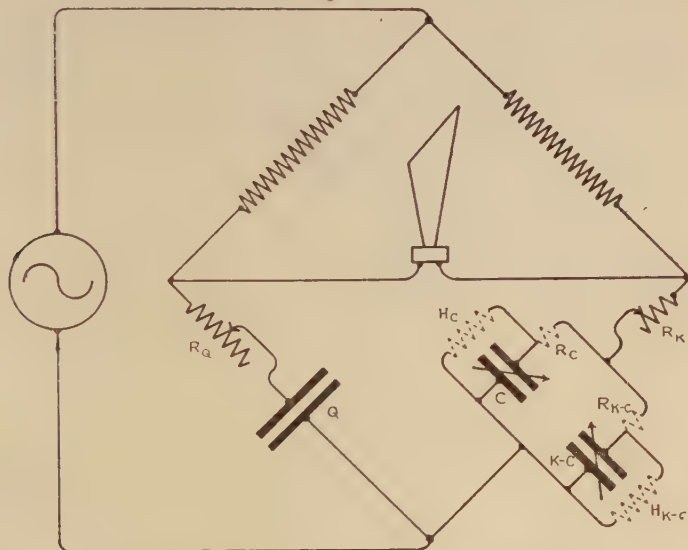
The condenser under test, of course, need not necessarily form part of the oscillator, but may be incorporated in another tuned circuit coupled to the oscillator, and containing also the standard condenser and the loss-measuring device. The presence of this additional tuned circuit certainly has the effect of filtering out harmonics from the working circuit, but, as it has already been shown that the detector is practically unaffected by them, this is not as great an advantage as at first sight might appear. The sensitivity of this arrangement is not as high, since, as is the case with the standard method, the coefficient of coupling cannot usefully be increased beyond a certain definite maximum without introducing oscillation hysteresis. It requires, moreover, an additional set of inductances to cover the whole frequency range. Looked at from other points of view, it has additional shortcomings. By using one of the circuits shown in figs. 1 and 3 the same maximum potential difference is applied to the condenser under test, whatever its capacity or the nature of its dielectric. This does not apply to the modification of the circuit now under consideration, or, indeed, to the standard method used in this country or elsewhere. Lastly, the losses of the material under test are not made good by regeneration, and this, as was shown in a previous paper (*Journ. of Scientific Instruments*, August 1925), is an important point when dealing with poor dielectrics.

In conclusion, I would like to acknowledge my indebtedness to Dr. G. Rotter, C.B.E., and to Dr. J. N. Pring for the kind interest they have shown in this work, and to the Director-General of Artillery for permission to publish it.

### Appendix.

The method by which the effective series resistances of the two supplementary condensers were determined appears to be of general utility not only in oscillation, but also in bridge, circuits intended for the measurement of condenser losses, and should obviate the necessity for the assumption so often made that the losses associated with the standard condensers used are themselves negligible. Fig. 6 shows.

Fig. 5.



the method applied to a Wien bridge suitable for measurements at acoustic frequencies, though it could be used just as readily in other bridge circuits such as those due to Heydweiller, Nernst, Grover, Hertwig, Fleming and Dyke, Scheering, Rosen, and others.

C and K-C are two separate variable condensers connected in parallel in one arm of the bridge, and they are set so that when the bridge is balanced the sum of their capacities is rather less than the maximum capacity of either of them individually.  $R_C$  and  $R_{K-C}$  represent their effective series resistances, and  $H_C$  and  $H_{K-C}$  the leakage in ohms<sup>-1</sup> associated with them.  $R_K$  is a small variable resistance in

series with the total capacity  $K$  in that arm of the bridge. In series with condenser  $Q$  is a resistance  $R_Q$  whose value does not require to be known.

If  $C_1$  and  $\overline{K-C_1}$  are the values of capacity and  $R_{K_1}$  of resistance which satisfy the conditions for balance, then the admittance of arm  $BD$ , neglecting small terms, is

$$H_C + R_C \omega^2 C_1^2 + H_{\overline{K-C}} + R_{\overline{K-C}} \omega^2 \overline{K-C_1}^2 + R_{K_1} \omega^2 K^2. \quad (1)$$

If  $C_2$  and  $K-C_2$  and  $R_{K_2}$  also satisfy the conditions for balance, we have also as the admittance

$$H_C + R_C \omega^2 C_2^2 + H_{\overline{K-C}} + R_{\overline{K-C}} \omega^2 \overline{K-C_2}^2 + R_{K_2} \omega^2 K^2. \quad (2)$$

Further, if  $C_3$ ,  $K-C_3$ , and  $R_{K_3}$  are other corresponding values of capacity and resistance, we have also

$$H_C + R_C \omega^2 C_3^2 + H_{\overline{K-C}} + R_{\overline{K-C}} \omega^2 \overline{K-C_3}^2 + R_{K_3} \omega^2 K^2. \quad (3)$$

These three statements are all equal to one another, and are sufficient to determine  $R_C$  and  $R_{\overline{K-C}}$ , the effective series resistances. Moreover, if, say, condenser  $C$  be cut out completely, and if  $R_{K_4}$  be the new resistance required to satisfy the balance conditions, then

$$H_{\overline{K-C}} + (R_{\overline{K-C}} + R_{K_4}) \omega^2 K^2 = \text{statements (1), (2), or (3),}$$

and is sufficient to determine the leakage  $H_{\overline{K-C}}$ . In a precisely similar manner the leakage associated with condenser  $C$  can be determined by completely cutting out condenser  $K-C$ .

## LXVII. Notices respecting New Books.

*The Geological Age of the Earth: the 27th Robert Boyle Lecture.*

By Prof. JOHN JOLY. (Oxford University Press. Pp. 18. 1s.)

THIS pamphlet is concerned chiefly with the relation of pleochroic halos to the measurement of geological time. Prof. Joly's discovery, that the smallest halo produced by the  $\alpha$  rays from small inclusions of uranium in certain micas has a rather larger radius than one would expect on other grounds, has not yet received a thoroughly satisfactory interpretation. Prof. Joly himself favours the view that the phenomenon indicates that the velocity of the  $\alpha$  particle ejected by uranium I was greater in early geological time than it is now, and, on the basis of an empirical law connecting the velocities of  $\alpha$  particles with the rates of decay of the emitting elements, is inclined to cast doubt on the constancy of the decay-period of uranium, and therefore on the validity of the uranium-lead ratio as a means of determining geological time. In the absence of a complete explanation of the abnormality in the size of the uranium halo it would perhaps be premature to form a definite opinion on

the validity of the argument, though one may feel that the arguments in the other direction advanced by Holmes\* are stronger.  
H. J.

*Gyromagnetic Electrons and a Classical Theory of Atomic Structure and Radiation.* By L. V. KING. (Montreal, at the Mercury Press, 1926.)

THE present work consists of two short papers given in the form of lectures to the McGill Physical Society in April 1926. They contain the first account given by Professor King of his theory by means of which he seeks to obtain the formulæ of Quantum Physics without introducing hypotheses which conflict with the classical Electromagnetic Theory. This is, evidently, a task of the greatest importance for contemporary physics, and if it can be accomplished many important results as regards physical principles will necessarily follow. The present outline of the theory can be regarded only as a preliminary account, and we await the detailed exposition of the steps by which, from the hypothesis of the Spinning Electron, the fundamental and well-established results of Spectrum Analysis, Black Body Radiation and Photo-Electricity may be derived. The full discussion must, of course, presuppose acquaintance with Professor King's important memoir 'On the Possibilities of a Vortex Electron Theory of Matter,' written in 1908; but unfortunately this memoir has never been available for the general scientific public. Now, however, with the new modifications which the present theory introduces, namely the idea that electronic precessions are due to electro-dynamic deformation, an idea which readily yields the key formula

$$h\nu = \frac{1}{2}m_0v^2,$$

the importance of this memoir becomes plainer, and we hope that Professor King will see his way to publish the relevant parts of it in the course of the detailed account of his new ideas which we await with the greatest interest.

*The Elements of Aerofoil and Airscrew Theory.* By H. GLAUERT, (Cambridge, at the University Press, 1926. 14s. net.)

ALL students of Aerodynamics will welcome this treatise by one of the acknowledged experts in this new branch of applied mathematics. Although there are still a very large number of outstanding problems which at present baffle the aerodynamician, the fact that a considerable body of results has now been established makes it very suitable and desirable that the subject should be treated in a text-book which is designed to appeal to students who do not possess a knowledge of hydrodynamics sufficient to enable them to assist in the advance of the subject themselves.

The aim of Aerofoil theory is to explain and to predict the force experienced by an aerofoil. Considerable insight has been obtained into the question of the behaviour of the aerofoil in the ordinary

\* Phil. Mag. (7) pp. 1055-1074 (1926).



working range below the critical angle, and a satisfactory theory has been reached for that part of the drag which is independent of the viscosity of the air. Although no complete theory is yet available which will deal with the behaviour of the aerofoil at and above the critical angle, certain results have been established as to the nature of the viscous drag. The airscrew presents problems which may be reduced to other problems relating to aerofoils, for the blades of the airscrew may evidently be regarded as aerofoils describing helical paths. It is interesting to record the fact that—as was to be expected—a satisfactory theory of the airscrew has been developed by extending and applying the fundamental principles of aerofoil theory.

*Fourfold Geometry, being the elementary geometry of the four-dimensional world.* By D. B. MAIR. (Methuen and Co. 1926.)

THE introduction of the Principle of Relativity marked an important stage in the development of the modern view of geometry which is one of the outstanding advances of our day. It is, of course, hardly true to attribute this revolution entirely to Relativity theory, for there were many signs from the time of Riemann onwards that a new view was being taken as to the logical status of Geometries as a whole. This entailed a wholly new conception of the nature of a geometry and a final clearing away of the confusions caused by confounding together mensuration and pure geometry, subjects which are now recognized to be of entirely different scope.

It is therefore very important that the actual detailed development of the new idea of geometry, upon which this great advance depends, should be available in text-book form for teaching purposes. Professor Mair has therefore performed a signal service by producing the present work. In his discussion of the "flat" fourfold space with which he is concerned, he presupposes only a small amount of knowledge in the reader; in fact it is only necessary to assume acquaintance in the student with the Cartesian method of treating geometry and with the meaning of conjugacy with respect to a conicoid in order to be able to recommend to him the book at present under review. This rather meagre technique which Professor Mair is content to assume the reader possesses necessarily adds to the number of elementary matters which have to be discussed. But it is of real value to those concerned with the mathematical exposition of these important ideas to be able to turn to this self-contained exposition.

It is interesting to notice that Professor Mair has felt called upon to introduce a number of new technical terms. As usual, the introduction of precisely defined terms leads to a considerable advance in clarity, and it is to be hoped that students of the subject will see that it is very much worth their while to become familiar with them.

---

[The Editors do not hold themselves responsible for the views expressed by their correspondents.]



THE  
LONDON, EDINBURGH, AND DUBLIN  
PHILOSOPHICAL MAGAZINE  
AND  
JOURNAL OF SCIENCE.

[SEVENTH SERIES.]

SUPPLEMENT, APRIL 1927.

LXVIII. *On Damping Effects in Exterior Ballistics.*  
By LAWRENCE WAINWRIGHT, M.Sc., Ph.D., Lieutenant,  
*United States Navy* \*.

NOTATION.

FIGURE 1 depicts the projectile and the sets of reference axes. The set  $xyz$  is fixed in space (motion of earth ignored in this analysis). The set  $\xi\eta\zeta$  has its origin at the centre of gravity,  $O$ , of the projectile and translates with it, but remains parallel to the set  $xyz$ . The set  $123$  has its origin at  $O$  and is rigidly attached to the projectile. The Eulerian angles  $\theta, \psi, \phi$  define the orientation of the projectile. The angle  $\theta$  will be referred to as the yaw, and the angle  $\psi$  as the precession.

We shall list here the different symbols used, though the assigned significance of some may not be clear until the reader has gone further.

$t$ : time ( $t_0 = 0$ ).

$w$ :  $\cos \theta$ .

$w_1 < w_2 < w_3$ : the three roots of the characteristic cubic ( $w_1$  corresponds to maximum yaw and  $w_2$  to minimum).

$w_0$ : the initial or a special value of  $w$  (as for a double root,  $w_1 = w_2 = w_0$ ).

$\theta_0, \theta_1, \theta_2$ : the corresponding values of  $\theta$ .

$\omega_1, \omega_2, \omega_3$ : the angular velocities about the axes 1, 2, 3.

$\omega^2 = \omega_1^2 + \omega_2^2$ .

$a_1, a_2, a_3$ : initial values of  $\omega_1, \omega_2, \omega_3$ .

\* Communicated by the Author.

$A_1, A_2, A_3$ : the moments of inertia about the axes 1, 2, 3.  
 $\lambda = A_3/A_1$ .

$\alpha = a_3\lambda$ .

$\mu$ : coefficient of the couple tending to increase yaw (considered constant unless specified contrarily).

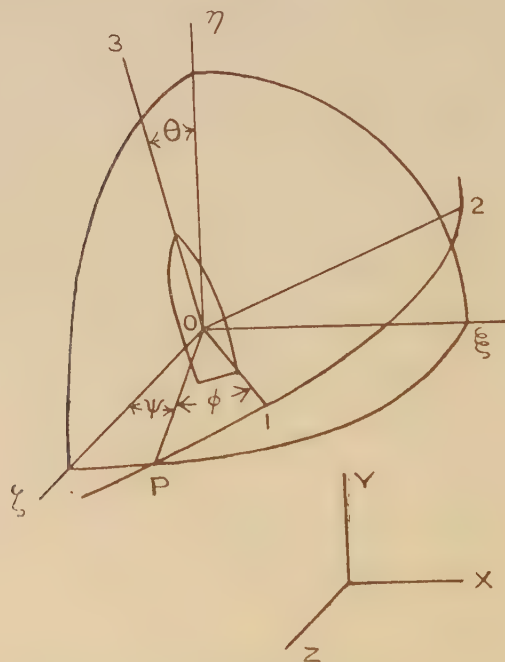
$c_1$ : energy constant (unless specified contrarily; does not include energy of spin).

$c_2$ : moment of momentum (about  $O\eta$ ) constant (unless specified contrarily).

$P$ : the period of  $\theta$ .

$\Delta\psi$ : the advance of  $\psi$  during  $P$ .

Fig. 1.



$\nu$ : coefficient of damping (wobble).

$\Delta w^i$ : change in  $w_i$  ( $i=0, 1, 2, 3$ ) during  $P$ .

$R = 1 - \frac{2\mu(w_1 + w_2)}{a_3^2\lambda^2}$ : a certain radicand.

$\rho = 8\mu/a_3^2\lambda^2$ : a parameter replacing  $\mu$  in tabular computations.

$K(\kappa), \Pi^1(n, \kappa)$ : standard elliptic function notation.

$C$ : a certain intermediate parameter (see eq. 8).

$W, V$ : abbreviations for certain algebraic expressions (see eqs. 18 ... 23).

Additional notation is introduced incidentally.

## ASSUMPTIONS.

The problem of the motion of a projectile is extraordinarily complicated. In such a case it is customary to make simplifying assumptions and treat the reduced problem. Then, as knowledge is gained from the study of the idealized case, the simplifying assumptions are gradually removed or made milder. The process is one of successive approximations. In the present problem, simplifying assumptions are necessitated both by the mathematical complexities and by ignorance of the physical laws involved. The justification of the assumptions here introduced rests upon the double ground of rendering the problem mathematically tractable and of leading to conclusions in close conformity to physical observation. We make the following principal assumptions:

- (a) That the projectile is symmetrical, both statically and dynamically.
- (b) That the centre of gravity of the projectile is moving in a straight line (in the direction  $O\eta$ ) with uniform velocity.
- (c) That there is a resultant force parallel to the direction of motion. That the magnitude of this force, and its point of application (forward of the centre of gravity on the 3-axis) may be considered for short intervals of time in a given problem as constant and independent of the position and orientation ( $\theta$  small) of the projectile, *i. e.* independent of  $x, y, z, \theta, \psi, \phi$ .
- (d) That we are treating such a case that, as ordinarily encountered in practice:  $w_1, w_2 > 0, 0$ ;  $w_1 \neq w_2$  (unless specified contrarily);  $w_1 < 1$ ;  $R > 0$  (explained later).
- (e) That the damping is zero until specifically introduced. That the damping due to the wobble is proportional to the angular velocity of wobble ( $\sqrt{\omega_1^2 + \omega_2^2}$ ), and acts oppositely.
- (f) That the perturbations are small and can be considered separately with sufficient approximation.

The basis for assumption (e) is briefly as follows:—The resistance of the air is known to vary, except in the region of the velocity of sound, approximately as the square of the velocity. Now consider a point on the projectile. It will have a velocity,  $v$ , due to the translation of the centre of gravity, and a velocity,  $\Delta v$ , due to wobble. Relative to the air, these velocities will have components  $\alpha v$  and  $\beta \Delta v$ ; and their sum squared will be  $\alpha^2 v^2 + 2\alpha\beta v\Delta v + \beta^2 (\Delta v)^2$ , where the third term will be very small. Now, as the damping force must vanish with  $\Delta v$ , it cannot depend upon the first

term. Hence, after a hypothetical integration over the surface of the projectile, we conclude that the damping force is, at least approximately, proportional to the angular velocity. Excluding the damping of the spin, which is considered separately, we have our assumption.

### THE EQUATIONS OF MOTION (UNDAMPED).

Let the couple tending to increase yaw be denoted by  $\mu A_1 \sin \theta$  (fig. 2). Then, from the geometrical relations

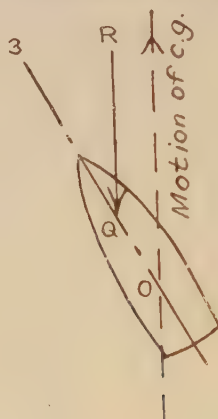


Fig. 2.

$$\overline{R \cdot OQ} = \mu A_1$$

and the laws of motion, we derive the equations of motion, which may be written, after dividing out  $A_1 = A_2 = \lambda A_3$ :

$$\left. \begin{aligned} \frac{d\omega_1}{dt} - (1-\lambda)\omega_2\omega_3 &= \mu \sin \theta \cos \phi, \\ \frac{d\omega_2}{dt} + (1-\lambda)\omega_3\omega_1 &= -\mu \sin \theta \sin \phi, \\ \frac{d\omega_3}{dt} &= 0, \\ \sin \theta \frac{d\psi}{dt} &= \omega_1 \sin \phi + \omega_2 \cos \phi, \\ \frac{d\theta}{dt} &= \omega_1 \cos \phi - \omega_2 \sin \phi, \\ \frac{d\phi}{dt} &= \omega_3 - \cos \theta \frac{d\psi}{dt}. \end{aligned} \right\} \dots (1)$$

$$\begin{aligned} \omega_1(0) &= a_1. & \theta(0) &= \theta_0. & \omega_1^2 + \omega_2^2 &= \omega^2. \\ \omega_2(0) &= a_2. & \psi(0) &= \psi_0. & a_1^2 + a_2^2 &= \omega_0^2. \\ \omega_3(0) &= a_3. & \phi(0) &= 0. & & \end{aligned}$$

From the first two, fourth, and fifth of (1) we obtain, on integration:

$$c_1 = \omega_1^2 + \omega_2^2 + 2\mu \cos \theta = \sin^2 \theta \left( \frac{d\psi}{dt} \right)^2 + \left( \frac{d\theta}{dt} \right)^2 + 2\mu \cos \theta, \quad (2)$$

where  $c_1$  is a constant determined by the initial conditions. From the assumption that there is no moment of force about the axis  $O\eta$ , it follows that the moment of momentum about  $O\eta$  is constant, giving:

$$c_2 = \sin^2 \theta \frac{d\psi}{dt} + a_3 \lambda \cos \theta, \quad (3)$$

where the constant,  $c_2$ , will be determined by the initial conditions. On eliminating  $d\psi/dt$  between (2) and (3), and writing  $w$  for  $\cos \theta$ , we obtain the characteristic cubic:

$$\begin{aligned} \left( \frac{dw}{dt} \right)^2 &= 2\mu w^3 - (c_1 + a_3^2 \lambda^2) w^2 + 2(c_2 a_3 \lambda - \mu) w + c_1 - c_2^2 = F(w) \\ &= 2\mu(w - w_1)(w - w_2)(w - w_3). \quad (4)^* \end{aligned}$$

$$w_1 \leq w_2 \leq w_3.$$

The general properties of the motion so defined are well known, occurring in the top problem, and it is not our intention to review them at length, as we are primarily interested in the question of damping. We have the usual relations among the roots:

$$\left. \begin{aligned} w_1 + w_2 + w_3 &= (c_1 + a_3^2 \lambda^2) / 2\mu, \\ w_1 w_2 + w_2 w_3 + w_3 w_1 &= (c_2 a_3 \lambda - \mu) / \mu, \\ w_1 w_2 w_3 &= (c_2^2 - c_1) / 2\mu. \end{aligned} \right\} \quad (5)$$

On solving for  $c_1$ ,  $c_2$ ,  $w_3$  in (5):

$$\left. \begin{aligned} c_1 &= -a_3^2 \lambda^2 + 2\mu(w_1 + w_2 + w_3), \\ c_2 &= \frac{a_3 \lambda (1 + w_1 w_2)}{w_1 + w_2} \pm \frac{a_3 \lambda \sqrt{(1 - w_1^2)(1 - w_2^2)} \sqrt{R}}{w_1 + w_2}, \\ w_3 &= -\frac{1 + w_1 w_2}{w_1 + w_2} + \frac{a_3^2 \lambda^2 (1 + w_1 w_2)}{\mu(w_1 + w_2)^2} \\ &\quad \pm \frac{a_3^2 \lambda^2 \sqrt{(1 - w_1^2)(1 - w_2^2)} \sqrt{R}}{\mu(w_1 + w_2)^2}. \end{aligned} \right\} \quad (6)$$

In the first of (6) we have written for brevity  $w_3$ , but it

\* The derivation of this equation is an abbreviation of my notes of lectures by Professor F. R. Moulton, of the University of Chicago.

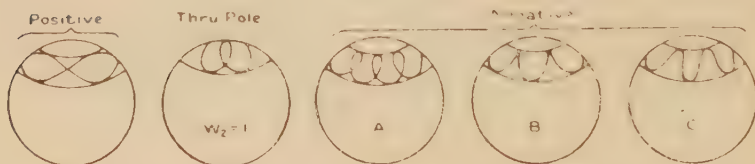


is to be understood to be replaced by the expression for it given in the third of (6).

The last stipulation in assumption (d) will now be clear. As  $c_2$  must be real in a physical problem, the second radicand in the expression for it must not be negative. Furthermore, it can be shown that the nearer the radicand approaches to zero the more unstable the motion; so we have assumed it definitely positive. The value of this radicand is one of the criteria of stability.

Corresponding to the double sign, two types of motion are distinguished—called “positive” for the upper sign (+) and “negative” for the lower (−). Between these two lies the case of oscillations passing through the pole, *i. e.* when  $w_2 = 1$ . It is possible further to subdivide the negative type into two cases divided by a limiting case. Of these three negative cases only one is likely to occur in actual firings, as shown by experimental data. Fig. 3 gives a qualitative idea of these types of motion.

Fig. 3.



### THE PERIOD OF OSCILLATION AND THE PRECESSIONAL ADVANCE.

#### *The Period.*

As the right member of (4) does not contain the time explicitly, we obviously have:

$$P = 2 \int_{w_1}^{w_2} \frac{dw}{\sqrt{F(w)}} = \frac{4K(\kappa_0)}{\sqrt{2\mu(w_3 - w_1)}}, \quad \kappa_0^2 = \frac{w_2 - w_1}{w_3 - w_1}, \quad (7)$$

where  $K$  is Legendre's complete integral of the first kind, and can readily be obtained from tables. It will be seen that  $P$ , as so far defined, depends upon four parameters:  $w_1, w_2, \mu, a_3\lambda$ . However, by introducing  $\rho = 8\mu/a_3^2\lambda^2$ , it is fortunately possible to obtain  $a_3\lambda P$  as a function of only three parameters:  $w_1, w_2, \rho$ . As  $a_3\lambda = \alpha$  is relatively well determined in proving ground work, the conversion from  $\rho$  to  $\mu$ , from  $\alpha P$  to  $P$ , and *vice versa*, involves no difficulty.

TABLE I.

		$\theta_1$							Type
$\theta_2$		0°.	5°.	10°.	15°.	20°.	25°.	30°.	
0.0	0°	6.283	6.277	6.259	6.229	6.188	6.134	6.069	(+)
	4		6.264	6.236	6.197	6.146	6.083	6.009	(-)
	8		6.283	6.275	6.254	6.222	6.178	6.122	(+)
0.2	0°			6.206	6.157	6.097	6.025	5.941	(-)
	4			6.282	6.271	6.249	6.214	6.168	(-)
	8								
0.4	0°	6.623	6.616	6.594	6.557	6.506	6.441	6.363	
	4		6.600	6.568	6.521	6.460	6.385	6.296	(+)
	8		6.622	6.610	6.584	6.544	6.489	6.421	(-)
0.6	0°			6.533	6.475	6.404	6.319	6.221	(+)
	4			6.617	6.602	6.572	6.528	6.469	(-)
	8								
0.8	0°	7.025	7.016	6.988	6.943	6.880	6.800	6.704	
	4		6.998	6.959	6.901	6.827	6.737	6.629	(+)
	8		7.022	7.006	6.973	6.921	6.852	6.768	(-)
1.0	0°			6.917	6.849	6.763	6.662	6.545	(+)
	4			7.012	6.991	6.951	6.894	6.820	(-)
	8								
1.2	0°	7.510	7.498	7.463	7.405	7.326	7.226	7.106	
	4		7.477	7.429	7.358	7.266	7.153	7.022	(+)
	8		7.504	7.483	7.438	7.372	7.285	7.177	(-)
1.4	0°			7.379	7.296	7.191	7.068	6.926	(+)
	4			7.488	7.457	7.403	7.329	7.234	(-)
	8								
1.6	0°	8.112	8.096	8.050	7.975	7.872	7.743	7.591	
	4		8.070	8.009	7.919	7.801	7.660	7.495	(+)
	8		8.102	8.072	8.012	7.924	7.809	7.671	(-)
1.8	0°			7.949	7.844	7.713	7.559	7.383	(+)
	4			8.074	8.030	7.957	7.857	7.732	(-)
	8								
2.0	0°	8.886	8.865	8.802	8.700	8.562	8.390	8.191	
	4		8.832	8.751	8.632	8.477	8.291	8.079	(+)
	8		8.870	8.827	8.743	8.622	8.467	8.283	(-)
2.2	0°			8.675	8.539	8.369	8.170	7.945	(+)
	4			8.824	8.759	8.656	8.518	8.350	(-)
	8								
2.4	0°	9.935	9.904	9.814	9.668	9.471	9.234	8.962	
	4		9.861	9.748	9.581	9.366	9.112	8.827	(+)
	8		9.908	9.841	9.717	9.542	9.323	9.068	(-)
2.6	0°			9.645	9.460	9.229	8.960	8.662	(+)
	4			9.830	9.730	9.577	9.379	9.142	(-)
	8								
2.8	0°	11.471	11.423	11.280	11.051	10.752	10.396	10.001	
	4		11.360	11.188	10.934	10.612	10.239	9.830	(+)
	8		11.423	11.311	11.112	10.838	10.505	10.129	(-)
3.0	0°			11.039	10.764	10.425	10.039	9.606	(+)
	4			11.282	11.115	10.870	10.564	10.210	(-)
	8								

Table I. gives values of  $\alpha P$  corresponding to a complete practical range of  $w_1$ ,  $w_2$ ,  $\rho$ . While there may well be some question of the sufficient approximation of the assumptions for the extreme values of  $w_1$  and  $\rho$  used in the table, it may be pointed out that the stability will be poor for these extreme values and a close approximation is not needed.

As a matter of fact, the formula (7) was not used in computing this table, but for reasons which have no bearing

on the present discussion the following equivalent formula was used :

$$P = \frac{4(1+\kappa)K(\kappa)}{\sqrt{2\mu(w_3-w_1)}}, \quad \kappa = \frac{\sqrt{C}-1}{\sqrt{C}+1}, \quad C = \frac{w_3-w_1}{w_3-w_2}. \quad (8)$$

For use in computations it would be advisable to expand Table I. by interpolation, so that only first differences need be taken into account. Lagrange's interpolation formula is well adapted to this case.

In computing Table I., five-place cosines were used as initial data. Thenceforth six significant figures were carried, except in a very few cases (mostly for large  $\rho$ ) where cancellations reduced the number to five, once in an item. The  $4K(\kappa)$  changed very slowly, and it was interpolated by slide-rule apportionment of the first difference. Some difficulty was experienced with the calculating machine used, but the results when differenced (4 figures) were smooth out to the fifth difference at least. Any errors which may remain are almost certainly a matter of one or two units in the last place. In this connexion it may not be amiss to point out that present-day experimental errors in exterior ballistics do not justify more than three significant figures in this table.

*The Advance.*

From (3) we have :

$$\frac{d\psi}{dt} = \frac{c_2 - a_3\lambda w}{1-w^2}, \quad \dots \dots \dots (9)$$

and as  $d\psi/dw = \frac{d\psi/dt}{dw/dt}$ , we make use of (4) to obtain :

$$\Delta\psi = 2 \int_{w_1}^{w_2} \frac{d\psi}{dw} dw = 2 \int_{w_1}^{w_2} \frac{c_2 - a_3\lambda w}{(1-w^2)\sqrt{F(w)}} dw. \quad (10)$$

This integral normalizes into two of Legendre's complete elliptic integrals of the third kind. The result is :

$$\Delta\psi = \frac{4a_3\lambda}{(w_1+w_2)\sqrt{2\mu(w_3-w_1)}} \left\{ \left[ (1+w_2) \right. \right. \\ \left. \pm (1-w_1)\sqrt{\frac{1-w_2^2}{1-w_1^2}}\sqrt{R} \right] \cdot \Pi^1(n_1, \kappa_0) + \left[ (1-w_2) \right. \\ \left. \pm (1+w_1)\sqrt{\frac{1-w_2^2}{1-w_1^2}}\sqrt{R} \right] \cdot \Pi^1(n_2, \kappa_0) \left. \right\}, \quad (11)$$

where

$$n_1 = \frac{w_2-w_1}{1+w_1}, \quad n_2 = -\frac{w_2-w_1}{1-w_1}, \quad \kappa_0^2 = \frac{w_2-w_1}{w_3-w_1}.$$

From (7) and (11) we readily deduce the following limiting values for  $\mu=0$ :

Type.	$\Delta\psi$ .	$\alpha P$ .
$w_2 < 1$	$\begin{matrix} + & 2\pi \\ - & 0 \end{matrix}$	$\frac{\sqrt{2} \pi (w_1 + w_2)}{\sqrt{1 + w_1 w_2 \pm \sqrt{(1 - w_1^2)(1 - w_2^2)}}$
$w_2 = 1$	$\pi$	$\sqrt{2} \pi \sqrt{1 + w_1}$

$$\left. \vphantom{\begin{matrix} + & 2\pi \\ - & 0 \end{matrix}} \right\} \quad (12)$$

For  $w_1 = w_2 = w_0 < 1$ , we have

$$\left. \begin{aligned} P &= \frac{2\pi}{\sqrt{2\mu(w_3 - w_0)}}, \\ \Delta\psi &= \frac{\alpha P}{2w_0} (1 \pm \sqrt{R}). \end{aligned} \right\} \quad \dots \quad (13)$$

The complete elliptic integral of the third kind in (11) can be expressed in terms of integrals of the first and second kinds, which can be obtained from tables. For practical use, a table similar to Table I. can be prepared.

#### A DAMPING IMPULSE.

##### *Opposing the Wobble.*

We consider a momentary impulse opposing  $\omega$ , and seek to determine its effect on  $w_1$  and  $w_2$ . We first consider the case  $w_1 \neq w_2$ . We have from (4), when  $w = w_1$ :

$$F(w_1) = 2\mu w_1^3 - (c_1 + a_3^2 \lambda^2) w_1^2 + 2(c_2 a_3 \lambda - \mu) w_1 + c_1 - c_2^2 = 0. \quad (14)$$

As  $w_1 \neq w_2$ ,  $\partial F / \partial w_1 \neq 0$ , so by implicit function theory:

$$\frac{\delta w_1}{\delta c_1} = - \frac{\frac{\partial F}{\partial c_2} \frac{\delta c_2}{\delta c_1} + \frac{\partial F}{\partial c_1}}{\frac{\partial F}{\partial w_1}} = \frac{2(c_2 - a_3 \lambda w_1) \frac{\delta c_2}{\delta c_1} - (1 - w_1^2)}{6\mu w_1^2 - 2(c_1 + a_3^2 \lambda^2) w_1 + 2(c_2 a_3 \lambda - \mu)} \quad (15)$$

In order to evaluate  $\delta c_2 / \delta c_1$ , we use from (1), (2), (3):

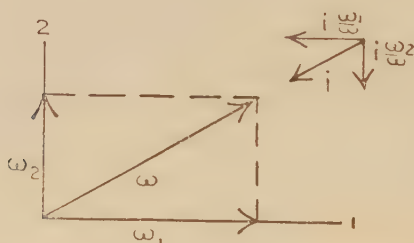
$$\left. \begin{aligned} c_2 &= w_1 \sin \theta \sin \phi + w_2 \sin \theta \cos \phi + a_3 \lambda w \\ &= \frac{\text{M. of M. about } O\eta}{A_1}, \\ c_1 &= w_1^2 + w_2^2 + 2\mu w = \frac{2 \text{ energy}}{A_1} - a_3^2 \lambda^2. \end{aligned} \right\} \quad (16)$$

We assume that the damping impulse acts oppositely to

the direction of motion, and that its line of action passes through O3 (from symmetry), but make no assumption as to the law of correspondence of the impulse to  $\omega$ . Consider the analogy of a falling body:  $2 \text{ energy}/m = v^2 + 2gh$ . A damping impulse would diminish  $v^2$ , but leave  $2gh$  unchanged. Thus the impulse considered will diminish  $\omega_1^2 + \omega_2^2$ , but leave  $2\mu v$  unchanged. Further, as the impulse is assumed to have its line of action through O3, it will change  $\omega_1 \sin \theta \sin \phi + \omega_2 \sin \theta \cos \phi$ , but not  $a_3 \lambda v$ . We may say that were the impulse great enough to arrest the wobble it would still leave  $2\mu v$  and  $a_3 \lambda v$  unaltered.

Consider the damping impulse to effect a slight diminution

Fig. 4.



of  $\omega$ , leaving  $\omega - i$ . Then, in connexion with fig. 4, we shall obviously have

before :	$\omega$	$\omega_1$	$\omega_2$	
after :	$\omega - i$	$\omega_1 \left(1 - \frac{i}{\omega}\right)$	$\omega_2 \left(1 - \frac{i}{\omega}\right)$ ,	
before :	$\omega_1 \sin \theta \sin \phi + \omega_2 \sin \theta \cos \phi + a_3 \lambda v$			
after :	$\left(1 - \frac{i}{\omega}\right) (\omega_1 \sin \theta \sin \phi + \omega_2 \sin \theta \cos \phi) + a_3 \lambda v$ <span style="float: right;"><math>c_2</math></span>			
before :	$\omega_1^2 + \omega_2^2 + 2\mu v$			
after :	$\left(1 - \frac{i}{\omega}\right)^2 (\omega_1^2 + \omega_2^2) + 2\mu v$ <span style="float: right;"><math>c_1</math></span>			

(neglecting the second order of the small quantity  $i/\omega$ ) :

$$\delta c_2 = -\frac{i}{\omega} (\omega_1 \sin \theta \sin \phi + \omega_2 \sin \theta \cos \phi),$$

$$\delta c_1 = -2 \frac{i}{\omega} (\omega_1^2 + \omega_2^2),$$

whence

$$\frac{\delta c_2}{\delta c_1} = \frac{1}{2} \frac{\omega_1 \sin \theta \sin \phi + \omega_2 \sin \theta \cos \phi}{\omega_1^2 + \omega_2^2} = \frac{1}{2} \frac{c_2 - a_3 \lambda v}{c_1 - 2\mu v}. \quad (17)$$



Substituting (17) in (15), making use of (5), (6), and observing the symmetry of  $w_1$  and  $w_2$ , we obtain :

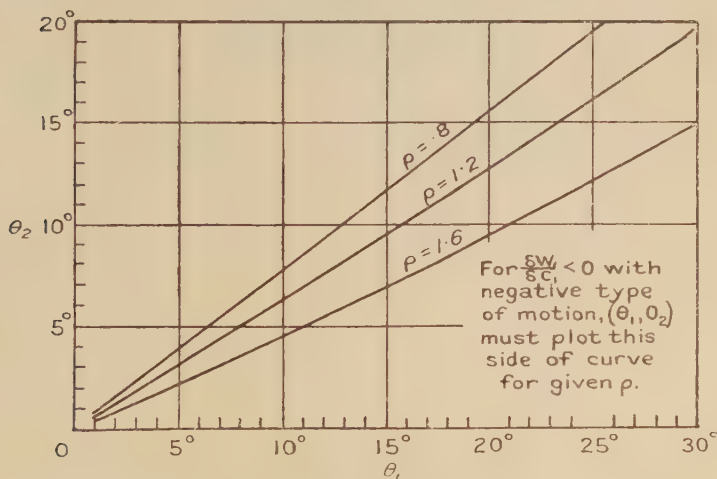
$$\left. \begin{aligned} \frac{\delta w_1}{\delta c_1} &= -[\sqrt{1-w_1^2} \sqrt{R} \pm \sqrt{1-w_2^2}] \cdot W_1, \\ \frac{\delta w_2}{\delta c_1} &= -[\sqrt{1-w_2^2} \sqrt{R} \pm \sqrt{1-w_1^2}] \cdot W_2, \\ W_i &= \frac{(-1)^i (w_i - w) a_3^2 \lambda^2 \sqrt{1-w_i^2} \sqrt{R}}{2\mu(w_1 + w_2)(w_2 - w_1)(w_3 - w_i)(c_1 - 2\mu w)} \end{aligned} \right\} \quad (18)$$

( $i = 1, 2$ ).

Under our hypotheses, when  $w_1 < w < w_2$ , we always have  $W_i > 0$ , finite. Hence the signs of the variations will be opposite to the signs of the brackets. As  $\delta c_1 < 0$ , the impulse will increase  $w_i$ , and hence decrease  $\theta_i$ , for a positive bracket.

For the upper signs, it is obvious that both brackets are positive. For the lower sign, it is also seen that the bracket for  $\delta w_1 / \delta c_1$  is positive for  $(1 - w_2)$  sufficiently small

Fig. 5.



or zero. We determine the zeroes of this bracket to be  $w_2 = w_1 + 2\mu(1 - w_1^2) / a_3^2 \lambda^2$  and  $w_2 = -w_1$ ; the latter value being excluded by hypothesis. Thus, for the lower sign, the bracket for  $\delta w_1 / \delta c_1$  will be positive if

$$w_2 = 1 \quad \text{or} \quad w_2 > w_1 + \frac{2\mu}{a_3^2 \lambda^2} (1 - w_1^2). \quad . \quad . \quad (19)$$

In fig. 5 is given a graphic means of determining whether  $\theta_1, \theta_2, \rho$  fulfil the second of (19), and Table II. gives the values from which it was plotted. Several experimental values were plotted, and all found to fulfil the condition. The condition  $w_2 = w_1 + 2\mu(1 - w_1^2)/a_3^2\lambda^2$  corresponds to a motion of negative type B (fig. 3), the branches of the cusp being tangent. The bracket for  $\delta w_2/\delta c_1$  has no zeroes under the hypotheses.

TABLE II.

$\rho$ .	$\theta_1 \dots 5^\circ$ .	$10^\circ$ .	$15^\circ$ .	$20^\circ$ .	$25^\circ$ .	$30^\circ$ .
1.6	2°25	4°53	6°91	9°43	12°10	14°96
1.2	3°16	6°35	9°58	12°88	16°28	19°76
0.8	3°86	7°75	11°66	15°60	19°60	23°63

By examining  $W_i$ , we see that  $\delta w_i/\delta c_1 = 0$  for  $w = w_i$ , and  $\delta w_2/\delta c_1 = 0$  for  $w_2 = 1$ . Thus, an impulse has no effect on  $w_i$  when occurring at  $w = w_i$ ; and an impulse has no tendency (under the hypotheses) to increase a zero minimum yaw. When the minimum yaw is decreasing, it will approach 0 asymptotically.

We now examine the case  $w_1 = w_2 = w_0 < 1$ . We cannot use (14), for, due to the double root,  $\partial F/\partial w_0 = 0$ ; but this last fact furnishes us the necessary relation for forming our implicit function derivatives. We have:

$$F_1(w_0) = 6\mu w_0^2 - 2(c_1 + a_3^2\lambda^2)w_0 + 2(c_2 a_3\lambda - \mu) = 0. \quad (20)$$

As  $w_0 < 1 < w_3$ ,  $\partial F_1/\partial w_0 \neq 0$ ; and we proceed as before, obtaining:

$$\left. \begin{aligned} \frac{\delta w_0}{\delta c_1} &= [\sqrt{R} \pm 1] \cdot W_0, \\ W_0 &= \frac{a_3^2\lambda^2(1 - w_0^2)\sqrt{R}}{8\mu w_0(w_3 - w_0)(c_1 - 2\mu w_0)}. \end{aligned} \right\} \dots (21)$$

Under our hypotheses, we always have  $W_0 > 0$ , finite. As  $\sqrt{R} < 1$ , the sign of 1 in the bracket obviously predominates. Hence for the upper sign  $\theta_0$  decreases, while for the lower sign it increases.

In all cases, the upper sign (+) corresponds to the loop-around-the-pole (+) type of motion; the lower sign (-) to the negative types.

Summary :—

Angle.	Type of Motion.	Effect on Angle.
$\theta_1$	$\left\{ \begin{array}{l} + \\ - \end{array} \right\}$	decreases
	$\left\{ \begin{array}{l} > w_1 + 2\mu(1-w_1^2)/a_3^2\lambda^2 \\ = 1 \\ \text{not} \end{array} \right\}$	decreases
		decreases
$\theta_2$	$\left\{ \begin{array}{l} + \\ - \end{array} \right\}$	increases
		decreases
$\theta_0$	$\left\{ \begin{array}{l} + \\ - \end{array} \right\}$	decreases
		increases

*Opposing the Spin.*

By an analogous process we arrive at :

$$\left. \begin{aligned} \frac{\delta w_1}{\delta a_3} &= [\sqrt{1-w_1^2} \pm \sqrt{1-w_2^2} \sqrt{R}] V_1, \\ \frac{\delta w_2}{\delta a_3} &= [\sqrt{1-w_2^2} \pm \sqrt{1-w_1^2} \sqrt{R}] V_2, \\ V_i &= \frac{(-1)^i (w_i - w) a_3 \lambda^2 \sqrt{1-w_1^2}}{\mu(w_1 + w_2)(w_2 - w_1)(w_3 - w_i)}; \end{aligned} \right\} \quad (22)$$

and for  $w_1 = w_2 = w_0 < 1$  :

$$\left. \begin{aligned} \frac{\delta w_0}{\delta a_3} &= [1 \pm \sqrt{R}] V_0, \\ V_0 &= \frac{a_3 \lambda^2 (1 - w_0^2)}{2\mu w_0 (w_3 - w_0)}. \end{aligned} \right\} \quad (23)$$

The discussion is altogether similar to the preceding, so we merely give :

Summary :—

Angle.	Type of Motion.	Effect on Angle.
$\theta_1$	$\pm$	increases
$\theta_2$	$\left\{ \begin{array}{l} + \\ - \end{array} \right\}$	increases
	$R < \frac{1-w_2^2}{1-w_1^2}$	decreases
	$R > \frac{1-w_2^2}{1-w_1^2}$	increases
$\theta_0$	$\pm$	increases

*Decreasing  $\mu$ .*

The couple coefficient,  $\mu$ , will decrease with decreasing velocity of translation, and with decreasing air density. It will therefore decrease, in an ordinary trajectory, at

least until the apex is passed. On the descending branch, the density will presumably increase, beginning at the apex; but the tangential velocity will not begin to increase until the apex has been left somewhat behind. In an ordinary trajectory, the decrease in  $\mu$  during the first part will be proportionately much greater than the increase during the last part. We consider an impulsive decrease of  $\mu$ , and proceed as before, obtaining :

$$\left. \begin{aligned} \frac{\delta w_i}{\delta \mu} &= -(-1)^i \frac{(1-w_i^2)(w_i-w)}{\mu(w_2-w_1)(w_3-w_i)} \quad (i=1, 2), \\ \frac{\delta w_0}{\delta \mu} &= \frac{w_0^2}{2\mu(w_3-w_0)} \quad (w_1=w_2=w_0 < 1). \end{aligned} \right\} \quad (24)$$

From (24) it is evident that, under our hypotheses, an impulsive decrease in  $\mu$ , for either a positive or negative type of motion, decreases  $\theta_1$  and  $\theta_2$ , unless the impulse occurs at the corresponding value of  $\theta$ ; that the effect on  $\theta_2$  is zero for  $\theta_2=0$ ; and that  $\theta_0$  is always increased.

#### CONTINUOUS DAMPING.

##### *Opposing the Wobble.*

Introducing now a continuous damping force, oppositely directed to and proportional to  $\omega$ , equations (1) are modified to become

$$\left. \begin{aligned} \frac{d\omega_1}{dt} - (1-\lambda)\omega_2\omega_3 &= -\mu \sin \theta \cos \phi - \nu\omega_1, \\ \frac{d\omega_2}{dt} + (1-\lambda)\omega_1\omega_3 &= -\mu \sin \theta \sin \phi - \nu\omega_2, \\ \text{(the remaining equations, and the initial} & \end{aligned} \right\} \quad (25)$$

conditions, unaltered).

From the first two and fifth of (25) we obtain, after integration :

$$\sin^2 \theta \left( \frac{d\psi}{dt} \right)^2 + \left( \frac{d\theta}{dt} \right)^2 = \omega_0^2 e^{-2\nu t} + 2\mu e^{-2\nu t} \int_0^t e^{2\nu t} \sin \theta \frac{d\theta}{dt} dt. \quad (26) *$$

From the equality of the rate of change of moment of momentum about  $O\eta$  to the moments of the external forces, we obtain, after integration :

$$\sin^2 \theta \frac{d\psi}{dt} = \left[ \sin^2 \theta \frac{d\psi}{dt} \right]_0 + a_3 \lambda e^{-\nu t} \int_0^t e^{\nu t} \sin \theta \frac{d\theta}{dt} dt. \quad (27) *$$

\* These equations are taken from my notes of Professor Moulton's lectures.

We make use of integration by parts to rearrange (26), (27):

$$\left. \begin{aligned} & \sin^2 \theta \left( \frac{d\psi}{dt} \right)^2 + \left( \frac{d\theta}{dt} \right)^2 + 2\mu \cos \theta \\ &= (\omega_0^2 + 2\mu \cos \theta_0) e^{-2vt} + 4\nu\mu e^{-2vt} \int_0^t e^{2vt} \cos \theta \, dt, \\ & \sin^2 \theta \frac{d\psi}{dt} + a_3 \lambda \cos \theta \\ &= \left[ \sin^2 \theta \frac{d\psi}{dt} + a_3 \lambda \cos \theta \right]_0 e^{-vt} + \nu a_3 \lambda e^{-vt} \int_0^t e^{vt} \cos \theta \, dt. \end{aligned} \right\} \quad (28)$$

Now define :

$$\left. \begin{aligned} c_1^0 &= (\omega_0^2 + 2\mu \cos \theta_0), \\ c_2^0 &= \left[ \sin^2 \theta \frac{d\psi}{dt} + a_3 \lambda \cos \theta \right]_0, \\ c_1 &= c_1^0 e^{-2vt} + 4\nu\mu e^{-2vt} \int_0^t e^{2vt} w \, dt, \\ c_2 &= c_2^0 e^{-vt} + \nu a_3 \lambda e^{-vt} \int_0^t e^{vt} w \, dt, \\ & \quad w = \cos \theta, \end{aligned} \right\} \quad \dots \quad (29)$$

where, evidently,  $c_1, c_2$  are not constants. They will, however, play rôles formally analogous to the  $c_1, c_2$  of undamped motion; and  $c_1^0, c_2^0$  have the values of  $c_1, c_2$  of undamped motion.

Substituting (29) in (28) and eliminating  $d\psi/dt$  between the two equations (28), we arrive at an equation formally the same as (4) :

$$\begin{aligned} \left( \frac{dw}{dt} \right)^2 &= 2\mu w^3 - (c_1 + a_3^2 \lambda^2) w^2 + 2(c_2 a_3 \lambda - \mu) w + c_1 - c_2^2 = F(w) \\ &= 2\mu(w - w_1)(w - w_2)(w - w_3) \quad w_1 \leq w_2 \leq w_3, \dots \quad (30) \end{aligned}$$

where, evidently,  $w_1, w_2, w_3$  are no longer constants. However,  $dw/dt$  and  $F(w)$ , formally a cubic, vanish together when the oscillation in yaw reverses. Now, at any instant of time, even when  $dw/dt \neq 0$ ,  $c_1$  and  $c_2$  have definite values which define uniquely the roots of  $F(w)$ . Hence  $F(w_i) = 0$  ( $i=1, 2, 3$ ) at any instant of time. Fixing our attention on  $w_i$  ( $i=1, 2$ ), and supposing all the roots distinct, we have,



by implicit function theory :

$$\left. \begin{aligned} \frac{dw_i}{dt} &= - \frac{\frac{\partial F}{\partial c_1} \frac{dc_1}{dt} + \frac{\partial F}{\partial c_2} \frac{dc_2}{dt}}{\frac{\partial F}{\partial w_i}} \\ &= (-1)^i \frac{(1-w_i^2) \frac{dc_1}{dt} - 2(c_2 - a_3 \lambda w_i) \frac{dc_2}{dt}}{2\mu(w_3 - w_i)(w_2 - w_1)} \quad (i=1, 2), \end{aligned} \right\} \quad (31)$$

where we have made use of the relations (5). From (29) it follows that

$$\left. \begin{aligned} \frac{dc_1}{dt} &= -2\nu c_1^0 e^{-2\nu t} - 8\nu^2 \mu e^{-2\nu t} \int_0^t e^{2\nu t} w dt + 4\nu \mu w \\ &= 2\nu(2\mu w - c_1), \\ \frac{dc_2}{dt} &= -\nu c_2^0 e^{-\nu t} - \nu^2 a_3 \lambda e^{-\nu t} \int_0^t e^{\nu t} w dt + \nu a_3 \lambda w \\ &= \nu(a_3 \lambda w - c_2). \end{aligned} \right\} \quad (32)$$

On substituting (32) in (31) we have :

$$\frac{dw_i}{dt} = (\nu - 1) \frac{(c_2 - a_3 \lambda w_i)(c_2 - a_3 \lambda w) - (1 - w_i^2)(c_1 - 2\mu w)}{\mu(w_3 - w_i)(w_2 - w_1)} \quad (i=1, 2) \quad (33)$$

Making further use of (5), (6), and writing  $w_3$ , for brevity, in place of its expanded form in (6), though understanding the substitution to have been made, (33) becomes :

$$\frac{dw_i}{dt} = \nu(-1)^i \frac{a_3^2 \lambda^2 (1 - w_i^2) R \pm \sqrt{(1 - w_1^2)(1 - w_2^2)} \sqrt{R}}{\mu(w_1 + w_2)(w_2 - w_1)(w_3 - w_i)} (w_i - w) \quad (i=1, 2). \quad (34)$$

We denote the general  $w$  now by  $w_0$ , and adjoin (30) to (34), when we have a system of differential equations of the form :

$$\frac{dw_i}{dt} = \nu f_i(w_j, \nu, t) \quad (i, j = 0, 1, 2). \quad (35)$$

By the general theory of differential equations, (35) can be solved in the form :

$$w_i = w_i^0 + w_i^1 \nu + w_i^2 \nu^2 + \dots \quad (i = 0, 1, 2), \quad (36)^*$$

which is valid for  $\nu$  or  $t$  sufficiently small (Poincaré ;

\* The superscripts on the  $w$ 's (0, 1, 2, ...) are not exponents, but functional indices corresponding to the powers of  $\nu$ .

Moulton). The  $w_i^k$  are functions of  $t$ , given by

$$\left. \begin{aligned} w_i^0 &= w_i(0), \\ w_i^1 &= \int_0^t f_i(w_j^0, 0, t) dt, \\ w_i^2 &= \int_0^t \left[ \frac{\partial f_i}{\partial v} + \sum_{j=0}^2 \frac{\partial f_i}{\partial w_j} w_j^1 \right] dt, \\ &\dots \dots \dots \end{aligned} \right\} \dots \dots (37)$$

It follows from (37) that  $v \frac{dw_i^1}{dt}$  ( $i=1, 2$ ) will be the same in form as (34), with the variable  $w_1, w_2$  in (34) assigned their initial values, and the general  $w$  in (34) tracing the values in undamped motion. We evaluate (36) to the first power in  $v$ ; performing the integration indicated in the second of (37), for one period, as a power series in  $\kappa$  (defined in equation 8) to the second degree. This gives an expression for  $\Delta w_i$  ( $i=1, 2$ ) which should be sufficiently accurate for experimental purposes. A similar procedure yields  $\Delta w_0$ . The results are :

$$\left. \begin{aligned} \frac{\alpha}{v} \Delta w_1 &= \frac{4(1 + \frac{3}{2}\kappa + \kappa^2) \alpha P}{\rho(w_1 + w_2)} \cdot \frac{(1 - w_1^2) R \pm \sqrt{(1 - w_1^2)(1 - w_2^2)} \sqrt{R}}{w_3 - w_1}, \\ \frac{\alpha}{v} \Delta w_2 &= \frac{4(1 - \frac{1}{2}\kappa) \alpha P}{\rho(w_1 + w_2)} \cdot \frac{(1 - w_2^2) R \pm \sqrt{(1 - w_1^2)(1 - w_2^2)} \sqrt{R}}{w_3 - w_2}, \\ \frac{\alpha}{v} \Delta w_0 &= \frac{2\pi \sqrt{2} w_0^2 (1 - w_0^2) (R \pm \sqrt{R})}{\left[ (1 + w_0^2) \pm (1 - w_0^2) \sqrt{R} - \frac{\rho w_0}{4} (1 + 3w_0^2) \right]^2} \end{aligned} \right\} (38)$$

The  $P$  in (38) will be, for practical purposes, the  $P$  of undamped motion. To determine it exactly we may proceed as follows. From (7) we can derive an equation of the form :

$$\frac{dP}{dt} = v f(w_i, v, t) \quad (i=1, 2), \dots \dots (39)$$

to which we adjoin (35), and solve as before :

$$P = P^0 + P^1 v + P^2 v^2 + \dots, \dots \dots (40)$$

where

$$\left. \begin{aligned} P^0 &= P(0), \\ P^1 &= \int_0^t f(w_i^0, 0, t) dt, \\ &\dots \dots \dots \end{aligned} \right\} \dots \dots (41)$$

Thus, for a complete oscillation (for use in 38) :

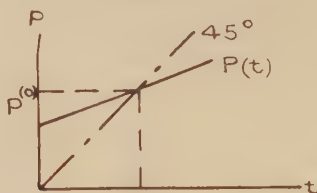
$$P = P^0 + v \int_0^P f(w_i^0, 0, t) dt + \dots \quad (\text{see fig. 6}). \quad (42)$$

On deriving with respect to  $P$ , we obtain

$$1 = \nu f(w_i^0, 0, P) + \dots, \dots \dots (43)$$

which can be solved for  $P$ . However, since  $f$  does not contain  $P$  explicitly, it follows that  $P = P^0$  to the first power in  $\nu$ .

Fig. 6.



In Table III. are given values of  $\frac{\alpha}{\nu} \Delta w_i$  ( $i=0, 1, 2$ ), and

TABLE III.

$$\frac{\alpha}{\nu} \Delta w_0 \quad (w_1 = w_2 = w_0).$$

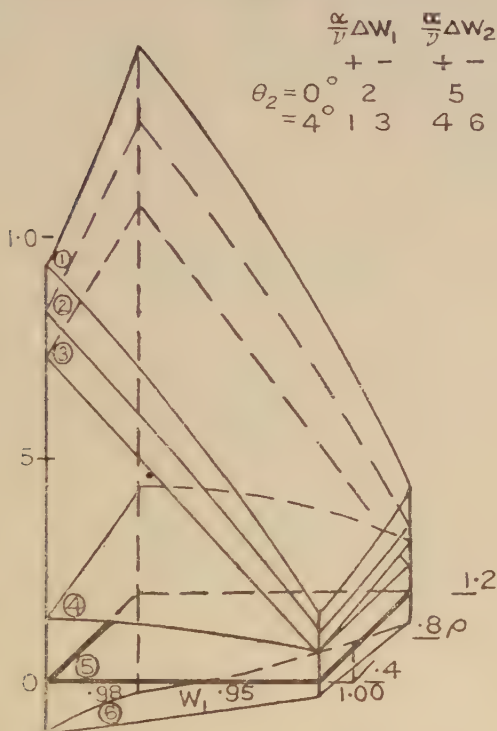
$\rho$ .	Type.	$w_0 \dots 10^\circ$ .	$20^\circ$ .	$30^\circ$ .
0.4	(+)	.2157	.7450	1.3097
	(-)	-.0124	-.0476	-.0994
0.8	(+)	.2659	.8863	1.4876
	(-)	-.0351	-.1311	-.2639
1.2	(+)	.3577	1.1195	1.7446
	(-)	-.0844	-.3005	-.5654

$$\frac{\alpha}{\nu} \Delta w_i \quad (i=1, 2).$$

$\rho$ .	$\theta_1 \dots$	$10^\circ$ .	$20^\circ$ .		$30^\circ$ .		$\theta_2$ .
0.4		.1052	0	.4006	0	.8320	0
0.8		.1210	0	.4550	0	.9260	0
1.2		.1469	0	.5399	0	1.0643	0
	Type.	(1)	(2)	(1)	(2)	(1)	(2)
0.4	(+)	.1508	.0636	.4812	.1072	.9285	.1412
	(-)	.0585	-.0305	.3156	-.0761	.7229	-.1166
0.8	(+)	.1812	.0813	.5596	.1355	1.0506	.1782
	(-)	.0590	-.0436	.3438	-.1029	.7885	-.1531
1.2	(+)	.2357	.1151	.6891	.1907	1.2347	.2437
	(-)	.0548	-.0702	.3792	-.1547	.8732	-.2198
		(1)	(2)	(1)	(2)	(1)	(2)
0.4	(+)	.1946	.1579	.5566	.2376	1.0172	.3020
	(-)	.0113	-.0270	.2275	-.1199	.6083	-.2046
0.8	(+)	.2385	.1966	.6560	.2979	1.1610	.3746
	(-)	-.0037	-.0478	.2279	-.1690	.6405	-.2751
1.2	(+)	.3187	.2687	.8285	.4077	1.3811	.5000
	(-)	-.0382	-.0919	.2109	-.2656	.6656	-.4053

a part of them are also portrayed in fig. 7. The table can be interpolated for practical use. Graphic interpolation should be sufficiently accurate in view of the probably approximate nature of the physical law assumed.

Fig. 7.



Starting with assumed, or observed, values of  $w_1, w_2, \alpha, \rho, v$ , and knowing or assuming the type of motion, curves of  $w_1, w_2$  can be constructed period by period, at the beginning of each new period re-entering Table III. (or the equivalent curves) to redetermine  $\Delta w_1, \Delta w_2$  for that period. It will be noted that the surfaces in fig. 7 are approximately plane, so that the law for  $dw_i/dt$  is approximately exponential\*. This process, suitably modified, should furnish a convenient means for determining  $v$  from observed data; the  $\Delta w_i$  due to decrease of  $\omega_3$  and  $\mu$  being regarded as negligible.

\* In computing  $\Delta w_1$  for a fixed  $w_2 < 1$ , the values for  $\Delta w_1$  should not converge on zero; for a  $w_1 > w_2$  violates the definitions.

*Other Forms of Damping.*

The method used for determining  $\Delta w_i$  for the wobble-damping is applicable to the  $\omega_3$  and  $\mu$  forms of damping, but it is probably futile to carry it through until the experimental technique has been sufficiently developed to detect these probably relatively small effects. The method will very likely also prove effective in examining the effect of the curvature of the trajectory on stability.

University of Chicago,  
9th May, 1924.

LXIX. *Potential of Systems of Electric Charges.*

By C. N. WALL \*.

## TABLE OF CONTENTS.

	Page
I. Introduction .....	660
II. Potential of a Line System of Charges .....	662
III. Potential of a Space System of Charges: Expansion in a Double Fourier Series .....	665
IV. Potential of a Space System of Charges: Expansion in a Series of Spherical Harmonics .....	678
V. Potential of a Space System of Charges: Expansion in a Series of Cylindrical Harmonics .....	686
VI. Calculation of Potential for a Special System .....	687
VII. Conclusion .....	688

I. *Introduction.*

THE theory of crystal structure and space lattices suggests the problem of determining the potential due to an infinite set of positive and negative point charges distributed in certain space configurations. Indeed, the theory can hardly be called complete without a solution of this problem since, in one sense, a crystal may be regarded as a set of electric doublets having a certain arrangement in space.

The problem of determining the potential of such a system of charges has been attacked, with more or less success, by Born †, Kornfeld ‡, Madelung §, Ewald ||, and others.

\* Communicated by Professor Jakob Kunz, Ph.D.

† M. Born, *Ency. d. math. Wiss.* v. 25; *Dynamik der Kristallgitter*, ii. § 25; M. Born and H. Kornfeld, *Phys. Zeit.* xxiv. p. 121 (1923).

‡ H. Kornfeld, *Zeit. f. Phys.* xxii. p. 27 (1924).

§ E. Madelung, *Phys. Zeit.* xix. p. 524 (1919).

|| P. P. Ewald, *Ann. d. Phys.* lxiv. p. 253 (1921).



In attacking the problem, various methods of procedure have been used. One method consists in setting up a double Fourier series with periodic properties appropriate to the given system of charges. The coefficients of this series are chosen in such a way that the function represented by the series satisfies Laplace's equation and also the boundary conditions required by the system.

In another method, use is made of the relation,

$$\frac{1}{R} = \frac{1}{\sqrt{\pi}} \int_0^{\infty} e^{-R^2 t} \frac{dt}{\sqrt{t}}.$$

This relation usually enables one to express the potential of the system in the form of a definite integral of Theta-functions. Although this form is very compact, it is not a convenient one for purposes of computation.

A third method consists in associating with each potential term an exponential factor which serves to wipe out the effect of charges very distant from the origin of the system. This method applied to the theory of crystal structure necessitates the fading away of the crystal as the distance from a fixed origin in the crystal is increased.

The defect which appears to be common to all of these methods is their speciality; that is, they lead to only one type of expansion for the potential in question. Now it is known that every solution of Laplace's equation which is analytic in a certain region can be expressed in that region as a series of spherical harmonics. The potential can also be expressed in a series of cylindrical harmonics. It is true that such expansions may not be natural ones for this problem, but one cannot be certain of that fact until one has obtained the expansions.

The purpose of this paper is to indicate a method which leads to expansions of the potential, due to certain systems of point charges, into double Fourier series, into series of spherical harmonics, and into series of cylindrical harmonics.

The method devised is based upon the possibility of expressing the potential due to a point charge as a special form of Whittaker's general solution of Laplace's equation\*. After so expressing the potential, several courses of procedure are open, each of which leads to a different type of expansion.

Since the method which we are going to employ is a synthetic method, that is, the expansions are built up step by step, it is rather difficult to make the argument entirely rigorous from the standpoint of analysis. But the functions

\* Whittaker, *Math. Ann.* vol. lvii. p. 333 (1902); Whittaker & Watson, *Modern Analysis*, 3rd ed., Chap. xviii.

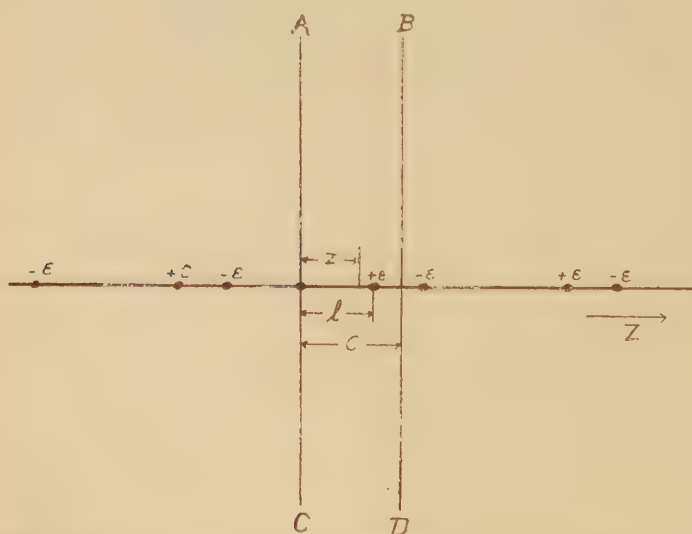
employed are those of applied mathematics whose behaviour seldom causes any trouble, as long as operations upon them are justified physically. Very likely the easiest way in which to make the argument entirely rigorous would be to start with the various expansions for the potential and then to show that they actually represent the potential in question. But such a process tells us nothing of the method of obtaining the expansions. For this reason we shall adopt the synthetic and more heuristic method of determining the potential.

In some cases it is of considerable value to know the potential due to a single line of point charges. As a preliminary exercise we shall treat this case. After that we shall develop a method of expanding the potential, due to an infinite set of charges distributed in space, into a double Fourier series, a series of spherical harmonics, and a series of cylindrical harmonics.

## II. Potential of a Line System of Electric Charges.

Let us consider an infinite system of positive and negative point charges distributed along the  $z$ -axis as shown in fig. 1.

Fig. 1.



We wish to determine the potential at any point  $z$  in a certain interval on the  $z$ -axis, due to these point charges.

Let  $0 \leq \frac{z}{l} \leq 1 - \delta$ , where  $\delta$  is an arbitrarily small positive

number. Then the potential at any point  $z$  in this interval may be written in the form

$$\begin{aligned}
 U &= \epsilon \left\{ \frac{1}{l-z} - \frac{1}{l+z} + \frac{1}{2c-l+z} - \frac{1}{2c-l-z} \right. \\
 &\quad + \sum_{n=1}^{\infty} \left[ \frac{1}{l-z+n2c} - \frac{1}{l+z+n2c} \right. \\
 &\quad \left. \left. + \frac{1}{-l+z+(n+1)2c} - \frac{1}{-l-z+(n+1)2c} \right] \right\} \\
 &= \frac{\epsilon}{2c} \left\{ \frac{2c}{l-z} - \frac{2c}{l+z} + \frac{2c}{2c-l+z} - \frac{2c}{2c-l-z} \right. \\
 &\quad + \sum_{n=1}^{\infty} \left[ - \frac{\frac{l-z}{2c}}{n \left( \frac{l-z}{2c} + n \right)} \right. \\
 &\quad \left. + \frac{\frac{l+z}{2c}}{n \left( \frac{l+z}{2c} + n \right)} - \frac{\frac{2c-l+z}{2c}}{n \left( \frac{2c-l+z}{2c} + n \right)} + \frac{\frac{2c-l-z}{2c}}{n \left( \frac{2c-l-z}{2c} + n \right)} \right] \right\}.
 \end{aligned}
 \tag{1}$$

In order to sum the series appearing in equation (1) we make use of the logarithmic derivative of the Gamma-function. It may be expressed by the equation\*

$$\frac{d}{dw} [\log \Gamma(w)] = -\gamma - \frac{1}{w} + w \sum_{n=1}^{\infty} \frac{1}{n(w+n)},$$

where  $\gamma$  is Euler's constant. It follows at once that

$$\epsilon \frac{d}{dz} \left[ \log \Gamma \left( \frac{l \pm z}{2c} \right) \right] = \pm \frac{\epsilon}{2c} \left\{ -\gamma - \frac{2c}{l \pm z} + \sum_{n=1}^{\infty} \frac{\frac{l \pm z}{2c}}{n \left( \frac{l \pm z}{2c} + n \right)} \right\}$$

and

$$\begin{aligned}
 \epsilon \frac{d}{dz} \left[ -\log \Gamma \left( \frac{2c-l \pm z}{2c} \right) \right] \\
 = \mp \frac{\epsilon}{2c} \left\{ -\gamma - \frac{2c}{2c-l \pm z} + \sum_{n=1}^{\infty} \frac{\frac{2c-l \pm z}{2c}}{n \left( \frac{2c-l \pm z}{2c} + n \right)} \right\}
 \end{aligned}$$

\* *L. c.*, Chap. 12, § 12.16.

It may be noted that the sum of the right-hand members of the above four equations is identical with the right-hand member of equation (1), provided term by term addition is allowed. This is certainly justified because of the restriction placed on  $z$ . Therefore  $U$  is given by the equation

$$U = \epsilon \frac{d}{dz} \left[ \log \left\{ \frac{\Gamma\left(\frac{l-z}{2c}\right) \Gamma\left(\frac{l+z}{2c}\right)}{\Gamma\left(\frac{2c-l-z}{2c}\right) \Gamma\left(\frac{2c-l+z}{2c}\right)} \right\} \right]. \quad (2)$$

Obviously equation (2) may be written in the form \*

$$U = \frac{\epsilon}{2c} \left\{ - \frac{\Gamma'\left(\frac{l-z}{2c}\right)}{\Gamma\left(\frac{l-z}{2c}\right)} + \frac{\Gamma'\left(\frac{l+z}{2c}\right)}{\Gamma\left(\frac{l+z}{2c}\right)} - \frac{\Gamma'\left(\frac{2c-l-z}{2c}\right)}{\Gamma\left(\frac{2c-l-z}{2c}\right)} + \frac{\Gamma'\left(\frac{2c-l+z}{2c}\right)}{\Gamma\left(\frac{2c-l+z}{2c}\right)} \right\}. \quad (3)$$

If we define the  $\Psi$ -function of  $w$  as  $\frac{\Gamma'(w)}{\Gamma(w)}$  then we obtain

$$U = \frac{\epsilon}{2c} \left\{ -\Psi\left(\frac{l-z}{2c}\right) + \Psi\left(\frac{l+z}{2c}\right) - \Psi\left(\frac{2c-l-z}{2c}\right) + \Psi\left(\frac{2c-l+z}{2c}\right) \right\}. \quad (4)$$

The case for  $1 + \delta \leq \frac{z}{l} \leq \frac{c}{l}$  may be developed in the same manner. Knowing  $U$  for the two intervals we can determine  $U$  along the entire  $z$ -axis, except in the immediate neighbourhood of the point charges, by the relations

$$U(z) = -U(-z) \quad \text{and} \quad U(z \pm 2c) = U(z).$$

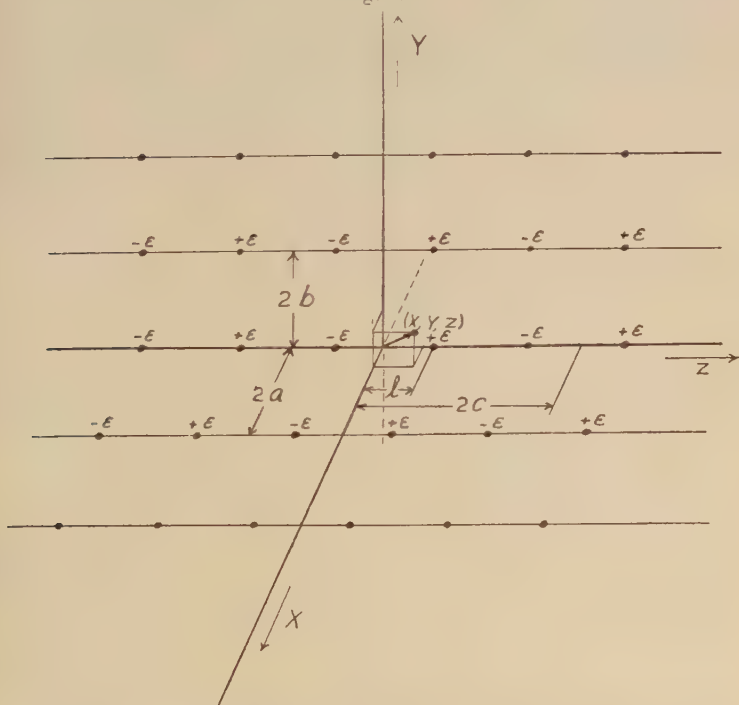
Evidently, the problem which we have just solved is identical with that of determining the potential along the  $z$ -axis due to a point charge of strength  $\epsilon$  placed between two parallel infinite conducting planes, at distances  $l$  and  $c-l$  from the planes.

\* J. H. Jeans, 'Electricity and Magnetism,' p. 291, prob. 44.

III. *Potential of a Space System of Electric Charges :  
Expansion in a Double Fourier Series.*

Let us consider an infinite set of positive and negative point charges of strength  $\epsilon$  distributed throughout space in the manner shown in fig. 2. The positions of all of the positive charges and of all of the negative charges are given respectively by the rectangular coordinates,  $(\lambda 2a, \mu 2b, \nu 2c + l)$ , and  $(\lambda 2a, \mu 2b, \nu 2c - l)$ , where  $\lambda, \mu$ , and  $\nu$  are allowed to run over all of the positive and negative integers including zero.

Fig. 2.



We desire to determine the potential of this system at any point in space  $(x, y, z)$  except in the immediate neighbourhoods of the point charges. In order to do this we shall first determine the potential of the system with  $x, y$ , and  $z$  confined to the intervals

$$0 \leq \frac{x}{a} \leq 1, \quad 0 \leq \frac{y}{b} \leq 1, \quad \text{and} \quad 0 \leq \frac{z}{l} \leq 1 - \delta,$$

where  $\delta$  is an arbitrarily small positive number. Thi



amounts to confining the point  $(x, y, z)$  to a small rectangular parallelepiped enclosed by the planes  $x=a$ ,  $x=0$ ,  $y=b$ ,  $y=0$ ,  $\frac{z}{l}=1-\delta$ , and  $z=0$ . After having determined the potential for points within this region it is an easy matter to do the same for the case where  $x$  and  $y$  are confined to the same intervals as before but  $z$  is confined to the interval  $1+\delta \leq \frac{z}{l} \leq \frac{c}{l}$ . Then, by certain obvious relations,

we can use these results to ascertain the potential at any desired point in space except in the immediate neighbourhoods of the point charges.

First, let us consider any positive charge to the right of the  $x$ - $y$ -plane and the corresponding negative charge to the left. The potential of these two type charges at a point  $(x, y, z)$  within the elementary parallelepiped we shall designate by  $V_{\lambda, \mu, \nu}$ , where  $V_{\lambda, \mu, \nu}$  is given by the equation

$$V_{\lambda, \mu, \nu} = \epsilon \left\{ \frac{1}{[(\nu 2c + l - z)^2 + (\lambda 2a - x)^2 + (\mu 2b - y)^2]^{1/2}} - \frac{1}{[(\nu 2c + l + z)^2 + (\lambda 2a - x)^2 + (\mu 2b - y)^2]^{1/2}} \right\}. \quad (1)$$

In equation (1)  $\nu$  may be any positive integer including zero, while  $\lambda$  and  $\mu$  may be any positive or negative integers including zero. By summing  $V_{\lambda, \mu, \nu}$  with respect to  $\nu$  from 0 to  $\infty$  and with respect to  $\lambda$  and  $\mu$  from  $-\infty$  to  $+\infty$ , we obtain the potential at  $(x, y, z)$  due to all of the positive charges to the right and all of the negative charges to the left of the  $x$ - $y$ -plane. If we then carry out the same process for the case of all of the negative charges to the right and all of the positive charges to the left of the  $x$ - $y$ -plane, we can obtain the entire potential. We shall proceed to carry out the first case in some detail.

The expression for  $V_{\lambda, \mu, \nu}$ , given in equation (1), is not in a form amenable to summation. It can be expressed in the desired form by means of the relation

$$\frac{1}{[z_1^2 + x_1^2 + y_1^2]^{1/2}} = \frac{1}{2\pi} \int_{-\pi}^{\pi} \frac{du}{z_1 + i(x_1 \cos u + y_1 \sin u)}, \quad (2)$$

where  $z_1 > 0$  \*. It is a simple matter to demonstrate the validity of equation (2) by the use of contour integration and the theory of residues. By the substitution  $\phi = u - \alpha$ ,

\* *L. c.* p. 391, ex. 1.

where  $\cos \alpha = \frac{x_1}{\sqrt{x_1^2 + y_1^2}}$ , and then the further substitution  $t = e^{i\phi}$ , where  $t$  is a complex variable whose modulus is unity, we obtain

$$\int_{-\pi}^{\pi} \frac{du}{z_1 + i(x_1 \cos u + y_1 \sin u)} = \frac{-2}{\sqrt{x_1^2 + y_1^2}} \int^{(0+)} \frac{dt}{t^2 - \frac{2iz_1 t}{\sqrt{x_1^2 + y_1^2}} + 1}, \quad (3)$$

where the path of integration in the  $t$ -plane is a unit circle around the origin taken in a positive sense. A little consideration shows that equation (3) is valid and we may, therefore, write equation (1) in the form

$$V_{\lambda, \mu, \nu} = \frac{\epsilon}{2\pi} \int_{-\pi}^{\pi} \left\{ \frac{1}{\nu 2c + l - z + i[(\lambda 2a - x) \cos u + (\mu 2b - y) \sin u]} - \frac{1}{\nu 2c + l + z + i[\dots]} \right\} du. \quad (4)$$

Next, we make use of the relation

$$\frac{1}{w^s} = \frac{1}{\Gamma(s)} \int_0^\infty e^{-wt} t^{s-1} dt, \quad . \quad . \quad . \quad (5)$$

where  $(Rw) > 0$  and  $R(s) > 0$ . This relation follows at once from the definition of the Gamma-function as a definite integral; that is,

$$\Gamma(s) = \int_0^\infty e^{-x} x^{s-1} dx,$$

where  $R(s) > 0$ . By setting  $x = wt$  where  $R(w) > 0$  equation (5) is obtained.

Since all of the terms in equation (4) satisfy the conditions connected with equation (5) it is possible, with the aid of equation (5), to express  $V_{\lambda, \mu, \nu}$  by the relation

$$V_{\lambda, \mu, \nu} = \frac{\epsilon}{\pi} \int_{-\pi}^{\pi} \int_0^\infty \left\{ e^{it(x \cos u + y \sin u)} e^{-t\nu 2c} \sinh(zt) e^{-it} - e^{-it(\lambda 2a \cos u + \mu 2b \sin u)} \right\} dt du. \quad (6)$$

Equation (6) gives a form for  $V_{\lambda, \mu, \nu}$  which is suitable for summing with respect to  $\nu$ ,  $\lambda$ , and  $\mu$ .

We shall first sum  $V_{\lambda, \mu, \nu}$  with respect to  $\nu$  from 0 to  $\infty$ . It is an easy matter to show that we may sum behind the

integral signs in equation (6) so that we obtain upon summing

$$\sum_{\nu=0}^{\infty} V_{\lambda, \mu, \nu} = V_{\lambda, \mu} = \frac{e}{\pi} \int_{-\pi}^{\pi} \int_0^{\infty} \left\{ e^{it(x \cos u + y \sin u)} \cdot \frac{\sinh(zt) e^{-t}}{1 - e^{-t}} \cdot e^{-it(\lambda 2a \cos u + \mu 2b \sin u)} \right\} dt du. \quad (7)$$

It remains to sum  $V_{\lambda, \mu}$  with respect to  $\lambda$  and  $\mu$  from  $-\infty$  to  $+\infty$ . Instead of doing this in the ordinary manner we shall employ the Cesàro I method of summation\*.

Consider the series

$$\sum_{\lambda=-(k-1)}^{k-1} e^{-it\lambda 2a \cos u} = 1 + 2 \cos(t 2a \cos u) + 2 \cos(2t 2a \cos u) + \dots + 2 \cos[(k-1)t 2a \cos u].$$

We may write this series in the form

$$S_k = u_0 + u_1 + u_2 + \dots + u_{k-1},$$

where  $\begin{cases} u_j = 2 \cos(jt 2a \cos u) \\ j \neq 0 \\ u_0 = 1 \end{cases}$

We now consider the expression

$$\frac{S_1 + S_2 + S_3 + \dots + S_k}{k} = \frac{1}{k} [ku_0 + (k-1)u_1 + (k-2)u_2 + \dots + u_{k-1}].$$

If  $\lim_{k \rightarrow \infty} \frac{1}{k} [S_1 + S_2 + \dots + S_k]$  exists, then the series  $\sum_{j=0}^{\infty} u_j$  is said to be summable Cesàro I or (CI). Further, this limit is equal to  $\sum_{j=0}^{\infty} u_j$  provided the latter series converges.

Let us denote Cesàro I summation by the symbol S(CI) so that

$$\begin{aligned} S(CI) e^{-it\lambda 2a \cos u} &= \frac{1}{k} [k + (k-1)2 \cos(t 2a \cos u) + (k-2)2 \cos(2t 2a \cos u) \\ &\quad + \dots + 2 \cos[(k-1)t 2a \cos u]] \\ &= \frac{1}{k} [k + (k-1)(\rho + \rho^{-1}) + (k-2)(\rho^2 + \rho^{-2}) + \dots \\ &\quad + (\rho^{k-1} + \rho^{1-k})], \end{aligned}$$

\* L. c., Chap. 8, § 8.43.

where  $2 \cos (t2a \cos u) = \rho + \rho^{-1}$ . But we have

$$\begin{aligned} & [k + (k-1)(\rho + \rho^{-1}) + (k-2)(\rho^2 + \rho^{-2}) + \dots + (\rho^{k-1} + \rho^{1-k})] \\ & = (\rho^{1-k} + \rho^{2-k} + \dots + \rho^{-1} + 1 - \rho - \rho^2 - \dots - \rho^k)(1 - \rho)^{-1} \\ & = (1 - \rho)^{-2}(\rho^{1-k} - 2\rho + \rho^{k+1}) = \frac{(\rho^{k/2} - \rho^{-k/2})^2}{(\rho^{1/2} - \rho^{-1/2})^2}. \end{aligned}$$

Therefore,

$$\sum_{\lambda=-(k-1)}^{k-1} S(\text{CI}) e^{-it\lambda 2a \cos u} = \frac{1}{k} \frac{\sin^2 (kta \cos u)}{\sin^2 (ta \cos u)}. \quad (8)$$

In a like manner,

$$\sum_{\mu=-(r-1)}^{r-1} S(\text{CI}) e^{-it\mu 2b \sin u} = \frac{1}{r} \frac{\sin^2 (rtb \sin u)}{\sin^2 (tb \sin u)}. \quad (9)$$

We are now in a position to sum  $V_{\lambda, \mu}$ , (CI), with respect to  $\lambda$  and  $\mu$ . It is perfectly evident for physical reasons that the order of the summations is immaterial so that we are justified in carrying them out in any manner we please. Indeed, we might have summed with respect to  $\lambda$  and  $\mu$  first, and then with respect to  $\nu$ . In summing with respect to  $\lambda$  and  $\mu$  we shall set  $r=k$ . This enables us to replace a double limit by a single limit. We obtain, by use of equations (7), (8), and (9),

$$\begin{aligned} \sum_{\substack{\lambda=-\infty \\ \mu=-\infty}}^{\infty} S(\text{CI}) V_{\lambda, \mu} &= V_1 = \frac{\epsilon}{\pi} \lim_{k \rightarrow \infty} \frac{1}{k^2} \int_{-\pi}^{\pi} \int_0^{\infty} \left\{ e^{it(x \cos u + y \sin u)} \right. \\ &\quad \left. \frac{\sinh (zt) e^{-lt}}{1 - e^{-t2c}} \frac{\sin^2 (kta \cos u) \sin^2 (ktb \sin u)}{\sin^2 (ta \cos u) \sin^2 (tb \sin u)} \right\} dt du. \end{aligned} \quad (10)$$

The expression for  $V_1$  given in equation (10) represents, in a compact form, the potential at any point in the elementary parallelepiped, due to all of the positive charges to the right and all of the negative charges to the left of the  $x$ - $y$ -plane as shown in fig. 2.

We have now to determine the potential in the same region due to the remainder of the charges. The argument is essentially the same as the one which we have just completed. We have only to replace  $+l$  by  $-l$  in equation (4) and change the sign of the right-hand member. If we then sum the resulting expression with respect to  $\nu$  from 1 to  $\infty$ , and

with respect to  $\lambda$  and  $\mu$  (Cesàro I) from  $-\infty$  to  $+\infty$ , we obtain

$$V_2 = -\frac{\epsilon}{\pi} \lim_{k \rightarrow \infty} \frac{1}{k^2} \int_{-\pi}^{\pi} \int_0^{\infty} \left\{ e^{it(x \cos u + y \sin u)} \frac{\sinh(zt) e^{lt}}{e^{t2c} - 1} \cdot \frac{\sin^2(kt a \cos u) \sin^2(ktb \sin u)}{\sin^2(ta \cos u) \sin^2(tb \sin u)} \right\} dt du. \quad (11)$$

This expression for  $V_2$  represents the potential at any point in the parallelepiped due to all of the negative charges to the right and all of the positive charges to the left of the  $x$ - $y$ -plane.

The total potential, that is the potential due to the entire set of charges, is evidently  $V_1 + V_2$ . Adding equations (10) and (11), we obtain the total potential in the form

$$V = V_1 + V_2 \\ = \frac{\epsilon}{\pi} \lim_{k \rightarrow \infty} \frac{1}{k^2} \int_{-\pi}^{\pi} \int_0^{\infty} \left\{ e^{it(x \cos u + y \sin u)} \frac{\sinh(zt) \sinh[(c-l)t]}{\sinh(ct)} \cdot \frac{\sin^2(kt a \cos u) \sin^2(ktb \sin u)}{\sin^2(ta \cos u) \sin^2(tb \sin u)} \right\} dt du, \quad (12)$$

since 
$$\frac{e^{-lt}}{1 - e^{-t2c}} - \frac{e^{lt}}{e^{t2c} - 1} = \frac{\sinh[(c-l)t]}{\sinh(ct)}.$$

By breaking the path of integration of  $u$  into four parts, that is  $-\pi$  to  $-\frac{\pi}{2}$ ,  $-\frac{\pi}{2}$  to  $0$ ,  $0$  to  $\frac{\pi}{2}$ , and  $\frac{\pi}{2}$  to  $\pi$ , and making the customary transformations, we get

$$V = \frac{4\epsilon}{\pi} \lim_{k \rightarrow \infty} \frac{1}{k^2} \int_0^{\pi/2} \int_0^{\infty} \left\{ \cos(tx \cos u) \cos(ty \sin u) \cdot \sinh(zt) \cdot \frac{\sinh[(c-l)t]}{\sinh(ct)} \cdot \frac{\sin^2(kt a \cos u) \sin^2(ktb \sin u)}{\sin^2(ta \cos u) \sin^2(tb \sin u)} \right\} dt du. \quad (13)$$

Although the expression for  $V(x, y, z)$  given in equation (13) is in a very compact form, it is obviously not suitable for purposes of computation. We shall proceed to evaluate this expression.

In equation (13) let us make the following transformations of the integration variables:

$$\left. \begin{aligned} t \cos u &= \frac{\pi \xi}{a}, \\ t \sin u &= \frac{\pi \eta}{b} \end{aligned} \right\} \cdot \cdot \cdot \cdot \cdot \cdot \quad (14)$$



Then,

$$\begin{aligned}
 V(x, y, z) &= \frac{4\epsilon}{ab} \lim_{k \rightarrow \infty} \frac{1}{k^2} \int_0^\infty \int_0^\infty \\
 &\cdot \left\{ \cos\left(\frac{\pi\xi}{a}x\right) \cos\left(\frac{\pi\eta}{b}y\right) \sinh\left[\pi z \sqrt{\left(\frac{\xi}{a}\right)^2 + \left(\frac{\eta}{b}\right)^2}\right] \right. \\
 &\quad \left. \sinh\left[\pi(c-l) \sqrt{\left(\frac{\xi}{a}\right)^2 + \left(\frac{\eta}{b}\right)^2}\right] \right. \\
 &\quad \left. \cdot \frac{\sinh\left[\pi c \sqrt{\left(\frac{\xi}{a}\right)^2 + \left(\frac{\eta}{b}\right)^2}\right]}{\left[\left(\frac{\xi}{a}\right)^2 + \left(\frac{\eta}{b}\right)^2\right]^{1/2}} \right\} \frac{\sin^2(\pi k\xi) \sin^2(\pi k\eta)}{\sin^2(\pi\xi) \sin^2(\pi\eta)} d\xi d\eta \\
 &= \frac{4\epsilon}{ab} \lim_{k \rightarrow \infty} \frac{1}{k^2} \int_0^\infty \int_0^\infty f(\xi, \eta) \frac{\sin^2(\pi k\xi) \sin^2(\pi k\eta)}{\sin^2(\pi\xi) \sin^2(\pi\eta)} d\xi d\eta,
 \end{aligned}
 \tag{15}$$

where

$$\begin{aligned}
 f(\xi, \eta) &= \cos\left(\frac{\pi\xi}{a}x\right) \cos\left(\frac{\pi\eta}{b}y\right) \\
 &\cdot \frac{\sinh\left[\pi z \sqrt{\left(\frac{\xi}{a}\right)^2 + \left(\frac{\eta}{b}\right)^2}\right] \sinh\left[\pi(c-l) \sqrt{\left(\frac{\xi}{a}\right)^2 + \left(\frac{\eta}{b}\right)^2}\right]}{\left[\left(\frac{\xi}{a}\right)^2 + \left(\frac{\eta}{b}\right)^2\right]^{1/2} \sinh\left[\pi c \sqrt{\left(\frac{\xi}{a}\right)^2 + \left(\frac{\eta}{b}\right)^2}\right]}.
 \end{aligned}
 \tag{16}$$

Consider the double integral

$$\frac{1}{k^2} \int_{q-1/2}^{q+1/2} \int_{p-1/2}^{p+1/2} f(\xi, \eta) \frac{\sin^2(\pi k\xi) \sin^2(\pi k\eta)}{\sin^2(\pi\xi) \sin^2(\pi\eta)} d\xi d\eta,$$

where  $p$  and  $q$  are any two positive integers. Its similarity to single integrals used in connexion with single Fourier series leads us to suspect that this double integral approaches  $f(p, q)$  as  $k$  goes to infinity. This is actually the case, as we shall prove.

Since

$$\frac{1}{k^2} \int_{q-1/2}^{q+1/2} \int_{p-1/2}^{p+1/2} \frac{\sin^2(\pi k\xi) \sin^2(\pi k\eta)}{\sin^2(\pi\xi) \sin^2(\pi\eta)} d\xi d\eta = 1,$$

it follows that

$$f(p, q) = \frac{1}{k^2} \int_{q-1/2}^{q+1/2} \int_{p-1/2}^{p+1/2} f(p, q) \frac{\sin^2(\pi k\xi) \sin^2(\pi k\eta)}{\sin^2(\pi\xi) \sin^2(\pi\eta)} d\xi d\eta.$$

Let  $\phi(\xi, \eta) = f(\xi, \eta) - f(p, q)$ , and then consider the double integral

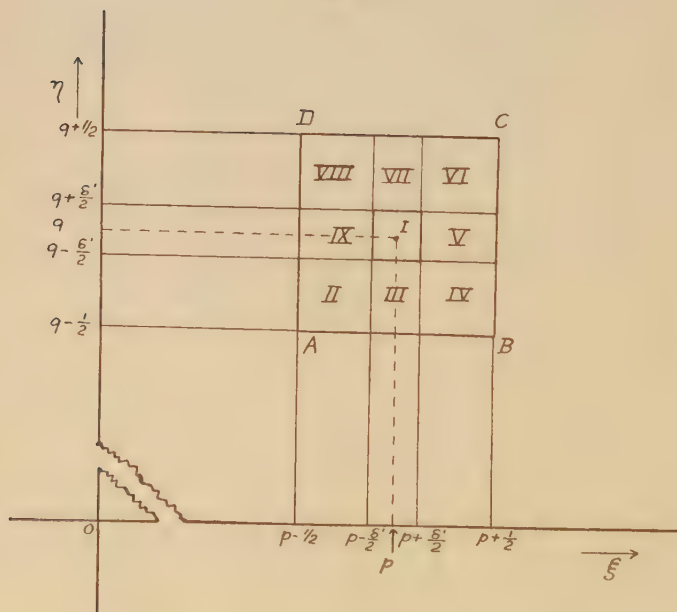
$$\frac{1}{k^2} \int_{q-1/2}^{q+1/2} \int_{p-1/2}^{p+1/2} \phi(\xi, \eta) \frac{\sin^2(\pi k \xi)}{\sin^2(\pi \xi)} \frac{\sin^2(\pi k \eta)}{\sin^2(\pi \eta)} d\xi d\eta.$$

To prove our point it is sufficient to show that this double integral goes to zero as  $k$  goes to infinity.

Given an arbitrary positive number  $\epsilon'$ , we can choose  $\delta'$  independent of  $k$  and different from zero such that  $|\phi(\xi, \eta)| < \epsilon'$  whenever

$$\left\{ \begin{array}{l} |\xi - p| \leq \frac{\delta'}{2} \\ |\eta - q| \leq \frac{\delta'}{2} \end{array} \right\}.$$

Fig. 3



Geometrically the situation is illustrated by fig. 3. As long as the point  $(\xi, \eta)$  remains within the small square (I) of sides  $\delta'$  as shown in the figure, then  $|\phi(\xi, \eta)| < \epsilon'$ . The double integral is to be taken over the large square ABCD as shown.

In order to prove that the double integral vanishes over ABCD as  $k$  goes to infinity, we shall break it up into nine pieces in the following manner :

$$\begin{aligned} & \frac{1}{k^2} \int_{q-1/2}^{q+1/2} \int_{p-1/2}^{p+1/2} \phi(\xi, \eta) \frac{\sin^2(\pi k \xi)}{\sin^2(\pi \xi)} \frac{\sin^2(\pi k \eta)}{\sin^2(\pi \eta)} d\xi d\eta \\ &= \frac{1}{k^2} \left\{ \left[ \int_q^{q+\delta'/2} \int_{p-\delta'/2}^{p+\delta'/2} \text{(I)} + \int_{q-1/2}^{q-\delta'/2} \int_{p-1/2}^{p-\delta'/2} \text{(II)} \right. \right. \\ & \quad + \int_{q+1/2}^{q-\delta'/2} \int_{p-\delta'/2}^{p+\delta'/2} \text{(III)} + \int_{q-1/2}^{q-\delta'/2} \int_{p+\delta'/2}^{p+1/2} \text{(IV)} \\ & \quad + \int_{q-\delta'/2}^{q+\delta'/2} \int_{p+\delta'/2}^{p+1/2} \text{(V)} + \int_{q+\delta'/2}^{q+1/2} \int_{p+\delta'/2}^{p+1/2} \text{(VI)} \\ & \quad + \int_{q+\delta'/2}^{q+1/2} \int_{p-\delta'/2}^{p+\delta'/2} \text{(VII)} + \int_{q+\delta'/2}^{q+1/2} \int_{p-1/2}^{p-\delta'/2} \text{(VIII)} \\ & \quad \left. + \int_{q-\delta'/2}^{q+\delta'/2} \int_{p+1/2}^{p-\delta'/2} \text{(IX)} \right] \\ & \quad \cdot \phi(\xi, \eta) \frac{\sin^2(\pi k \xi)}{\sin^2(\pi \xi)} \frac{\sin^2(\pi k \eta)}{\sin^2(\pi \eta)} d\xi d\eta \Big\}. \quad \dots \quad (17) \end{aligned}$$

It is obvious that each of the nine parts in equation (17) represents the double integral taken over one of the nine regions into which the square ABCD has been broken, so that the sum represents the double integral taken over the entire square. Further, Parts II, IV, VI, and VIII are similar in character, as are Parts III, V, VII, and IX. Part I is unique. It will be sufficient, therefore, to consider in detail only Parts I, II, and III, since they are characteristic of the entire group.

Consider Part I. Surely

$$\begin{aligned} & \left| \frac{1}{k^2} \int_q^{q+\delta'/2} \int_{p-\delta'/2}^{p+\delta'/2} \phi(\xi, \eta) \frac{\sin^2(\pi k \xi)}{\sin^2(\pi \xi)} \frac{\sin^2(\pi k \eta)}{\sin^2(\pi \eta)} d\xi d\eta \right| \\ & \leq \frac{1}{k^2} \int_q^{q+\delta'/2} \int_{p-\delta'/2}^{p+\delta'/2} \frac{\sin^2(\pi k \xi)}{\sin^2(\pi \xi)} \frac{\sin^2(\pi k \eta)}{\sin^2(\pi \eta)} |\phi(\xi, \eta)| d\xi d\eta \\ & < \frac{\epsilon'}{k^2} \int_q^{q+\delta'/2} \int_{p-\delta'/2}^{p+\delta'/2} \frac{\sin^2(\pi k \xi)}{\sin^2(\pi \xi)} \frac{\sin^2(\pi k \eta)}{\sin^2(\pi \eta)} d\xi d\eta \\ & < \frac{\epsilon'}{k^2} \int_q^{q+1/2} \int_{p-1/2}^{p+1/2} \frac{\sin^2(\pi k \xi)}{\sin^2(\pi \xi)} \frac{\sin^2(\pi k \eta)}{\sin^2(\pi \eta)} d\xi d\eta = \epsilon'. \end{aligned}$$

Therefore for Part I we have

$$\left| \frac{1}{k^2} \int_{q-\delta'/2}^{q+\delta'/2} \int_{p-\delta'/2}^{p+\delta'/2} \phi(\xi, \eta) \frac{\sin^2(\pi k \xi) \sin^2(\pi k \eta)}{\sin^2(\pi \xi) \sin^2(\pi \eta)} d\xi d\eta \right| < \epsilon', \quad (18)$$

where  $\epsilon'$  is an arbitrarily small positive number.

Let us now consider Part II. We have

$$\left| \frac{1}{k^2} \int_{q-1/2}^{q-\delta'/2} \int_{p-1/2}^{p-\delta'/2} \phi(\xi, \eta) \frac{\sin^2(\pi k \xi) \sin^2(\pi k \eta)}{\sin^2(\pi \xi) \sin^2(\pi \eta)} d\xi d\eta \right| < \frac{1}{k^2 \sin^4\left(\pi \frac{\delta'}{2}\right)} \int_{q-1/2}^{q-\delta'/2} \int_{p-1/2}^{p-\delta'/2} |\phi(\xi, \eta)| d\xi d\eta < \frac{M}{k^2 \sin^4\left(\pi \frac{\delta'}{2}\right)}, \quad (19)$$

where  $M$  and  $\delta'$  are positive constants independent of  $k$  and different from zero. By taking  $k$  large enough, we can make the last member in relation (19) as small as we please. Since this member bounds Part II, we can make Part II as small as we please by taking  $k$  sufficiently large.

In the last place we consider Part III. We have

$$\left| \frac{1}{k^2} \int_{q-1/2}^{q-\delta'/2} \int_{p-\delta'/2}^{p+\delta'/2} \phi(\xi, \eta) \frac{\sin^2(\pi k \xi) \sin^2(\pi k \eta)}{\sin^2(\pi \xi) \sin^2(\pi \eta)} d\xi d\eta \right| < \frac{M'}{k^2 \sin^2\left(\pi \frac{\delta'}{2}\right)} \int_{p-\delta'/2}^{p+\delta'/2} \frac{\sin^2(\pi k \xi)}{\sin^2(\pi \xi)} d\xi = \frac{M'}{k^2 \sin^2\left(\pi \frac{\delta'}{2}\right)} \int_{p-1/2}^{p+1/2} \frac{\sin^2(\pi k \xi)}{\sin^2(\pi \xi)} d\xi = \frac{M'}{k \sin^2\left(\pi \frac{\delta'}{2}\right)}, \quad (20)$$

where  $M'$  and  $\delta'$  are positive constants different from zero and independent of  $k$ . Again, by taking  $k$  sufficiently large we can make Part III arbitrarily small.

By relations (18), (19), and (20) we see that Parts I, II, and III can be made arbitrarily small, the first by a proper choice of  $\epsilon'$ , the latter two by making  $k$  sufficiently large. In the same way the remaining parts can be made arbitrarily small by choosing a sufficiently large value of  $k$ . Since there are only a finite number of parts, it follows that their sum may be made arbitrarily small. Therefore, we have

$$\lim_{k \rightarrow \infty} \frac{1}{k^2} \int_{q-1/2}^{q+1/2} \int_{p-1/2}^{p+1/2} \phi(\xi, \eta) \frac{\sin^2(\pi k \xi) \sin^2(\pi k \eta)}{\sin^2(\pi \xi) \sin^2(\pi \eta)} d\xi d\eta = 0,$$

or finally,

$$f(p, q) = \lim_{k \rightarrow \infty} \frac{1}{k^2} \int_{q-1/2}^{q+1/2} \int_{p-1/2}^{p+1/2} f(\xi, \eta) \frac{\sin^2(\pi k \xi)}{\sin^2(\pi \xi)} \frac{\sin^2(\pi k \eta)}{\sin^2(\pi \eta)} d\xi d\eta. \quad (21)$$

By the same type of argument it can be shown that

$$\frac{1}{2}f(0, q) = \lim_{k \rightarrow \infty} \frac{1}{k^2} \int_{q-1/2}^{q+1/2} \int_0^{1/2} f(\xi, \eta) \frac{\sin^2(\pi k \xi)}{\sin^2(\pi \xi)} \frac{\sin^2(\pi k \eta)}{\sin^2(\pi \eta)} d\xi d\eta, \quad (22)$$

$$\frac{1}{2}f(p, 0) = \lim_{k \rightarrow \infty} \frac{1}{k^2} \int_0^{1/2} \int_{p-1/2}^{p+1/2} f(\xi, \eta) \frac{\sin^2(\pi k \xi)}{\sin^2(\pi \xi)} \frac{\sin^2(\pi k \eta)}{\sin^2(\pi \eta)} d\xi d\eta, \quad (23)$$

and

$$\frac{1}{4}f(0, 0) = \lim_{k \rightarrow \infty} \frac{1}{k^2} \int_0^{1/2} \int_0^{1/2} f(\xi, \eta) \frac{\sin^2(\pi k \xi)}{\sin^2(\pi \xi)} \frac{\sin^2(\pi k \eta)}{\sin^2(\pi \eta)} d\xi d\eta, \quad (24)$$

provided that in the last case we define  $f(0, 0)$  as  $\lim_{\substack{\xi \rightarrow 0 \\ \eta \rightarrow 0}} f(\xi, \eta)$ .

Now, going back to equation (15) we see that it may be written in the form

$$\begin{aligned} V(x, y, z) &= \frac{4e}{ab} \lim_{k \rightarrow \infty} \frac{1}{k^2} \left\{ \left[ \int_0^{1/2} \int_0^{1/2} + \sum_{q=1}^{\infty} \int_{q-1/2}^{q+1/2} \int_0^{1/2} + \sum_{p=1}^{\infty} \int_0^{1/2} \int_{p-1/2}^{p+1/2} \right. \right. \\ &\quad \left. \left. + \int_{1/2}^{\infty} \int_{1/2}^{\infty} \right] f(\xi, \eta) \frac{\sin^2(\pi k \xi)}{\sin^2(\pi \xi)} \frac{\sin^2(\pi k \eta)}{\sin^2(\pi \eta)} d\xi d\eta \right\} \\ &= \frac{4e}{ab} \lim_{k \rightarrow \infty} \frac{1}{k^2} \left\{ \left[ \int_0^{1/2} \int_0^{1/2} + \sum_{q=1}^{\infty} \int_{q-1/2}^{q+1/2} \int_0^{1/2} + \sum_{p=1}^{\infty} \int_0^{1/2} \int_{p-1/2}^{p+1/2} \right. \right. \\ &\quad \left. \left. + \sum_{p=1}^{\infty} \sum_{q=1}^{\infty} \int_{q-1/2}^{q+1/2} \int_{p-1/2}^{p+1/2} \right] f(\xi, \eta) \frac{\sin^2(\pi k \xi)}{\sin^2(\pi \xi)} \frac{\sin^2(\pi k \eta)}{\sin^2(\pi \eta)} d\xi d\eta \right\} \\ &= \frac{4e}{ab} \sum_{p=0}^{\infty} \sum_{q=0}^{\infty} \epsilon_{p,q} f(p, q)^*, \quad (25) \end{aligned}$$

where

$$\epsilon_{0,0} = \frac{1}{4}, \quad \epsilon_{0,j} = \epsilon_{i,0} = \frac{1}{2}, \quad \text{and} \quad \epsilon_{i,j} = 1, \quad i \neq 0, \quad j \neq 0.$$

\* It is not difficult to justify these operations.



By the use of equation (18) we finally obtain

$$V(x, y, z) = \frac{4\epsilon}{ab} \sum_{p=0}^{\infty} \sum_{q=0}^{\infty} \left\{ \epsilon_{p,q} \frac{\sinh \left[ z\pi \sqrt{\left(\frac{p}{a}\right)^2 + \left(\frac{q}{b}\right)^2} \right] \sinh \left[ \pi(c-l) \sqrt{\left(\frac{p}{a}\right)^2 + \left(\frac{q}{b}\right)^2} \right]}{\left[ \left(\frac{p}{a}\right)^2 + \left(\frac{q}{b}\right)^2 \right]^{1/2} \sinh \left[ \pi c \sqrt{\left(\frac{p}{a}\right)^2 + \left(\frac{q}{b}\right)^2} \right]} \right. \\ \left. \cdot \cos \left( \frac{\pi p}{a} x \right) \cos \left( \frac{\pi q}{b} y \right) \right\} \dots \dots \dots (26)$$

The value of  $V(x, y, z)$ , given in the form of a double Fourier series in equation (26), represents the potential due to an infinite set of positive and negative point charges distributed in space as shown in fig. 2, at any point within the elementary parallelepiped; that is, in the intervals  $0 \leq \frac{x}{a} \leq 1$ ,  $0 \leq \frac{y}{b} \leq 1$ , and  $0 \leq \frac{z}{l} \leq 1 - \delta$ . This double Fourier series evidently converges absolutely and uniformly within this region.

The case where  $1 + \delta \leq \frac{z}{l} < \frac{c}{l}$  still remains to be considered.

A little thought makes it evident that the potential function for this case will be the same as that for the first case, except that the  $z$  and  $l$  will be interchanged. This enables us to write the solution at once for the case  $1 + \delta \leq \frac{z}{l} < \frac{c}{l}$  in the form

$$\bar{V}(x, y, z) = \frac{4\epsilon}{ab} \sum_{p=0}^{\infty} \sum_{q=0}^{\infty} \left\{ \epsilon_{p,q} \frac{\sinh \left[ (\pi l) \sqrt{\left(\frac{p}{a}\right)^2 + \left(\frac{q}{b}\right)^2} \right] \sinh \left[ \pi(c-z) \sqrt{\left(\frac{p}{a}\right)^2 + \left(\frac{q}{b}\right)^2} \right]}{\left[ \left(\frac{p}{a}\right)^2 + \left(\frac{q}{b}\right)^2 \right]^{1/2} \sinh \left[ \pi c \sqrt{\left(\frac{p}{a}\right)^2 + \left(\frac{q}{b}\right)^2} \right]} \right. \\ \left. \cdot \cos \left( \frac{\pi p}{a} x \right) \cos \left( \frac{\pi q}{b} y \right) \right\} \dots \dots \dots (27)$$

Thus by equations (26) and (27) we have defined two potential functions,  $V(x, y, z)$  and  $\bar{V}(x, y, z)$ . In the development of  $V$ , the variables  $x$ ,  $y$ , and  $z$  were restricted

to the intervals  $0 \leq \frac{x}{a} \leq 1$ ,  $0 \leq \frac{y}{b} \leq 1$ , and  $0 \leq \frac{z}{l} \leq 1 - \delta$ . For

$\bar{V}$  the corresponding intervals were  $0 \leq \frac{x}{a} \leq 1$ ,  $0 \leq \frac{y}{b} \leq 1$ ,

and  $1 + \delta \leq \frac{z}{l} \leq \frac{c}{l}$ . Now the series defining  $V$  converges

for  $0 \leq \frac{z}{l} \leq 1$  provided not both  $x$  and  $y$  are zero. Also the

series defining  $\bar{V}$  converges for  $1 \leq \frac{z}{l} \leq \frac{c}{l}$  provided not both

$z$  and  $y$  are zero. Further,  $V(x, y, l) = \bar{V}(x, y, l)$  provided not both  $x$  and  $y$  are zero. Physically then, at least, we have a right to assume that  $V(x, y, z)$  represents the potential due to the system in the region defined by

the intervals  $0 \leq \frac{x}{a} \leq 1$ ,  $0 \leq \frac{y}{b} \leq 1$ , and  $0 \leq \frac{z}{l} \leq 1$  provided

the point  $(0, 0, l)$  is excluded from this region by inclosing it in a sphere of radius  $\delta$ , arbitrarily small. Also, we may assume the same for the function  $\bar{V}$  in the region defined by

the intervals  $0 \leq \frac{x}{a} \leq 1$ ,  $0 \leq \frac{y}{b} \leq 1$ , and  $1 \leq \frac{z}{l} \leq \frac{c}{l}$  with the

small sphere around  $(0, 0, l)$  excluded. This enables us to define a function  $\Phi(x, y, z)$  which gives the potential through-

out the entire region defined by the intervals  $0 \leq \frac{x}{a} \leq 1$ ,

$0 \leq \frac{y}{b} \leq 1$ , and  $0 \leq \frac{z}{l} \leq \frac{c}{l}$ , where the point  $(0, 0, l)$  has been

excluded by drawing a small sphere of radius  $\delta$  around it.

For  $0 \leq \frac{z}{l} \leq 1$ ,  $\Phi(x, y, z) = V(x, y, z)$ , and for  $1 \leq \frac{z}{l} \leq \frac{c}{l}$ ,

$\Phi(x, y, z) = \bar{V}(x, y, z)$ .

But a knowledge of the potential throughout the region indicated enables us to determine it throughout the entire space, except in the immediate neighbourhoods of the charges, by the obvious relations

$$\left. \begin{aligned} \Phi(-x, y, z) &= \Phi(x, y, z), \\ \Phi(x, -y, z) &= \Phi(x, y, z), \\ \Phi(x, y, -z) &= -\Phi(x, y, z), \\ \Phi(x \pm 2a, y, z) &= \Phi(x, y, z), \\ \Phi(x, y \pm 2b, z) &= \Phi(x, y, z), \\ \Phi(x, y, z \pm 2c) &= \Phi(x, y, z). \end{aligned} \right\} \quad (28)$$

By means of the relations (28) we can consider our potential function as given throughout a parallelepiped whose sides coincide with the planes  $x = \pm a$ ,  $y = \pm b$ , and  $z = \pm c$ , the charges within this region being excluded by small spheres. Within this parallelepiped there are two poles, one a positive and the other a negative. Both poles are of the first order. Over the end faces of the prism,  $z = \pm c$ , the potential vanishes identically; over the side faces,  $x = \pm a$ ,  $y = \pm b$ , the normal flux vanishes identically. These facts are obviously true from a physical viewpoint. They may be verified by means of equations (26) and (27).

Therefore the surface integral,  $\iint \Phi \frac{\partial \Phi}{\partial n} ds$ , taken over the surface of the prism must vanish since  $\Phi = 0$  over the end faces and  $\frac{\partial \Phi}{\partial n} = 0$  over the side faces. This fact, coupled with Green's theorem, proves the uniqueness of the solutions we have obtained\*. These characteristics of the potential function in question are somewhat analogous to the properties of elliptic functions.

Before concluding this paper we intend to make a few rough calculations by means of equations (26) and (27) of the potential of a very simple system of charges which is a special case of the system just treated. However, we will first expand the potential of the general system into a series of spherical harmonics. This will be our next task.

#### IV. *Potential of a Space System of Electric Charges : Expansion in a Series of Spherical Harmonics.*

The method, which we have employed in determining the potential of an infinite set of charges distributed in space as shown in fig. 2 is not limited to the development of that potential in a double Fourier series. By a slight modification of the method it is possible to develop the potential around the origin in a series of spherical harmonics. Without more ado we will proceed with this problem. Since much of the argument is quite similar to that which has already been made, it will be sufficient merely to sketch the development of this expansion.

As before, we consider the potential due to a single positive charge to the right of the  $x$ - $y$ -plane and the corresponding negative charge to the left of the plane. This potential may

\* J. H. Jeans, 'Electricity and Magnetism,' p. 163.

be written as

$$V_{\lambda, \mu, \nu} = \epsilon \left\{ \frac{1}{[(\nu 2c + l - z)^2 + (\lambda 2a - x)^2 + (\mu 2b - y)^2]^{1/2}} - \frac{1}{[(\nu 2c + l + z)^2 + (\lambda 2a - x)^2 + (\mu 2b - y)^2]^{1/2}} \right\}, \quad (1)$$

where the symbols have the same significance as in section III. As before,  $\lambda$  and  $\mu$  may be any positive or negative integer, while  $\nu$  may be any positive integer including zero. Furthermore, as fig. 2 indicates,  $l$  shall be less than  $c$ . Finally, we shall impose the condition that

$$\left| \frac{z + i(x \cos u + y \sin u)}{l} \right| \leq 1 - \delta,$$

where  $\delta$  is an arbitrarily small positive number and  $u$  is confined to the interval  $-\pi \leq u \leq \pi$  \*. The reason for this condition will appear shortly.

Equation (1) may be written in the form

$$\begin{aligned} V_{\lambda, \mu, \nu} &= \frac{\epsilon}{2\pi} \int_{-\pi}^{\pi} \left\{ \frac{1}{\nu 2c + l - z + i[(\lambda 2a - x) \cos u + (\mu 2b - y) \sin u]} - \frac{1}{\nu 2c + l + z + i[(\lambda 2a - x) \cos u + (\mu 2b - y) \sin u]} \right\} du \\ &= \frac{\epsilon}{2\pi} \int_{-\pi}^{\pi} \left\{ \frac{1}{\nu 2c + l + i(\lambda 2a \cos u + \mu 2b \sin u)} \right. \\ &\quad \left. - \frac{1}{\left[ 1 - \frac{z + i(x \cos u + y \sin u)}{\nu 2c + l + i(\lambda 2a \cos u + \mu 2b \sin u)} \right]} \right. \\ &\quad \left. - \frac{1}{\left[ 1 - \frac{-z + i(x \cos u + y \sin u)}{\nu 2c + l + i(\lambda 2a \cos u + \mu 2b \sin u)} \right]} \right\} du. \quad (2) \end{aligned}$$

\* This is equivalent to the condition:

$$\frac{\sqrt{x^2 + y^2 + z^2}}{l} \leq 1 - \delta.$$

Since the second brackets quantity in the integrand of equation (2) consists of two terms of the form  $\frac{1}{1-t}$ , each term may be expanded into a power series, these series added term by term, and then the resulting series integrated term by term by virtue of the condition

$$\left| \frac{z + ix(\cos u + y \sin u)}{l} \right| \leq 1 - \delta.$$

Carrying out these operations, we obtain

$$\begin{aligned} V_{\lambda, \mu, \nu} = \frac{\epsilon}{2\pi} \sum_{n=0}^{\infty} \int_{-\pi}^{\pi} \{ [z + i(x \cos u + y \sin u)]^{n+1} \\ - [-z + i(x \cos u + y \sin u)]^{n+1} \} \\ \cdot \left\{ \frac{1}{[\nu 2c + l + i(\lambda 2a \cos u + \mu 2b \sin u)]^{n+2}} \right\} du. \quad (3) \end{aligned}$$

Let us now expand the second brackets quantity in the integrand of equation (3) into a Fourier series. Then

$$\begin{aligned} \frac{1}{[\nu 2c + l + i(\lambda 2a \cos u + \mu 2b \sin u)]^{n+2}} \\ = \frac{1}{2} \alpha_0^{(n+1)} + \sum_{m=1}^{\infty} [\alpha_m^{(n+1)} \cos mu + \beta_m^{(n+1)} \sin mu], \end{aligned}$$

where

$$\alpha_m^{(n+1)} = \frac{1}{\pi} \int_{-\pi}^{\pi} \left\{ \frac{1}{[\nu 2c + l + i(\lambda 2a \cos w + \mu 2b \sin w)]^{n+2}} \right\} \cos mw \, dw.$$

Since

$$\int_0^{\infty} e^{-wt} t^{s-1} dt = \frac{\Gamma(s)}{w^s},$$

where  $R(w) > 0$  and  $R(s) > 0$ , we may write the above coefficients in the form

$$\begin{aligned} \alpha_m^{(n+1)} = \frac{1}{\pi(n+1)!} \\ \int_{-\pi}^{\pi} \int_0^{\infty} \left\{ \frac{\cos mw}{\sin mw} t^{n+1} e^{-t\nu 2c} e^{-lt} e^{-it\lambda 2a \cos w} e^{-it\mu 2b \sin w} \right\} dt \, dw. \end{aligned} \quad (4)$$

If we now substitute the Fourier series which we have obtained for the second brackets quantity in equation (3) and



then integrate term by term \*, we get

$$\begin{aligned}
 V_{\lambda, \mu, \nu} = \frac{\epsilon}{2\pi} \sum_{n=0}^{\infty} \left\{ \frac{1}{2} \alpha_0^{(n+1)} \int_{-\pi}^{\pi} \{ [z + i(x \cos u + y \sin u)]^{n+1} \right. \\
 - [-z + i(x \cos u + y \sin u)]^{n+1} \} du \\
 + \sum_{m=1}^{n+1} [\alpha_m^{(n+1)}] \int_{-\pi}^{\pi} \{ [z + i(x \cos u + y \sin u)]^{n+1} \\
 - [-z + i(x \cos u + y \sin u)]^{n+1} \} \cos mu \, du \\
 + \beta_m^{(n+1)} \int_{-\pi}^{\pi} \{ [z + i(x \cos u + y \sin u)]^{n+1} \\
 \left. - [-z + i(x \cos u + y \sin u)]^{n+1} \} \sin mu \, du \right\}.
 \end{aligned}
 \tag{5}$$

It is evident that for  $m > n+1$  every integral of the form

$$\int_{-\pi}^{\pi} \left\{ [z + i(x \cos u + y \sin u)]^{n+1} - [-z + i(\dots)]^{n+1} \right\} \frac{\cos mu}{\sin mu} du$$

vanishes by virtue of orthogonality conditions.

Now †

$$\begin{aligned}
 \int_{-\pi}^{\pi} [\pm z + i(x \cos u + y \sin u)]^{n+1} \frac{\cos mu}{\sin mu} du \\
 = \frac{2\pi i^m (n+1)!}{(n+m+1)!} \cdot \frac{\cos m\phi}{\sin m\phi} \rho^{n+1} P_{n+1}^{(m)}(\pm \cos \theta), \tag{6}
 \end{aligned}$$

where  $x, y$ , and  $z$  have been expressed in terms of polar coordinates; that is,

$$\left\{ \begin{aligned}
 z &= \rho \cos \theta, & -z &= \rho \cos (\pi - \theta) = -\rho \cos \theta, \\
 x &= \rho \sin \theta \cos \phi, & x &= \rho \sin (\pi - \theta) \cos \phi = \rho \sin \theta \cos \phi, \\
 y &= \rho \sin \theta \sin \phi, & y &= \rho \sin \theta \sin \phi.
 \end{aligned} \right\}
 \tag{7}$$

Therefore, noting that

$$P_{n+1}^{(m)}(-\cos \theta) = (-1)^{n+m+1} P_{n+1}^{(m)}(\cos \theta),$$

\* This operation is justified since the Fourier series is uniformly convergent in the interval  $-\pi \leq u \leq \pi$ . Carslaw, 'Fourier's Series and Integrals,' pp 168, 169.

† *L. c.* Chap. 18, § 18.31.

equation (5) may be written in the form

$$\begin{aligned} V_{\lambda, \mu, \nu} = & \frac{\epsilon}{2\pi} \sum_{n=0}^{\infty} \left\{ \frac{1}{2} \alpha_0^{(n+1)} 2\pi \rho^{n+1} P_{n+1}(\cos \theta) [1 - (-1)^{n+1}] \right. \\ & + \sum_{m=1}^{n+1} \frac{2\pi i^m (n+1)!}{(n+m+1)!} \cdot \rho^{n+1} P_{n+1}^{(m)}(\cos \theta) [1 - (-1)^{n+m+1}] \\ & \times [\alpha_m^{(n+1)} \cos m\phi + \beta_m^{(n+1)} \sin m\phi] \Big\} \dots \dots \dots (8) \end{aligned}$$

In equation (8) we note that only the coefficients  $\alpha_m^{(n+1)}$  and  $\beta_m^{(n+1)}$  involve  $\lambda$ ,  $\mu$ , and  $\nu$ , so that a summation of  $V_{\lambda, \mu, \nu}$  with respect to  $\lambda$ ,  $\mu$ , and  $\nu$  involves, essentially, a summation of each of the coefficients with respect to  $\lambda$ ,  $\mu$ , and  $\nu$ . We have expressed these coefficients in such a form (equation 4) that the summation can be carried out without difficulty. The question of the legitimacy of the procedure arises. The argument may be made rigorous by expressing  $V_{\lambda, \mu, \nu}$  in the form of a finite series with a remainder. The above operations may then be carried out on this finite series and the remainder. After the operations, the absolute value of the resulting remainder turns out to be bounded by a quantity of the form

$$M \left| \frac{z + i(x \cos u + y \sin u)}{l} \right|^N,$$

where  $M$  is a positive constant and  $N$  is a positive integer which may be taken as large as we please. Since

$$\left| \frac{z + i(x \cos u + y \sin u)}{l} \right| < 1 - \delta,$$

by hypothesis, the upper bound of the absolute value of the resulting remainder, and hence the remainder itself, may be made arbitrarily small by choosing  $N$  sufficiently large; that is, the remainder goes to zero as  $N$  goes to infinity. This justifies the procedure of summing each of the coefficients in the infinite series, and also proves the convergence of the resulting series.

Turning now to equation (4) and summing the coefficients  $\alpha_m^{(n+1)}$  and  $\beta_m^{(n+1)}$ , first with respect to  $\nu$ , and then with respect to  $\lambda$  and  $\mu$ , (Cesàro I), we obtain

$$\begin{aligned} S(\text{CI}) \sum_{\lambda=-\infty}^{\infty} \sum_{\nu=0}^{\infty} \frac{\alpha_m^{(n+1)}}{\beta_m^{(n+1)}} = & \frac{1}{\pi(n+1)!} \lim_{k \rightarrow \infty} \frac{1}{k^2} \int_{-\pi}^{\pi} \int_0^{\infty} \left\{ \cos mw \, t^{n+1} \right. \\ & \left. \cdot \frac{e^{-tt}}{1 - e^{-t^2 c}} \frac{\sin^2(kt a \cos w) \sin^2(kt b \sin w)}{\sin^2(t a \cos w) \sin^2(t b \sin m)} \right\} dt dw. \quad (9) \end{aligned}$$

For  $\sin mw$  the integrand is an odd function of  $w$ , and therefore the double integral vanishes. Thus

$$\sum_{\substack{\lambda=-\infty \\ \mu=-\infty}}^{+\infty} \sum_{\nu=0}^{\infty} \beta_m^{(n+1)} = 0.$$

This means, of course, that in the expansion of the potential no terms involving  $\sin m\phi$  will appear. This is to be expected, since the potential will certainly be an even function of  $\phi$ .

Further, if  $m$  is odd, it may easily be shown, by breaking the double integral into four parts as

$$\int_{-\pi}^{-\pi/2} \int_0^{\infty} + \int_{-\pi/2}^0 \int_0^{\infty} + \int_0^{\pi/2} \int_0^{\infty} + \int_{\pi/2}^{\pi} \int_0^{\infty},$$

that the double integral vanishes. Thus for odd  $m$

$$\sum_{\substack{\lambda=-\infty \\ \mu=-\infty}}^{+\infty} \sum_{\nu=0}^{\infty} \alpha_m^{(n+1)} = 0.$$

This result is, likewise, to be expected, since it is evident that the potential at  $\phi$  and at  $\pi - \phi$ , for a given  $\rho$  and  $\theta$ , must be identical. Therefore  $\cos m\phi = \cos m(\pi - \phi)$ . This is only true provided  $m$  is an even integer.

It is now possible, with the aid of equations (8) and (9), to write

$$\begin{aligned} \sum_{\substack{\lambda=-\infty \\ \mu=-\infty}}^{+\infty} \sum_{\nu=0}^{\infty} V_{\lambda, \mu, \nu} &= V_1(\rho, \theta, \phi) \\ &= \epsilon \sum_{n=0}^{\infty} \rho^{2n+1} \left\{ \alpha_0^{(2n+1)} P_{2n+1}(\cos \theta) \right. \\ &\quad \left. + 2 \sum_{m=1}^n [\alpha_{2m}^{(2n+1)} \cos 2m\phi P_{2n+1}^{(2m)}(\cos \theta)] \right\}, \end{aligned} \quad (10)$$

where

$$\begin{aligned} \alpha_{2m}^{(2n+1)} &= \frac{(-1)^m (2n+1)!}{(2n+2m+1)!} \left[ \sum_{\substack{\lambda=-\infty \\ \mu=-\infty}}^{+\infty} \sum_{\nu=0}^{\infty} \alpha_{2m}^{(2n+1)} \right] \\ &= \frac{(-1)^m 4}{\pi (2n+2m+1)!} \lim_{k \rightarrow \infty} \frac{1}{k^2} \int_0^{\pi/2} \int_0^{\infty} \left\{ \cos(2mw) \right. \\ &\quad \left. \cdot t^{2n+1} \frac{e^{-lt}}{1-e^{-t^2c}} \cdot \frac{\sin^2(kt a \cos w) \sin^2(kt b \sin w)}{\sin^2(ta \cos w) \sin^2(tb \sin w)} \right\} dt dw. \end{aligned} \quad (11)$$

The function  $V_1(\rho, \theta, \phi)$  defined by equations (10) and (11) evidently represents the potential in the region defined by the relation

$$\left| \frac{z + i(x \cos u + y \sin u)}{l} \right| \leq 1 - \delta,$$

due to all of the positive charges to the right and all of the negative charges to the left of the  $x$ - $y$ -plane. In an exactly similar manner, we can determine the potential  $V_2(\rho, \theta, \phi)$  due to the remainder of the charges. The function  $V_2(\rho, \theta, \phi)$  is given by the equation

$$V_2(\rho, \theta, \phi) = \epsilon \sum_{n=0}^{\infty} \rho^{2n+1} \left\{ b_0^{(2n+1)} P_{2n+1}(\cos \theta) + 2 \sum_{m=1}^n b_{2m}^{(2n+1)} \cos 2m\phi P_{2n+1}^{(2m)}(\cos \theta) \right\}, \quad (12)$$

where

$$b_{2m}^{(2n+1)} = - \frac{(-1)^{m4}}{\pi(2n+2m+1)!} \lim_{k \rightarrow \infty} \frac{1}{k^2} \left\{ \int_0^{\pi/2} \int_0^{\infty} \left\{ \cos(2mw) \right. \right. \\ \times t^{2n+1} \frac{e^{kt}}{e^{t2c} - 1} \cdot \frac{\sin^2(kt a \cos w) \sin^2(ktb \sin w)}{\sin^2(ta \cos w) \sin^2(tb \sin w)} \Big\} dt dw. \\ \left. \left. \left. \right. \right. \right\} \quad (13)$$

These relations are also valid provided

$$\left| \frac{z + i(x \cos u + y \sin u)}{l} \right| \leq 1 - \delta.$$

Adding equations (10) and (12) term by term, which process is surely justifiable, we obtain

$$V(\rho, \theta, \phi) = V_1(\rho, \theta, \phi) + V_2(\rho, \theta, \phi) \\ = \epsilon \sum_{n=0}^{\infty} \rho^{2n+1} \left\{ A_0^{(2n+1)} P_{2n+1}(\cos \theta) + 2 \sum_{m=1}^n \left[ A_{2m}^{(2n+1)} \cos 2m\phi P_{2n+1}^{(2m)}(\cos \theta) \right] \right\}, \quad (14)$$

where

$$A_{2m}^{(2n+1)} = \frac{(-1)^{m4}}{\pi(2n+2m+1)!} \lim_{k \rightarrow \infty} \frac{1}{k^2} \int_0^{\pi/2} \int_0^{\infty} \left\{ \cos(2mw) t^{2n+1} \right. \\ \times \frac{\sinh[(c-l)t]}{\sinh(ct)} \cdot \frac{\sin^2(kt a \cos w) \sin^2(ktb \sin w)}{\sin^2(ta \cos w) \sin^2(tb \sin w)} \Big\} dt dw. \\ \left. \left. \left. \right. \right. \right\} \quad (15)$$

The total potential  $V(\rho, \theta, \phi)$  of the system of charges under consideration is given by means of equations (14) and (15). The potential is expressed as a series of spherical harmonics in which all of the constants of the system appear in the coefficients  $A_{2m}^{(2n+1)}$ . These coefficients are written in the form of double integrals which closely resemble the double integral involved in Section III. The evaluation of these double integrals is made in the same manner as in Section III. We obtain, after several steps,

$$A_{2m}^{(2n+1)} = \frac{(-1)^m 4\pi^{2n+1}}{(2n+2m+1)! ab} \sum_{p=0}^{\infty} \sum_{q=0}^{\infty} \left\{ \epsilon_{p,q} \cos \left[ 2m \tan^{-1} \left( \frac{qa}{pb} \right) \right] \right. \\ \left. \cdot \left[ \left( \frac{p}{a} \right)^2 + \left( \frac{q}{b} \right)^2 \right]^n \cdot \frac{\sinh \left[ \pi(c-l) \sqrt{\left( \frac{p}{a} \right)^2 + \left( \frac{q}{b} \right)^2} \right]}{\sinh \left[ \pi c \sqrt{\left( \frac{p}{a} \right)^2 + \left( \frac{q}{b} \right)^2} \right]} \right\} \quad (16)$$

Equations (14) and (16) completely determine the potential  $V(\rho, \theta, \phi)$  in the region defined by the relation,

$$\left| \frac{z + i(x \cos u + y \sin u)}{l} \right| \leq 1 - \delta,$$

where  $\delta$  is an arbitrarily small positive number.

The expansion in spherical harmonics is characterized by certain features which make it more useful, in some cases, than the expansion in a double Fourier series. After the coefficients have once been computed for a definite system, in the case of the expansion in spherical harmonics, the computation of the potential at any point  $(\rho, \theta, \phi)$  is a relatively simple matter. This is due to the fact that the constants of the system only appear in the coefficients  $A_{2m}^{(2n+1)}$  and are not connected with the variables  $\rho, \theta$ , and  $\phi$ . However, in the case of the double Fourier series, the constants of the system are linked up with the variables  $x, y$ , and  $z$  in trigonometric and hyperbolic functions. This tends to increase the difficulty of any considerable computation.

Furthermore, it is often advantageous to know the potential of such a system as we have been considering, with the two central charges at  $(0, 0, l)$  and  $(0, 0, -l)$  omitted. In the



case of the expansion in spherical harmonics it is an easy matter to subtract from the total potential, the potential due to these two charges, since the latter potential can be expressed in a series of spherical harmonics as follows :

$$V_{0,0,0} = \epsilon \left\{ \frac{1}{\sqrt{\rho^2 + l^2 - 2\rho l \cos \theta}} - \frac{1}{\sqrt{\rho^2 + l^2 + 2\rho l \cos \theta}} \right\} \\ = \epsilon \sum_{n=0}^{\infty} \frac{2}{l^{2n+2}} \rho^{2n+1} P_{2n+1}(\cos \theta), \quad (17)$$

provided  $\frac{\rho}{l} \leq 1 - \delta$ ,  $\delta$  being arbitrarily small. Subtracting this series term by term from that given in equation (14), we obtain

$$V'(\rho, \theta, \phi) = V(\rho, \theta, \phi) - V_{0,0,0}(\rho, \theta, \phi) \\ = \epsilon \sum_{n=0}^{\infty} \rho^{2n+1} \left\{ \left[ A_0^{(2n+1)} - \frac{2}{l^{2n+1}} \right] P_{2n+1}(\cos \theta) \right. \\ \left. + 2 \sum_{m=1}^n \left[ A_{2m}^{(2n+1)} \cos 2m\phi \right] l^{\frac{2m}{2n+1}} (\cos \theta) \right\}. \quad (18)$$

$V'(\rho, \theta, \phi)$ , as defined in equation (18), gives the potential of the system with the two central charges omitted.

If we set  $\theta=0$ , equation (18) becomes

$$V'(\rho, 0, \phi) = \epsilon \sum_{n=0}^{\infty} \rho^{2n+1} \left[ A_0^{(2n+1)} - \frac{2}{l^{2n+1}} \right]. \quad (19)$$

The function  $V'(\rho, 0, \phi)$  surely exists for  $\rho < l$ . Physically it should exist for  $\rho=l$  since the charge there has been removed. It is quite likely, then, that the series in equation (19) actually converges for  $\rho=l$ , although the author has not been able to verify this conjecture. In many cases it is of some importance to know the value of  $V'(l, 0, \phi)$  since it gives the so-called exciting potential. Equation (19) gives us a means of calculating this potential, even though we are certain of the convergence of series involved for  $\rho < l$  only. We can certainly take the  $\lim_{\rho \rightarrow l} V'(\rho, 0, \phi)$ .

#### V. *Potential of a Space System of Electric Charges: Expansion in a Series of Cylindrical Harmonics.*

It has been shown in the two preceding sections how we may expand the potential of our system into a double Fourier

series and into a series of spherical harmonics. A similar type of argument leads to an expansion in cylindrical harmonics. Since the expansion turns out to be very cumbersome in form, we will merely write down the result.

$V(\rho, \phi, z)$

$$= \frac{8\epsilon}{ab} \sum_{m=0}^{\infty} \sum_{p=0}^{\infty} \sum_{q=0}^{\infty} \left\{ (-1)^m \epsilon_{m,p,q} \cos(2m\phi) \cdot \cos \left[ 2m \tan^{-1} \left( \frac{qa}{pb} \right) \right] \right. \\ \times \frac{\sinh \left[ \pi z \sqrt{\left( \frac{p}{a} \right)^2 + \left( \frac{q}{b} \right)^2} \right] \sinh \left[ \pi(c-l) \sqrt{\left( \frac{p}{a} \right)^2 + \left( \frac{q}{b} \right)^2} \right]}{\left[ \left( \frac{p}{a} \right)^2 + \left( \frac{q}{b} \right)^2 \right]^{1/2} \sinh \left[ \pi c \sqrt{\left( \frac{p}{a} \right)^2 + \left( \frac{q}{b} \right)^2} \right]} \\ \times J_{2m} \left[ \pi \rho \sqrt{\left( \frac{p}{a} \right)^2 + \left( \frac{q}{b} \right)^2} \right] \left. \right\},$$

where  $\epsilon_{0,0,0} = \frac{1}{8}$ ;  $\epsilon_{0,0,k} = \epsilon_{i,0,0} = \epsilon_{0,j,0} = \frac{1}{4}$ ;  $\epsilon_{i,j,0} = \dots = \frac{1}{8}$  and  $\epsilon_{i,j,k} = l$ ;  $i \neq 0$ ,  $j \neq 0$ ,  $k \neq 0$ .

It is evident that the triple series defining  $V(\rho, \phi, z)$  is of little value in its present form. This is chiefly due to the fact that the constants and summation variables of the system are connected with  $\rho$ ,  $\phi$ , and  $z$  in several functions.

## VI. Calculation of Potential for a Special System.

We have calculated the potential at a few points for a very special and simple system of charges. The constants of the system are:  $a=b=c=\pi$ ,  $l=\frac{\pi}{2}$ , and  $\epsilon=1$ . The potential of this system has been calculated at three points on the  $z$ -axis,  $\frac{\pi}{8}$ ,  $\frac{\pi}{4}$ , and  $\frac{3\pi}{8}$ , first by means of the double Fourier series, and then by means of the series of spherical harmonics. Only the first three coefficients in the series of spherical harmonics were evaluated. They were:

$$A_0^{(1)} = 0.74, \quad A_0^{(3)} = 0.31, \quad \text{and} \quad A_0^{(5)} = 0.10.$$

The results of the calculations are given in the following table, along with the potential due to the two central charges alone.

$z$ .	Potential Fourier Series.	Potential Spherical Harmonics.	Potential Central Charges.
0 .....	0.00	0.00	0.00
$\frac{\pi}{8}$ .....	0.34	0.31	0.34
$\frac{2\pi}{8}$ .....	0.78	0.76	0.85
$\frac{3\pi}{8}$ .....	1.80	1.61	2.18
$\frac{4\pi}{8}$ .....	$\infty$	$\infty$	$\infty$

### VII. Conclusion.

The method which we have devised enables us to express the potential of an infinite system of charges, fairly general in character, by means of several different, well-known, expansions. The question arises as to whether or not a more general system of charges could be treated by the same method. As an illustration, we might consider the case in which the positive charges have the coordinates,  $(\lambda 2a + x_0, \mu 2b, \nu 2c + l)$ , and the negative charges, the coordinates,  $(\lambda 2a - x_0, \mu 2b, \nu 2c - l)$ . In this case the axis of the electric doublets, instead of being parallel to the  $z$ -axis, would make a certain angle with it. The author has carried this case far enough to assure himself that no special difficulties would arise. The indications are that a solution of such a problem only amounts to the interposition of a few more simple factors in the formulæ.

In conclusion, the author wishes to acknowledge the invaluable aid and encouragement given to him in the preparation of this paper by Professor Jakob Kunz.

Laboratory of Physics,  
University of Illinois,  
May, 1926.

LXX. *A Graphical Method for Determining the Whirling Speeds of Loaded Shafts.* By H. H. JEFFCOTT, *Sc.D.*\*

1. **T**HE most usual case in which the whirling speeds have to be calculated is that of a shaft of diameter uniform throughout its length, carrying a number of masses disposed in any manner along its length, and supported by bearings at its ends. It is intended in this note to give an account of a graphical method by which the whirling speeds of such a shaft may be approximately determined in a simple and rapid manner. This method is not to be confused with that by which the deflexion of a loaded shaft may be determined graphically by use of the bending-moment diagram. The employment of the diagrams given below enables the whirling speeds themselves to be directly and rapidly ascertained.

2. When the elastic central line of a light rotating vertical shaft which carries a perfectly balanced concentrated load  $m$  is deflected from its rest position, the load is acted upon outwardly by centrifugal force due to the rotation and inwardly by the elastic force tending to bring the shaft back to its undeflected position.

Each of these forces is proportional to the displacement  $u$ . If the speed is so low that the elastic restoring force ( $Eu$ ) is greater than the centrifugal force ( $m\omega^2u$ ), the shaft will be brought back to its undeflected position. If, however,  $E = m\omega^2$  so that for small values of the displacement the centrifugal and elastic forces are equal to one another, there will be no tendency for the shaft to return to its undeflected position, and it will remain bent. While rotating in this deflected form the centrifugal force gives rise to reactions at the bearings. The speed at which the centrifugal force is equal to the elastic restoring force and at which, accordingly, the shaft may continue to rotate in the deflected condition, is called a whirling speed or critical speed of transverse vibration.

When there is a number of concentrated masses on a light shaft, there is an equal number of whirling speeds corresponding to the possible types of vibration in which the elastic and centrifugal forces can balance each other. Thus with two concentrated loads on a light shaft the axis is bent in one loop with a node at each bearing corresponding to the first whirling speed, and in two loops with one of the masses in each at the second whirling speed.

\* Communicated by the Author.

3. If the load on the rotating shaft were balanced in an ideally perfect manner and were not acted upon by any extraneous force, there would be no agency to produce deflexion in the shaft, and in this ideal condition, if the speed be gradually raised, it should pass through the whirling speed without deflexion and consequent vibration.

In practice, however, the loads upon the shaft are never thus ideally balanced and are out of balance to a small extent, depending on the precision with which the rotor is constructed and on the adjustments that are subsequently effected to make the balance as perfect as is practically possible. The problem met with in practice is, therefore, the determination of the whirling speeds on the basis that the load is not quite perfectly balanced.

The behaviour of a light shaft carrying a single concentrated load slightly out of balance has been investigated elsewhere\*, and it has been shown that the damping due to viscous resistance within the shaft exercises an important influence on the nature of the vibration. The amplitude of the vibration is smaller the more perfectly the load is balanced; while the greater the imperfection of the balance of the load, the wider will be the range of the speeds over which vibration of a given magnitude can take place.

In the simple case under consideration, at a speed a little below the whirling speed the greatest deflexion lies on the side of the shaft-axis on which lies the out-of-balance of the load. During the passage of the shaft through the whirling speed the point of maximum deflexion gradually shifts round till, at a speed a little higher than the whirling speed, the point of maximum deflexion is diametrically opposite the position on the shaft it previously occupied. Thus the molecular friction within the shaft limits the magnitude of the vibration and influences its character.

In the case just considered the moment of inertia is assumed to exercise a negligible effect. When the load on the shaft consists of a disk-shaped mass or masses which are relatively of large diameter, the moment of inertia of the load exercises an influence on the vibration of the shaft and on the speed at which it whirls.

4. In order to permit lubrication and free rotation of the shaft in its bearings, it is necessary to provide a small clearance between the journal and the bearings. The British Engineering Standards Association recommend an allowance on a 1-in. journal of from  $\cdot001$  to  $\cdot003$  in. for first quality

\* Phil. Mag. xxxvii. pp. 304 *et seq.* (March 1919).



running-fits, and from  $\cdot004$  to  $\cdot011$  in. for third quality running-fits. For a 6-in. journal the corresponding figures are  $\cdot0025$  to  $\cdot0075$  in. and  $\cdot01$  to  $\cdot0275$  in. respectively. As the bearing-length is ordinarily from  $1\frac{1}{2}$  to 3 times the bearing diameter, it will be seen that these clearances permit a small amount of angular play of the shaft in the bearing amounting to as much as  $\cdot007$  radian reckoned from the central position. The position of the centre of the shaft may therefore be eccentric by a serious amount before the bearing exerts any restriction on angular displacement. A little consideration of this difference between the diameters of the journal and the bearing shows that a considerable vibration may be set up at the middle part of the shaft without the bearing exercising restriction on the journal. Thus, for example, if a uniform shaft 4 ft. long carries a central load of 500 lb. and rotates at 1000 r.p.m., it may be deflected without experiencing angular restriction from the bearings to such an extent that a centrifugal force amounting to as much as 1200 lb. wt. may be set up with consequent reactions on the bearings rotating in direction.

Accordingly for a shaft supported in two bearings it is usual to make the calculation of whirling speeds on the basis that the shaft is freely supported at each bearing, as considerable vibration is possible before the restriction of the bearing is called into play.

5. So far we have disregarded any possible effect of gravity on the whirling speeds. A horizontal shaft experiences the action of the uniform field of force due to gravity acting in a downward direction. When the shaft is stationary its centre line is deflected to a form and extent depending on the spacing and magnitudes of the loads it supports. If it be rotated very slowly it will be seen that, at any section, the shaft rotates around the deflected position of its elastic central line. In other words, when the shaft is at rest all its points and all the particles of the loads are deflected by gravity to an equilibrium position; and when the shaft is rotating slowly, all its points and all the particles of the loads rotate about the deflected elastic central line in the same way to the first order of small quantities as they would rotate about the undeflected central line if gravity were annulled. Thus the motion is defined by a rotation round the undeflected axis of the shaft coupled with a deflexion due simply to gravity.

If the loaded shaft be rotating and its axis be displaced from the deflected position, the centrifugal force acting from the deflected centre will be opposed by the elastic force

towards that centre due to that displacement. The further elastic force due to the deflexion of the axis from its unstrained position is balanced by gravity.

As a result of these considerations we may omit the effect of gravity when determining the whirling speeds of a horizontal shaft, and we observe that the motion is round the gravitationally-deflected position of the neutral axis instead of round its unstrained position. At an exceedingly high speed of rotation, namely the speed corresponding to the free period of longitudinal vibration of the shaft, the deflexion due to gravity will become less. This speed, however, in all cases arising in practice, usually exceeds greatly the working speed of the shaft.

6. We may now proceed to obtain an expression for the whirling speeds of a light uniform shaft loaded by a number of masses (whose moments of inertia will be regarded later on as exercising a negligible influence on the whirling speeds) distributed in any given manner along the shaft, which is supported freely at each end. First, it is necessary to find an expression for the deflexion, supposed small, of the loaded shaft at any point.

Let  $l$  be the length of the shaft,  $d$  its diameter,  $I$  its moment of inertia of cross-section about the diameter perpendicular to the plane of bending intersecting the neutral axis, so that  $I = \frac{\pi d^4}{64}$ , and let  $E$  be Young's Modulus of elasticity. Also let a force  $X$  acting perpendicularly to the length of the shaft in the plane of bending, and a couple  $M$  about a line at right-angles to the shaft-axis and to the plane of bending, be applied at a point distant  $z_1$  from one bearing which is taken as the origin. Then, following the Bernoulli-Eulerian method, it is easy to see that the displacement  $u$  at any point  $z$  on the shaft between  $o$  and  $z_1$  is given by

$$6EIlu = Xz_1(l-z)(2lz - z^2 - z_1^2) - M(l-z)(3z_1^2 - 2lz + z^2). \quad (1)$$

For any point  $z$  on the shaft between  $z_1$  and  $l$  the displacement  $u$  is given by

$$6EIlu = Xz(l-z_1)(2lz_1 - z_1^2 - z^2) - Mz\{l^2 - z^2 - 3(l-z_1)^2\}.$$

If the force and the couple be due to rotation, and if  $m_1$  be the mass of the load at the point  $z_1$ ,  $k_1$  be its radius of gyration about the line perpendicular to the plane of bending intersecting the axis of the shaft,  $\omega$  be the angular velocity of rotation of the shaft, and  $u_1$  be the displacement at the point  $z_1$ , then

$$X = m_1\omega^2u_1 \quad \text{and} \quad M = -m_1k_1^2\omega^2\left(\frac{du}{dz}\right)_1.$$

When there are several forces and couples acting along the shaft, the total displacement at any point due to the joint action of all the loads is equal to the sum of the displacements (being small) at that point due severally to each of the loads and couples.

Accordingly we can write

$$\frac{6EIu_r}{l^3\omega^2} = \sum_{s=0}^{s=r} \left\{ m_s A'_{rs} u_s + m_s k_s^2 B'_{rs} \left( \frac{du}{dz} \right)_s \right\} + \sum_{s=r}^{s=n} \left\{ m_s A_{rs} u_s + m_s k_s^2 B_{rs} \left( \frac{du}{dz} \right)_s \right\}. \quad (2)$$

where

$$A'_{rs} l^4 = z_s (l - z_r) (2lz_r - z_r^2 - z_s^2),$$

$$A_{rs} l^4 = z_r (l - z_s) (2lz_s - z_s^2 - z_r^2),$$

$$B'_{rs} l^4 = (l - z_r) (3z_s^2 - 2lz_r + z_r^2),$$

$$B_{rs} l^4 = z_r \{ l^2 - z_r^2 - 3(l - z_s)^2 \}.$$

In most practical problems the terms in  $k$  may be neglected.

Accordingly, if we omit the terms in  $k$  and write  $t = \frac{z}{l}$ , we have

$$\frac{6EIu_r}{l^3\omega^2} = \sum_{s=0}^{s=r} m_s A'_{rs} u_s + \sum_{s=r}^{s=n} m_s A_{rs} u_s, \quad . \quad . \quad (3)$$

where now

$$A'_{rs} = t (1 - t_r) (2t_r - t_r^2 - t_s^2)$$

and

$$A_{rs} = t_r (1 - t_s) (2t_s - t_s^2 - t_r^2).$$

Here it is to be noted that  $A'_{rs}$  and  $A_{rs}$  are functions of the positions of the loads  $m_s$  upon the shaft and of the position at which the deflexion is being calculated; and their values may be tabulated for different values of  $t_s$  and  $t_r$ , *i.e.* for different values of the loaded point  $t_s$  and of the point  $t_r$  at which the deflexion is being determined.

$A'_{rs}$  is employed when  $r > s$ , or, in other words, when the deflexion is considered at the point  $r$  which is farther from the origin than the particular load point indicated by  $s$ .

Conversely, when  $r < s$ ,  $A_{rs}$  is used.

It will be noticed that the expression for  $A'_{rs}$  is changed into that for  $A_{rs}$  by changing  $t_r$  to  $t_s$  and  $t_s$  to  $t_r$ . Thus  $A'_{rs} = A_{sr}$ , and  $A'_{sr} = A_{rs}$ .

If we write  $x$  for  $t_r$  and  $y$  for  $1 - t_s$ , we have the form

$$\frac{A}{xy} = 1 - (x^2 + y^2).$$

7. A table for  $A'_{rs}$  and  $A_{rs}$  for different values of  $t_r$  and  $t$  is given here.

$t_r$ 

$t_s$	0	.05	.1	.15	.2	.25	.3	.35	.4	.45	.5	.55	.6	.65	.7	.75	.8	.85	.9	.95	1.0
0	0																				
.05	0	45																			
.1	0	84	162																		
.15	0	117	227	325																	
.2	0	143	280	405	512																
.25	0	163	321	467	596	704															
.3	0	178	350	511	658	783	882														
.35	0	187	369	542	698	836	951	1035													
.4	0	191	378	555	720	866	990	1087	1152												
.45	0	191	378	557	724	873	1001	1107	1181	1224											
.5	0	187	370	545	710	860	990	1099	1180	1230	1250										
.55	0	179	354	523	681	827	955	1061	1145	1202	1230	1224									
.6	0	167	332	490	640	777	900	1005	1088	1148	1180	1181	1152								
.65	0	153	303	449	586	713	826	925	1005	1061	1099	1107	1087	1035							
.7	0	136	270	399	522	635	738	826	900	955	990	1001	990	951	882						
.75	0	117	232	343	449	547	635	713	777	827	860	873	866	836	783	704					
.8	0	96	190	281	363	449	522	586	640	681	710	724	720	698	658	596	512				
.85	0	73	145	215	281	343	399	449	490	523	545	557	555	542	511	467	405	325			
.9	0	49	93	145	190	232	270	303	332	354	370	378	378	369	350	321	280	227	162		
.95	0	25	49	73	96	117	136	153	167	179	187	191	191	187	178	163	143	117	84	45	
1.0	0	0	0	0	0	0	0	0	0	0	0	0	0	0	0	0	0	0	0	0	0

Values of  $A_{rs} \times 10,000$ .

8. Reverting now to the simple case of a single load of negligible moment of inertia on a light uniform shaft, equation (3) becomes (for  $r > s$ )

$$6EIu_r = m_s l^3 \omega^2 A'_{rs} u_s. \quad \dots \dots \dots (4)$$

If the point  $r$  is chosen so as to coincide with the load-point  $s$  of the shaft, we find that, if

$$6EI = m_s l^3 \omega^2 A'_{ss}. \quad \dots \dots \dots (5)$$

holds true, the elastic and centrifugal forces are equal to each other whatever small value we give to the displacement of the load, and accordingly the whirling speed is determined by the equation

$$\omega^2 = \frac{6EI}{m_s l^3 A'_{ss}}. \quad \dots \dots \dots (6)$$

More generally, for a number of loads, for which the effects of the moments of inertia are negligible, supported on a light uniform shaft, we first write down the displacement equation (3), and let  $r$  be given successively the values corresponding to the different load-points  $s$ . By eliminating the various values of  $u_s$  we find the whirling speeds are given by the determinantal equation :

$$\begin{vmatrix} W_1 A'_{11} - \phi & W_2 A_{12} & W_3 A_{13} & \dots \\ W_1 A'_{21} & W_2 A'_{22} - \phi & W_3 A_{23} & \dots \\ W_1 A'_{31} & W_2 A'_{32} & W_3 A'_{33} - \phi & \dots \\ \dots & \dots & \dots & \dots \end{vmatrix} = 0, \quad (7)$$

where

$$\phi = \frac{6EIg}{l^3 \omega^2} \quad \text{and} \quad W_1 = m_1 g, \text{ etc.}$$

When the number of loads is large, and when in addition the moments of inertia may not be neglected, the determinant is usually of a high order and consequently is tedious to solve. In ordinary cases in which the load may be regarded as made up of a number of separate parts suitably spaced along the uniform shaft, the order of the determinant is not inconveniently great, and its solution may be obtained by an arithmetical or a graphical method.

9. When using arithmetical methods, the determinantal equation (7) may perhaps most conveniently be solved in the following way :—

In the determinant the values of  $m_1 A'_{11}$ , etc. are all known in terms of the data of the problem, and may be evaluated conveniently by use of the table in paragraph (7).



Assume a suitable value for  $\phi$ , and on substituting we have a purely numerical determinant, which may be evaluated in the following straightforward way:—

Let the numerical determinant be represented by

$$\Delta \equiv \begin{vmatrix} a_1 & b_1 & c_1 & \dots \\ a_2 & b_2 & c_2 & \dots \\ a_3 & b_3 & c_3 & \dots \\ . & . & . & . \end{vmatrix}.$$

Multiply across the first row by  $\frac{1}{a_1}$ , the second by  $\frac{1}{a_2}$  etc., and at the same time the determinant itself by  $a_1, a_2$ , etc.

$$\text{Then } \Delta = a_1 a_2 a_3 \dots \begin{vmatrix} 1 & \frac{b_1}{a_1} & \frac{c_1}{a_1} & \dots \\ 1 & \frac{b_2}{a_2} & \frac{c_2}{a_2} & \dots \\ 1 & \frac{b_3}{a_3} & \frac{c_3}{a_3} & \dots \\ . & . & . & . \end{vmatrix}$$

$$= a_1 a_2 a_3 \dots \Delta',$$

where  $\Delta'$  stands for the determinant on the right.

Subtract the first row of  $\Delta'$  from each of the other rows in turn, and we find

$$\Delta' = \begin{vmatrix} 1 & \frac{b_1}{a_1} & \frac{c_1}{a_1} & \dots \\ 0 & \frac{b_2}{a_2} - \frac{b_1}{a_1} & \frac{c_2}{a_2} - \frac{c_1}{a_1} & \dots \\ 0 & \frac{b_3}{a_3} - \frac{b_1}{a_1} & \frac{c_3}{a_3} - \frac{c_1}{a_1} & \dots \\ . & . & . & . \end{vmatrix}$$

$$= \begin{vmatrix} \frac{b_2}{a_2} - \frac{b_1}{a_1} & \frac{c_2}{a_2} - \frac{c_1}{a_1} & \dots \\ \frac{b_3}{a_3} - \frac{b_1}{a_1} & \frac{c_3}{a_3} - \frac{c_1}{a_1} & \dots \\ . & . & . \end{vmatrix}$$

$$= \begin{vmatrix} a_1' & b_1' & \dots \\ a_2' & b_2' & \dots \\ . & . & . \end{vmatrix} \text{ say, } = \Delta_1, \text{ where } a_1' = \frac{b_2}{a_2} - \frac{b_1}{a_1} \text{ etc.}$$

Accordingly  $\Delta = a_1 a_2 a_3 \dots \Delta_1$ , where  $\Delta_1$  is a numerical determinant of order lower by 1 than  $\Delta$ .

Proceed in like manner with  $\Delta_1$ , reducing it to the product  $a_1' a_2' \dots \Delta_2$ , where  $\Delta_2$  is of order lower by 1 than  $\Delta_1$ , and so on.

Thus the arithmetical value of the determinant may be obtained. A value sufficiently approximate (especially with the first trial values of  $\phi$ ) may be obtained by carrying the several arithmetical operations to three or four significant figures; slide rule accuracy is often sufficient.

Now an odd number of real roots of the equation in  $\phi$  lie between those values of  $\phi$  which give opposite signs to the values of the determinant  $\Delta$ . Accordingly further trial values of  $\phi$  are to be chosen lying between such values when found, and so situated that the resulting determinant will be as nearly zero as may be.

Some indication of the location of the roots is obtained by observing that their sum is numerically equal to the sum of the constituents of  $\Delta$  along the principal diagonal of the determinant: *i. e.*,

$$W_1 A'_{11} + W_2 A'_{22} + \dots,$$

while the product of the roots is equal to the value of  $\Delta$  when  $\phi=0$ . Accordingly it is convenient to proceed in the following way.

First it is observed that when  $\phi$  is  $+\infty$  the value of  $\Delta$  is  $+\infty$  if the order  $n$  of the determinant is even, and  $-\infty$  if  $n$  is odd.

Also  $\phi=-\infty$  makes  $\Delta=+\infty$  whether  $n$  is even or odd.

Calculate the sum  $S$  of  $W_1 A'_{11}$ ,  $W_2 A'_{22}$ , etc., along the principal diagonal, and evaluate the determinant  $\Delta_0$  in which  $\phi$  is made equal to zero.

The sum of the  $n$  roots is  $S$ , and their product is  $\Delta_0$ . Physical considerations indicate that they are positive. Hence a trial value for  $\phi_1$  somewhat less than  $S$  is indicated, as this corresponds to a value of  $\omega$  in the neighbourhood of the first whirling speed.

Find the value of  $\Delta$  for this value  $\phi_1$  of  $\phi$  in the manner explained. Next try a value of  $\phi_2$  close to  $\phi_1$ , and proceed until adjacent values of  $\phi$  give small values of  $\Delta$  having opposite signs. The location of the first whirling speed is thus ascertained.

When this first root has been approximately determined, trial may be made of a considerably smaller value of  $\phi$  with a view to finding the root that corresponds to the second whirling speed.

It is usually sufficient for practical requirements to find the first two, or occasionally three, whirling speeds, so the process may be terminated when roots known to correspond closely to the first two or three whirling speeds have been obtained.

10. Alternatively, graphical methods may be employed for obtaining the determinantal equation in arithmetical form, and also for solving this equation. By the use of these graphical methods the approximate determination of the whirling speeds is greatly facilitated.

Before we proceed to evaluate the determinantal equation (7) by graphical means, it is convenient to rewrite equation (3) in the form

$$\psi u_r = \sum_{s=0}^{s=r} \chi'_{rs} u_s + \sum_{s=r}^{s=n} \chi_{rs} u_s, \quad \dots \dots (9)$$

and consequently equation (7) takes the form

$$\begin{vmatrix} \chi'_{11} - \psi & \chi_{12} & \chi_{13} & \dots\dots\dots \\ \chi'_{21} & \chi'_{22} - \psi & \chi_{23} & \dots\dots\dots \\ \chi'_{31} & \chi'_{32} & \chi'_{33} - \psi & \dots\dots\dots \\ \dots\dots\dots & \dots\dots\dots & \dots\dots\dots & \dots\dots\dots \end{vmatrix} = 0, \quad (10)$$

where, for  $r > s$ ,

$$\chi'_{rs} = W_s A'_{rs} \frac{l^3}{6EIg} \times \left( \frac{2\pi}{60} \right)^2 \times 10^7,$$

and for  $r < s$ ,

$$\chi_{rs} = W_s A_{rs} \frac{l^3}{6EIg} \times \left( \frac{2\pi}{60} \right)^2 \times 10^7.$$

$\psi \equiv \frac{10^7}{N^2}$ , where  $N$  is the speed in revs. per min.

Further, it is convenient to take  $\chi'_{rs}$  in factors which may all be represented to one scale in the diagram by lines of convenient length. Thus we take

$$\begin{aligned} \chi'_{rs} &= 1.2851 \times 100 A'_{rs} \times \left( \frac{W_s}{20} \times \frac{1}{10} \right) \\ &\times \left\{ \frac{1}{10} \times \left( \frac{l}{5} \times \frac{1}{2d} \right)^3 \times \frac{1}{2d} \right\}, \quad (11) \end{aligned}$$

in which Young's Modulus is taken as  $3 \times 10^7$  lb. weight per sq. in. and  $W$  is equal to  $mg$ ,  $g$  being expressed in inches per sec. per sec.

The diagram is constructed to give the product of these



at unit distance from the horizontal axis, and a curve through the origin, at each point on which the abscissa is one-tenth of the cube of the ordinate. Finally, through the origin a straight line is drawn, at each point on which the abscissa is 1.285 times the corresponding ordinate. The method of using this diagram is indicated in paragraph (16).

12. On the lower half of the paper two curved loops passing through the origin O are to be drawn in the way indicated in fig. 1. One loop OLA MO is in the S.W., and one ONB TO is in the S.E. quadrant. Also in the S.E. quadrant a curved line OC is drawn which for part of its length is almost straight.

Each loop is a reflexion of the other in the vertical axis. The origin O corresponds to both ends of the shaft, while the points A and B correspond to its middle point. The right-hand halves of each loop OMA and OTB correspond to points on one-half of the shaft nearest the origin, and the left halves OLA and ONB of the loops correspond to points on the second half of the shaft. In finding the value of  $A'_{rs}$  or  $\chi'_{rs}$  if the number  $r$  is greater than  $s$ , we choose the point  $r$  on the left loop OA, and from it draw a line to the point  $s$  on the right loop OB. On the other hand, if  $r$  is less than  $s$ , the values of  $A_{rs}$  and of  $\chi_{rs}$  are obtained by choosing the point  $r$  on the right loop OB and drawing a line to it from the point  $s$  on the left loop OA. Thus the greater of  $r$  and  $s$  is always chosen on the left loop OA, and a straight line is drawn from it to the lesser of  $r$  and  $s$  on the right loop OB.

Equal horizontal scales are drawn below the two loops as shown. The scales are such that the points A and B correspond to the middle point of the shaft.

To find the position on the loops of any other load-point  $s$  of the shaft, choose the position of  $s$  as a fraction of the length of the shaft on each of the horizontal scales in turn. Proceed vertically from these points to meet the curve X'O'X, and then horizontally to meet the appropriate sides of the loops as indicated. These points on the loops correspond to the position  $s$  on the shaft. Do this for all the load positions and for both loops, marking the resulting points thereon.

The loops OA and OB have been so constructed that if a straight line be drawn from a load-point L on one loop to another load-point T on the other loop, the line LT intersects the vertical axis in the point R, and if from R a horizontal line be drawn meeting the curve OC in S, then the length



RS or its equivalent OU is equal to  $100A'_{rs}$ , where  $r$  and  $s$  correspond to the positions of the loads at L and T, and  $A'_{rs}$  is the position function of paragraph (6). Thus the various values of  $A'_{rs}$  and  $A_{rs}$  corresponding to the different load positions are at once obtained.

13. The curves OLA and OMA in fig. 1 have as the coordinates of their points that correspond to the divisions of the length of the shaft into twentieths the following approximate values:—

$t$ .	OX'.	OY'.
0	0	0
0.05	1.80	0.75
0.1	3.38	1.89
0.15	4.16	3.02
0.2	5.24	4.44
0.25	6.34	5.85
0.3	6.82	6.89
0.35	7.36	7.74
0.4	8.12	8.50
0.45	8.50	8.74
0.5	10.00	8.92
0.55	9.42	8.25
0.6	8.88	7.36
0.65	8.30	6.27
0.7	7.55	5.05
0.75	6.50	3.77
0.8	5.46	2.62
0.85	4.16	1.56
0.9	2.83	0.77
0.95	1.46	0.28
1.0	0	0

The curve OC passes through the points whose coordinates are

OX.	OY'.
0	0
2.0	1.49
10.5	7.10
12.5	8.92

and it is practically straight between the two intermediate points in this table.

14. Let us now suppose that we possess the data for a particular loaded shaft for which the whirling speeds are required. It will be found convenient to carry out the various operations on a sheet of tracing-paper pinned over the construction diagram drawn on squared paper.

Let the load consist of a number of masses whose weights are  $W_1, W_2, W_3$ , etc., lb. spaced along the shaft at positions  $z_1, z_2, z_3$ , etc.

Let the effects of the moments of inertia of the loads on the whirling speeds be negligible, and further let the shaft be of uniform diameter  $d$  inches, and of length between centres of bearings at its ends  $l$  inches. We proceed with the diagram (fig. 1) as follows:—

There are two fundamental lines and one fundamental curve in the N.W. quadrant (fig. 1), viz. a horizontal straight line QF distant 1 unit from the horizontal axis, an oblique straight line OJ through the origin such that for each of its points the abscissa is equal to 1.285 times the ordinate, and a curve OH through the origin for each point of which the abscissa is equal to one-tenth of the cube of the ordinate.

In the N.W. quadrant take a length OD representing to scale twice the diameter of the shaft ( $2d$ ). From D draw a line vertically intersecting in F the horizontal line QF, which is drawn at unit distance from the horizontal axis: *i. e.*, OQ or DF is equal to one unit of the scale of the diagram. Next join OF and produce it. Mark the point E so that OE represents one-fifth of the length of the shaft to the same scale, *i. e.*  $OE = \frac{l}{5}$ , and draw a vertical line EG meeting

the line OF in G. Through G draw a horizontal line GH to meet in H the curve OH. Through H draw a vertical line to meet the line OF in I, and IJ horizontally to meet the straight line OJ in J. Through J draw a vertical line JK meeting the horizontal line QF in K. Join OK and produce it. Then the line OK is such that for each point upon it the ratio of the abscissa to the ordinate is  $0.6425 \times 10^{-4} \times \frac{l^3}{d^4}$ .

The diagram should be constructed to suitable scales for  $d, l$ , and  $W$ , so that the construction lines in the N.W. and N.E. quadrants lie conveniently for the operations. It may also be convenient in the N.W. quadrant to draw the line JK to meet the horizontal line distant 10 units from the horizontal axis (instead of meeting the horizontal line 1 unit from the horizontal axis), in which case the expression for  $\psi$  must be written as  $\frac{10^6}{N^2}$  instead of  $\frac{10^7}{N^2}$ .

There is one fundamental line in the N.E. quadrant, viz. a

vertical line through P at a distance 10 units from the vertical axis. On this vertical line through P mark off from P lengths  $PW_1, PW_2, PW_3, \dots$  representing  $\frac{W_1}{20}, \frac{W_2}{20}, \dots$  to the same scale as before. Join  $OW_1, OW_2, OW_3, \dots$  and produce these lines. For each point on  $OW_s$  the ratio of the ordinate to the abscissa is  $\frac{W_s}{200}$ .

In the lower half of the chart are the two loops OA and OB, the curved line OC, and the curve  $X'O'X$ , which enables points to be selected on the loops OA and OB corresponding to any specified positions along the shaft. Mark the points on the loops corresponding to the given load positions.

The value of  $\chi'_{rs}$  is obtained from the completed diagram by the following procedure.

From the load-point  $r$  (when  $r$  is greater than  $s$ ) on the loop OA draw a straight line to the load-point  $s$  on the loop OB; where this line cuts the vertical axis in R draw a horizontal line to meet the curved line OC in S. Draw a vertical line through S to meet the horizontal axis in U, and produce this line till it meets the radial line corresponding to  $W_s$  in the N.E. quadrant at the point V. Through V draw a horizontal line to meet the line OK in W in the N.W. quadrant, and WZ vertically to meet the horizontal axis in Z. Then the length OZ represents to the scale of the diagram the value of the function  $\chi'_{rs}$ , and similarly of  $\chi_{rs}$ . Thus the values of  $\chi$  in the determinant are found arithmetically, and the solution may be obtained by the method described in paragraph (10).

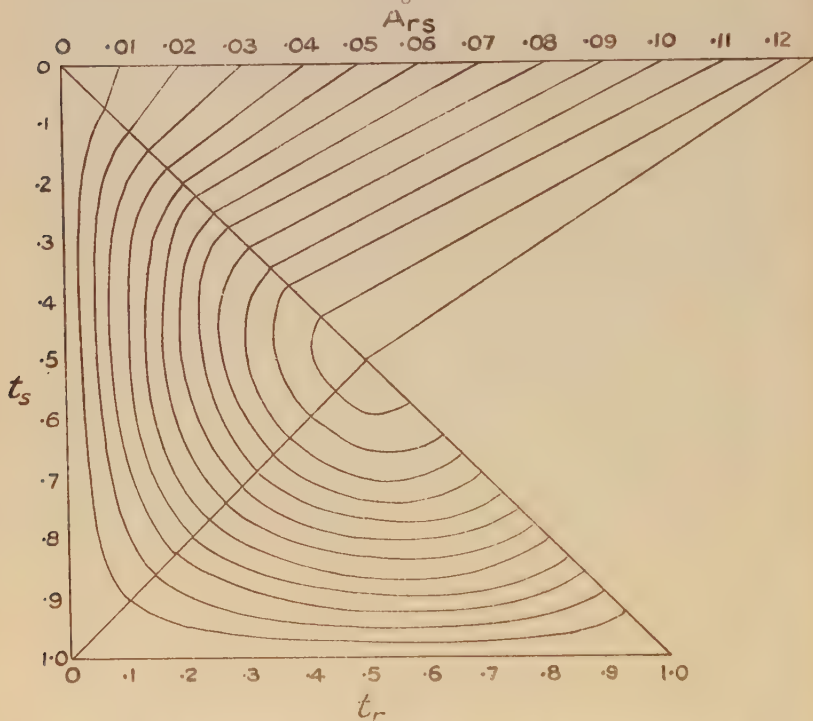
15. Instead of employing the two loops for the purpose of finding the values of  $A'_{rs}$  and  $A_{rs}$ , we may arrange  $t_r$  and  $t_s$  along axes at right angles to one another, and draw on the triangular diagram a series of contour lines corresponding to the values of  $A'_{rs}$  and  $A_{rs}$  consequent on choosing particular values of  $t_r$  and  $t_s$  (see fig. 2).

The curves of this family may be produced to meet the horizontal axis of the diagram at distances from the origin corresponding to the respective values of  $A_{rs}$ . By drawing these curves sufficiently closely to one another suitable accuracy may be obtained.

On this diagram the larger of  $r$  and  $s$  is measured downwards from zero at the apex, and the lesser of  $r$  and  $s$  is measured along the base towards the right. These two

704 Dr. H. H. Jeffcott on a Graphical Method for  
coordinate positions fix a point on the contour diagram which  
gives the corresponding value of  $A'_{rs}$  or  $A_{rs}$ .

Fig. 2.



16. It is worthy of note that if  $u'_r$  is the deflexion due to gravity at the point  $t_r$  of the shaft when at rest,

$$\theta u'_r = g \sum_{s=0}^{s=r} W_s A'_{rs} + g \sum_{s=r}^{s=n} W_s A_{rs}, \quad \dots \quad (12)$$

where

$$\theta \equiv \frac{6EIg}{\beta}.$$

With this may be compared the centrifugal displacement  $u_r$ , which is given by

$$\theta u_r = \omega^2 \sum_{s=0}^{s=r} W_s A'_{rs} u_s + \omega^2 \sum_{s=r}^{s=n} W_s A_{rs} u_s.$$

Thus the position functions  $A'_s$  and  $A_{rs}$  for gravitational deflexion are the same as for centrifugal displacement in a single loop, and the methods here set out may therefore be

applied to gravitational deflexions so far as they are relevant. Also if we use the quantities  $\chi$ , we have for the gravitational deflexion  $u'_r$  at a point  $r$  on the shaft

$$\frac{u'_r}{g} \times \left(\frac{2\pi}{60}\right)^2 \times 10^7 = \sum_{s=0}^{s=r} \chi'_{rs} + \sum_{s=r}^{s=n} \chi_{rs}$$

or

$$284 \cdot 1 u'_r = \sum_{s=0}^{s=r} \chi'_{rs} + \sum_{s=r}^{s=n} \chi_{rs}, \quad . \quad . \quad . \quad (13)$$

the dimensions being inches and pounds, assuming  $E = 3 \times 10^7$  lb. per sq. inch.

Fig. 1 gives approximately the values of  $\chi'_{rs}$  and  $\chi_{rs}$  at the various load-points.

17. It should be observed that if a single load is placed on the shaft at a point not far from the origin, then by drawing a tangent from that point to the appropriate side of the other loop (fig. 1) it will be seen that the maximum gravitational deflexion occurs, not at the centre of the shaft, but at a point a short distance away from it on the side nearer the load. Further, as the position of the load is gradually altered to the middle of the shaft, the position of maximum deflexion approaches the middle point of the shaft.

This may be readily be verified. The gravitational deflexion  $u'_1$  at the point  $z_1$  on the shaft is given by the equation

$$u'_1 = \frac{W}{6EI} z_1(l-a)(2la-a^2-z_1^2),$$

where the load  $W$  is placed at a point distant  $a$  from the origin, and  $z_1$  is not greater than  $a$ . If  $z_1$  is regarded as variable and  $a$  is constant, by differentiating with respect to  $z_1$  the expression for  $u'_1$  we find that the maximum value of  $u'_1$  occurs at the position  $z_1$ , given by

$$z_1^2 = \frac{a}{3} (2l-a), \quad \text{in which } z_1 \nless a.$$

Hence if

$$\begin{aligned} a &= \frac{l}{2} & z_1 &= \frac{l}{2}, \\ a &= l & z_1 &= \frac{l}{3} = 0 \cdot 577l. \end{aligned}$$

Similarly if  $z_1 \nless a$ , it may be shown that if

$$\begin{aligned} a &= \frac{l}{2} & z_1 &= \frac{l}{2}, \\ a &= 0 & z_1 &= 0 \cdot 423l. \end{aligned}$$



Further, it may be shown, by regarding  $z_1$  as constant and  $a$  variable and differentiating  $u'_1$  with respect to  $a$ , that the maximum value of  $u'_1$  at  $z_1$  is given by

$$z_1^2 = l^2 - 3(l-a)^2 \quad \text{if } z_1 \neq$$

and therefore the deflexion at  $z_1$  is greatest when the load is at the position  $a$  given by this equation.

If

$$z_1 = \frac{l}{2} \quad a = \frac{l}{2},$$

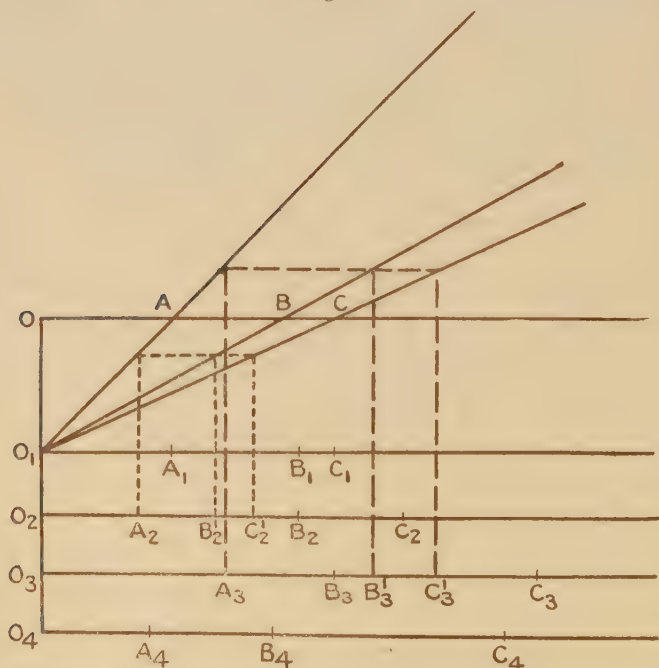
$$z_1 = 0 \quad a = 0.423l;$$

and in like manner if  $z_1 = l$ ,  $a = 0.577l$ .

18. The arithmetical determinant  $\Delta$  of paragraph (9) may be evaluated by graphical means in the following manner:—

Draw a number of horizontal lines (fig. 3), on squared

Fig. 3.



paper at convenient distances apart, and a vertical line intersecting them in  $O_1, O_2, O_3, \dots$ . On these lines mark off lengths representing to scale the values of the various

constituents of the determinant, and to right or left of the vertical line according to whether the corresponding constituent is positive or negative.

Thus on the horizontal line through  $O_1$ ,  $O_1A_1$  represents  $a_1$ ;  $O_1B_1$  represents  $b_1$ ;  $O_2A_2$  represents  $a_2$ ; and so on.

On the vertical line mark the point  $O$  above  $O_1A_1$  (which is the topmost of the horizontal lines) so that  $O_1O=a_1$ , and through  $O$  draw a horizontal line. From  $A_1, B_1, C_1, \dots$  draw vertical lines to meet the horizontal line through  $O$  in  $A, B, C, \dots$ . Join  $O_1$  to  $A, B, C, \dots$  and proceed in the following way. From the point  $A_2$  go vertically to meet the line  $O_1A$ , then horizontally to meet the line  $O_1B$ , then vertically downwards to meet  $O_2A_2$  in  $B'_2$ .

Next proceed vertically from  $A_2$  to  $O_1A$ , proceed horizontally to  $O_1C$ , and vertically to  $O_2A_2$ , meeting it at  $C'_2$ . Proceed in a similar manner from  $A_3$ , namely vertically to  $O_1A$ , horizontally to  $O_1B$ , and vertically to  $O_3A_3$  in  $B'_3$ . Likewise to  $C'_3$ , and so on according to the number of constituents in the determinant. This procedure is to be carried out for each of the constituents (except the first) in the first column. The result is that the original determinant is equal approximately to  $a_1$  multiplied by a determinant of order lower by 1 and consisting of the following constituents:—

$B'_2B_2, C'_2C_2$ , etc., . . . ,  $B'_3B_3, C'_3C_3$ , etc., . . . and the first constituent is positive if  $B'_2$  is to the left of  $B_2$ , and negative if to the right of  $B_2$ , and similarly for the other constituents.

We proceed in like manner to evaluate this second determinant and reduce it to one of an order lower by unity, multiplied by the leading constituent  $a'_2$ . Finally, the original determinant is approximately equal to the product of the leading constituents of the various determinants obtained in this manner down to the last.

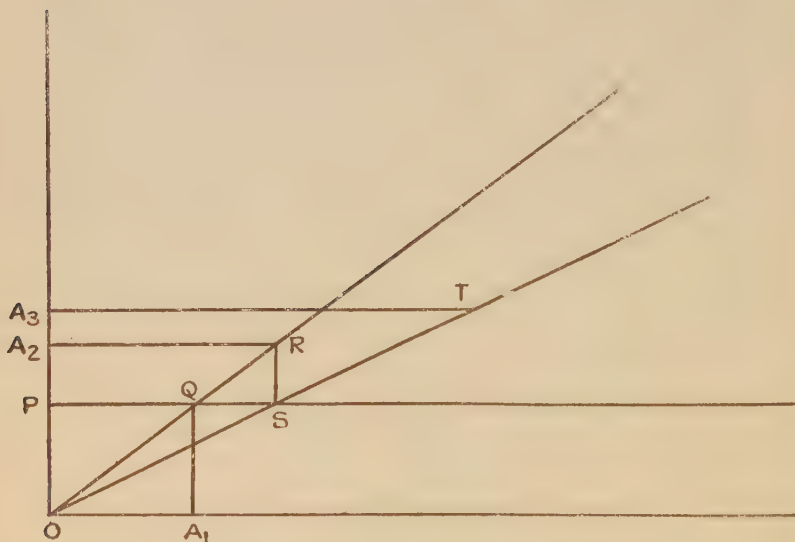
The lengths of these lines may be multiplied together graphically in the following way:—

On squared paper draw horizontal and vertical axes through the origin  $O$  (fig. 4), and through a point  $P$  on the vertical axis where  $OP=1$  draw the horizontal line  $PQ$ . On the horizontal axis mark off  $A_1$  so that  $OA_1$  is equal to the length  $a_1$  of the first of the lines to be multiplied together. Draw a vertical line through  $A_1$  to meet the line  $PQ$  in  $Q$ . Join  $OQ$  and produce it. Mark off on the vertical axis the point  $A_2$  so that the length  $OA_2=a'_2$ , the second of the lines to be multiplied together, and draw the horizontal line  $A_2R$  to meet the line  $OQ$  in  $R$ . Through  $R$  draw a vertical line meeting  $PQ$  in  $S$ , and join  $OS$  and produce it. Mark  $A_3$

so that  $OA_3 = a''_3$ . Draw a horizontal line through  $A_3$  meeting  $OS$  in  $T$ , then the length  $A_3T$  is the product of  $a_1, a'_2, a''_3$  to the scale of the diagram. Continue the process for the number of factors required.

We thus obtain the value of  $\psi$  or  $\frac{10^7}{N^2}$ . If the values of  $a_1, a'_2, \dots$  are relatively large, it may be necessary to make  $OP$  equal to 10 units or 100 units, with consequent modification in the value of the graphical product.

Fig. 4.



The addition to the diagram of a radial line and two curves would enable the value of  $N$  to be read off directly if desired.

19. The following examples illustrate the procedure.

1. A single concentrated load at the centre of a light uniform shaft freely supported at its ends. Diameter of shaft 1.5 inches, length of shaft 40 inches, load 80 lb. Find the whirling speed and the gravitational deflexion at the centre.

(a) By graphical method. First find the radial line in the N.W. quadrant that corresponds to the given values of  $d$  and  $l$ . In the N.E. quadrant construct the radial line corresponding to the given load. Then in the lower half of the diagram join the points on the two loops that correspond

to the position of the load. From the intersection with the vertical axis proceed horizontally to the curve OC, vertically to meet the radial line of the N.E. quadrant, then horizontally to meet the radial line in the N.W. quadrant, and then vertically to the horizontal axis, on which the intercept from the origin is equal to  $\chi$ .

This intercept is quickly found to be 4.05. Then by equation (10), paragraph (10),  $\frac{10^7}{N^2} = \psi = \chi = 4.05$ . Therefore  $N = 1571$  revs. per min.

(b) By arithmetical method, using equation (6) and the table for  $A_{rs}$  in paragraph (7).

Here

$$\begin{aligned} t_s &= 0.5 \\ W_s &= 80 \\ l &= 40 \\ d &= 1.5 \\ E &= 3 \times 10^7 \\ A_{rs} &= 0.125. \end{aligned}$$

$$\omega^2 = \frac{6EIg}{W_s l^3 A_{rs}}.$$

After arithmetical reduction we find

$$\omega = 163.8.$$

$$\therefore N = 1565 \text{ revs. per min.}$$

(c) The gravitational deflexion at the centre of the shaft in this example is by equation (12), paragraph (16) :

$$u' = \frac{gm_s A_{rs} l^3}{6EI} = \frac{W_s A_{rs} l^3}{6EI}.$$

Therefore  $u' = \frac{W l^3}{48EI}$ , which is the well-known formula for the deflexion at the middle point of the shaft under central load.

Hence  $u' = 0.0143$  inch.

(d) By equation (13) of paragraph (15) we have

$$\begin{aligned} 284.1 u' &= 4.05 \\ u' &= 0.0143 \text{ inch.} \end{aligned}$$

2. Three equal concentrated loads on a light uniform shaft supported in two bearings at positions distant respectively from one end by  $\frac{1}{4}$ ,  $\frac{1}{2}$ ,  $\frac{3}{4}$  of the length.

Diameter of shaft 1 inch, length of shaft 30 inches, each

load 80 lb. Find the three whirling speeds and the gravitational deflexions at the positions of the loads.

(a) By graphical method.

Using the diagram in fig. 1, drawn to a suitable scale, first construct in the N.W. quadrant the radial line that corresponds to the given values of  $d$  and  $l$ .

In the N.E. quadrant draw the radial lines that correspond to the three loads. As these loads are equal to one another, these radial lines coincide.

Next in the lower half of the diagram mark on the two loops the positions of the loads.

Then to find the arithmetical values of  $\chi_{rs}$  we choose the load positions  $r$  and  $s$ , one on each loop, the greater numerically to be on the left loop. The line joining these points on the loops intersects the vertical axis of the diagram, and a horizontal line through this intersection cuts the curve OC in a point from which a vertical line is drawn to meet the appropriate radial line in the N.E. quadrant, and then horizontally to meet the radial line in the N.W. quadrant, of which intersection the abscissa represents to scale the value of  $\chi_{rs}$ .

In this way the values of  $\chi'_{11}$ ,  $\chi_{12}$ , etc., are found. It is not necessary to scale off these abscissæ, for their lengths may be incorporated directly into the graphical solution of the determinantal equation.

Working with a small-scale diagram, we find that the values of  $\chi_{rs}$  substituted in equation (10) of paragraph (10) lead to the equation :

$$\begin{vmatrix} 4.9 - \psi & 6.0 & 3.8 \\ 6.0 & 8.7 - \psi & 6.0 \\ 3.8 & 6.0 & 4.9 - \psi \end{vmatrix} = 0.$$

The sum of the roots of this equation is 18.5. They are found to be  $\psi = 17.185, 1.1, 0.215$ .

$$\text{Now} \quad \psi = \frac{10^7}{N^2}.$$

Hence  $N = 763, 3015, 6820$  revs. per min.

Similar approximate values may be obtained more readily by solving the determinantal equation graphically in the manner described in paragraph (18).

(b) By arithmetical method using the determinantal equation (7) and the table for  $A_{rs}$  in paragraph (7).



Here

$$t_s = 0.25, 0.5, 0.75$$

$$W_s = 80, 80, 80$$

$$l = 30$$

$$d = 1$$

$$E = 3 \times 10^7.$$

Hence from Table I.:

$$\begin{array}{lll} A'_{11} = .0704 & A_{12} = .0860 & A_{13} = .0547 \\ A'_{21} = .0860 & A'_{22} = .1250 & A_{23} = .0860 \\ A'_{31} = .0547 & A'_{32} = .0860 & A'_{33} = .0704. \end{array}$$

Now each load is 80 lb.

Hence the whirling speeds are given by

$$\begin{vmatrix} 5.632 - \phi & 6.88 & 4.376 \\ 6.88 & 10.00 - \psi & 6.88 \\ 4.376 & 6.88 & 5.632 - \phi \end{vmatrix} = 0.$$

The sum of the roots is 21.264.

By subtracting the first column from the third, and then adding the third row to the first, the determinant is reduced to one of the second order, and finally it is equal to

$$(\phi - 1.256)\{(\phi - 10)^2 - 94.6688\} = 0.$$

Hence  $\phi = 19.728, 1.256, 0.272.$

Now

$$\phi = \frac{6EIg}{\omega^2 l^3}, g = 386, \text{ and } \frac{6EIg}{l^3} = 1.264 \times 10^5$$

since

$$I = \frac{\pi d^4}{64}.$$

Hence

$$\omega^2 = 6406, \quad 100620, \quad 464614$$

and

$$\omega = 80.04, \quad 317.2, \quad 681.6.$$

Hence

$$N = 764, \quad 3029, \quad 6560, \text{ revs. per min.}$$

Alternatively the determinantal equation may be solved

by trying likely values for  $\phi$ , and proceeding until adjacent values of  $\phi$  give opposite signs to the value of  $\Delta$ . A root lies between those values of  $\phi$ , and its proximity to either value may be estimated from the corresponding values of  $\Delta$ .

Thus since the sum of the roots is 21.264, a trial value of 20 may be chosen to begin with. This will be found to give a negative value to  $\Delta$ , and as  $\phi = +\infty$  also gives a negative value, it may be concluded that the greatest root is less than 20. A trial of 19 gives a positive value to  $\Delta$ , and hence the root lies between 19 and 20. Also the values of  $\Delta$  indicate that the root is probably nearer 20 than 19. 19.5 gives a positive value, so that the root lies between 19.5 and 20. Continuing in this way the value of  $\phi$  may be found to the desired degree of approximation.

In like manner  $\phi = 1$  gives a negative value to  $\Delta$ , while  $\phi = 1.5$  gives a positive value.

Also  $\phi = 0$  gives a positive value to  $\Delta$ , and  $\phi = 0.5$  gives a negative value.

Hence real roots lie between 0 and 0.5, and between 1 and 1.5, in addition to that between 19.5 and 20.

By continuing this process, sufficiently close values of  $\phi$  and hence of the whirling speeds may be obtained.

The types of vibration corresponding to the three whirling speeds are respectively :—

- (1) Deflexion in one loop with nodes at the bearings, the three loads being deflected to one side of the axis.
- (2) Deflexion in two loops with nodes at the bearings and at an intermediate point, two adjacent loads being deflected to one side and the third load (near one end of the shaft) being deflected to the other side of the axis.
- (3) Deflexion in three loops with nodes at the bearings and at two intermediate points, the central load being deflected to the opposite side of the axis to the two other loads.

(c) The gravitational deflexions at the positions 0.25, 0.5, and 0.75 on the shaft may be found thus :—

By equation (12) of paragraph (16) :

$$\frac{\theta u'_r}{g} = \sum_{s=0}^{s=r} W_s A'_{rs} + \sum_{s=r}^{s=n} W_s A_{rs},$$

where

$$\theta = \frac{6EIg}{l^3} = 1.264 \times 10^5.$$

Hence

$$\frac{\theta}{g}u_1' = W_1A'_{11} + W_2A'_{12} + W_3A'_{13},$$

$$\frac{\theta}{g}u_2' = W_1A'_{21} + W_2A'_{22} + W_3A'_{23},$$

$$\frac{\theta}{g}u_3' = W_1A'_{31} + W_2A'_{32} + W_3A'_{33}.$$

Now

$$g = 386, W_1 = W_2 = W_3 = 80, \frac{\theta}{g} = 327.4, W_1A'_{11} = 5.632, \text{ etc.,}$$

as in Section (b) of this example.

$$\therefore 327.4u_1' = 5.632 + 6.88 + 4.376 = 16.888,$$

$$327.4u_2' = 6.88 + 10 + 6.88 = 23.76,$$

$$327.4u_3' = 4.376 + 6.88 + 5.632 = 16.888.$$

Hence

$$u_1' = u_3' = 0.052 \text{ inch,}$$

$$u_2' = 0.073 \text{ inch.}$$

(d) Alternatively it is more rapid to use equation (13) of paragraph (16) when the diagram (fig. 1) is available, for we have directly from the diagram the values of  $\chi_{rs}$ , as in section (a) of this example, and

$$284.1u_r' = \sum_{s=0}^{s=r} \chi'_{rs} + \sum_{s=r}^{s=r} \chi_{rs}.$$

Thus

$$284.1u_1' = 14.7 \quad u_1' = 0.052 \text{ inch} = u_3',$$

$$284.1u_2' = 20.7 \quad u_2' = 0.073 \text{ inch.}$$

LXXI. *Electric Double-Refraction in Relation to the Polarity and Optical Anisotropy of Molecules.*—Part I. *Gases and Vapours.* By Prof. C. V. RAMAN, F.R.S., and K. S. KRISHNAN\*.

### 1. Introduction.

AS is well known, Kerr discovered that fluids when placed in an electrostatic field exhibit a feeble birefringence. The accepted explanation of the effect is that the electrostatic field exercises an orientative influence on the molecules, that the latter possess an intrinsic optical anisotropy, and that, in consequence of the molecular orientation, the fluid as a whole becomes optically anisotropic. In

\* Communicated by the Authors.

the original form of the theory, due to Langevin, it is assumed that the molecules are both electrostatically and optically anisotropic, and that the orientative action of the field is due to the couple exerted by it on the induced doublets in the molecules. In the later form of the theory, due to Born \*, the orientative effect exerted by the field on the permanent electric doublet, if any, present in the molecule is also taken into account. We propose in the series of papers of which this is the first, to discuss the available data regarding electric double-refraction in the light of these theories, and to correlate them with what is known regarding the optical anisotropy of molecules from observations on light-scattering, and regarding the permanent electric moment from the observed variation of the dielectric constant with temperature.

## 2. The Kerr Constant Data for Gases and Vapours.

The simplest case to consider is naturally that of gases and vapours, as here the mutual influence of the molecules is negligible. The available data regarding the Kerr constant in the gaseous state are, however, very scanty, and the corresponding data regarding light-scattering have also not been obtained for all the substances. The variation of dielectric constant with temperature is also not known for many vapours. Such figures as are available are, however, very interesting, and are collected together in Table I. The second column gives the Kerr constant for the sodium line for one atmosphere pressure at 20° C., compiled from the measurements of Leiser †, Hansen ‡, and Szivessy §. Column 3 gives the ratio,  $r$ , of the components of polarization in the light transversely scattered by the vapours, when the incident light is unpolarized, from the measurements by Rayleigh ||, Cabannes ¶ and others. The last column gives the permanent electric moments of the molecules as calculated by Zahn \*\* and others.

\* For a good account of the subject, see P. Debye, Marx's 'Handbuch der Radiologie,' Bd. vi. pp. 754-776.

† R. Leiser, *Ver. d. Deutsch. Phys. Gesell.* xiii. p. 903 (1911).

‡ D. E. Hansen, quoted by G. Szivessy, *Jahrbuch der Radioaktivität*, xvi. p. 414 (1920).

§ G. Szivessy, *Zeits. f. Phys.* xxvi. p. 323 (1924).

|| Lord Rayleigh, *Proc. Roy. Soc. A*, xcv. p. 155 (1918).

¶ J. Cabannes and J. Granier, *Comptes Rendus*, clxxxii. p. 885 (1926); *Journ. d. Physique* [VI], p. 429 (1923). See also K. R. Ramanathan and N. G. Srinivasan, *Phil. Mag.* i. p. 491 (1926), and W. H. Martin and A. F. W. Cole, *Chem. Abs.* xx. p. 1752 (1926).

\*\* C. T. Zahn, *Phys. Rev.* xxvii. p. 455 (1926); and also C. P. Smyth, *Journ. Amer. Chem. Soc.* xlvi. p. 2151 (1924).

TABLE I.

Gas or Vapour.	Kerr const. for the D line for 1 atm. press. at 20° C., $K \times 10^{10}$ .	Depolari- zation factor, $r \times 100$ .	Approximate value of the permanent moment, $\times 10^{18}$ .
Ethyl chloride .....	8.7	1.64	2.3 (?)
Methyl bromide.....	8.2	.....	Polar.
Acetaldehyde .....	10.0	.....	1.69 (from liquid at 10° C.).
Methyl chloride.....	5.45	1.52	Polar.
Ethyl nitrate .....	15.0	.....	1.57 (from liquid at 20° C.)
Phosgene.....	1.4	.....	.....
Carbon dioxide .....	0.24 (at 17° 5 C.).	9.8	Non-polar.
Cyanogen .....	0.68	12.0 (?)	0.62 (from liquefied gas at 23° C.).
Hydrogen cyanide.....	14.7	.....	1.22 (from liquid at 21° C.).
Acetylene .....	0.29	4.6	Non-polar.
Ammonia .....	0.59 (at 17° 9 C.).	1.0	1.44
Nitrous oxide .....	0.48	12.2	Non-polar.
Chlorine .....	0.35	4.1	Non-polar.
Hydrogen chloride ...	0.90	1.0	1.03
Hydrogen sulphide ...	0.26	1.0	1.02
Sulphur dioxide.....	-1.67 (at 17° 3 C.).	4.9 (?)	1.61
Nitrogen .....	No appreciable double re- fraction at 2 atm. press.	3.75	Non-polar.
Oxygen .....		6.45	Non-polar.
Nitric oxide .....		2.6	Slightly polar.
Carbon monoxide .....		3.4	Almost non-polar ( $\mu = 0.13 \times 10^{-18}$ ).

It is very significant that all the substances which possess a large Kerr constant have molecules which are electrically polar. Amongst the non-polar molecules, the gases  $\text{CO}_2$  and  $\text{N}_2\text{O}$  are distinguished by the possession of a large optical anisotropy, as will be evident from the values of the depolarization factor in column 3 of the table, and yet, as will be seen from the data, they exhibit only a relatively feeble Kerr effect; oxygen, which is strongly anisotropic



optically but is also non-polar, shows hardly any observable Kerr effect. This suggests immediately that, in the case of molecules which are electrically polar, the orientative influence of an electrostatic field is chiefly due to the couple exerted on the permanent electric doublet present in the molecule. The expression for the Kerr constant of a vapour sufficiently rare to obey Boyle's law is

$$K = \frac{n_p - n_s}{\lambda E^2} \\ = \frac{3\pi\nu}{\lambda} (\theta_1 + \theta_2), \quad . \quad . \quad . \quad . \quad (1)$$

where  $\nu$  is the number of molecules per unit volume,  $\lambda$  is the wave-length of the incident light,  $E$  the acting electrostatic field, and  $n_p$  and  $n_s$  are the refractive indices for light-vibrations along and perpendicular to the field.

$$\theta_1 = \frac{1}{45kT} [(A-B)(A'-B') + (B-C)(B'-C') \\ + (C-A)(C'-A')], \quad (2)$$

$$\text{and } \theta_2 = \frac{1}{45k^2T^2} [(A-B)(\mu_1^2 - \mu_2^2) + (B-C)(\mu_2^2 - \mu_3^2) \\ + (C-A)(\mu_3^2 - \mu_1^2)], \quad (3)$$

where  $k$  is the Boltzmann constant per molecule;  $T$  is the absolute temperature;  $A, B, C$  are the moments induced in a molecule along its three principal axes of optical anisotropy by unit electric force in the incident light-waves acting respectively along these directions;  $A', B', C'$  are similar moments induced along the same three directions by unit *electrostatic* field; and  $\mu_1, \mu_2, \mu_3$  are the components along these directions of the permanent electric moment of the molecule.

### 3. Electrically Non-Polar Molecules.

For a non-polar molecule such as  $\text{CO}_2$ ,  $\theta_2 = 0$  and we are only concerned with  $\theta_1$ . It is not unreasonable in such cases to assume, as has been done by Gans\*, that

$$\frac{A'}{A} = \frac{B'}{B} = \frac{C'}{C}.$$

Then this ratio  $= \frac{\delta - 1}{n_0^2 - 1}$ , where  $\delta$  is the dielectric constant of the vapour and  $n_0$  is the refractive index of the vapour

\* R. Gans, *Ann. der Physik*, lxx. p. 97 (1921).

outside the field. The expression (2) for  $\theta_1$  therefore reduces to

$$\theta_1 = \frac{1}{45kT} \frac{\delta - 1}{n_0^2 - 1} [(A - B)^2 + (B - C)^2 + (C - A)^2]. \quad (4)$$

Now, from the theory of light-scattering by optically anisotropic molecules the factor of depolarization,  $r$ , of the transversely-scattered light is given by

$$r = \frac{6[(A - B)^2 + (B - C)^2 + (C - A)^2]}{10 \left[ \frac{3(n_0 - 1)^2}{2\pi\nu} \right]^2 + 7[(A - B)^2 + (B - C)^2 + (C - A)^2]}. \quad (5)$$

From (1), (4), and (5) we may readily obtain as the relation between the Kerr constant and the factor of depolarization

$$K = \frac{3(n_0 - 1)(\delta - 1)}{4\pi\nu\lambda kT} \cdot \frac{r}{6 - 7r}. \quad \dots \quad (6)$$

Table II. gives the values of the Kerr constant calculated from  $r$  according to this expression, for a few non-polar molecules for which data are available. The close agreement between the calculated and observed values shows the validity of the assumptions made.

TABLE II.

Gas or Vapour.	Depolarization factor. $r \times 100$ .	$(n_0 - 1) \times 10^4$ for D line per atm. at 20° C.	$(\delta - 1) \times 10^4$ per atm. at 20° C.	Kerr constant per atm. at 20° C. $K \times 10^{10}$ .	
				Calculated.	Observed.
Carbon dioxide ...	9.8	4.18	8.93	0.28	0.24 (at 17° 5 C.).
Nitrous oxide .....	12.2	4.73	10.6	0.48	0.48
Acetylene .....	4.6	5.62	12.43	0.23	0.29
Chlorine .....	4.1	7.28	.....	0.30	0.35
Nitrogen .....	3.75	2.79	5.40	0.04	Not appreciable.
Oxygen .....	6.45	2.52	5.06	0.06	
Carbon monoxide.	3.4	3.12	6.38	0.05	

#### 4. Polar Molecules : Determination of Electric Moment.

For polar molecules  $\theta_1$  is usually small in comparison with  $\theta_2$ ; and since it appears as a small correction term in the expression for the Kerr constant, we may, to a sufficient

approximation, determine  $\theta_1$  in the same way as for non-polar molecules. There is one difference, however, between the two cases: for non-polar molecules the ratio  $\frac{A'}{A} = \dots = \frac{\delta - 1}{n_0^2 - 1}$ , where  $\delta$  is the *observed* dielectric constant; for polar molecules, on the other hand, this ratio  $= \frac{\epsilon - 1}{n_0^2 - 1}$ , where  $\epsilon$  is the contribution to the dielectric constant  $\delta$  from the *induced* electric moments alone of the molecules, the contributions from the permanent moments being entirely omitted.  $\epsilon$  can be evaluated from the temperature variation of the dielectric constant at a constant density by means of the well-known formula of Debye,

$$\delta = \epsilon + \frac{a}{T}, \quad \dots \dots \dots (7)$$

where  $a$  is a constant for the molecule independent of the temperature. Theoretically,  $\epsilon$  should be equal to the square of the refractive index extrapolated for infinite wave-length, provided, of course, the values of refractive index used for extrapolation refer to a region of the spectrum far removed from absorption bands.

$\theta_2$ , however, cannot be evaluated completely unless we know the position of the permanent electric moment and the form of the optical ellipsoid of the molecule. In the simple cases, however, when the optical ellipsoid is a spheroid of revolution, say  $B = C$ , and the permanent moment is either parallel to the axis of the spheroid (*i. e.* the  $A$ -axis) or is inclined to it at some known angle  $\alpha$ ,  $\theta_2$  can be connected numerically with the optical anisotropy of the molecule as determined from observations on light-scattering. Thus, in expression (3) for  $\theta_2$ , putting  $B = C$  and  $\mu_1^2 = \mu^2 \cos^2 \alpha$  and  $\mu_2^2 + \mu_3^2 = \mu^2 \sin^2 \alpha$ , and using eqn. (5), we have

$$\theta_2 = \pm \frac{(n_0 - 1)\mu^2}{30\pi\nu k^2 T^2} (2 \cos^2 \alpha - \sin^2 \alpha) \sqrt{\frac{5r}{6 - 7r}}, \quad \dots (8)$$

the  $+$  or  $-$  sign being taken according as the optical ellipsoid is prolate or oblate, *i. e.* according as  $A \gtrless B (= C)$ .

Thus we get a simple relation connecting the Kerr constant with the factor of depolarization and the permanent moment of the molecules. Instead of calculating the Kerr constant, however, it would be of greater interest to calculate the permanent moments from the known values of  $K$  and  $r$ ; and we give here as examples the calculations for a few simple cases.

(1) *HCl*.—From direct considerations of symmetry the optical ellipsoid will be one of revolution about the line joining the H- and Cl-nuclei, and this direction will also be the axis of the electric doublet of the molecule. Now let us assume with Bragg \* that the optical anisotropy of a molecule is due, at least in a large measure, to the mutual influence of the electric doublets induced in the different atoms of the molecule by the field of the light-waves. In the case of *HCl* it directly follows that the optical polarizability of the molecule along the line of the nuclei will be greater than for perpendicular directions; *i. e.*,  $A > B = C$  and  $\alpha = 0$ .

From Table I.  $K = 0.90 \times 10^{-10}$  per atm., from which we get, using eqn. (1),

$$\theta_1 + \theta_2 = 2.23 \times 10^{-35};$$

while from the value  $r = 0.010$  for the depolarization factor,

$$\theta_1 = 0.07 \times 10^{-35},$$

so that

$$\theta_2 = 2.16 \times 10^{-35};$$

and hence we obtain

$$\mu = 1.04 \times 10^{-18} \text{ E.S.U.},$$

agreeing perfectly with the value

$$\mu = 1.03 \times 10^{-18} \text{ E.S.U.}$$

obtained recently by Zahn from dielectric constant measurements.

(2) *CH<sub>3</sub>Cl*.—Here the three H-atoms may reasonably be assumed to lie at the corners of an equilateral triangle, the C- and Cl-atoms lying on a line drawn through the centroid of the triangle perpendicular to its plane. Considerations of symmetry require the axis of the permanent doublet to be along the latter line and the optical ellipsoid to be one of revolution about this line, which, on actual calculation of the optical anisotropy by Bragg's method, is found to be the major axis. Thus we have, as before,

$$A > B = C \quad \text{and} \quad \alpha = 0.$$

The value  $K = 5.45 \times 10^{-10}$  per atm. gives

$$\theta_1 + \theta_2 = 1.35 \times 10^{-34}.$$

\* W. L. Bragg, Proc. Roy. Soc. A, cv. p. 370 (1924); cvi. p. 346 (1924). See also K. R. Ramanathan, same Proc. viii. p. 684 (1925).

From  $r=0.0152$

$$\theta_1=0.03 \times 10^{-34};$$

$$\therefore \theta_2=1.32 \times 10^{-34},$$

whence

$$\mu=1.66 \times 10^{-18} \text{ E.S.U.}$$

(3)  $C_2H_5Cl$ .—Here there is some uncertainty regarding the form of the optical ellipsoid. However, we shall assume for simplicity

$$A > B = C \quad \text{and} \quad \alpha = 0.$$

From the values in Table I. we get, as before,

$$\theta_1 + \theta_2 = 2.16 \times 10^{-34},$$

$$\theta_1 = 0.07 \times 10^{-34};$$

$$\therefore \theta_2 = 2.09 \times 10^{-34},$$

which corresponds to

$$\mu = 1.76 \times 10^{-18} \text{ E.S.U.}$$

It has already been mentioned that  $\theta_2$  is usually large in comparison with  $\theta_1$ . The above calculation shows that actually, in the cases of  $HCl$  and  $C_2H_5Cl$ ,  $\theta_2$  is 30 times larger than  $\theta_1$ , and for  $CH_3Cl$  it is about 40 times larger.

Regarding  $CH_3Cl$  and  $C_2H_5Cl$ , we have no reliable data for the dielectric constant from which to calculate the permanent moment independently and compare with the values obtained here. However, we have no reason to doubt that they are the proper values (especially for  $CH_3Cl$ ). In fact, in certain special cases where we can be certain about the form of the optical ellipsoid and the position of the axis of the electric doublet, this method of calculating the electric moment of the molecule promises to be at least as sensitive as the dielectric constant method. Thus, for instance, in the case of  $CH_3Cl$  Hansen gives the value of the Kerr constant relative to carbon bisulphide liquid to three significant digits. Assuming therefore that the value is correct to 3 per cent. (which would admit of an error as high as 6 per cent. in the measurement of  $r$ ), the calculated value of the permanent moment will be correct to less than 2 per cent.

### 5. Polar Molecules : Determination of Electric Axis.

In the case of molecules having an axis of optical symmetry, to which the permanent doublet is inclined at a known angle, we have seen that it is possible to calculate the



permanent moment from the value of the Kerr constant and the constant of depolarization of the scattered light.

*Vice versa*, if the moment is known from measurements of the dielectric constant, the inclination of the electric doublet to the optic axis can be found. The latter procedure promises to be of interest in certain cases, *e.g.* some of the simple derivatives of benzene. Regarding the benzene molecule, we have strong reasons to believe that the optical ellipsoid is an oblate spheroid of revolution with its axis perpendicular to the plane of the ring\*. If one or more of the H-atoms be replaced by other atoms or groups which are not themselves strongly anisotropic optically, we can still, to a first approximation, consider the derivative to have an axis of optical symmetry; and thus, if we know the values of the Kerr constant, of the factor of depolarization, and of the permanent moment, we can locate the direction of the moment with respect to the axis. In the case of simple derivatives like chlorobenzene or bromobenzene, for example, it would be particularly interesting to ascertain whether the moment lies in the plane of the ring, since it might probably throw light on the vexed question whether the ring is plane or puckered. But, unfortunately, we have no data for the Kerr constant of any of the benzene derivatives in the vapour state, even though a fair number of them have been studied with respect to their light-scattering. However, we shall have something more to say on this point when we discuss the case of the liquids.

### 6. Explanation of Negative Kerr Constants.

Probably the strongest argument in favour of Born's theory of electric double-refraction is the natural explanation it offers for the negative value of the Kerr constant obtained in some cases. If the permanent electric moment of the molecule lies along directions of smaller optical polarizability of the molecule, then, owing to the couple exerted by the external field on the doublet, the molecule tends to orientate with the direction of smaller optical polarizability along the field. Hence the refractive index for light-vibrations parallel to the field is less than for vibrations perpendicular to it; i. e.,  $n_p < n_s$  and the medium exhibits a negative double-refraction. It is significant in this connexion to note that in all cases in which the Kerr constant is negative the molecule is known to be electrically polar.

As an instructive illustration of the dependence of the sign of the Kerr effect on the constitution of the molecule,

\* K. R. Ramanathan, Proc. Roy. Soc. A, cx. p. 123 (1926).

let us consider here the chloromethanes. Monochloromethane has a positive value for the Kerr constant, and this, we have seen, agrees with that expected from theoretical considerations. On the other hand, di- and tri-chloromethanes are known to exhibit a negative Kerr effect in the liquid state. We shall presently see that this is also in agreement with what we should expect on theoretical grounds.

(1)  $\text{CHCl}_3$ .—First let us take  $\text{CHCl}_3$ . Analogous to the structure of  $\text{CH}_3\text{Cl}$ , already mentioned, the three Cl-atoms may be assumed to lie at the vertices of an equilateral triangle with the C- and H-atoms on a line perpendicular to its plane. From direct considerations of symmetry it is obvious, as for  $\text{CH}_3\text{Cl}$ , that the optical ellipsoid of the molecule will be a spheroid of revolution with its axis along the line of the C- and H-atoms, which will also be the axis of the permanent doublet. Now, by far the greatest contribution to the refractivity of the molecule comes from the three chlorine atoms; and since they are in a plane, owing to the mutual influence of the doublets induced in them, the optical polarizability of the  $\text{CHCl}_3$  molecule perpendicular to this plane will be smaller than for directions in the plane: *i.e.*, the optical polarizability of the molecule along the axis of its permanent doublet is less than for perpendicular directions. Hence its double-refraction in an electric field will be negative.

In our previous notation

$$A < B = C \quad \text{and} \quad \alpha = 0,$$

and it is obvious from eqn. (8) that  $\theta_2$  will be negative.

(2)  $\text{CH}_2\text{Cl}_2$ .—Here we may reasonably assume the two Cl-atoms to lie at the ends of a straight line and the two H-atoms at the ends of another, the two lines being perpendicular to each other and to the line joining their middle points. The C-atom will lie on the last line, which will also, from considerations of symmetry, be the axis of the electric doublet of the molecule. Regarding the optical ellipsoid of the molecule, we are obviously not justified, consistently with the above structure, in assuming an axis of symmetry. But since the contribution to the refractivity of the molecule from the C- and the two H-atoms is much smaller than the contribution from the two Cl-atoms, we may, without being altogether wide of the mark, consider the optical ellipsoid to be a prolate spheroid with its axis along the line joining the two Cl-atoms; *i.e.*, perpendicular to the axis of the electric

doublet. Hence we have

$$A > B = C \quad \text{and} \quad \alpha = \frac{\pi}{2};$$

so that here again, according to (8),  $\theta_2$  will be negative.

(3)  $\text{CH}_3\text{Cl}$ .—Here, as we have seen in para. (4) above,

$$A > B = C \quad \text{and} \quad \alpha = 0,$$

and hence  $\theta_2$  is positive.

More extensive data regarding the Kerr constant and light-scattering in gases and vapours with electrically polar molecules are obviously desirable, and we have initiated experimental work with this object.

### 7. Summary.

1. An attempt is made in this paper to correlate, on the basis of Born's theory of electric double-refraction (Kerr effect), the available data on the Kerr effect of gases and vapours, with the optical anisotropy of molecules as determined from observations on light-scattering, and with the polarity of the molecules as determined from dielectric constant measurements.

2. In the case of molecules which are electrically polar, it is found that the orientative action of an electrostatic field on the molecule is due chiefly to the couple exerted on the permanent electric doublet present, and is much larger than would be the case if the molecules were non-polar.

3. For non-polar molecules, with the simplifying assumptions of Gans regarding the relation between the constants of electric and optical anisotropy, we can calculate the values of the Kerr constant from the factor of depolarization of the scattered light in good agreement with the observed values.

4. In the case of polar molecules having an axis of optical symmetry, to which the permanent moment is parallel or is inclined at a known angle, it is possible to calculate the value of the moment from the Kerr constant and the factor of depolarization. Calculations are given for a few cases.

5. On the other hand, if the moment of the doublet is known, its direction can be determined from the same data. The applicability of the method to simple benzene derivatives is pointed out.

6. The significance of the negative value of the Kerr constant is discussed in the light of Born's theory, with special reference to its dependence on molecular structure, as evidenced in the chloromethanes.

LXXII. *Electric Double-Refraction in Relation to the Polarity and Optical Anisotropy of Molecules.*—Part II. *Liquids.*  
By Prof. C. V. RAMAN, F.R.S., and K. S. KRISHNAN \*.

1. *Introduction.*

IN Part I.† the electric double-refraction (Kerr effect) in gases and vapours was discussed in relation to the optical anisotropy of molecules as determined from observations on light-scattering. It was found that in the case of electrically non-polar molecules their electrostatic anisotropy is sufficient to account for the orientative couple exerted by the field on them, and thus for the observed double-refraction. On the other hand, in the case of molecules known to be electrically polar, the orientative couple is in a large measure due to the permanent doublets present in them, and the actual magnitudes involved were shown in certain simple cases to be in quantitative agreement with what one should expect from Born's theory of the Kerr effect. In this part we propose to extend the discussion to the case of liquids. Here, of course, owing to our imperfect knowledge of the liquid state, the problem is more complicated. There are, however, certain prominent features of the phenomenon which are of interest, and admit of at least an approximate comparison between observation and theory.

2. *Kerr Constant Data in Liquids.*

The electric double-refraction in liquids has been studied extensively by Schmidt ‡, Leiser §, McComb ¶, and others, while data for the scattering of light in some 65 liquids (chiefly organic) are available from measurements made by K. S. Krishnan ¶. In the following Table (I.) are given the data for some typical cases. Column 2 gives the relative values of the Kerr constant, carbon bisulphide, as usual, being taken as 100; column 3 gives the factor of depolarization of the scattered light; and column 4 the values of the dielectric constant.

\* Communicated by the Authors.

† *Suprà*, p. 713.

‡ W. Schmidt, *Ann. der Physik*, vii. p. 142 (1902).

§ For collected data, see H. Kauffmann, 'Beziehungen zwischen physikalischen Eigenschaften und chemischer Konstitution,' *Euke, Stuttgart*, 1920, pp. 385-389.

¶ H. E. McComb, *Phys. Rev.* xxix. p. 525 (1909).

¶ K. S. Krishnan, *Phil. Mag.* l. p. 697 (1925).

TABLE I.

Liquid.	Kerr constant, $CS_2=100$ .	Depolarization factor. $r \times 100$ .	Dielectric constant $\delta$ at $20^\circ C$ .
Hexane .....	1.73	9.9	1.729
Cyclohexane .....	2.30	8	2.05
Heptane .....	3.26	11.4	.. ...
Octane .....	4.21	12.9	1.945
$\beta$ -iso amylene .....	7.9	25.8	2.191
Propyl chloride .....	234	16.3	7.70
Methylene chloride .....	-36	31	8.3
Ethylene chloride.....	146	36	9.96
Chloroform .....	-103	24.0	4.853
Carbon tetrachloride .....	2.3	5.3	2.190
Carbon bisulphide.....	100	68.5	2.593
Acetic acid.....	130	45.5	6.02
Propionic acid .....	43	41	3.12 (at $18^\circ C$ .)
Ethyl ether .....	-19.2	8.0	4.351
Benzene .....	18.4	47	2.284
Toluene .....	23.3	51	2.368
Ethyl benzene .....	23.4	53	2.417
<i>m</i> -Xylene .....	26.6	56	2.392
<i>p</i> -Xylene .....	22.6	58.3	2.15
Chlorobenzene .....	280	57.5	5.65
Bromobenzene .....	280	63.5	5.2
Nitrobenzene.....	7900	74	36.95
Aniline .....	-38	60	6.936
<i>o</i> -Nitrotoluene .....	5400	82	26.2
<i>m</i> -Nitrotoluene .....	5520	83	23.6
Benzyl alcohol .....	-477	62	13.0
Water.....	123	8.5	80.5
Methyl alcohol .....	30	6.0	31.2
Ethyl alcohol .....	23.8	5.3	25.8
Propyl alcohol .....	-78	7.1	22.2
Butyl alcohol.....	-113	9.3	19.2
Isobutyl alcohol .....	-111	7.3	20.0
Trimethyl carbinol .....	154	4.1	11.4
Ethyl formate ...	138	21.3	8.27
Ethyl acetate.....	52	23.0	6.11
Acetone .....	505	20.0	22.58



It will be seen that, just as in the case of vapours, all the liquids which have a large Kerr constant are characterized by the possession of strongly polar molecules, as will be evident from the dielectric constant data in column 4. In fact, the variations in the values of the Kerr constant are even more pronounced than in the case of vapours. This is really what we should expect from theoretical considerations. The influence of the electrical polarity of the molecules on the Kerr effect is here twofold. One is its direct contribution to the orientative couple exerted on the molecule by the external field, just as in the gaseous state. The other arises in the following way: owing to the influence of neighbouring molecules, the actual field tending to orientate any particular molecule is  $\frac{\delta+2}{3}$  times the external imposed field, where  $\delta$  is the dielectric constant. Since, in the case of polar molecules, the value of the dielectric constant is large, and since the double refraction varies as the square of the acting field, the enormous influence of the polarity of the molecules on the magnitude of the Kerr effect is readily understood.

The theoretical expression for the Kerr constant of a liquid is

$$K = \frac{\pi\nu(n_0^2+2)^2}{3n_0\lambda} \left(\frac{\delta+2}{3}\right)^2 (\theta_1 + \theta_2), \quad \dots \quad (1)$$

where the different letters have the same significance as in Part I.,  $\theta_1$  and  $\theta_2$  being given, as before, by the relations

$$\theta_1 = \frac{1}{45kT} [(A-B)(A'-B') + (B-C)(B'-C') + (C-A)(C'-A')], \quad \dots \quad (2)$$

$$\theta_2 = \frac{1}{45k^2T^2} [(A-B)(\mu_1^2 - \mu_2^2) + (B-C)(\mu_2^2 - \mu_3^2) + (C-A)(\mu_3^2 - \mu_1^2)]. \quad \dots \quad (3)$$

For convenience we shall denote the term on the right-hand side of equation (1), which is proportional to  $\theta_1$ , by  $K_1$ , and the term proportional to  $\theta_2$  by  $K_2$ , so that

$$K = K_1 + K_2.$$

### 3. Non-Polar Molecules.

In the case of non-polar molecules  $\theta_2 = 0$ , and with the assumptions of Gans regarding the relation between the

constants of electrostatic and optical anisotropy, viz.,  $\frac{A'}{A} = \frac{B'}{B} = \frac{C'}{C}$ , this ratio =  $\frac{\delta-1}{\delta+2} \frac{n_0^2-1}{n_0^2+2}$ , and hence the expression for  $\theta_1$  reduces to

$$\theta_1 = \frac{1}{45kT} \frac{\delta-1}{\delta+2} \cdot \frac{n_0^2+2}{n_0^2-1} [(A-B)^2 + (B-C)^2 + (C-A)^2]. \quad (4)$$

It remains to evaluate the constants of optical anisotropy in the above expression from scattering measurements. It might be imagined that the anisotropic constants would be characteristic of the molecule, and could thus be easily evaluated from the vapour state, as in Part I.; but, as a matter of fact, owing probably to temporary molecular groupings, the optical anisotropy calculated from the liquid state is, in general, found to be less than that calculated from the vapour; and in any discussion concerning the liquids it is only appropriate that we should use the former value for the optical anisotropy. Two slightly different expressions have been proposed connecting the depolarization factor  $r$  with the constants of optical anisotropy—

$$r = \frac{6[(A-B)^2 + (B-C)^2 + (C-A)^2]}{10kT\beta\nu\left(\frac{n_0^2+2}{3}\right)^2(A+B+C)^2 + 7[(A-B)^2 + (B-C)^2 + (C-A)^2]} \quad (5a)$$

and

$$r = \frac{6[(A-B)^2 + (B-C)^2 + (C-A)^2]}{10kT\beta\nu(A+B+C)^2 + 7[(A-B)^2 + (B-C)^2 + (C-A)^2]}, \quad (5b)$$

where  $\beta$  is the isothermal compressibility and  $(A+B+C)$  is given by the relation

$$\frac{n_0^2-1}{n_0^2+2} = \frac{4\pi}{3} \nu \frac{A+B+C}{3}. \quad (6)$$

Since the experimental data available at present are not sufficient to decide definitely between the two expressions \*, we shall use both of them here. From (4) and (5) we thus have

$$\theta_1 = \frac{9\beta(\delta-1)(n_0^2-1)}{8\pi^2\nu(\delta+2)(n_0^2+2)} \cdot \left(\frac{n_0^2+2}{3}\right)^2 \cdot \frac{r}{6-7r} \quad (7a)$$

or

$$\theta_1 = \frac{9\beta(\delta-1)(n_0^2-1)}{8\pi^2\nu(\delta+2)(n_0^2+2)} \cdot \frac{r}{6-7r}, \quad (7b)$$

\* See K. S. Krishnan, *Proc. Ind. Assn. Sc.* ix. p. 251 (1926).

728 Prof. C. V. Raman and Mr. K. S. Krishnan on  
and hence

$$K = \frac{\beta(n_0^2 - 1)(n_0^2 + 2)(\delta - 1)(\delta + 2)}{24\pi n_0 \lambda} \left( \frac{n_0^2 + 2}{3} \right)^2 \cdot \frac{r}{6 - 7r} \quad (8a)$$

or

$$K = \frac{\beta(n_0^2 - 1)(n_0^2 + 2)(\delta - 1)(\delta + 2)}{24\pi n_0 \lambda} \cdot \frac{r}{6 - 7r} \quad (8b)$$

Table II. shows the values of the Kerr constant calculated according to these expressions for all the non-polar liquids for which we have the necessary data.

TABLE II.

Liquid.	$\times 100.$	$n_0.$	$\delta.$	Kerr constant $\times 10^7.$		
				Calculated according to		Observed.
				(8a)	(8b)	
Pentane .....	7.5	1.356	...	0.082	0.050	0.050
Isopentane .....	5.6	1.353	...	0.059	0.036	0.050
Hexane .....	9.9	1.375	1.729	0.074	0.044	$\begin{cases} 0.045 \\ 0.056 \end{cases}$
Cyclohexane .....	8	1.427	2.05	0.080	0.044	0.074
Heptane .....	11.4	1.386	...	0.102	0.060	$\begin{cases} 0.071 \\ 0.105 \end{cases}$
Octane.....	12.9	1.397	1.945	0.116	0.067	$\begin{cases} 0.077 \\ 0.136 \end{cases}$
Carbon tetrachloride.	5.3	1.461	2.190	0.068	0.036	0.074
Carbon bisulphide ...	$\begin{cases} 68.5 \\ 64.0 \end{cases}$	1.627	2.593	$\begin{cases} 0.79 \\ 7.24 \end{cases}$	$\begin{cases} 4.08 \\ 3.02 \end{cases}$	3.226
Benzene .....	47	1.501	2.284	1.45	0.72	0.593
<i>m</i> -Xylene .....	56	1.497	2.392	2.20	1.10	0.858
<i>p</i> -Xylene .....	58.3	1.496	2.15	1.96	0.98	$\begin{cases} 0.74 \\ 0.73 \end{cases}$

All the constants refer to the D line and 20° C.

Considering the uncertainties in the evaluation of the anisotropic constants from  $r$ , the agreement between the calculated and observed values in Table II. should be considered satisfactory. Equation (8b), which corresponds to the relation (5b) for the optical anisotropy, gives better agreement in the case of highly refractive liquids. In the

following discussion we shall use the same expression for the anisotropy consistently; the main conclusions, however, will not be seriously affected when the relation (5a) is used.

### Polar Molecules.

Here also  $\theta_1$  can be evaluated in the same way as for non-polar molecules, the ratio  $\frac{A'}{A} = \dots$  being now equal to  $\frac{\epsilon - 1}{\epsilon + 2} \frac{n_0^2 - 1}{n_0^2 + 2}$ , where  $\epsilon$  is given by Debye's relation

$$\frac{\delta - 1}{\delta + 2} = \frac{\epsilon - 1}{\epsilon + 2} + \frac{4\pi}{3} \nu \frac{\mu^2}{3kT}. \quad (9)$$

$\mu$  is the "effective value" of the permanent electric moment of the molecule, which is different in general from the real moment of the individual molecules, owing to the well-known phenomenon of association of polar molecules; its actual magnitude varies naturally with temperature. Hence  $\epsilon$  can not be evaluated easily from the temperature dependence of the dielectric constant, as in the vapour state; but it is possible to calculate it on the basis of Debye's dipole-theory from dielectric constant measurements at different temperatures of very dilute solutions of the liquid in a non-polar solvent like benzene, carbon bisulphide, or carbon tetrachloride\*. However, for the purpose of our present discussion we can take  $\epsilon$  to a first approximation to be equal to the square of the refractive index extrapolated for zero frequency.

Thus we obtain the relation

$$K_1 = \frac{\beta(n_0^2 - 1)(n_0^2 + 2)(\epsilon - 1)(\delta + 2)^2}{24\pi n_0 \lambda (\epsilon + 2)} \frac{r}{6 - 7r}. \quad (10)$$

The problem of determining  $\theta_2$ , however, is very complicated. It is possible to evaluate  $\theta_2$  only when we know the form of the optical ellipsoid and the position of the permanent electric moment. Even in the gaseous state, where these quantities refer to the *individual molecules*, our information regarding them extends only to very simple cases. When, on the other hand, we have to deal, as in the liquid state, with certain "effective values" of these quantities which, we have *prima facie* reasons to believe, can no longer be identified with the values for the individual molecules, the problem is naturally very complicated. We

\* See P. Debye, *Handbuch der Radiologie*, Bd. vi. p. 633.

have therefore to limit ourselves to a more or less general discussion.

Let us first consider a somewhat simple case, say chloroform. It has already been shown in Part I. that the optical ellipsoid of the  $\text{CHCl}_3$  molecule is an oblate spheroid of revolution, with the permanent doublet along its axis.

The value of the permanent moment calculated according to equation (9) from the dielectric constant for the liquid at  $20^\circ \text{C}$ ., taking  $\epsilon$  to be equal to the square of the refractive index extrapolated for infinite wave-length, comes out to be equal to  $1.07 \times 10^{-18}$  e.s.u., which is slightly less than the value  $1.25 \times 10^{-18}$  calculated by Smyth\* from the vapour.

Also the optical anisotropy, defined by, say,

$$\frac{(A-B)^2 + (B-C)^2 + (C-A)^2}{(A+B+C)^2},$$

calculated from the liquid state =  $0.17$ , as against  $0.28$  from the vapour.

For reasons already indicated we shall take the former value and assume that the axis of the electric moment has the same position in the molecule as in the state of vapour. On calculation we get

$$K_1 = 0.47 \times 10^{-7} \quad \text{and} \quad K_2 = -5.9 \times 10^{-7},$$

$$\text{and therefore} \quad K = -5.4 \times 10^{-7},$$

as compared with the observed value  $-3.32 \times 10^{-7}$ . The assumption made in the calculation that the permanent doublet is along the direction of minimum optical polarizability would give to the calculated Kerr constant the maximum possible negative value. If, however, owing to molecular association in the liquid state, the position of the effective moment is altered, the calculated value of the Kerr constant would be diminished, and would then agree better with the observed value. Even as it stands, the results of the calculation furnish strong support to Born's expression for the Kerr constant in preference to that due to Langevin. The latter gives for chloroform the value  $+1.02 \times 10^{-7}$ , which has the wrong sign, and is also numerically much smaller than the observed value.

A negative value for the Kerr constant cannot be explained on the basis of Langevin's theory unless we make the improbable assumption that the maximum electrostatic polarizability of the molecule is along directions of smaller

\* C. P. Smyth, *Journ. Am. Chem. Soc.* xlv. p. 2151 (1924).



optical polarizability—an assumption which cannot be reconciled with the ideas of Bragg regarding the cause of electrostatic and optical anisotropy, viz., as being due to atomic interaction.

### 5. *The General Case.*

In general there is considerable uncertainty both as regards the form of the optical ellipsoid and the position of the permanent moment, even for the individual molecules. For the present we shall, for the purpose of tentative calculations, assume that the effective optical ellipsoid is a spheroid of revolution whose axis coincides with the axis of the permanent doublet, the spheroid being taken as prolate or oblate according as the Kerr constant is positive or negative. This would obviously be far from the truth in most cases, and it is not surprising that we find in several cases large differences between the calculated and observed values as shown in Table III. It is significant, however, that the calculated values are always numerically higher than the observed, which is what we should expect, as the assumptions made are such as make the calculated value of the Kerr constant numerically a maximum.

TABLE III.

Liquid.	$K_1 \times 10^7.$	$K_2 \times 10^7.$	Kerr constant $\times 10^7.$	
			Calculated $= K_1 + K_2.$	Observed.
Propyl chloride .....	0.72	16.3	17.0	7.55
Methylene chloride ...	1.26	-9.6	-8.3	-1.16
Ethylene chloride .....	2.12	35.5	37.6	4.71
Acetic acid .....	1.18	12.2	13.4	4.19
Propionic acid .....	0.38	2.3	2.7	1.39
Ethyl ether.....	0.22	-1.49	-1.27	-0.618
Ethyl formate .....	0.74	18.2	18.9	4.45
Ethyl acetate .....	0.49	10.4	10.9	1.68
Acetone .....	3.6	120	124	16.3

### 6. *Monohydric Alcohols.*

Since the value of the Kerr constant depends on the angle between the axis of the electric moment of the molecule and its optic axis, which in its turn depends on the chemical structure of the molecule, we should expect certain

similarities in the behaviour of molecules of the same type. That is actually what we find, for instance, in the case of the monohydric alcohols. Table IV. shows in column 2 the observed values of  $K$ ; column 3 gives the values of  $K_1$  calculated according to equation (10); column 4 gives  $K - K_1 = K_2$ ; and the last column gives the values of  $K_2$  directly evaluated on the assumption that the optical ellipsoid is a prolate spheroid of revolution with the permanent moment perpendicular to the axis of the spheroid.

TABLE IV.

Liquid.	$K \times 10^7$ observed.	$K_1 \times 10^7$ .	$K - K_1 = K_2$ $\times 10^7$ .	$K_2 \times 10^7$ calculated directly.
Methyl alcohol .....	0.97	1.41	-0.44	-40
Ethyl alcohol.....	0.768	0.96	-0.19	-32
Propyl alcohol .....	-2.52	0.99	-3.51	-31
Butyl alcohol.....	-3.65	1.01	-4.66	-29
Isobutyl alcohol .....	-3.58	0.90	-4.48	-29

It will be seen that the values of  $K_2$  in column 4 are far smaller numerically than the values calculated according to the above assumptions. Theoretically the contribution from the permanent moment to the Kerr constant will be nothing when it makes an angle of  $54^\circ 44'$  with the axis of the optical spheroid (corresponding to the condition  $2 \cos^2 \alpha - \sin^2 \alpha = 0$ ). The small values of  $K_2$  in column 4 therefore suggest that in the case of the alcohols the permanent moments, instead of being perpendicular to the optical axis, are inclined to it at an angle not much greater than  $55^\circ$ . Indeed, there is reason to believe that in the monohydric alcohols the OH group, which is chiefly responsible for the polarity, is inclined to the hydrocarbon chain at an angle which may vary slightly with the length of the chain.

### 7. Some Benzene Derivatives.

Let us take another example—simple derivatives of benzene. As in Part I., the optical ellipsoids of these molecules can be roughly considered to be oblate spheroids of revolution. Table V. gives the calculations for some of

these molecules, assuming that the permanent moment is in the plane of the ring. In the case of aniline and benzyl alcohol, for which the Kerr constant is negative, the moment is taken to be perpendicular to the plane, a supposition which, however, is *a priori* much less probable than that of a moderate inclination to the plane of the ring.

TABLE V.

Liquid.	$K_1 \times 10^7$ .	$K_2 \times 10^7$ .	Kerr constant $\times 10^7$ .	
			Calculated $= K_1 + K_2$ .	Observed.
Toluene.....	0.80	0.31	1.11	0.753
Ethyl benzene .....	0.84	0.42	1.26	0.754
Chlorobenzene .....	3.15	10.3	13.5	9.1
Bromobenzene .....	3.99	10.0	14.0	9.1
Nitrobenzene .....	184	770	950	256
Aniline .....	3.74	-29	-25	-1.23
Benzyl alcohol.....	12.0	-130	-118	-15.4

For toluene and ethyl benzene the contribution from the electrical polarity of the molecule is very small. In other cases the calculated values of the Kerr constant are numerically larger than the observed values, thus pointing to an inclination of the permanent moments to the plane of the ring. Whether this inclination arises from a distortion, due to the heavy substituents, of the benzene ring, which is otherwise plane, or whether it is due to the fact that the ring is puckered, and consequently the substituent atoms like Cl or Br are attached to the ring at an angle, cannot be decided without further data, especially for the vapour.

### 8. Temperature Dependence of the Kerr Constant.

We now come to the question of the variation of the Kerr constant of liquids with temperature. We have seen that the value of the optical anisotropy and of the permanent moment calculated from the liquid state is less than that calculated from the vapour. As the temperature is raised, the values continually approach the value for the vapour.

Therefore any discussion of the temperature dependence of the Kerr constant of liquids must naturally take this variation into account. However, since the scattering measurements are not available at different temperatures, we shall, to a first approximation, assume the anisotropic constants to be independent of temperature, and shall only take into consideration the change in the effective value of the permanent moment  $\mu$ , as given by eqn. (9). We shall also suppose that when the effective value of  $\mu$  changes, its position with respect to the optic axes is not altered. With these assumptions the expression for the Kerr constant can be written in the form

$$K \propto \frac{(n_0^2 - 1)(n_0^2 + 2)(\delta + 2)^2}{n_0^3 T} \left(1 + \phi \frac{\mu^2}{T}\right), \quad (11)$$

where  $\phi$  is a constant independent of temperature.  $\phi$  can be evaluated from the known values of the quantities involved, at 20° C.

Table VI. includes all the liquids whose Kerr constant has been investigated over a long range of temperature. Column 3 gives the ratio of the values of  $K$  at the extreme limits of the range of temperature over which they have been studied, calculated according to (11). The observed values of the ratio are given in column 4 for comparison.

TABLE VI.

Liquid.	Limits of the range of temperature over which investigated.		Kerr const. at $t_2^\circ$ C. Kerr const. at $t_1^\circ$ C.		Observer*.
	$t_1$ (0° C.).	$t_2$ (0° C.).	Calculated.	Observed.	
Toluene .....	{ -78.5 -20	18 100	0.56 0.51	0.58 0.59	L. W. B.
Chlorobenzene ...	-20	100	0.30	0.39	B.
Bromobenzene ...	-20	100	0.33	0.41	B.
Nitrobenzene .....	5.5	25	0.76	0.74	S.
Ethyl ether.....	-78.5	18	0.17	0.26	L. W.
Chloroform ?.....	-20	55	0.40	0.42	B.

\* L. W.—N. Lyon and F. Wolfram, *Ann. der Phys.* lxxiii. p. 739 (1920).

B.—C. Bergholm, *Ann. der Phys.* lxxv. p. 128 (1921).

S.—G. Szivessy, *Zeit. f. Phys.* ii. p. 30 (1920).

Considering the nature of the assumptions made, the agreement between the calculated and the observed values is quite satisfactory, so that measurements on the temperature dependence of the Kerr constant of liquids, far from disproving Born's expression, actually support it.

### 9. *Summary.*

1. In this part the discussion of the available data on electric double-refraction in relation to the polarity and optical anisotropy of the molecules is extended to the liquid state.

2. It is found that, just as in the case of vapours, all the compounds which exhibit a large Kerr effect are characterized by the possession of electrically polar molecules, the influence of the polarity on the Kerr constant being here even more pronounced than in the case of vapours.

3. In the case of non-polar molecules the moments induced in the molecules when placed in an electrostatic field are sufficient to account quantitatively for the observed double-refraction.

4. In simple cases of polar liquids like chloroform, where we have definite information regarding the form of the optical ellipsoid and the position of the electric moment, the observed Kerr constant is in numerical agreement with that calculated on the basis of Born's theory, which takes into account also the orientative couples exerted by the external field on the permanent doublets present in the molecules.

5. Even in the general case there is nothing to throw doubt on the validity of Born's theory. In the case of alcohols, for instance, the contribution from the permanent moments to the Kerr constant is found to be very small, and this is explained on the assumption of suitable positions for the permanent moment, which are not improbable from our knowledge of their structure. In the cases of benzene derivatives, also, the moments are apparently inclined to the plane of the ring.

6. Measurements on the dependence on temperature of the electric double-refraction of liquids support the validity of Born's expression for the Kerr constant.



LXXIII. *On the Arc Spectrum of Lead.* By N. K. SUR\*.

THOUGH the arc spectrum of lead has been investigated by several investigators (Saunders, Meissner, Thorsen, Grotrian, McLennan, Zumstein, and again by Gieseler and Grotrian), and values of all fundamental and other terms as well as several Rydberg series have been obtained, the spectrum has not yet been completely explained from the standpoint of Hund's theory of complex spectra. If we start with the structure-diagram of Pb. and apply Hund's theory the situation becomes clearer. The structure-diagram of Pb, written according to Saha's method, is

2 K	8 L	18 M	32 N				
	O <sub>1</sub>	O <sub>2</sub>	O <sub>3</sub>	O <sub>4</sub>			
	2	6	10				
		P <sub>1</sub>	P <sub>2</sub>	P <sub>3</sub>	P <sub>4</sub>		
		2	2				
			Q <sub>1</sub>	Q <sub>2</sub>	Q <sub>3</sub>	Q <sub>4</sub>	
				R <sub>1</sub>	R <sub>2</sub>	R <sub>3</sub> .....	

The combination

(a)  $P_2P_2$  (two electrons in  $P_2$  level) gives  $^3P_{0,1}$ ,  $^1\bar{D}_2$ ,  $^1\bar{S}_0$  identified with  $^3P_0=59821$ ,  $^3P_1=52004$ ,  $^3P_2=49173$ ,  $^1D_2=P_2=38365$ ,  $^1S_0=P_0=30355$ , obtained by previous workers. The term values are taken from Gieseler and Grotrian's paper (*Zs. für Phys.* xxxii. p. 381, 1925).

(b)  $P_2Q_1$  (one electron in  $P_2$  level and another in  $Q_1$  level) gives us  $^1P_1$ ,  $^3\bar{P}_0$ ,  $^3P_1$ ,  $^3P_2$ .

(c)  $P_2P_3$  gives us  $^3\bar{P}_{0,1,2}$ ,  $^3D_{1,2,3}$ ,  $^3F_{2,3,4}$ ,  
 $^1P_1$ ,  $^1D_2$ ,  $^1F_3$ .

(d)  $P_2Q_2$  gives us  $^3P_{0,1,2}$ ,  $^3\bar{D}_{1,2,3}$ ,  $^3\bar{S}_1$ ,  
 $^1P_1$ ,  $^1D_2$ ,  $^1\bar{S}_0$ .

Terms from state (a) will combine with those from (b) and (c); terms from (d) will combine with those from (b) and (c). The terms  $^3P_{0,1,2}$ ,  $^1D_2$ ,  $^1S_0$  of (d) will be terms of higher Rydberg sequence to those from (a), but new terms like  $^3\bar{D}_{1,2,3}$ ,  $^3\bar{S}_1$ ,  $^1P_1$  will be obtained.

\* Communicated by Prof. M. N. Saha.

Now the previous workers have found that the fundamental levels ( $^3P_{0,1,2}$ ,  $^1D_2$ ,  $^1S_0$  from (a)) combine, as far as the selection principle for the inner quantum number would permit, with the following terms:—

$^2S_1 = 24536$  and its higher Rydberg sequence terms,

$^2X_0 = 24864$ ,

$X_1 = 10383$ ,

$X_2 = 11634$ .

Also with

$d_2 = 14380$ ,

$d_3 = 13494$ ,

$d_1 = 13754$ ,

$d_2' (?) = 13762$ ,

} and their higher Rydberg sequence terms.

Before identifying these terms, we may point out that some of the terms will be of the displaced type first discovered by Paschen and Meissner in the spectrum of neon, and since confirmed by Meissner in the spectrum of argon, and by Russell and Saunders in the spectrum of calcium. The value of the displacement constant has to be obtained from the spectrum of  $Pb^+$ . This will be similar to thallium, and a preliminary analysis shows that the difference between the values of  $^2P_1$  and  $^2P_2$  of  $Pb^+$  (as obtained from the data of Lang and Carroll, and the data on Zeeman effect by Back) is 19010. Hence terms of the Pb-spectrum arising from  $^2P_2$  level of  $Pb^+$  will be of the displaced type, *i. e.* the terms from a diagonal displacement (*e. g.*  $P_2Q_1$ ,  $P_2R_1$ ,  $P_2S_1$ ,  $P_2T_1 \dots$ ) will form a Rydberg sequence if 19010 is added to them, while the set of terms arising from  $^2P_1$  level of  $Pb^+$  will show a Rydberg sequence. These former terms will therefore be very small, and the second members of the series will be generally negative. But about the particular terms which arise from  $P_1$  (or  $P_{\frac{1}{2}}$ ) there are as yet no clear rules. The hypothesis of Jordan (*Zs. für Phys.* xxxiii. p. 563, 1925) is in disagreement with Paschen's results, and it seems that the point has still to be elucidated. We can see that of the terms arising from  $P_2P_2$ ,

$P_{\frac{1}{2}}P$  (stationary electron in  $P_{\frac{1}{2}}$ -orbit, second in any one of the P-orbits  $P_{\frac{1}{2}}$  or  $P_{\frac{3}{2}}$ ) gives us terms with  $j=0, 1$ .

$P_{\frac{3}{2}}P$  gives us terms with  $j=1, 2$ .

We can therefore identify

$$\left. \begin{matrix} {}^2S_1 \\ {}^2X_0 \end{matrix} \right\} \text{ as originating from } P_{\frac{1}{2}} (P_{\frac{1}{2}, \frac{3}{2}}).$$

$$\left. \begin{matrix} X_1 \\ X_2 \end{matrix} \right\} \text{ as originating from } P_{\frac{3}{2}} (P_{\frac{1}{2}, \frac{3}{2}}).$$

The second terms in the Rydberg sequence of  $X_1, X_2$  will be very small or negative. The state (c) gives twelve terms of which four arise from  $P_{\frac{1}{2}}$  level of  $Pb^+$  with  $j=1, 2, 2, 3$ , and eight arise from  $P_{\frac{3}{2}}$  level of  $Pb^+$  with  $j=0, 1, 2, 3; 1, 2, 3, 4$ . The four terms can be identified with the four  $d$  terms which follow a Rydberg sequence. Of the other eight terms, only one term denoted as  $f_3$  by Gieseler and Grotrian has been discovered. This must be  $\bar{f}_3$  as it combines with the fundamental  ${}^3P_2=49173$  and  $P_2=1\bar{D}_2=38365$ .

The author (Phil. Mag. ii. p. 633, 1926) has found four new series denoted by  $2S-mp_{1,2}, 2x-mp_{1,2}$ . Recently Back has established that  $j$  for  $2S=1$  and  $j$  for  $2x$  is 0. Hence the inner quantum numbers for both sets of terms are equal to 1, and not 1 and 2 as given originally. These states must arise from the combination  $P_2Q_2$ , which gives four terms with  $j=0, 1, 1, 2$  following a Rydberg sequence, and eight terms with  $j=1, 2, 0; 1, 2, 3$ , which will not follow a Rydberg sequence (or will follow if 19010 be added to them). Hence the two  $mp$  sets obtained are the terms arising from the  $P_{\frac{1}{2}}$  level of  $Pb^+$ , and of these one set will form the higher Rydberg sequence to the fundamental  ${}^3P_1$  (52004). The other  $p_1$  set (mentioned as  $mp_2$  in the above-mentioned paper) will have no member corresponding to the total quantum number 1, as this is forbidden by Pauli's rule. They will therefore form a sequence of  $mp_1$  terms combining with  $2S_1$  and  $2x_0$  or  $2S_0$ , and their first member will not be  ${}^2p_2=49173$ . The terms from the  $P_{\frac{3}{2}}$ -state of  $Pb^+$  will be very small in value.

Indications of the existence of small positive or negative terms have been already obtained, for which the reader is referred to the former paper in the Philosophical Magazine. These terms will only combine with the fundamental terms, and hence they can be obtained in the extreme ultraviolet or fluorite region.

Rydberg sequence of the displaced type has been discovered by Shenstone in the spectrum of CuI (Phys. Rev. Sept. 1926), and seems to be a general feature of the heavy elements.

It may be added that forbidden transitions are very frequent in the spectra of heavy elements like Pb, Bi, and Th, and explain the existence of combinations like  ${}^3P_1 - {}^1D_2$ ,  ${}^3P_1 - {}^1S_0$  mentioned in the above paper of the author.

Physics Department,  
University of Allahabad,  
November 3, 1926.

*Note added on correction of proof.*—After this note had been communicated for publication, a paper has been published by Gieseler and Grotrian (*Zs. f. Phys.* xxxix. p. 377, 1926), in which they have traversed identical grounds, though their reasoning is not quite the same as mine.

LXXIV. *The Theory of the Linear Electric Oscillator and its bearing on the Electron Theory.* By G. A. SCHOTT, F.R.S.\*

1. *INTRODUCTION.*—It has been the custom after the manner of Helmholtz and Lord Kelvin to describe the oscillatory discharge of an electrically-charged condenser through a resistance and self-induction by means of the equations of energy and motion of the ordinary mechanical oscillator with one degree of freedom, viz.

$$\frac{d}{dt}(\frac{1}{2}\dot{x}^2 + \frac{1}{2}\mu x^2) + \chi \dot{x}^2 = X\dot{x}, \quad . \quad . \quad . \quad (1)$$

$$\ddot{x} + \chi \dot{x} + \mu x = X. \quad . \quad . \quad . \quad (2)$$

It was soon recognized that the electric oscillator differs from the ordinary mechanical oscillator in so far as it radiates electromagnetic energy, and that a rigorous theoretical treatment should take account of this fact. H. Hertz, in the ninth of his *Electric Papers*, found that the electromagnetic energy of an electric oscillator of moment  $el \sin nt$  is radiated at the rate  $e^2 l^2 n^4 / 3c^3$  erg/sec. on the average. This result agrees with the law of Larmor and H. A. Lorentz, according to which an accelerated electron, moving with a velocity small compared with that of light, radiates electromagnetic energy at the rate  $2e^2 \ddot{x}^2 / 3c^3$ , and it requires the addition of a term of the form  $\theta \ddot{x}^2$  to the left-hand member of (1). In order, however, to secure the passage from the amended equation of energy to the corresponding equation

\* Communicated by the Author.

of motion by the division by  $\dot{x}$ , just as we pass from (1) to (2), we must add an additional term,  $-\frac{d}{dt}(\theta\dot{x}\ddot{v})$ , to the left-hand member of (1); in this manner we obtain the amended equations, viz.

$$\frac{d}{dt}(-\theta\dot{x}\ddot{x} + \frac{1}{2}\dot{x}^2 + \frac{1}{2}\mu\dot{x}^2) + \theta\ddot{x}^2 + \chi\dot{x}^2 = X\dot{x}, \quad (3)$$

$$-\theta\ddot{x} + \ddot{x} + \chi\dot{x} + \mu x = X. \quad (4)$$

Thus we obtain the equations first proposed by M. Planck for the linear electric oscillator in order to take account of the radiation of electromagnetic energy.

2. The oscillatory free motion of the system represented by (4) is determined in the usual way from prescribed initial conditions by putting

$$x = A\epsilon^{\alpha t} + \epsilon^{-kt}(B \cos nt + C \sin nt), \quad (5)$$

where  $\alpha$  and  $-k \pm in$  are the roots of the cubic indicial equation

$$-\theta p^3 + p^2\chi p + \mu = 0, \quad (6)$$

the frictional coefficient  $\chi$  being supposed zero, or, at any rate, small enough to ensure the existence of a pair of complex roots corresponding to damped free oscillations with  $k$  positive. Then the third root  $\alpha$  is clearly real and positive, being given by the equation

$$\alpha = 2k + \theta^{-1}. \quad (7)$$

Planck, in his first edition of his 'Theorie der Strahlung,' dismisses this root with the remark that it is physically unintelligible; if, however, we adopt the interpretation of similar roots in classical mechanics, we must regard it as indicating instability in the system. In order to see what degree of instability is to be expected, we shall consider two cases.

For the first case we take a Hertz oscillator of period  $T$  and wave-length  $\lambda$ , with capacity  $C$  and self-induction  $L$ , discharging across a spark-gap of length  $l$ . Hertz's expression for the radiation gives

$$\theta/T = 2l^2/3\lambda L = 8\pi^2 l^2 C/3\lambda^3.$$

With  $l=1$  cm.,  $C=1$  cm.,  $\lambda=100$  cm., we get

$$\theta = 2.6 \cdot 10^{-5} T,$$

a value which indicates great instability, since the real



exponential will be multiplied more than fifty times in one ten-thousandth of a period. Nearly the same value is got with  $C=1$  microfarad and  $\lambda=100$  m.; so great an instability is not met with in practice.

For the second case take a slowly-moving electron controlled by a quasi-elastic force; here we have

$$\theta = 2e^2/3c^3m = 6.2 \cdot 10^{-24} \text{ sec.},$$

with the usual values of  $c$ ,  $e$ , and  $m$ . This clearly gives a much higher degree of instability still.

3. These examples show that, though a rigorous treatment of the radiating electric oscillator undoubtedly requires us to take account of the loss of energy due to radiation, yet the obvious method of doing so leads to results not in accordance with experience. The difficulty is accentuated by the fact—obvious from (7)—that the smaller the radiation coefficient  $\theta$  is, the greater will be the exponent  $\alpha$ , and therefore also the instability; in fact, with Planck's correction infinitesimal radiation means infinite instability—a physically unintelligible result.

It might be urged that the Quantum theory avoids the difficulty, in so far as it postulates that all electric oscillators can only exist permanently in states in which there is no radiation at all, whilst radiation only occurs in the unstable states through which the oscillator passes as it goes from one stable state to another. This explanation is acceptable for the "microscopic" oscillators dealt with in the Quantum theory, but it will hardly avail for the "macroscopic" oscillators with which we are concerned, in wireless telegraphy for instance, which certainly radiate and for which nevertheless some representation or other is needed. Besides, up to the present the Quantum theory has not reached the stage in which it can dispense altogether with the results of classical electrodynamics, as, for example, in the explanation of interference, refraction, and dispersion: witness the use made of Bohr's Correspondence Principle and the attempt of Bohr, Kramers, and Slater to account for dispersion. Moreover, the recent promising attempt of E. Schrödinger\* to deduce Quantum conditions from the wave-equation implies a return to the principles of classical electrodynamics rather than a further departure from them. For these reasons a rigorous treatment of electronic problems on classical principles seems desirable.

\* "Quantisierung als Eigenwertproblem," *Ann. d. Physik*, vol. lxxix. pp. 361, 489, 734; vol. lxxx. p. 437 (1926).

4. Adopting the Electron theory as a basis, we may regard every linear electric oscillator as constituted by an assemblage of electrons, each oscillating to and fro parallel to the oscillator under the action of a controlling quasi-elastic force together with the forces due to the neighbouring electrons and possibly of a viscous resistance, explicable as the result of collisions in the well-known manner due to H. A. Lorentz. Each electron must be regarded as radiating electromagnetic energy according to the classical law, but the action on it of the remaining electrons of the assemblage will result in an absorption of energy, which is accompanied by a corresponding accelerating force following the same law as the reaction due to the electron's own radiation\*. Thus we may use equation (4), but with a diminished value of  $\theta$ ; if the assemblage of electrons were infinite, homogeneous, and isotropic, the resulting value of  $\theta$  would be zero, a limiting condition which obviously will not generally be reached. As we saw in § 3, a diminution in the value of  $\theta$  means an increase of the instability, so that we shall overestimate the stability if we take for  $\theta$  the value  $6 \cdot 2 \cdot 10^{-24}$  sec. given at the end of § 2.

Even if the assemblage of electrons be in a stationary state of motion initially in the absence of an external disturbing force, which may very well happen owing to the vanishing of the coefficient  $\Lambda$  of the real exponential in (5), yet in general the incidence of a disturbing force will introduce the real exponential. The part of the motion due to the latter will very soon outstrip the remainder to such an extent that it alone need be taken into account. When this stage is reached, the velocity of the electron becomes comparable with that of light, so that on the one hand relativistic corrections must be applied †, whilst, on the other hand, only the acceleration and radiation terms in (4) need be retained, because they are of the order  $\alpha^2$ , all the others being of lower order.

5. Let us write

$$\dot{x} = c\beta = c \tanh u, \quad \kappa = \sqrt{1 - \beta^2} = \operatorname{sech} u. \quad (8)$$

Then, if the conditions just mentioned be satisfied after a time  $t_1$ , corresponding to values  $x_1, \beta_1, u_1, \kappa_1$  of the other variables, we must from this time onwards replace (4) by ‡

$$\kappa^{-3}\ddot{x} - \theta(\kappa^{-4}\ddot{\ddot{x}} + 3c^{-2}\kappa^{-6}\dot{x}\ddot{x}) = 0. \quad (9)$$

\* C. W. Oseen, *Physik. ZS*

† Schott, 'Electromagnetic Radiation,' p. 176.

‡ Schott, *loc. cit.*

Multiplying by  $\kappa$  and integrating from  $t_1$  to  $t$ , we obtain with (8)

$$u - \theta \cosh u \cdot \dot{u} = u_1 - \theta \cosh u_1 \cdot \dot{u}_1 = b, \quad \text{say.} \quad (10)$$

Hence, separating the variables, we obtain

$$\left. \begin{aligned} t - t_1 &= \theta \int_{u_1}^u \frac{\cosh u \, du}{u - b}, & x - x_1 &= a \int_{u_1}^u \frac{\sinh u \, du}{u - b}, \\ x - ct &= x_1 - ct_1 - a \int_{u_1}^u \frac{e^{-u} \, du}{u - b}, & \text{where } a &= 2e^2/3c^2 m. \end{aligned} \right\} \quad (11)$$

$a$  is the conventional radius of the electron, *i. e.*  $1.84 \cdot 10^{-13}$  cm., when we are dealing with an isolated electron, whilst it will be smaller for an assemblage of electrons.

We see from (11) that  $x$  increases without limit with  $t$  and ultimately only in direct proportion to it, instead of exponentially as before. Thus the relativistic corrections diminish the instability very considerably, but do not remove it entirely. Moreover, an assemblage of electrons is less stable than an isolated electron, but not very much so.

6. It is well known that the equations (1) and (2), as well as these equations with the proper relativistic corrections, can be deduced from the Electron theory of H. A. Lorentz with the help of appropriate assumptions as to the structure of the electron, provided always that the size of the electron be small enough to allow us to adopt Abraham's hypothesis of quasistationary motion. That is to say, in the expression for the resultant internal mechanical force on the electron due to the mutual actions of its elementary charges, all terms involving higher powers of the radius of the electron than the inverse first power are assumed to be negligible, and that, too, without any proof being given that the series is convergent. On this view, equations (3) and (4) form a second approximation in which the zero power of the radius is retained. Since, as we have found, these two approximations yield contradictory results, the method cannot be sound, and it becomes important to find a more rigorous one.

We notice that the method of H. A. Lorentz works with the retarded potentials and assumes that this is allowable even when the motion is discontinuous, as in the present case, where the incidence of a disturbing force might, and on the view taken in classical mechanics actually does, produce a discontinuity in the acceleration of the electron. This difficulty is being investigated at present; the results so far obtained show that no difficulty arises so long as the

velocity of the electron is continuous during the whole motion, but that the retarded potentials require correction in cases of impulsive motions.

It follows that a rigorous method must take account of higher powers of the radius of the electron, even though it is known to be only of the order  $10^{-11}$  to  $10^{-13}$  cm., according to the view of its structure that we adopt. This is due to the fact, which will appear in the course of the investigation, that the coefficients in the series increase rapidly as the power increases. Fortunately, the more complete investigation has been carried out already for the rectilinear motion of a rigid spherical electron with uniform volume density\*, and is easily extended to the case of uniform surface density. Obviously the results will be true very approximately for a slowly-moving deformable electron, like that of H. A. Lorentz, at any rate sufficiently so for atomic problems, in which the velocity of the electron rarely exceeds a few hundredths of the velocity of light.

7. *Rigorous expression for the internal mechanical force.*—The mechanical force per unit electric charge,  $f$ , which is parallel to the  $x$ -axis, the direction of motion, is given by †

$$-f = \sum_{k=0}^{k=\infty} \frac{(-1)^k}{k!} \left[ \frac{\partial^k}{\partial \xi^k} I \{x(t+\tau) + x(t)\}^k \right]_{\tau=0} \\ + \sum_{k=0}^{k=\infty} \frac{(-1)^k}{(k+1)!} \left[ \frac{\partial^k}{\partial \xi^k} ID^2 \{x(t+\tau) - x(t)\}^{k+1} \right]_{\tau=0}, \quad (12)$$

where  $\xi$  denotes the  $x$ -coordinate of an element  $de$  of electric charge referred to the electric centre ( $x$ ) of the electron as origin, the corresponding radius vector being  $r$ ,  $D$  denotes the symbolic operator  $\partial/\partial \tau$ , and  $I$  denotes another symbolic operator, which is defined for a uniform spherical electron of internal and external radii  $f$  and  $a$  by the equation ‡

$$I = \frac{3e}{a^3 - f^3} \left\{ \frac{e^{-rD}}{rD} \int_0^r \sinh r'D \cdot r' dr' + \frac{\sinh rD}{rD} \int_r^\infty e^{-r'D} r' dr' \right\} \\ = \frac{3e}{(a^3 - f^3)r^3} \{ rD - f(aD) \sinh rD - g(bD) e^{-rD} \}. \quad (13)$$

The functions  $f$  and  $g$  are symbolic operators defined by

$$f(aD) = (1 + aD)e^{-aD}, \quad g(bD) = bD \cosh bD - \sinh bD. \quad (14)$$

\* Schott, *Ann. d. Physik*, (4) xxv. p. 63 (1908).

† *Ibid.* p. 74, equation (20).

‡ Schott, *l. c.* p. 68; (13) is a generalization of equation (13) there.

In order to find the resultant internal force on the electron, we multiply (12) by  $de$  and integrate over the whole electron, making use of (13) and (14) and treating the operator  $D$  as a constant in the usual way. We can facilitate the integration by using the following lemma:—

If  $\phi$  denote a function of  $r$  alone, and  $d\omega$  an element of solid angle, whilst  $\xi = r\mu$ , then we have \*

$$\left. \begin{aligned} \iint \frac{\partial^k \phi}{\partial \xi^k} d\omega &= \frac{4\pi}{(k+1)r} \frac{d^k(r\phi)}{dr^k}, \text{ when } k \text{ is even} \\ &= 0, \text{ when } k \text{ is odd.} \end{aligned} \right\} \quad (15)$$

Then we find that the resultant internal mechanical force  $F$  on the whole electron is given by

$$\begin{aligned} F = \frac{18e^2}{(a^3 - b^3)^2} &\left[ D^{-4} \{ f(aD) [g(bD) - g(bD)] \right. \\ &\quad \left. - g(bD) [f(aD) - f(bD)] \} \right. \\ &\quad \times \sum_{j=0}^{j=\infty} \frac{D^{2j+1} \{ x(t+\tau) - x(t) \}^{2j+1}}{(2j+3)(2j+1) \lfloor 2j+1 \rfloor} \Big]_{\tau=0}. \end{aligned} \quad (16)$$

The term arising from  $j=0$  and the first term of  $\int I de$  both involve  $[x(t+\tau) - x(t)]^{\tau=0}$  as a factor and therefore vanish identically.

8. *The uniform spherical surface electron.*—We shall limit ourselves to this model, because the results are much the simplest. We put  $b = a - \delta$  in (16) and proceed to the limit when  $\delta$  vanishes, a process which requires some care. Retaining terms of the two lowest orders in  $\delta$ , we find that the terms in the first line of (16) reduce to

$$\frac{2e^2}{a^2} \left( 1 + \frac{2\delta}{a} + \dots \right) \left( \frac{1}{\delta D} - \frac{1}{aD} - \epsilon^{-aD} \sinh aD + \dots \right).$$

When this expression is substituted in (16), the two terms in the former which involve  $1/D$  give rise to vanishing terms of the type  $[D^{2j} \{ x(t+\tau) - x(t) \}^{2j+1}]_{\tau=0}$ . Thus we obtain in the limit

$$F = -\frac{e^2}{a^2} \left[ (1 - \epsilon^{-2aD}) \sum_{j=0}^{j=\infty} \frac{D^{2j+1} \{ x(t+\tau) - x(t) \}^{2j+1}}{(2j+3)(2j+1) \lfloor 2j+1 \rfloor} \right]_{\tau=0}. \quad (17)$$

The differentiations with respect to  $\tau$ , indicated by the

\* *Ibid.* p. 74.



operator  $D$ , must be effected before  $\tau$  is put to zero. Bearing this in mind, we see that the term  $j=0$  gives on expansion in powers of  $a$

$$\begin{aligned} F &= -\frac{e^2}{a} \left[ \left( \frac{2}{3c^2} \frac{\partial^2}{\partial \tau^2} - \frac{2a}{3c^3} \frac{\partial^3}{\partial \tau^3} + \dots \right) \{x(t+\tau) - x(t)\} \right]_{\tau=0} \\ &= -\frac{2e^2}{3c^2 a} \ddot{x} + \frac{2e^2}{3c^3} \ddot{x} - \dots = -m\ddot{x} + m\theta \ddot{x} - \dots \quad (18) \end{aligned}$$

The terms written down in (18) agree with those used by Planck in his equation (4), § 1, since the mass is given by  $m=2e^2/3c^2a$  for a uniform spherical surface charge of radius  $a$ , when the velocity is small enough.

So far we have used retarded potentials as usual, but in view of the use of advanced potentials, suggested by W. Ritz, and advocated by Nordström and also by Leigh Page\* in equal amounts with the retarded potentials so as to annul the radiation, we may note that for the advanced potentials we must change the sign of  $c$  and therefore also of  $D$  throughout. Thus on the hypothesis of Nordström and Leigh Page we get in place of (17)

$$F = -\frac{e^2}{a^2} \left[ \sinh 2aD \sum_{j=0}^{j=\infty} \frac{1^{2j+1}}{(2j+3)(2j+1)} \{x(t+\tau) - x(t)\}^{2j+1} \right]_{\tau=0}. \quad (19)$$

9. *The convergence of the series.*—It is important to gain some idea of the rate of convergence of the series (17) and (19), and for this purpose it will suffice to consider the case where the coordinate is an exponential function of the time, since this occurs most frequently in practice. Accordingly we shall write

$$\left. \begin{aligned} x(t) &= A\epsilon^{pt}, & x(t+\tau) - x(t) &= (\epsilon^u - 1)A\epsilon^{pt}, \\ u &= p\tau, & \beta &= (Ap/c)\epsilon^{pt}, \\ \Delta &= \frac{\partial}{\partial u}, & D &= p\Delta/c, & \zeta &= 2ap/c. \end{aligned} \right\} \quad (20)$$

Then we obtain from (17)

$$\begin{aligned} F &= -\frac{e^2}{a^2} \left[ (1 - \epsilon^{-\zeta\Delta}) \sum_{s=0}^{j=\infty} \frac{(\beta\Delta)^{2j+1} (\epsilon^u - 1)^{2j+1}}{(2j+3)(2j+1)} \frac{2j+1}{2j+1} \right]_{u=0} \\ &= -\frac{e^2}{a^2} \sum_{j=0}^j \sum_{s=0}^s \frac{(-1)^{s-1} (1 - \epsilon^{-s\zeta}) (s\beta)^{2j+1}}{(2j+3)(2j+1)} \frac{s}{|s|} \frac{2j+1}{2j+1-s}. \quad (21) \end{aligned}$$

For a selected value of  $s$  the  $j$  series ultimately converge

\* Phys. Rev. ser. 2, vol. xxiv. p. 296 (1924).

absolutely, like the series for  $\sinh s\beta$ ; hence we can change the order of summation. We put  $s=2i+1$ , or  $2i$ , according to circumstances, and then put  $j=i+k$ ; then we obtain without difficulty

$$F = -\frac{e^2}{a^2} \int_0^\beta \frac{d\beta}{\beta^3} \int_0^\beta \sum_{i=0}^{i=\infty} \times \left\{ \frac{[1 - e^{-(2i+1)\zeta}] [(2i+1)\beta]^{2i+1} \cosh [(2i+1)\beta]}{(2i+1)!} - \frac{[1 - e^{-2i\zeta}] [2i\beta]^{2i} \sinh [2i\beta]}{(2i)!} \right\} \beta d\beta. \quad (22)$$

Obviously the convergence of the series (17) for  $F$  depends upon that of simpler series of the type

$$S = \sum_{i=0}^{i=\infty} \frac{[(2i+1)\beta e^{\beta-\xi}]^{2i+1}}{(2i+1)!}, \quad \dots \quad (23)$$

where  $\xi$  is the real part of  $\zeta$ , and the same thing holds for (19). The series  $S$  converges whenever  $e\beta e^{\beta-\xi} < 1$ , or  $\log(1/\beta) > 1 + \beta - \xi$ .

When  $\xi$  vanishes, the upper limit for  $\beta$  is 0.278; when  $\xi$  is positive, the limit is higher— $\xi=0.1$  gives 0.301,  $\xi=1$  gives 0.568; when  $\xi$  is negative, the limit is lower— $\xi=-0.1$  gives 0.255,  $\xi=-1$  gives 0.12.

The values of  $\xi$  usually met with are small, so that the limit for  $\beta$  will usually be appreciably greater than 0.25; hence we see that the series (17), and equally so (19), converge so long as the velocity of the electron does not exceed one-fourth of that of light, and the coordinate does not increase faster than a real exponential with positive exponent.

Moreover, since in most atomic problems the velocity is only a few hundredths of that of light, whilst the second term ( $i=1$ ) in (22) is only of the order  $\beta^2$  in comparison with the first ( $i=0$ ), it will be sufficient to reject all such higher terms throughout. This amounts to retaining only the term  $j=0$  in the sum which occurs in (17) and (19), a procedure contrasting vividly with that adopted hitherto. Here we reject higher powers of the velocity of the electron, but retain higher powers of the radius; hitherto the procedure has been to reject higher powers of the radius, but retain those of the velocity, whereby the relativistic and analogous expressions for the electromagnetic momentum and radiation used, for instance by H. A. Lorentz, M. Abraham, and also by the writer in 'Electromagnetic

Radiation,' have been obtained. Whether or not  $\beta$  be small enough to justify the new procedure in any particular case must be decided *a posteriori*.

10. *The corrected equation of motion of the linear electric oscillator.*—Rejecting all terms in (17) except the term  $j=0$ , we obtain

$$F = -\frac{e^2}{3a^2}(1-\epsilon^{-2aD})Dx = -\frac{c^2m}{4a^2}(1-\epsilon^{-2aD})2aDx, \quad \left. \vphantom{\frac{e^2}{3a^2}} \right\} \quad (24)$$

where now  $D = \partial/c\partial t$ ,  $m = 2e^2/3c^2a$ .

With, as before, a quasi-elastic force  $-m\mu x$ , a frictional resistance  $-m\chi\dot{x}$ , and an external force  $mX$  we obtain, instead of (2),

$$\left. \begin{aligned} \{\mu_1 + (1 + \chi_1 - \epsilon^{-2aD})2aD\}x &= 4\theta^2 X, \\ \text{where } \theta &= a/c, \quad \mu_1 = 4\theta^2\mu, \quad \chi_1 = 2\theta\chi. \end{aligned} \right\} \quad (25)$$

In precisely the same way we obtain from (19)

$$\{\mu_1 + (\chi_1 + \sinh 2aD)2aD\}x = 4\theta^2 X \quad (26)$$

for the hypothesis of Nordström and Leigh Page.

As we have seen, (2) and (4) constitute respectively first and second approximations to both (25) and (26), which differ only in the higher terms. The differences will appear clearly if we consider the nature of the free motion, arising in each case from the sudden incidence of the disturbing force  $X$  and given by the appropriate equation without second member. This equation is a linear differential equation, though of infinite degree, and its solution is determined in the usual way as a sum of exponentials of the form  $\Lambda e^{\rho t}$ . The exponents  $\rho$  of these exponentials are the roots of an indicial equation, which is now of infinite degree, *i. e.* transcendental. For (25) we find

$$\mu_1 + (1 + \chi_1 - \epsilon^{-\zeta})\zeta = 0, \quad \zeta = 2ap/c = 2\theta p; \quad (27)$$

whilst for (26) we obtain

$$\mu_1 + (\chi_1 + \sinh \zeta)\zeta = 0. \quad (28)$$

The stability of the oscillator depends upon the roots of these equations: if all the possible values of  $\zeta$  have a negative, or zero, real part  $\xi$ , the oscillator is stable, otherwise not. If any one value of  $\zeta$  have a zero real part, then a periodic disturbing force, however small, of the proper frequency will give rise to infinite resonance and upset the oscillator, even if it be stable in the usual sense.

11. As far as squares of  $\zeta$ , both (27) and (28) with the help of (25) reduce to

$$\left. \begin{aligned} \mu_1 + \chi_1 \zeta + \zeta^2 &= 0, \\ \text{whence} \end{aligned} \right\} \quad (29)$$

$$\zeta = -\frac{1}{2}\chi_1 \pm i\sqrt{(\mu_1 - \frac{1}{4}\chi_1^2)}, \quad \rho = -\frac{1}{2}\chi \pm i\sqrt{(\mu - \frac{1}{4}\chi^2)},$$

which are the equations for the frequency and damping coefficient of the ordinary mechanical oscillator. If  $\nu_0$  and  $\lambda_0$  be its frequency and wave-length, and  $\alpha_0$  its damping coefficient, we have at once

$$\mu = 4\pi^2\nu_0^2, \quad \chi = 2\alpha_0, \quad \mu_1 = (4\pi a/\lambda_0)^2, \quad \chi_1 = 4\theta\alpha_0 = 4a\alpha_0/c. \quad (30)$$

These equations enable us to obtain estimates of the values of  $\mu_1$  and  $\chi_1$ . With

$$a = 1.87 \cdot 10^{-5} \text{ A.U.}, \quad \lambda_0 = 6000 \text{ A.U.}, \quad \alpha = 3 \cdot 10^7 \text{ sec.}^{-1},$$

as found by Wien and his successors, we get

$$\mu_1 = 1.6 \cdot 10^{-15}, \quad \chi_1 = 7.5 \cdot 10^{-16},$$

both very small. For X-rays with

$$\lambda_0 = 2 \text{ A.U.} \quad \text{and} \quad \alpha_0 = 3 \cdot 10^9 \text{ sec.}^{-1},$$

as found by F. Kirchner, we get

$$\mu_1 = 1.4 \cdot 10^{-8}, \quad \chi_1 = 7.5 \cdot 10^{-14},$$

both still small.

Putting  $\zeta = \xi + i\eta$ , we see from (29) that  $\xi$  and  $\eta^2$  may both be regarded as small quantities of the first order, at any rate for visible spectrum lines, and nearly so for characteristic X-rays.

12. *The classical electron theory.*—The discussion of the remaining roots of (27) and (28) is much facilitated by using a graphic method. Equating real and imaginary parts separately to zero, we obtain from (27)

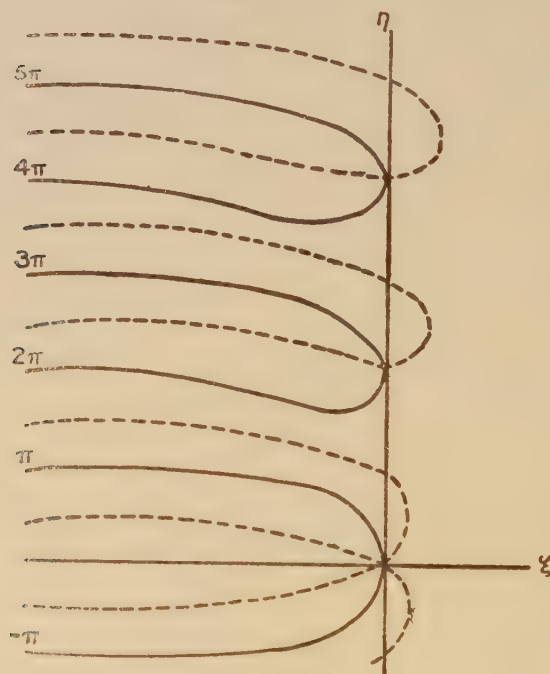
$$[\mu_1 + (1 + \chi_1)\xi]\epsilon^\xi = \xi \cos \eta + \eta \sin \eta, \quad (1 + \chi_1)\epsilon^\xi = \cos \eta - \xi \sin \eta / \eta. \quad (31)$$

A factor  $\eta$  in the second equation has been discarded, because  $\eta = 0$  only gives real values of  $\xi$  from the first equation, when  $\mu_1$  is less than  $\frac{1}{4}\chi_1^2$ ; we reject this case because it gives no vibrations at all.

The equations (31) give two curves in the  $(\xi, \eta)$  plane,

shown in fig. 1 by the dotted and full lines respectively, both curves being of course symmetrical with respect to the real axis. Their intersections determine the roots of (27), those of (29) corresponding to the two intersections near the origin, the values of  $\xi$  and  $\eta$  being necessarily very much exaggerated in the diagram. All the roots have small negative values of  $\xi$ , whilst  $\eta$  is nearly equal to an integral

Fig. 1.



multiple of  $2\pi$ ; in fact, bearing these results in mind, we find that an approximate calculation by means of (31) gives for the large roots

$$\xi = -\chi_1 - \frac{\mu_1^2}{8\pi^2 k^2}, \quad \eta = 2k\pi + \frac{\mu_1}{2k\pi}, \quad k \text{ an integer.} \quad (32)$$

The frequencies are approximately equal to  $c\eta/4\pi\alpha = kc/2a$ , and the wave-lengths to  $2a/k$ , and are infinite in number;



with the conventional value of  $a, 1.87 \cdot 10^{-13}$  cm., the longest wave-length, given by  $k=1$ , is about one-eleventh of the shortest wave-length found by Millikan for the cosmic rays, but for a larger value, such as that suggested by A. H. Compton for his spherical electron, the wave-length would be correspondingly greater. All the values of  $\xi$  are negative, even in the absence of friction ( $\chi_1=0$ ), although in that case the damping coefficient is very small and diminishes with the wave-length, being proportional to its square.

Hence it follows from the classical electron theory that (1) the linear electric oscillator is stable, and (2) that a properly attuned periodic disturbing force will never produce infinite resonance. The instability found with Planck's radiation correction is spurious and due to an unjustifiable method of approximation; in fact, in problems concerning the stability of electronic systems the quasi-stationary hypothesis is unreliable.

13. *The hypothesis of Nordström and Leigh Page.*—Equating real and imaginary parts of (28) separately to zero, we obtain

$$\left. \begin{aligned} \mu_1 + (\chi_1 + \sinh \xi \cos \eta) \xi - \eta \cosh \xi \sin \eta &= 0, \\ \chi_1 + \sinh \xi \cos \eta + \xi \cosh \xi \sin \eta / \eta &= 0, \end{aligned} \right\} \quad (33)$$

where the factor  $\eta$  has been discarded from the second equation as before.

We need only consider points near the  $\eta$ -axis, for which  $\xi$  is small of the order  $\chi_1$ . Neglecting second-order terms, we find

$$\left. \begin{aligned} \eta \sin \eta &= \mu_1, \quad \text{whence} \quad \eta = k\pi + \frac{\mu_1 \cos k\pi}{k\pi} + \dots, \\ \xi &= -\frac{\chi_1}{\cos \eta + \sin \eta / \eta} = -\chi_1 \cos k\pi + \dots, \end{aligned} \right\} \quad (34)$$

approximately for the large roots for which  $k$  is an integer.

Comparing (34) with (32), we see that the main difference between them lies in the fact that, although  $\eta$  is determined by the same equation in each case, yet in the present one all values of  $k$  are admissible, odd as well as even; whereas in the previous one only even values could be used, because otherwise  $\cos \eta$  would be negative, and the second equation (31) could not be satisfied. But now the second equation (34) shows that, whilst the even values of  $k$  give

negative values of  $\xi$  and therefore correspond to damped vibrations as before, on the other hand the odd values of  $k$ , which now occur, give positive values of  $\xi$  and correspond to vibrations of continually increasing amplitude, leading to instability. This is a direct consequence of the presence of frictional resistance indicated by a finite though small positive value of  $\chi_1$ .

If, on the other hand,  $\chi_1$  be zero, the second equation (33) reduces to  $\xi=0$ , or to

$$\xi^{-1} \tanh \xi + \eta^{-1} \tan \eta = 0. \quad (35)$$

This equation has no real pair of solutions other than  $\xi=0$ ,  $\eta=0$ , already excluded, since the first equation cannot be satisfied. Thus, in the absence of friction, we have an infinity of undamped vibrations: there is stability, but owing to the absence of damping there will be infinite resonance, even for the vibration of lowest frequency corresponding to the ordinary mechanical oscillator.

Thus we see that, on the hypothesis of Nordström and Leigh Page, owing to the total absence of radiation in the absence of friction, the linear electric oscillator is liable to infinite resonance and incapable of permanent existence, unless it is completely protected from outside disturbances with the proper periods. On the other hand, when friction is present the oscillator is unstable.

The example of the linear electric oscillator shows that electrically charged systems behave quite differently from ordinary mechanical systems, without charge but otherwise similarly constituted. It is dangerous to draw conclusions respecting the properties of electrical systems from the ascertained properties of similar mechanical systems, at any rate where questions of stability are concerned, such as arise when we are dealing with problems of atomic structure. A more complete and rigorous formulation of electron mechanics is needed for this purpose than that which we possess at present.

Freiburg i/B.,  
Aug. 20, 1926.

LXXV. *On the Sparking Potentials of Glow Discharge-Tubes.*

By JAMES TAYLOR, M.Sc., Ph.D., A.Inst.P., Fellow of the International Education Board, and Earl Grey Memorial Fellow; The Physical Laboratory of the University, Utrecht\*.

## PART II.

## ON THE ELECTRODE SURFACE EFFECTS OF DISCHARGE-TUBES.

*Introduction.*

IN continuation of the subject of the sparking potentials of glow discharge-tubes we shall now consider in more detail the polarization effects which were mentioned in Part I. of this paper<sup>1</sup>.

The importance of surface films on the electrodes of discharge-tubes has been noted by numerous experimenters. Compton and Ross carried out some experiments on "charged surface layers formed on the electrodes of vacuum tubes"<sup>2</sup>. Züher observed a polarization of sparking gaps<sup>3</sup>, but attributed the preponderant part of the effect to polarization of the insulating material of the gap. In the usually accepted explanation of the Rutherford-Geiger  $\alpha$ -particle counter, it is assumed that a film of high resistance exists on the surface of the counter point<sup>4</sup>. Zeleny<sup>5</sup> considers the action as being due to a gas film on the pointed electrode, and on this basis explains many of his observations on point-to-plate discharges. He is further of opinion that the time-lag in the production of the discharge is accounted for by the presence of such films<sup>6</sup>.

It has been observed that the first spark through a tube which has been unused for some time frequently passes more easily and without appreciable time lag at a lower potential than succeeding ones. This was the case with many of the tubes described in this work. On the other

\* Communicated by Professor Ornstein.

<sup>1</sup> James Taylor, *Phil. Mag.*, Feb. 1927, p. 368.

<sup>2</sup> Compton & Ross, *Phys. Rev.* vi. 3. p. 207 (1915); Ratner, *Phil. Mag.* xliii. p. 193 (1922).

<sup>3</sup> Züher, *Ann. d. Phys.* lxxvi. p. 231 (1925).

<sup>4</sup> For literature on the subject see Jönsson, *Zeit. f. Phys.* xxxvi. 6. p. 426 (1926).

<sup>5</sup> Zeleny, *Phys. Rev.* xvi. p. 102 (1920); xix. p. 566 (1922); xxiv. p. 255 (1924).

<sup>6</sup> Zeleny, *Phys. Rev.* xvi. p. 102 (1920).

hand, it appears in certain cases that the first spark passes less readily than the following<sup>7</sup>. These and other observations point to a change in the electrodes on the passage of a discharge<sup>7</sup>.

For the type of tube chiefly considered in this paper many electrode fatigue effects have been signalled<sup>8</sup>. It is known that the sparking potential is altered and is made much more constant when the electrodes have been purged and heated to redness for some time by means of an electric discharge. This stabilization appears to result from the destruction or modification of certain gas-layers and impurities<sup>9</sup>. Certain results of Ryde<sup>10</sup> show that surface films may play a very considerable role in causing changes of the sparking potentials. Clarkson in some work upon argon-nitrogen tubes<sup>11</sup> concludes that many of the anomalies inherent in such tubes may be attributed to films of gas absorbed on the cathode. Apart from changes caused by intense discharges which may radically alter the nature or condition of such surface films, there are fatigue effects which occur in tubes where only small energy transferences are taking place<sup>11, 12</sup>. Such effects were also observed in tube (2)<sup>13</sup> of the present work. Campbell<sup>14</sup>, in experiments on point and sphere sparking gaps in air, concluded that "some very easily variable surface condition of the plug" played a considerable role.

The above results point to a very considerable influence of the electrode condition upon the processes of the discharge and upon the sparking potential itself.

In the experiments to be described, most of the discharge-tubes were very carefully prepared and treated as described in Part I. of this paper<sup>1</sup> in order to avoid unnecessary complications due to impurities. The sparking potentials were determined under definite conditions, and it was demonstrated that the effects to be described were not due to electrostatic effects on the walls of the discharge-tube owing to accumulation of charge thereon. This was shown by experiments in which the walls were charged from an

<sup>7</sup> Townsend, 'Electricity in Gases,' p. 345 (1915).

<sup>8</sup> See for example, Shaxby & Evans, Proc. Phys. Soc. Lond. xxxvi. 4. p. 257 (1925); and discussion following on this paper.

<sup>9</sup> Dubois, *Compt. Rend.* clxxv. p. 947 (1922); Taylor & Clarkson, Phil. Mag. xlix. pp. 338-339 (1925); Taylor, Clarkson, & Stephenson, Journ. Scient. Instrs. ii. 5. p. 155 (1925).

<sup>10</sup> Proc. Phys. Soc. Lond. xxxvi. 4. pp. 249-250 (1925).

<sup>11</sup> Clarkson, Proc. Phys. Soc. Lond. xxxviii. 1, pp. 13-14 (1926).

<sup>12</sup> Taylor, 'Nature,' Correspondence, Sept. 24, 1924.

<sup>13</sup> For the description of this tube which was utilized in Part I. of this paper, see Taylor, *loc. cit.* p. 371.

<sup>14</sup> Campbell, Phil. Mag. xxxviii. pp. 226-228 (1919).

external source to a potential of several hundreds of volts, and it was found to be without influence on the values of the sparking potentials determined. Further, owing to the actual form of the tubes the polarization could not be due to charges on the electrode supports, etc.

### *Experimental Methods.*

In determining the sparking potentials the following method—unless otherwise stated—was utilized.

A source of steady and constant potential of which the value could be varied was placed in series with a resistance of 450,000 ohms and the discharge-tube whose constants were being investigated. The latter was shunted by a capacity of 0.5 microfarad, and the potentials at which discharges were produced were determined by means of the thermionic-valve electrostatic voltmeter referred to in Part I. of this paper. (This voltmeter was used throughout so that the results obtained were directly comparable with those obtained in the experiments on the "corona"). In determining the sparking potential the voltage across the circuit was gradually raised till a flash occurred. The time occupied in the process of raising the potential was usually 15 to 20 secs., but provided this was not excessively long consistent results were obtained.

In certain cases sodium was introduced into the tubes by electrolysis through the glass, as described in Part I.<sup>15</sup>

### *Polarization.*

"Polarization" is used throughout this paper to denote the effect which gave rise to a temporary increase in the value of the sparking potential on the passage of a flash or discharge.

### *Experimental Results.*

#### *Tube (2).*

This tube, described in Part I., consisted of nickel electrodes 5 cm. in diameter and 15 mm. apart at the centres. The electrodes were slightly curved (20 cm. in diameter), and the filling gas was neon-helium mixture at 7.8 mm. pressure.

It was found initially that the sparking potential was slightly variable (between 208 and 211 volts). The light of a 60 watt lamp, falling on the negative electrode from a

<sup>15</sup> See also R. C. Burt, *Phil. Mag.* xlix. p. 1168 (1925); *Journ. Opt. Soc. xi.* p. 87 (1925). Taylor, *Exp. Wire. & Wire. Engin.* 111. p. 39 (1926).



short distance away, did not appreciably affect the value of the sparking potential, so that effects due to external ionizing factors of small intensity could be neglected.

Some experiments were made in which the tube was connected directly to a low-resistance potentiometer: the sparking potentials were determined by gradually increasing the voltage across the terminals of the tube and noting when a discharge occurred. Initially the sparking potential was 210, but after a few flashes the value rose to 214 volts. After 45 discharges of short time duration had taken place the value had risen to 218 volts and remained at this value with further flashing. A discharge was then sent through the tube in the reverse direction, and it was found immediately afterwards that the sparking potential (in the normal direction) had fallen to 209 volts again, but increased in the same way as before when flashing was continued. The polarized tube was rested for four hours: the sparking potential had fallen by the end of this time to 204 volts, and there was no appreciable time-lag in the production of the discharge at this potential, even in darkness. After eight discharges of short duration the sparking potential rose to 211.5 volts. The tube was then run a great deal with the discharge first in one direction and then in the other. At the end of this "overrunning" the tube was symmetrical with respect to the sparking potential values and of value 212 volts.

With prolonged "overrunning" the sparking potential rose to 225 volts, but after a rest of one half-hour fell to 221, whilst when the electrode which had been employed as anode when the tube was "overrun" was utilized as cathode in sparking, the value was 210 volts. It is not proposed, however, here to deal with discharges of this nature which radically affect the surface of the electrode by the bombardment and heating of the electrodes, but with the less violent method of flashes from a condenser and high resistance (described above). Using this method it was found that the sparking potential rose from 206 volts to 213 volts after 300 flashes. The tube was then rested for four minutes. In this time the sparking potential had fallen to 208 volts; it rose again to 213 after 200 flashes. Fifty flashes were then put through the tube in the reverse direction. It was then found that the sparking potential in the normal direction had fallen to 210 volts but again rose to 213 after flashing for some time. About 450 flashes were then passed through in the reverse direction and the sparking potential in the normal direction redetermined. The value was 208 volts,

and rose again after flashing in the normal direction, to a steady value of 213. After a rest of one minute the sparking potential had fallen to 210.5.

At this point the tube was accidentally broken, so it was not possible to continue the experiments.

#### *Tube (4).*

Tube (4) was a Philips' Tungsten arc lamp consisting of tungsten electrodes of spherical form about 2 mm. in diameter and separated by a distance of 1 or 1.5 mm. The filling gas was neon-helium mixture at about half an atmosphere pressure. Before using the tube the cap was removed and the magnesium electrode—which is normally utilized to "strike" the arc—was short-circuited to the tungsten electrode opposite it. In this way the tungsten spheres alone functioned in the discharge.

The static sparking potential was found to be 206 volts, at which value a number of flashes were obtained. After flashing for some time the value of the sparking potential rose to 216 volts and was still increasing. The tube was rested for several minutes, and it was found that the sparking potential had then fallen to 213 volts. With continued flashing the sparking potential rose to about 260 volts, and finally no flashes could be obtained with the potentials available. Occasionally, however, blue-coloured, concentrated sparks passed across the electrodes in place of the usual red flashes due to neon. On reversing the electrodes so that the cathode was used as anode, flashes were obtained at about 235 volts initially, but the sparking potential rose to 250 volts after flashing had taken place for some time. At this point normal flashes ceased and gave place to the blue concentrated spark mentioned above (at much higher potentials). After a rest of half-an-hour the tube had completely recovered and the sparking potential fallen to the initial value of 206 volts.

With tube (4) it was found that irradiating the cathode by the light from a small half-watt lamp at 20 cm. distance exerted a considerable influence on the value of the measured sparking potential, if the tube was only slightly polarized. Thus in dim illumination, when the tube was polarized and gave a value of about 220 volts for the sparking potential, the sparking potential was 206 volts when the cathode was irradiated by the light from the small half-watt lamp. This effect of light was not observed with unpolarized electrodes or with fully polarized electrodes.

It should be noted here that tube (4) had not been

specially treated to avoid traces of impurities such as electro-negative gases, so that it is quite possible that the filling gas was not very pure. In the tubes which had been specially prepared to avoid such impurities no appreciable effect of light upon the value of the sparking potential was ever observed.

Sodium was then introduced electrolytically by means of the usual method, only instead of a filament a discharge between the tungsten electrodes was used.

The static sparking potential was then found to be 140 volts. The tube polarized very slowly and a sparking potential of 146 volts was finally attained. No difference of sparking potential was found when the cathode was irradiated. The effect of the sodium had thus been to lower the sparking potential by 66 volts, and to reduce the polarization from more than 50 volts to 5 or 6 volts.

#### *Tube (1).*

This tube was described in Part I. It consisted of parallel rectangular electrodes of iron (18.5 by 18.5 mm.) and 3.5 mm. apart, filled with neon-helium mixture at a pressure of about 10 mm. The tube had not been specially treated to remove gas impurities from the electrodes and filling gas. It was found that the time of lag in the production of a discharge was very considerably altered by irradiating the cathode by light, and attained large values after flashing had taken place for some time. Thus, although the actual static value of the sparking potential was always the same, yet under experimental conditions where the process of raising the potential across the discharge-tube in determining a sparking potential occupied only 15 or 20 secs., large differences were found according to the extent to which the cathode was irradiated. When the polarization of the tube became large, no influence of irradiation could be detected. Considerable polarizations were observed in this tube (of 30 volts or more), but the effects were neither constant nor repeatable, and differed markedly from the tubes which had been treated to avoid impurities.

#### *Tube (3).*

This tube was identical in form with tube (2), but comprised in addition a side-tube and tungsten filament for the introduction of sodium by electrolysis.

The constants of the tube were determined very shortly after it had been made. So far as the static sparking potentials were concerned, it was symmetrical to within about

half a volt,  $v_c$  being 213 volts with electrode A as cathode and 212·5 with B as cathode. On examining the polarization effects it was found that the tube became stably polarized with either A or B as cathode in about 6 flashes (the interval between the flashes was not too great, usually of one half-minute or so, otherwise the tube "recovered" considerably), and afterwards flashed regularly with a definite sparking potential value. The total polarization was about 7 volts with A as cathode and 9 volts with B as cathode (see Table I.).

TABLE I.

Polarization in volts. A cathode.	No. of flashes.	Polarization in volts. B cathode.	No. of flashes.
5	4	8	5 or 6
6·5	6 or 7	10	4 or 5
7·5	6 or 7	10	6
5·7	6	8	6
8	6	6·5	8
9·5	10	11	6
Averages ... 7	6·5	9	6

When the tube had become polarized it could be depolarized or "recovered" in two ways:—

(1) By passing a few flashes in the reverse direction (cathode changed to anode).

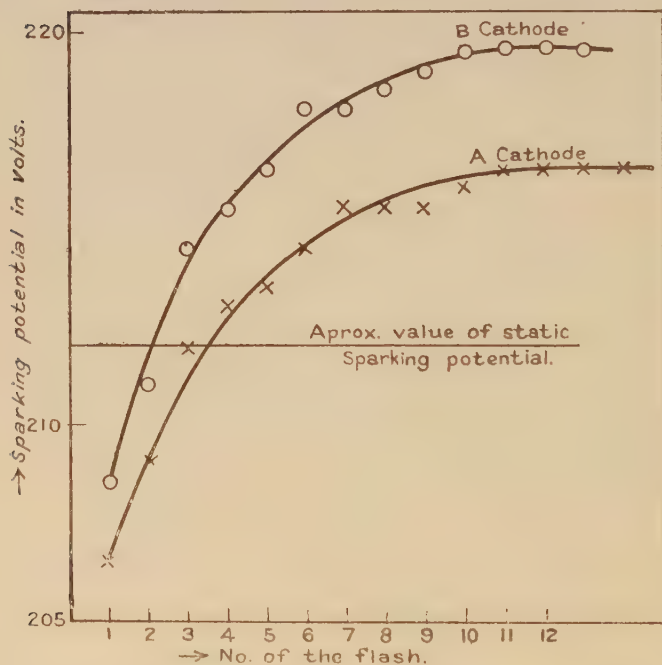
(2) By resting the tube for about half-an-hour.

When the tube had been rested for some hours the first flash was produced at 212 volts approximately (the static sparking potential). On the other hand, if the tube had been used with A as cathode until it was polarized and was then reversed, B being utilized as cathode, it was found that the sparking potential was usually of the order of 208 or 209 volts, for the first flash, after which it rose until a steady value was attained when the tube became polarized. If the effects be interpreted as being due to "electrical double layers" on the cathode, we see that an electrical double layer set up on polarization may actually lower the value of the sparking potential when the electrodes are reversed\*. The magnitude of the effect, however, was rarely comparable with that of the actual polarization effects.

\* It should be noted that this does not prove that an appreciable part of the sparking potential change is connected with the anode condition, but simply that the anode may have acquired a surface charge which affects the value of the sparking potential when this electrode becomes cathode.

The graphs of fig. 1 show the increase of the sparking potential with flashing. The actual form of course depended upon the interval between flashes etc., but the general nature was always the same.

Fig. 1.—Graphs showing examples of the increase of the Sparking Potential with flashing. Both graphs were taken after the tube had been polarized and immediately reversed. Results taken on Tube (3).



Sodium was next introduced electrolytically into the side-tube, in small quantity sufficient to give some vapour. The sodium vapour was not, however, pulled over to the discharge-tube electrodes by an electric field, so that only a small quantity, if any, would be condensed on the electrodes. On examining the sparking potentials and polarization effects it was found that they were the same as before the introduction of sodium vapour.

Sodium was then introduced for several hours, and the vapour was pulled over to the discharge-tube electrodes by maintaining a discharge between the electrodes and the glass



side-tube (the side-tube, contained in molten sodium nitrate, is of course the anode). Owing to the form of the tube more sodium was pulled over to the electrode B than to the electrode A.

The sparking potentials and polarization effects were then redetermined. The static sparking potential with B as cathode had fallen to 172 volts and the polarization effect was too small to be measured.

With A as cathode the static sparking potential had fallen to 192 volts and the polarization produced a rise of the sparking potential to about 198 for regular flashing. The polarization was thus of the order of 6 volts. A short time later the sparking potential for B as cathode was 172 volts and a polarization of about 1 volt was observed, whilst the static sparking potential for A was 195 and a polarization of 4 volts only was observable.

Results taken 10 days later showed but little alteration, the static sparking potential for B as cathode being 174.5 and for A as cathode 198.5, whilst the polarization in the former case was 1 volt and in the latter case 5 volts. These changes were probably the result of a certain amount of absorption of the sodium on the surface of the electrodes, but are very little greater than changes observable in any discharge-tube from the time when it has just been completed and after a fortnight's use.

Now apart from the introduction of sodium the conditions of the tube remained identical throughout the experiments. The first introduction of sodium into the side-tube (although in sufficient quantity to be visible) made no observable difference in the results, for it was not pulled over to the electrodes. It was evident therefore that it was not a "clean-up" of gas or the presence of sodium vapour which caused the differences. The seat of the phenomena must therefore be sought upon the surface of the electrodes themselves.

Summarizing the results on the effect of the introduction of sodium upon all the discharge-tubes used, we find the following. The effect is dual. First of all there is a reduction of the actual sparking potential value, and secondly there is a very considerable diminution of the polarization effects observed. Further, it is to be seen from the results on tube (3) that the effect of sodium upon the electrodes is of a progressive nature and depends upon the amount of sodium on the electrodes. It may be assumed, in accordance

with Langmuir's theory<sup>16</sup>, that a film of atomic thickness of sodium on the electrode will act in all ways as a sodium electrode—this is also supported from the results of X-ray practice upon very thin anticathodes. If the quantity of sodium upon the electrodes is insufficient for this then there will be bare patches.

#### *General Classification.*

We may divide the electrode surface phenomena roughly into three headings:—

- (1) Those which give rise to permanent changes.
- (2) Those which give rise to changes which are temporary but not reversible, or are only partially reversible and are of large magnitude.
- (3) Those which give rise to reversible and temporary changes of a repeatable nature.

(1) The effects included under this heading are those which are brought about by heavy discharges such as are used in "overrunning" discharge-tubes for the stabilization of their constants" and which cause an actual alteration—usually visible—of the surface of the electrodes.

It is not certain whether these effects are primarily due to an actual alteration of the surface of the cathode or to a "clean-up" of the filling gas or impurities. It was therefore considered to be of interest to carry out some experiments with a view to elucidating this.

#### *Change of Sparking Potential with the Surface Condition of the Electrodes.*

A tube No. (5) similar in form to tube (2) was used. The electrodes were not "overrun" or "baked out" in constructing. The filling gas was carefully purified neon-helium mixture (97 per cent. neon, 3 per cent. helium), and the sparking potentials were determined over a range of pressures (see graph of fig. 2).

The tube was then "overrun" for about one and a half hours at 0.1 amp. direct current. A considerable amount of sputtering occurred during this time. The discharge-tube was then filled again with carefully purified neon-helium mixture and the sparking potentials were determined over the same range of pressures as before.

It was found that an increase in the sparking potential of over 60 volts had taken place though the gas was of exactly

<sup>16</sup> Langmuir, J. Am. Chem. Soc. xxxvii. p. 1139; xxxviii. p. 2221 (1916); Phys. Rev. viii. p. 149 (1916); J. Am. Chem. Soc. xl. p. 1316 (1918).

the same nature as previously. The tube recovered considerably with time (see Table II.), but on attaining equilibrium the values of the sparking potential were still some

Fig. 2.— Graphs showing the change of the Sparking Potentials with the surface conditions of the Electrodes. Results on tube (5).

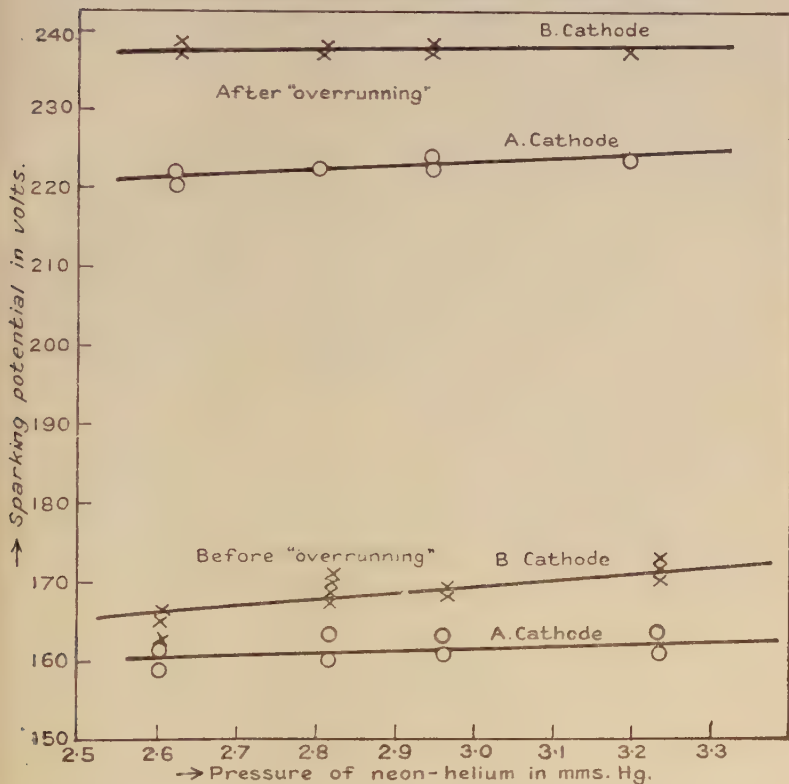


TABLE II.

Results taken with Tube (5), showing partial recovery from "overrunning."

SPARKING POTENTIAL.		TIME since being "overrun."	PRESSURE of neon-helium.
A cathode.	B cathode.		
224	238	0 hours.	3.2 mm.
222	237.5	about 0.5 hours.	do.
196	215	20 hours.	do.
190	209	44 hours.	do.
187	205	5 days.	do.

Voltages constant after this.

30 volts higher than originally. In this tube the polarization was extremely small and there was a tendency for a small decrease of the sparking potential after continued flashing.

It is to be concluded that the nature and condition of the cathode exert a very profound influence on the magnitude of the sparking potentials: indeed, the changes in the above experiment were as great as those observed on the introduction of sodium on to the electrodes.

Experiments of a similar nature have been conducted recently by Janitzky<sup>17</sup>.

(2) Under the heading (2) are to be classed most of the effects observed with tubes (1) and (4) before the introduction of sodium. These tubes were those which were likely to contain traces of active gases and in which the electrodes had not been "baked out" or "overrun." The problem arises then as to whether the polarization effects are due to the presence of active gases as impurity in the neon-helium mixture or to some surface condition of the electrodes. Some experiments were made with hydrogen to test this.

#### *Experiments with Hydrogen.*

A discharge-tube having a palladium wire fused into the bulb so that hydrogen could be introduced by diffusion, was filled with pure neon-helium gas, and sodium was introduced on to the electrodes. The sparking potential was determined—121 volts—and the polarization was found to be negligibly small.

Hydrogen was then introduced in small quantity; the sparking potential was immediately redetermined and found to be 220 volts. There was no measurable polarization.

It is to be concluded from the above experiment that the presence of the active gas hydrogen is not itself sufficient to produce polarization effects. This is probably true of other gases, but the writer has not been able so far to conduct definite experiments in this direction.

We may conclude consequently that the seat of the polarization phenomena is the surface of the electrodes, and since abnormally large and erratic polarization effects did not occur in those tubes whose electrodes had been thoroughly "baked out" and "overrun," or were "sodiumated," it is very probable that the effects are due to the presence of layers of active gases absorbed or occluded at the electrode surfaces. It is possible that many of the photoelectric effects signalled

<sup>17</sup> Janitzky, *Zts. f. Phys.* xxxv. p. 27 (1925).

in connexion with the neon glow-lamp<sup>18</sup> have arisen from such causes.

(3) The effects classed under this heading are those dealt with mainly in this work and appear to exist in tubes which have been carefully treated to avoid gases of the active kind in the neon-helium mixture and whose electrodes have been "baked out" for several hours at 300° C. and "overrun."

### *Theory of Sparking.*

Before proceeding to a proposed explanation of the polarization effects it is necessary to describe briefly a new Theory of Sparking which it is proposed to adopt. The hypothesis is merely incidental to the present work and is reserved for future treatment.

The mechanism of the initiation of the spark and glow discharge is not known. The widely accepted theory is that of Townsend<sup>19</sup>. Another theory has been put forward more recently by Holst and Oosterhuis<sup>20</sup>.

With regard to the development of currents in the regime before a self-sustained discharge is obtained, experimental evidence is fairly decisive "in showing that ionization is principally due to the direct effect of collisions of electrons with molecules of the gas." The question remains "which of the other modes of generating ions contributes the additional effect required in order to explain the disruptive discharge"<sup>21</sup>.

In a recent paper<sup>21</sup> Prof. Townsend criticises the theory of Holst and Oosterhuis, and discusses three different methods by which the additional ionization might be brought about. He rejects all except the first method which assumes the production of the extra ionization by the collisions of the positive ions with the gas molecules. The process of production of the extra ionization from electronic emission from the cathode by bombardment of the positive ions is rejected on several counts, one of the weightiest being that such a method necessitates the assumption that the number of electrons set free at the negative electrode is independent of the velocity with which the positive ions impinge on the cathode.

There is, however, at least one method by which electrons

<sup>18</sup> See *e.g.* Oswald & Tarrant, Proc. Phys. Soc. Lond. xxxvi. p. 241 (1924); A. Lamberts, *Phys. Zeits.* xxvi. p. 254 (1925).

<sup>19</sup> 'Electricity in Gases,' J. S. Townsend (Oxford) 1915, p. 322.

<sup>20</sup> Holst & Oosterhuis, *Phil. Mag.* xlv. p. 1117 (1923).

<sup>21</sup> Townsend, *Phil. Mag.* xlv. p. 44 (1923).



may be ejected from the cathode by neutralization of the positive ions on reaching the cathode, which will be independent of the velocity of the positive ions. Sir J. J. Thomson recently put forward this idea in connexion with the electric discharge in gases<sup>22</sup>, and at the time of writing this paper, a further study has just appeared<sup>23</sup>. Briefly we may describe the idea as follows:—The positive ions of the gas arrive at the cathodic surface under the electric field and are neutralized there by the electrons falling into the vacant orbits. As a consequence radiation is emitted, of which a part falls upon the cathode surface and gives rise to photoelectric effects which result in the expulsion of electrons. We assume here that these photoelectrons in turn produce ionization by collision and provide the additional source of ionization necessary to initiate the self-sustained electric discharge.

It is readily to be seen how this hypothesis can be fitted into Formulæ (B) of Townsend's paper<sup>21</sup>, or the relation obtained by Holst and Oosterhuis<sup>20</sup>.

Nevertheless there are still difficulties in the light of certain experimental evidence in accepting such a theory as outlined above; it is hoped, however, to continue work in this direction, and a fuller consideration of the theory will be given in a later paper.

According to the foregoing hypothesis the sparking potential of a discharge-tube should be intimately connected with the photoelectric properties of the cathode surface, and changes of the nature and condition of the surface should entail considerable changes of this function. The results with tube (3) after the introduction of sodium illustrate well this change: the sparking potential was progressively lowered with increase of the quantity of sodium on the electrode, showing that in this type of tube where the field is uniform, the sparking potential is a function of the composition of the cathode over a considerable area, a result in accordance with the idea that the value is a function of the photoelectric emissivity of the cathode. The results with tube (5) are also in accordance with the above hypothesis, for it is known that the photoelectric properties of metals vary considerably according to the state of the surface and the occluded gases thereon<sup>24</sup>.

<sup>22</sup> Sir J. J. Thomson, *Phil. Mag.* xlviii. p. 1 (1924); *ibid.* xlix. May 1925.

<sup>23</sup> Sir J. J. Thomson, *Phil. Mag.* ii. p. 675 (1926).

<sup>24</sup> See *e.g.* Welo, *Phil. Mag.* xlv. p. 593 (1925); Chien Cha, *Phil. Mag.* xlix. p. 262 (1925).

The partial recovery of tube (5) was probably brought about by the further diffusion of gas from the metal of the cathode to the surface (*cp.* with the results of Welo, see note 24).

It is evident that such surface-films of gas on the cathode of a discharge-tube will exert a considerable effect upon the photoelectric power of the cathode surface and consequently upon the magnitude of the sparking potential if the process initiating a self-sustained electric discharge is regarded as above.

### *Theory of Polarization Phenomena.*

We shall adopt the hypothesis that the polarization effects are occasioned by the action of the discharge upon layers of gas absorbed or occluded upon the discharge-tube electrodes.

The explanation of the rotational fatigue effect (see note 12) becomes clear if we assume that there is a gas film at the cathode surface and that the part of this film immediately beneath the negative glow becomes positively charged by the electronic emission of the cathode and the bombardment by the positive ions of the discharge. This electrically charged double-layer cannot immediately dissipate its charge, and consequently a polarization layer is formed at the surface of the cathode. The effect of this layer is twofold. It actually decreases the field between the cathode surface and the edge of the negative glow, and further it inhibits the emission of electrons from the cathode. It is consequently easier for the discharge to pass at an adjacent portion of the cathode that has not been subject to the action of the discharge. The discharge may consequently rotate and the period of rotation depends on the time for the "recovery" of the cathodic gas-layer.

It is necessary to consider such films in their relation to the sparking potentials. The passage of a discharge will be accompanied, in a way described above, by a charging-up positively of the gas-layer at the cathode surface which is giving off electrons and is being bombarded by positive ions at the same time. Consequently a polarized layer is set up after a spark or discharge has taken place. The charge of this layer will disappear in a time depending upon the duration of the discharge, or upon the frequency of discharge if flashes are taking place, and upon the intensity of the discharge.

Now when a potential is placed across the polarized discharge-tube, the existence of the electrical double-layer will modify the conditions under which discharge occurs.

In the first place, such a layer will introduce an apparent resistance in the circuit due to the increased contact potential of the electrode to gas surface, and decrease the value of the field between the electrodes for a given potential across the discharge-tube terminals. Further, it will diminish the capacity of the cathode metal for emitting electrons and considerably alter the photoelectric properties of the cathode by introducing a fatigue effect.

In certain cases where active gases such as oxygen etc. were likely to exist as films on the electrode surfaces the polarizations were abnormal. In tubes (1) and (4) for example, it was found that after heavy flashing in one direction through the tube had taken place, the sparking potentials in both directions were considerably increased. This was probably due either to a formation of a negatively charged layer on the surface of the anode in addition to the positive layer on the cathode, or to a temporary change in the nature of the films on both electrodes.

In most of the tubes the polarization could be largely eliminated, as we saw, by passing flashes in the reverse direction. This effect is readily explainable. The positively charged outer layer of the cathode film becomes bombarded by electrons when the discharge is reversed, and this quickly neutralizes the positive layer and brings the tube into the unpolarized state.

In those tubes showing small and reversible polarization effects the condition of the anode appeared to exert little influence. This is illustrated in many results. A polarized tube, on being reversed, never showed a sparking potential value considerably less than the static value, and in the tube (3) polarizations of appreciable value were only obtained when the electrode which was relatively free from sodium was used as cathode. When the sparking potential with B (the electrode upon which there was most sodium) as cathode was 172 volts, the sparking potential with A as cathode was 192 volts and rose to 198 volts with flashing, that is to say there was a polarization of 6 volts. Now when the polarized tube was reversed so that B was again cathode and the sparking potential immediately determined, it was found still to be of the value 172 volts, so that an effect on electrode A capable of producing a change of 6 volts when A was cathode produced no appreciable change when A was anode. From this it may be concluded that in these cases the chief effects are located on the cathodic surface.

It is difficult to understand how such large polarizations as those observed in tubes (1) and (4) can be produced if it

is not due to an effect which either prevents the cathode from emitting electrons so readily or alters the photoelectric emissivity of the surface. The former explanation is applicable to the reversible polarizations and the latter to the electrode surface effects produced by intense discharges and "overrunning."

*General Remarks on Electrode Surface Phenomena.*

The electrode surface phenomena in discharge-tubes are of an intricate nature and the previous considerations can merely be considered as illustrative and introductory.

It should be remarked that the magnitude of the polarization effects depends upon the intensity of the discharges and their time-duration, upon the previous treatment of the electrodes, and many other factors. Further, the effects are not observed in all tubes, and this appears to be intimately connected with the nature of the gas-layer on the electrode surface. Indeed, in one tube a slight depreciation of the sparking potential was observed after flashing for some time. In this case the electrodes had not been treated at all, and it was found that about 0.25 c.c. of gas at atmospheric pressure was given off on "overrunning." There was probably a considerable water-vapour content.

Experiments with pure metal electrodes such as are produced by metallic evaporation in vacuum are in progress, and it is hoped that they will throw a considerable light upon the electrode surface phenomena.

It is a great pleasure to me to express my gratitude to the International Education Board for the Fellowship which enabled this work to be carried out, to Prof. Ornstein under whose supervision the research was done and to whom I am indebted for much valuable advice and assistance, and to Mr. Willemse, of the University Physical Laboratory at Utrecht, for continual assistance in the construction of the tubes and apparatus.

*Summary.*

The paper deals with the electrode surface effects of discharge-tubes and their relation to the sparking potentials. Experimental data are given for many tubes, and it is shown in the case of tubes containing neon-helium mixture as filling gas and having electrodes of nickel and iron (that have been thoroughly "baked out") that there is a temporary increase of the sparking potential with "flashing" or



discharge. This increase of the sparking potential is termed "polarization."

In certain cases very large polarizations were observed. Polarization could be reduced or eliminated in many cases by passing a discharge in the reverse direction through a polarized tube, or by resting it for a few hours.

Experiments showed that the polarizations were reduced to very small values by introduction of sodium upon the electrodes, and that the actual values of the sparking potentials were very considerably lowered at the same time.

A new Theory of the Sparking Potentials is given. It is assumed that electrons are given off from the cathode by the photoelectric effect of the radiation from the positive ions which are neutralized at the cathode surface. According to this hypothesis the sparking potential should be a function of the photoelectric emissivity of the cathode. Some experimental results in support of this are given.

Assuming the above hypothesis, a theory of the electrode surface phenomena is given in which it is assumed that the passage of a discharge modifies gas-layers which are occluded or absorbed on the electrodes. The modifications are of two kinds—a permanent one which changes the photoelectric emissive power of the cathode and is consequently accompanied by a change in the sparking potentials, and a temporary one due to the charging-up of the surface gas-layers and the consequent formation of electrical double-layers. These layers inhibit electronic emission from the cathode and bring about the "polarization" effects.

September 25th, 1926.

LXXVI. *The Magnetic Rotation of Solutions of certain Ferric Salts.* By CONSTANCE E. RICHARDS, M.Sc., and R. W. ROBERTS, M.Sc., *The University, Liverpool* \*.

**I**N the course of an investigation on the magnetic rotary dispersion of certain solutions of nickel and cobalt by one of us†, it was found necessary, in order to obtain effects characteristic of the solute, to take into account the rotation due to the solvent. To do this an appeal to two different theories was made, and it was found that the rotary dispersion curve of the solute obtained from these theories had certain common features. For the sharper isolation, however, of

\* Communicated by Prof. L. R. Wilberforce.

† Phil. Mag. xlix. p. 397 (1925).



the rotation due to paramagnetic ions in solution, it is desirable to deal with solutions in which this paramagnetic rotation preponderates over the diamagnetic rotation of the solvent.

It is well known that solutions of some iron salts in water and a few alcohols give very large negative rotations, and it occurred to us that a systematic study of the magnetic rotary dispersion of solutions of iron salts in water and alcoholic solvents would be of experimental and theoretical interest. A preliminary investigation of a negatively rotating iron salt was made by one of us in the year 1921 in the case of potassium ferricyanide\* (previously investigated by Siertsema)†. The present communication deals only with aqueous solutions of ferric salts.

The early researches of Verdet‡, H. Becquerel§, Quincke||, Du Bois¶, and Cotton\*\* on solutions of ferric chloride deal mainly with the rotation for comparatively few wave-lengths. More recently, however, Ingersoll†† has determined the magnetic rotation of a number of aqueous solutions of paramagnetic salts over the spectral range  $1\cdot35\ \mu$  to  $\cdot56\ \mu$ . It was hoped, with modern methods of producing monochromatic light of strong intensity and known wave-length, that the course of the rotary dispersion in the visible spectrum could be determined over a wider spectral range than formerly.

#### EXPERIMENTAL.

As the absorption of some of the ferric salts used increases with dilution‡‡, most of the work has been carried out with fairly concentrated solutions. Owing to the strong absorption, it was found necessary to put the solutions under test in a smaller cell than the one used for the previous work on Ni and Co solutions. The cell used in the recent investigation was made by grinding down the ends of a small piece of glass tubing to be as nearly normal to the axis of the tube as possible. The length of the tube amounted to 0·52 cm. To the ends of the tube were fixed square micro-cover glasses

\* *Loc. cit.*

† *Arch. Néer.* (2) v. p. 447 (1900).

‡ *Phil. Mag.* xii. (4th ser.) p. 483 (1856).

§ *Ann. Chim. et Phys.* (5) xii. p. 42 (1877).

|| *Wied. Ann.* xxiv. p. 606 (1885).

¶ *Wied. Ann.* xxxv. p. 137 (1885).

\*\* *Eclair. électr.* viii. pp. 162 & 198 (1896).

†† *J. O. A. S. America*, vol. vi. No. 7 (1922).

‡‡ Anderson, *Proc. Roy. Soc. Edin.* xxxiii. p. 35 (1912).

of thickness 0.0165 cm., and held in position by means of a small quantity of Chatterton cement. As the distance between the pole-pieces of the electromagnet used amounted to 1.2 cm., it was necessary to determine the variation of the magnetic potential across the ends of the tube with the position of the cell between the pole-pieces. This was done, with sufficient accuracy for our purpose, by observing the rotation produced by the cell when filled with water on reversal of the current through the electromagnet. From the mean of a large number of readings obtained with the cell in positions differing by 1 mm., it was found that the greatest change of rotation was produced when the cell was almost symmetrically placed with reference to the pole-pieces. This position was noted and the cell was always brought, throughout the course of the work, to this standard position.

As sources of illumination, a number of arcs were used. In the data to follow, observations are recorded on the lines 5780 (mean line), 5461, and 4358 of the vacuum arc spectrum of mercury, on the lines 5218, 5153, and 5105 of the open copper arc, on the lines 5330 and 4958 of the open iron arc, and also on the yellow sodium line. The greatest difficulty was experienced in taking observations in the red-orange part of the spectrum. A quartz mercury amalgam lamp gave a disappointing performance. The open arc between rotating electrodes of a silver cadmium alloy of the same composition as used by Lowry\*, was found with our arrangement not to be sufficiently steady for continuous observation. The most satisfactory source in this region was obtained by burning lithium carbonate between copper electrodes, as suggested by Lowry and Parker†. Readings could only be taken on the line 6104.

In order to detect any possible changes in the solutions with time, observations were made rapidly on all the lines in turn. This procedure was repeated a large number of times. With the exception of the ferric nitrate solution, the maximum variations from the mean for the readings in the successive series were found to be nearly the same as those obtained for pure water. In the case of the ferric nitrate solution a distinct variation of the rotation with temperature was observed. Owing to the hygroscopic nature of the ferric salts used, it was thought advisable to determine the strengths of the solutions by volumetric analysis of the iron content. The bichromate method was used.

\* *Phil. Mag.* xviii. p. 320 (1909).

† *Journ. Scient. Instr.* i. p. 16 (1923).

The refractive indices were obtained by means of a Pulfrich refractometer. The recorded results refer to room temperature at about 17° C. No temperature correction has been applied to them, as the determination of the refractive indices of the solutions was not regarded as of primary importance in this work, and the uncorrected values are sufficiently accurate for the purpose of the present calculations.

### FORMULÆ.

When we have paramagnetic ions in a diamagnetic medium experiment indicates that both the Hall Effect and the Molecular Current Effect must be taken into consideration. We readily find that if we retain only terms involving the first power of  $H$ , the external magnetic field, the rotation is given by the formula \*

$$\delta = \frac{e^3 H}{18\pi m c^4} \frac{(n^2 + 2)^2}{n} \sum_d \frac{\lambda_d^4 \lambda^2}{(\lambda^2 - \lambda_d^2)^2} + \frac{2\pi}{3c^3} n(n^2 + 2) \sum_p N_p \frac{e^2 q_p}{m_p T_p} \frac{\lambda_p^2}{\lambda^2 - \lambda_p^2}.$$

If we apply this result to a length of solution equal to 1 cm. in a magnetic field of 1 gauss, we find

$$R = x \left( \frac{n^2 + 2}{n_w^2 + 2} \right)^2 \frac{n_w}{n} R_w + \frac{(n^2 + 2)^2}{n \lambda^2} \sum_d \frac{a'_d}{(1 - \lambda^{-2} \lambda_d^2)} + \frac{n(n^2 + 2)}{\lambda^2} \sum_p \frac{a'_p}{1 - \lambda^{-2} \lambda_p^2},$$

where  $R$  and  $R_w$  are the Verdet constants for the solution and pure water respectively,  $x$  is the mass of water in 1 c.c. of solution,  $a'_d$  and  $a'_p$  are diamagnetic and paramagnetic constants, and the  $\sum_d$  and  $\sum_p$  extend over diamagnetic and paramagnetic electrons respectively.

$$\text{Let} \quad R'_w = x \left( \frac{n^2 + 2}{n_w^2 + 2} \right)^2 \frac{n_w}{n} R_w$$

$$\text{and} \quad R_s = R - R'_w,$$

then  $R_s$ , which may be regarded as the rotation due to the salt, is given by

$$\frac{R_s \lambda^2}{n(n^2 + 2)} = \sum_p \frac{a'_p}{1 - \lambda^{-2} \lambda_p^2} + \frac{n^2 + 2}{n^2} \sum_d \frac{a'_d}{(1 - \lambda^{-2} \lambda_d^2)^2}.$$

Approximate formulæ may be obtained if we regard the

\* *Loc. cit.*

diamagnetic part on the right-hand side of the above equation as small in comparison with the paramagnetic part, and if we suppose there is only one kind of paramagnetic electron, then

$$\frac{R_s \lambda^2}{n(n^2 + 2)} = \frac{a_p}{1 - \lambda^{-2} \lambda_p^2} \dots \dots \dots (1)$$

If the diamagnetic part is not negligible, as is probably the case for only weakly paramagnetic solutions, we can still allow for its effect approximately by treating  $\lambda_d$  as small in comparison with  $\lambda$ , and taking  $(n^2 + 2)/n^2$  as being constant, then

$$\frac{R_s \lambda^2}{n(n^2 + 2)} = \frac{a_p}{1 - \lambda^{-2} \lambda_p^2} + a_d, \dots \dots (1a)$$

where  $a_p$  and  $a_d$  are constants.

After the magnetic observations had been completed an important paper by Ladenburg\* has appeared in which a new formula for the magnetic rotation of a paramagnetic substance is deduced. His formula may be written in the form

$$R = \frac{e^3}{18\pi m^2 c^3} \frac{(n^2 + 2)^2}{n} \frac{1}{\lambda^2} \sum_d \frac{\lambda_d^4}{(1 - \lambda^{-2} \lambda_d^2)^2} \\ + \frac{1}{54\pi c^2 kT} \frac{(n^2 + 2)^2}{n\lambda} \sum_p \frac{\mu_p \rho_p \lambda_p^2}{1 - \lambda^{-2} \lambda_p^2},$$

whence, writing  $b'_d = e^3/18\pi m^2 c^3$ ,

$$R = R'_w + \frac{(n^2 + 2)^2}{n\lambda^2} \left\{ \sum_d \frac{b'_d \lambda_d^4}{(1 - \lambda^{-2} \lambda_d^2)^2} \right. \\ \left. + \frac{2e^2 \lambda}{27mc^2 kT} \sum_p \frac{N_p \mu_p \lambda_p^2}{1 - \lambda^{-2} \lambda_p^2} \right\},$$

and

$$\therefore \frac{R_s n \lambda^2}{(n^2 + 2)^2} = \sum_d \frac{b'_d \lambda_d^4}{(1 - \lambda^{-2} \lambda_d^2)^2} + \frac{2e^2 \lambda}{27mc^2 kT} \sum_p \frac{N_p \mu_p \lambda_p^2}{1 - \lambda^{-2} \lambda_p^2}.$$

If we assume that only one kind of paramagnetic electron is present, and also suppose that the free periods of the diamagnetic electrons lie far in the ultraviolet, then

$$\frac{R_s n \lambda^2}{(n^2 + 2)^2} = \frac{b_p \lambda}{1 - \lambda^{-2} \lambda_p^2} + b_d,$$

where

$$b_p = \frac{2e^2 N \mu \lambda_p^2}{27mc^2 kT},$$

\* *Zeits. f. Phys.* xxxiv. p. 898 (1925).

$b_d$  is a constant, and  $N$  is the total number of paramagnetic electrons per c.c. of solution. As a further approximation we may drop  $b_d$  and use the formula

$$\frac{R_p n \lambda}{(n^2 + 2)^2} = \frac{b_p}{1 - \lambda^{-2} \lambda_p^2} \cdot \cdot \cdot \cdot \cdot \cdot (2)$$

Besides differing in the expressions for the constants  $a_p$  and  $b_p$ , the paramagnetic rotation deduced from the Drude formula has a different dispersion from that given by the Ladenburg formula. In the latter case this rotation tends to zero for short waves on the high frequency side of the absorption band. This behaviour is absent in some cobalt solutions, the dispersion curve of the solution remaining almost parallel and below the water curve as far as the observations could be extended into the ultraviolet. On the other hand, the Drude formula predicts that the paramagnetic rotation for such waves would tend to a negative value. Too much must not be expected from either formula when applied to solutions, owing to the complicated processes existing in them. We have used formulæ (1) and (2) on all the salts except ferric nitrate, where the course of the rotary dispersion is much more complex than with the remaining solutions. It may be of interest to note that the position of the absorption band given by (1) in the case of a solution of  $K_3Fe(CN)_6$  is very near to the position determined by absorption measurements. Calculation gave the band to be at  $\cdot 427 \mu$ , and H. C. Jones and W. W. Strong\* state that absorption measurements indicate the presence of an absorption band near  $\cdot 420 \mu$ .

The values of  $\lambda_p$  given by the formula (2) are greater than those given by (1).

## RESULTS.

All the observations have been corrected for the rotation produced by the end plates. These corrected rotations have been reduced to give Verdet constants; the Verdet constant for water at the mean temperature  $20^\circ C.$  was taken to be  $0\cdot 01309$  min. per cm. gauss†. The average field obtained with the small cell in the standard position amounted to  $13,510$  gauss.

\* Carn. Inst. Pubn. No. 130, p. 28 (1910).

† Rodger & Watson, Phil. Trans. A, 186. p. 621 (1895).



*Water.*

Observations were made with both the large cell and the small cell. Good agreement was obtained between the Verdet constants deduced from these readings. The mean Verdet constants are here recorded.

$\lambda$ in $\mu$ .	$n$ .	$R_{40}$ .
·5893	1·3330	·0131
·5780	1·3334	·0136
·5461	1·3345	·0153
·5330	1·3349	·0160 <sup>b</sup>
·5218	1·3353	·0172
·5105	1·3358	·0175 <sup>b</sup>
·4958	1·3366	·0187

*Ferric Sulphate.* (Fig. 1.)

$$d = 1·190. \quad x = ·990.$$

$\lambda$ in $\mu$ .	$n$ .	$R$ .	$R'_{40}$ .	$R_s$ .
·6104 Li	1·3728	·0080	·0122	—·0042
·5893 Na	1·3737	·0083	·0133	—·0049
·5780 Hg	1·3741	·0088	·0138	—·0050
·5461 Hg	1·3760	·0094	·0155	—·0061
·5330 Fe	1·3768	·0098	·0163	—·0066
·5218 Cu	1·3773	·0107	·0170	—·0064
·5105 Cu	1·3780	·0108	·0179	—·0071
·4958 Fe	1·3800	·0108	·0191	—·0082

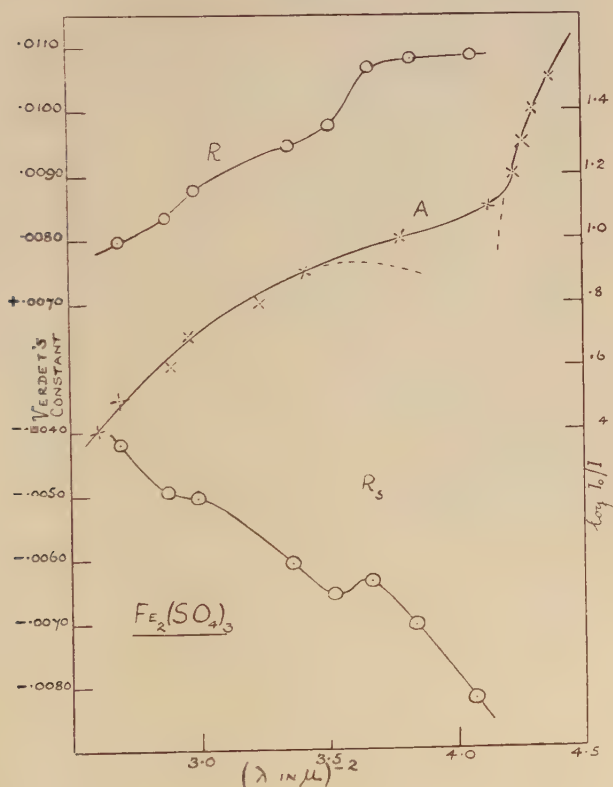
Although the rotation of this solution is positive, it will be seen from the graph that the salt produces a distinct negative rotation. The decided inflexions in the rotary dispersion curve indicate the presence of at least two absorption bands.

The absorption spectra of solutions of two different strengths of ferric sulphate have been investigated by Anderson \*. His curves, however, do not show the presence of an absorption band in the visible part of the spectrum. We are able to give the absorption spectrum of this solution through the kindness of Dr. R. A. Morton and Dr. R. W. Riding, who mapped it by means of the Hilger method. The  $\log I_0/I$  values in the graph marked A refer to length of solution equal to 2 cm.

\* *Loc. cit.*

It will be noticed that there is a close connexion between the courses of the absorption curve and the rotary dispersion curve. It must be admitted that the absorption bands in this solution are not completely isolated. Superimposed on these weak absorption bands is the effect due to the strong absorption band in the near ultraviolet, with the result that

Fig. 1.



these weak bands are not very pronounced. Many interesting examples of inflexions caused by weak bands have been recorded by Henri in his book on 'Etudes de Photochimie.'

Both the  $A$  and  $R$  curves indicate the presence of an absorption band with its maximum at about  $\lambda^{-2} = 3.6$ , i. e.  $\lambda = 0.53 \mu$ . There also appears to be a weak band in the neighbourhood of  $\lambda^{-2} = 3.1$ , i. e.  $\lambda = 0.57 \mu$ .

The rotations  $R_s$  for the last three wave-lengths in the above table provide the following values of  $\lambda_p$ :—

Pair.	$\lambda_p$ from (1).	$\lambda_p$ from (2).
5218 } 4958 }	·394 $\mu$	·424 $\mu$
5105 } 4958 }	·407	·437

*Ferric Nitrate.* (Fig. 2.)

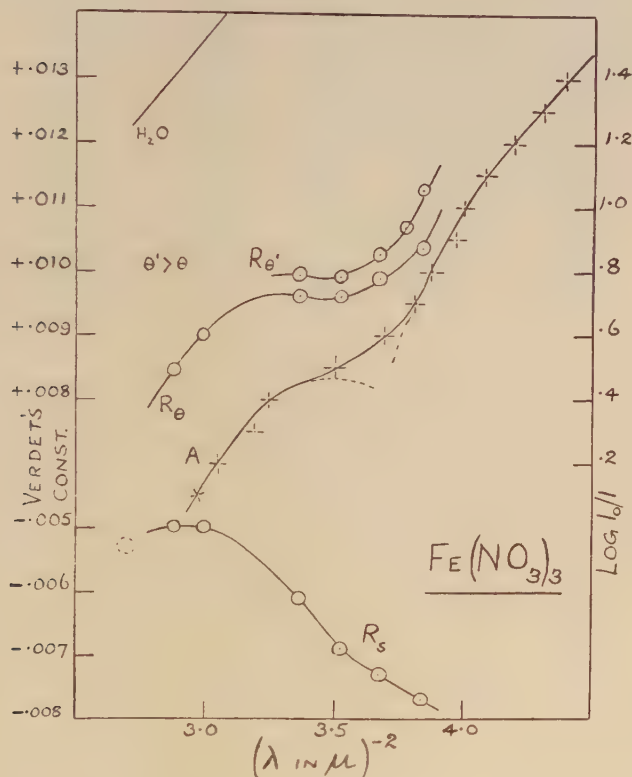
$$d = 1.190. \quad x = .996.$$

$\lambda$ .	$n$ .	$R$ .	$R'_{90}$ .	$R_s$ .
·5893	1.3797	·0085	·0135	—·0050
·5780	1.3804	·0090	·0140	—·0050
·5461	1.3818	·0096	·0157	—·0061
·5330	1.3827	·0096	·0165	—·0069
·5218	1.3836	·0099	·0172	—·0073
·5105	1.3863	·0104	·0181	—·0077

As with the preceding salt, the rotation produced by ferric nitrate is negative. There is a distinct bend in the rotary dispersion curve at about  $\lambda^{-2} = 3.5$ , *i. e.*  $\lambda = .535 \mu$ . The absorption curve of a normal solution of ferric nitrate also shows a bend at about the same value of  $\lambda^{-2}$ , as may be seen from the graph A, in which the values  $\log I_0/I$  for a length of solution equal to 1 cm. are plotted against  $\lambda^{-2}$ . These absorption measurements, kindly made for us by Drs. Morton and Riding, give added support to the accuracy of the magnetic observations. A further point of interest in connexion with this solution is that there is a distinct variation of the rotation with temperature. The upper magnetic curve  $R_\theta$  of fig. 2 has been drawn from observations made at the end of a run on the magnet when the coils had been warmed up through the passage of the current for about four hours. This change of rotation is in the opposite direction to the decrease of rotation of diamagnetic substances with increase of temperature, and is also much larger in magnitude than the corresponding change in the diamagnetic rotation. The change plainly refers to the decrease of the negative paramagnetic rotation of the ferric nitrate with increase of temperature. After we had observed this effect, we found that Elias had noted a pronounced increase of paramagnetic

rotation (which in his case was negative) with decrease of temperature in the case of nitrates of certain rare earths. It is curious that our solution is also of a paramagnetic nitrate.

Fig. 2.



Ladenburg has pointed out in his paper the significance of this temperature variation and has deduced on classical grounds that the paramagnetic rotation varies inversely as the absolute temperature.

### Ferric Chloride.

Four solutions of this salt of different strengths were examined. The results for two of these, which were investigated in the early stages of the work, are recorded in graphical form in fig. 5. The results for the other two, for which the

rotary dispersion has been more completely determined, are given in tabular and graphical form (figs. 3 and 4).

Fig. 3 has been constructed from the following data :—

$$d = 1.045. \quad x = .994.$$

$\lambda$ .	$n$ .	$R$ .	$R'_{90}$ .	$R_g$ .
.6104	1.3470	.0105	.0120	-.0015
.5893	1.3478	.0113	.0131	-.0019
.5780	1.3484	.0117	.0137	-.0020
.5461	1.3496	.0129	.0153	-.0024
.5330	1.3500	.0135	.0161	-.0026
.5218	1.3508	.0141	.0168	-.0027
.5105	1.3514	.0145	.0176	-.0031
.4958	1.3535	.0154	.0188	-.0034

Fig. 3.

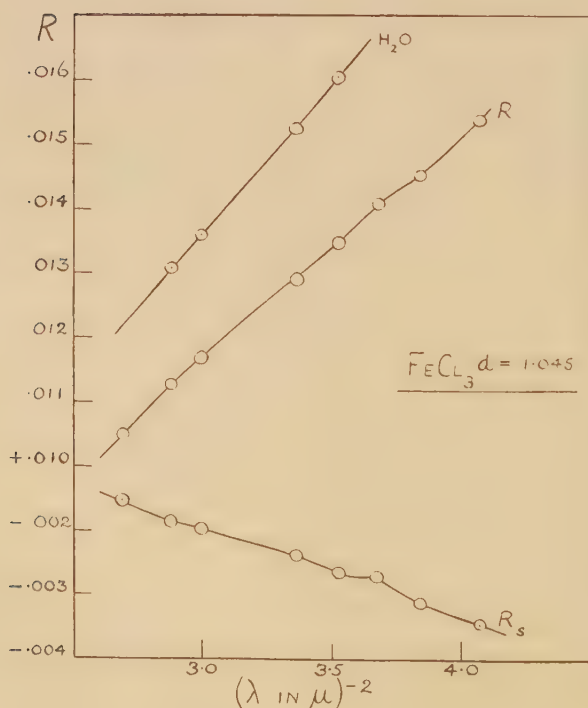


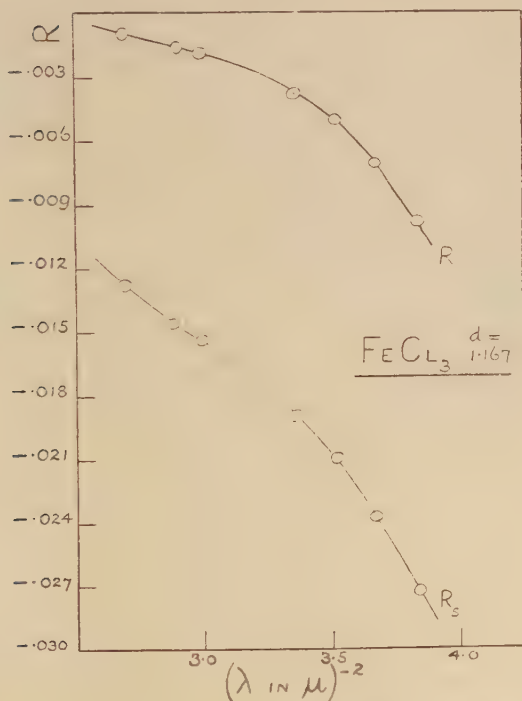


Fig. 4 has been constructed from the following data:—

$$d = 1.167. \quad x = .956.$$

$\lambda$ .	$n$ .	$R$ .	$R'_{10}$ .	$R_s$ .
.6104	1.3904	-.0009	.0119	-.0128
.5893	1.3911	-.0016	.0130	-.0146
.5780	1.3916	-.0019	.0135	-.0154
.5461	1.3933	-.0038	.0152	-.0190
.5330	1.3940	-.0050	.0159	-.0210
.5218	1.3959	-.0071	.0166	-.0237
.5105	1.3969	-.0099	.0174	-.0273

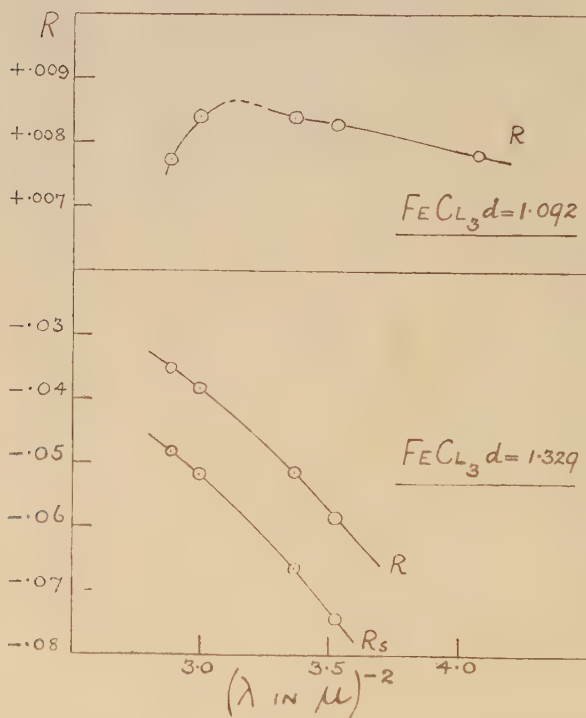
Fig. 4.



A glance at figs. 3, 4, and 5 shows how the rotation of the solution changes from positive to negative with increasing iron content. There is a marked change in the course of the rotary dispersion curve for the solution of density 1.092 in the neighbourhood  $\lambda^{-2} = 3.1$  ( $\lambda = .57 \mu$ ). This is probably due to some dehydration of the  $\text{FeCl}_3$  molecule taking place.

All trace of this process has vanished in the most concentrated solution investigated. The curve for this solution, as far as one can judge from four points, seems regular. The same kind of change happens with potassium ferricyanide, but in this case a smooth curve is obtained with a solution of a very much smaller concentration \*, namely 1.7 per cent.

Fig. 5.



It is very probable that the magnetic rotation of ferric chloride depends largely on its state of electrolytic dissociation. It is well known that aqueous solutions of ferric chloride are strongly acid. Elias † has observed the much stronger rotation produced in solutions of certain rare earths by the addition of small quantities of free acid, and remarks on the new dissociation state (which is more paramagnetic) thereby formed.

\* Roberts, *loc. cit.* Siertsema, *loc. cit.*

† *Ann. der Phys.* xxxv. p. 299 (1911).

Care has been taken with the solutions of density 1·045 and 1·167 to investigate their rotation when freshly made up. In this connexion it may be mentioned that Anderson has recorded the considerable changes in the absorption of some ferric solutions after a period of standing of six weeks.

The following table gives the results of the calculations for  $\lambda_p$  :—

Density.	Pair.	$\lambda_p$ from (1).	$\lambda_p$ from (2).
1·329	5893 }	·406 $\mu$ .	·441 $\mu$
	5461 }		
	5780 }	·403	·441
	5330 }		
1·167	5461 }	·418	·440
	5105 }		
	5330 }	·428	·446
	5105 }		
	5218 }	·427	·447
	5105 }		
1·045	5893 }	·35	·40
	4958 }		
	5461 }	·36	·40
	4958 }		

The values of  $\lambda_p$  derived from (2) are more consistent than those obtained from (1). In the case of the two stronger solutions the agreement between the values of  $\lambda_p$  in the fourth column is good. These values of  $\lambda_p$  are not far removed from  $\lambda_p = \cdot 437 \mu$  obtained with the  $\text{Fe}_2(\text{SO}_4)_3$  solution. We tentatively suggest that the chloride and sulphate solutions have the same magnetic absorption band.

#### *Ferric Ammonium Chloride.*

We have also made some observations on a solution of this double salt. The density of the solution was 1·091 gm./c.c. This solution gave a larger rotation than pure water, which may be explained on the grounds of the positive diamagnetic rotation of the ammonium and chlorine ions overpowering the negative rotation due to the ferric ions. We found that although the rotation of the salt is positive, there is a pronounced change in the rotary dispersion curve at about  $\lambda^{-2} = 3\cdot 1$  ( $\lambda = \cdot 57 \mu$ ) and a less pronounced change in the neighbourhood of  $\lambda^{-2} = 3\cdot 6$  ( $\lambda = \cdot 53$ ). The work on double salts is being continued and we hope to publish the results shortly.

We beg to express our best thanks to Professor L. R. Wilberforce for his kind interest and helpful advice in the course of the experimental work; to Mr. F. C. Guthrie, M.A., for his help with the volumetric analysis; and to Dr. R. A. Morton and Dr. R. W. Ridding for their measurements on the absorption spectra of ferric sulphate and ferric nitrate.

George Holt Physics Laboratory,  
The University of Liverpool.  
August 1926.

---

LXXVII. *Some Problems in the Conduction of Heat.* By  
GEORGE GREEN, D.Sc., *Lecturer in Physics in the Applied  
Physics Department of the University of Glasgow* \*.

MANY of the every-day problems in heat conduction arising in the laboratory involve the transference of heat from one medium to another. Problems of this type are as a rule difficult to solve by the methods usually given in the textbooks, and comparatively little attention has been given to them. It is proposed in the present paper to draw attention to a method specially suited to such problems, and to give one or two of the fundamental solutions required in applying the method. The main idea underlying the method employed is to treat all heat-conduction problems as problems in wave-motion. Instead of building up the solutions we require from instantaneous point sources or doublet sources, we build them up from wave-trains, and in this way the methods and principles employed in the solution of wave-motion problems become available for heat conduction. We accordingly commence by showing how the well-known expressions for the instantaneous point source and doublet source solutions can be obtained by means of wave-trains, and as it is simplest to deal with the case of plane waves, we begin by deriving the solutions corresponding to the instantaneous plane source and doublet source.

The general equation of conduction of heat in a uniform medium may be written in the form

$$\frac{\partial v}{\partial t} = \kappa \nabla^2(v), \quad . \quad . \quad . \quad . \quad . \quad (1)$$

where  $v$  represents the temperature, and  $\kappa$  the diffusivity. There are two solutions of the above equation representing

\* Communicated by the Author.

wave-trains travelling in the direction of  $x$  positive, namely

$$e^{-x\sqrt{\frac{k}{2\kappa}}} \cos \left( kt - x\sqrt{\frac{k}{2\kappa}} \right)$$

and

$$e^{-x\sqrt{\frac{k}{2\kappa}}} \sin \left( kt - x\sqrt{\frac{k}{2\kappa}} \right). \quad . \quad . \quad . \quad . \quad . \quad (2)$$

By changing  $x$  into  $-x$  we obtain the corresponding solutions representing wave-trains travelling from the origin in the direction of  $x$  negative. From these we may obtain any more general solution of the same type by summations or integrations after the manner of Fourier. For example, we might define the temperature conditions at the origin by

$$v(0, t) = \frac{\theta}{\pi} \int_0^\infty dk \cos kt, \quad . \quad . \quad . \quad . \quad . \quad (3)$$

which represents a finite temperature  $\theta$  at the instant  $t=0$  and zero temperature at any later time. The corresponding solution, representing the temperature throughout the positive half of the medium at any time, is given by

$$v = \frac{\theta}{\pi} \int_0^\infty dk e^{-x\sqrt{\frac{k}{2\kappa}}} \cos \left( kt - x\sqrt{\frac{k}{2\kappa}} \right). \quad . \quad . \quad (4)$$

When we add to this the corresponding expression containing only negative wave-trains, we obtain the solution for the temperature produced in the medium by the instantaneous generation of a temperature  $\theta$  at the origin at time  $t=0$ . The solution obviously fulfils the condition that the flow of heat from the origin at each instant in the positive direction is equal to the flow of heat from the origin in the negative direction. We can employ the integral contained in (3) in a similar way to represent initial conditions of heat supply at the origin. Thus if a quantity of heat  $Q$  per unit area of an infinite plane at the origin be instantaneously generated at time  $t=0$ , we have, with  $K$  representing conductivity of the medium,

$$\text{Lt}_{x=0} \left( -K \frac{\partial v}{\partial x} \right) = \frac{Q}{2\pi} \int_0^\infty dk \cos kt. \quad . \quad . \quad . \quad (5)$$

From this we obtain

$$-K \frac{\partial v}{\partial x} = \frac{Q}{2\pi} \int_0^\infty dk e^{-x\sqrt{\frac{k}{2\kappa}}} \cos \left( kt - x\sqrt{\frac{k}{2\kappa}} \right), \quad (6)$$



and also

$$v = \frac{Q\sqrt{2\kappa}}{4K\pi} \int_0^\infty dk \frac{e^{-x\sqrt{\frac{k}{2\kappa}}}}{k^{\frac{1}{2}}} \left\{ \cos\left(kt - x\sqrt{\frac{k}{2\kappa}}\right) + \sin\left(kt - x\sqrt{\frac{k}{2\kappa}}\right) \right\}$$

$$= \frac{Q\sqrt{\kappa}}{2K\pi} \int_0^\infty dk \frac{e^{-x\sqrt{\frac{k}{2\kappa}}}}{k^{\frac{1}{2}}} \cos\left(kt - x\sqrt{\frac{k}{2\kappa}} - \frac{\pi}{4}\right), \quad (7)$$

which, with the addition of the corresponding negative wave-trains, represents the solution for an instantaneous plane source,  $Q$ , half the heat generated being operative in producing wave-trains travelling in the positive direction of  $x$  and the other half in producing wave-trains travelling in the negative direction.

More general solutions corresponding to arbitrary conditions of temperature or heat supply, throughout space and time, can of course be derived from the above solutions by integrations with respect to  $x$  and  $t$ ; but it is obvious that we do not in this way obtain the complete solution of the differential equation of heat conduction. If in (3) and (5) above we replace the cosine by a sine and obtain the corresponding solutions, these solutions represent temperature or heat sources of a different type from those contained in (4) and (7) above. The four solutions referred to are of fundamental importance in heat-conduction problems, but it is impossible to solve all problems by summations of these alone, as we shall see in certain cases discussed below.

We shall now evaluate the integrals contained in (4) and (7), and also the integrals obtained when the cosines in (3) and (5) are replaced by sines. If we put  $\alpha^2 = \frac{x^2}{8\kappa t}$  and make the substitution  $y = k^{\frac{1}{2}}t^{\frac{1}{2}} - \alpha$  we can write equations (4) and (7) in the forms

$$v(x, t) = \frac{2\theta e^{-2\alpha^2}}{\pi t} \int_{-\alpha}^\infty dy (y + \alpha) e^{-2\alpha y} \cos(y^2 - \alpha^2), \quad (8)$$

$$v(x, t) = \frac{Q\sqrt{2\kappa} e^{-2\alpha^2}}{2K\pi\sqrt{t}} \int_{-\alpha}^\infty dy e^{-2\alpha y} \left\{ \cos(y^2 - \alpha^2) + \sin(y^2 - \alpha^2) \right\}, \quad (9)$$

respectively. The values of these integrals can be expressed

in terms of the two integrals which we shall denote by

$$I_c = \int_{-\alpha}^{\infty} dy e^{-2\alpha y} \cos(y^2 - \alpha^2), \quad \text{and} \quad I_s = \int_{-\alpha}^{\infty} dy e^{-2\alpha y} \sin(y^2 - \alpha^2). \quad (10)$$

When these expressions are integrated by parts, and also differentiated with respect to  $\alpha$ , and the results examined, it is found that

$$\frac{dI_c}{d\alpha} = e^{2\alpha^2} \quad \text{and} \quad \frac{dI_s}{d\alpha} = -e^{2\alpha^2}. \quad (11)$$

We find accordingly that

$$I_c + I_s = \sqrt{\frac{\pi}{2}}, \quad \text{and} \quad I_c - I_s = 2 \int_0^{\alpha} d\alpha e^{2\alpha^2}, \quad (12)$$

and it follows that the integrals contained in (4) and (7) have the values given by

$$v(x, t) = \frac{2\theta\alpha e^{-2\alpha^2}}{\pi t} (I_c + I_s) = \frac{\theta x e^{-\frac{x^2}{4\kappa t}}}{2\sqrt{\pi\kappa t^3}}, \quad (13)$$

$$v(x, t) = \frac{Q\sqrt{2\kappa} e^{-2\alpha^2}}{2K\pi\sqrt{t}} (I_c + I_s) = \frac{Q\sqrt{\kappa} e^{-\frac{x^2}{4\kappa t}}}{2K\sqrt{\pi t}}. \quad (14)$$

These solutions are evidently in agreement with that representing an instantaneous doublet and that representing an instantaneous plane source at the origin respectively. When the cosines in (3) and (5) are replaced by sines, the solutions obtained corresponding to (4) and (7) above are respectively

$$\begin{aligned} v(x, t) &= \frac{\theta}{\pi} \int_0^{\infty} dk e^{-k} \sqrt{\frac{k}{2\kappa}} \sin\left(kt - x\sqrt{\frac{k}{2\kappa}}\right) \\ &= \frac{\theta}{\pi t} \{1 - 2\alpha e^{-2\alpha^2} (I_c - I_s)\}, \end{aligned} \quad (15)$$

$$\begin{aligned} v(x, t) &= \frac{Q\sqrt{\kappa}}{2K\pi} \int_0^{\infty} dk e^{-k} \frac{\sqrt{k}}{k^{\frac{3}{2}}} \sin\left(kt - x\sqrt{\frac{k}{2\kappa}} - \frac{\pi}{4}\right) \\ &= \frac{Q\sqrt{2\kappa} e^{-2\alpha^2}}{2K\pi\sqrt{t}} (I_s - I_c). \end{aligned} \quad (16)$$

Any possible solution of the differential equation can be built up by summation or integration from the fundamental wave-trains referred to in (2), according to the usual Fourier method employed in the cases which we have dealt with above. In the case of plane waves it is of fundamental

importance to determine what happens when a wave-train arrives at a boundary at which radiation takes place or at which there is a change in the medium. We shall therefore consider these two problems taking first the case of two different media in contact.

From  $-\infty$  to  $+a$  let  $(K_1, \kappa_1)$  represent conductivity and diffusivity of the medium respectively, and from  $+a$  to  $+\infty$  let  $(K_2, \kappa_2)$  represent the corresponding quantities for medium 2. Assume that a periodic source of the type  $\theta \cos kt$  exists at the origin and that it is required to determine the temperature at any point in either medium. The conditions stated at the origin require the existence of a positive and a negative wave-train in medium 1 represented by

$$\theta e^{-x\sqrt{\frac{k}{2\kappa}}} \cos\left(kt - x\sqrt{\frac{k}{2\kappa}}\right)$$

and

$$\theta e^{x\sqrt{\frac{k}{2\kappa}}} \cos\left(kt + x\sqrt{\frac{k}{2\kappa}}\right) \text{ respectively.} \quad (17)$$

The negative wave-train travels onward without interruption, but the positive wave-train on arrival at the boundary of separation of the two media gives rise to a transmitted wave-train and to a reflected wave-train, in a manner exactly analogous to the transmission and reflexion of a plane wave in the corresponding optical problem. At the boundary of separation the phases of all three wave-trains must be in agreement at any instant; hence we take as our solution

$$v_1 = \theta e^{-x\sqrt{\frac{k}{2\kappa_1}}} \cos\left(kt - x\sqrt{\frac{k}{2\kappa_1}}\right) + A e^{(x-2a)\sqrt{\frac{k}{2\kappa_1}}} \cos\left(kt + (x-2a)\sqrt{\frac{k}{2\kappa_1}}\right). \quad (18)$$

for medium 1 on the positive side of the origin, and for medium 2 we take

$$v_2 = B e^{-(x-a')\sqrt{\frac{k}{2\kappa_2}}} \cos\left(kt - (x-a')\sqrt{\frac{k}{2\kappa_2}}\right) \quad \text{with} \quad a' = a\left(1 - \sqrt{\frac{\kappa_2}{\kappa_1}}\right), \quad (19)$$

where  $A$  and  $B$  are constants to be determined from the conditions to be fulfilled at the boundary  $x=a$ . These

conditions are ;

$$v_1 = v_2; \text{ and } K_1 \frac{\partial v_1}{\partial x} = K_2 \frac{\partial v_2}{\partial x}, \dots \quad (20)$$

and we obtain accordingly the values for A and B given by

$$A = \theta \frac{K_1 \sqrt{\kappa_2} - K_2 \sqrt{\kappa_1}}{K_1 \sqrt{\kappa_2} + K_2 \sqrt{\kappa_1}}; \quad B = \theta \frac{2K_1 \sqrt{\kappa_2}}{K_1 \sqrt{\kappa_2} + K_2 \sqrt{\kappa_1}}. \quad (21)$$

If the problem had been to determine the temperature throughout the two media produced by a periodic supply of heat  $q \cos kt$  at the origin, the solution obtained in a manner similar to that employed above would be given by

$$\begin{aligned} v_1 = & \frac{q}{2K_1} \sqrt{\frac{\kappa_1}{k}} e^{-x\sqrt{\frac{k}{2\kappa_1}}} \cos \left( kt - x\sqrt{\frac{k}{2\kappa_1}} - \frac{\pi}{4} \right) \\ & + \frac{A}{2K_1} \sqrt{\frac{\kappa_1}{k}} e^{-(x-2a)\sqrt{\frac{k}{2\kappa_1}}} \cos \left\{ kt + (x-2a)\sqrt{\frac{k}{2\kappa_1}} - \frac{\pi}{4} \right\}, \\ & \dots \dots \dots (22) \end{aligned}$$

$$\begin{aligned} v_2 = & \frac{B}{2K_2} \sqrt{\frac{\kappa_2}{k}} e^{-(x-a')\sqrt{\frac{k}{2\kappa_2}}} \cos \left\{ kt - (x-a')\sqrt{\frac{k}{2\kappa_2}} - \frac{\pi}{4} \right\}; \\ & a' = a \left( 1 - \sqrt{\frac{\kappa_2}{\kappa_1}} \right), \dots \dots \dots (23) \end{aligned}$$

where A and B have the values already determined, with  $q$  instead of  $\theta$ .

It is worthy of note that in each of these cases the values obtained for A and B are independent of  $k$ . When we integrate the expressions contained in (22) and (23) with respect to  $k$  to obtain the solution representing the effect of an instantaneous generation of a quantity of heat  $q$  at the origin at time  $t=0$ , the integrals appearing are those already evaluated, the solution being

$$v_1 = \frac{q\sqrt{\kappa_1} e^{-\frac{x^2}{4\kappa_1 t}}}{2K_1 \sqrt{\pi t}} + \frac{A\sqrt{\kappa_1} e^{-\frac{(2a-x)^2}{4\kappa_1 t}}}{2K_1 \sqrt{\pi t}}, \dots \dots \dots (24)$$

$$v_2 = \frac{B\sqrt{\kappa_2} e^{-\frac{(x-a')^2}{4\kappa_2 t}}}{2K_2 \sqrt{\pi t}}, \quad a' = a \left( 1 - \sqrt{\frac{\kappa_2}{\kappa_1}} \right). \dots \quad (25)$$

These expressions show that the effect of an instantaneous plane source of heat at the origin at  $t=0$  in medium 1 is the same as if medium 1 extended throughout space, and an instantaneous generation of heat of amount A took place at  $x=2a$  at time  $t=0$  in addition to the heat  $q$  generated at

the origin ; and the effect in medium 2 is the same as that produced by the instantaneous generation of a quantity of heat  $B$  at point  $x=a'$  at  $t=0$  in a uniform medium 2 extending throughout space.

When an instantaneous plane source of heat  $k$  exists at the plane of separation of the two media, we first find the solution corresponding to a periodic supply of heat  $q \cos kt$  at the boundary plane which is taken as origin. The conditions to be fulfilled in this case are

$$v_1 = v_2 : K_1 \frac{\partial v_1}{\partial x} - K_2 \frac{\partial v_2}{\partial x} = q \cos kt. \quad (26)$$

As the wave-train in medium 2 is a positive train and that in medium 1 a negative train, the solution is evidently given by (see (7) above)

$$v_1 = \frac{A \sqrt{\kappa_1} e^{x \sqrt{\frac{k}{2\kappa_1}}}}{2K_1 \sqrt{k}} \cos \left( kt + x \sqrt{\frac{k}{2\kappa_1}} - \frac{\pi}{4} \right), \quad (27)$$

$$v_2 = \frac{B \sqrt{\kappa_2} e^{-x \sqrt{\frac{k}{2\kappa_2}}}}{2K_2 \sqrt{k}} \cos \left( kt - x \sqrt{\frac{k}{2\kappa_2}} - \frac{\pi}{4} \right), \quad (28)$$

and the values of  $A$  and  $B$ , obtained by means of the above conditions, are given by

$$A = q \frac{2K \sqrt{\kappa_2}}{K_1 \sqrt{\kappa_2} + K_2 \sqrt{\kappa_1}}; \quad B = q \frac{2K_2 \sqrt{\kappa_1}}{K_1 \sqrt{\kappa_2} + K_2 \sqrt{\kappa_1}}. \quad (29)$$

The solution for an instantaneous plane source  $q$  at the origin is derived from the above by integration with respect to  $k$  as before. The instantaneous source  $q$  is equivalent to an instantaneous source of amount  $\frac{A}{2}$  supplying heat to medium 1 only, and an instantaneous source of amount  $\frac{B}{2}$  supplying heat to medium 2 only.

Let us return again to the case of two media in contact at the plane  $x=a$ . If the condition to be fulfilled at the origin is that temperature or heat supply is given as a function of the time  $t$ , the required solutions are derived in the usual way from the solutions which we have already obtained by integrations with respect to  $t$ . But it must be kept in mind that the terms represented by the reflected wave-trains, while they are necessary to fulfil the conditions at the boundary of



separation, may violate in turn the conditions to be fulfilled at the origin or at another boundary. In that case additional wave-trains must be introduced in order to fulfil the required conditions at the origin, and thereafter additional terms must be introduced to fulfil the conditions at the boundary of separation of the media  $x=a$ , alternately.

Consider now a uniform medium extending from  $-\infty$  to  $+a$  and let radiation take place at the boundary  $x=a$  into a region kept at temperature zero. As in the previous case we shall take first the wave-trains representing temperature conditions produced in a uniform medium by a periodic heat supply  $q \cos kt$  maintained at the origin, namely

$$\frac{q \sqrt{\kappa} e^{-x \sqrt{\frac{k}{2\kappa}}}}{2K \sqrt{k}} \cos \left( kt - x \sqrt{\frac{k}{2\kappa}} - \frac{\pi}{4} \right)$$

and

$$\frac{q \sqrt{\kappa} e^{x \sqrt{\frac{k}{2\kappa}}}}{2K \sqrt{k}} \cos \left( kt + x \sqrt{\frac{k}{2\kappa}} - \frac{\pi}{4} \right). \quad \dots (30)$$

The negative wave-train proceeds without interruption, but the positive wave-train on arrival at the boundary  $x=a$  again gives rise to a transmitted and to a reflected wave-train. The most general case is that in which the reflected wave-trains belong to both the types which we have referred to in (2) above. Hence we take as the solution giving the temperature within the medium

$$\begin{aligned} v = & \frac{q \sqrt{\kappa} e^{-x \sqrt{\frac{k}{2\kappa}}}}{2K \sqrt{k}} \cos \left( kt - x \sqrt{\frac{k}{2\kappa}} - \frac{\pi}{4} \right) \\ & + \frac{A \sqrt{\kappa} e^{(x-2a) \sqrt{\frac{k}{2\kappa}}}}{2K \sqrt{k}} \cos \left\{ kt + (x-2a) \sqrt{\frac{k}{2\kappa}} - \frac{\pi}{4} \right\} \\ & + \frac{B \sqrt{\kappa} e^{(x-2a) \sqrt{\frac{k}{2\kappa}}}}{2K \sqrt{k}} \sin \left\{ kt + (x-2a) \sqrt{\frac{k}{2\kappa}} - \frac{\pi}{4} \right\}, \\ & \dots \dots (31) \end{aligned}$$

where A and B are constants to be determined by the condition to be fulfilled at the boundary  $x=a$ . From the condition  $-K \frac{\partial v}{\partial x} = hv$  at  $x=a$ , we find that the values

of A and B are given by

$$A = q \frac{K^2 \frac{k}{\kappa} - h^2}{K^2 \frac{k}{\kappa} + 2hK \sqrt{\frac{k}{2\kappa} + h^2}} :$$

$$B = -q \frac{2hK \sqrt{\frac{k}{2\kappa}}}{K^2 \frac{k}{\kappa} + 2hK \sqrt{\frac{k}{2\kappa} + h^2}} . \quad . \quad . \quad (32)$$

The solution corresponding to an instantaneous heat source of amount  $q$  at the origin, at  $t=0$ , follows immediately from the above, being

$$v = \frac{q\sqrt{\kappa} e^{-\frac{x^2}{4\kappa t}}}{2K\sqrt{\pi t}} + \frac{\sqrt{\kappa}}{2K\pi} \int_0^\infty dk \frac{e^{(x-2a)\sqrt{\frac{k}{2\kappa}}}}{k^{\frac{1}{2}}} \left[ A \cos \left\{ kt + (x-2a) \sqrt{\frac{k}{2\kappa} - \frac{\pi}{4}} \right\} + B \sin \left\{ kt + (x-2a) \sqrt{\frac{k}{2\kappa} - \frac{\pi}{4}} \right\} \right] . \quad (33)$$

The solutions corresponding to a temperature  $\theta$  instantaneously generated at the origin can be obtained in a similar manner :

$$v = \frac{\theta x e^{-\frac{x^2}{4\kappa t}}}{2\sqrt{\pi \kappa t^3}} + \frac{1}{\pi} \int_0^\infty dk e^{(x-2a)\sqrt{\frac{k}{2\kappa}}} \left[ A \cos \left\{ kt + (x-2a) \sqrt{\frac{k}{2\kappa}} \right\} + B \sin \left\{ kt + (x-2a) \sqrt{\frac{k}{2\kappa}} \right\} \right] , \quad . \quad . \quad (34)$$

$\theta$  replacing  $q$  in the values of A and B given by (32).

These results cannot now be interpreted in terms of the ordinary plane source or plane doublet source solutions. The terms containing A and B represent, however, sources of a special type at the plane  $x=2a$ . Approximate evaluations of the integrals representing these sources can always be obtained by making use of the principle of stationary-phase or group-velocity. In the integrals containing A and B the phase of the periodic term is stationary at the value of  $k$  given by  $k^{\frac{1}{2}} = \frac{(2a-x)}{2\sqrt{2\kappa t}}$ , and according to the principle we may insert this value of  $k$  in the amplitude terms A and B.

Equation (33) then may be written in the form

$$v = \frac{q\sqrt{\kappa}e^{-\frac{x^2}{4\kappa t}}}{2K\sqrt{\pi t}} + \frac{A\sqrt{\kappa}}{2K\pi} \int_0^\infty dk \frac{e^{\frac{(x-2a)\sqrt{k}}{2\kappa}}}{k^{\frac{1}{2}}} \cos \left\{ kt + (x-2a)\sqrt{\frac{k}{2\kappa}} - \frac{\pi}{4} \right\} \\ + \frac{B\sqrt{\kappa}}{2K\pi} \int_0^\infty dk \frac{e^{\frac{(x-2a)\sqrt{k}}{2\kappa}}}{k^{\frac{1}{2}}} \sin \left\{ kt + (x-2a)\sqrt{\frac{k}{2\kappa}} - \frac{\pi}{4} \right\}, \quad \dots \quad (35)$$

in which the integrals represent sources of the types referred to on pp. 785-787, for which the values are given in (13), (14) and (15), (16).

When the medium does not extend to  $-\infty$  the above solution is incomplete. Each of the reflected wave-trains on arrival at a boundary gives rise to two wave-trains similar to the trains represented by the A and B terms in (31). The complete solution accordingly consists of a succession of terms, similar to an infinite system of images in each boundary. In the same way if the conditions given at the origin determine the temperature there as a function of the time, each wave-train reflected at the boundary  $x=a$  violates this condition and additional terms must be introduced to maintain the required conditions at the origin and at the boundary  $x=a$  alternately.

Several of the problems dealt with above have been solved by special methods\*, the solutions obtained by different methods being identical in form. Solutions applicable to the case of a bar which loses heat by radiation at both ends are also well known†, but they differ completely in form from the corresponding solutions obtained by the method employed in the present paper. It would be interesting to demonstrate the equivalence of the solutions, but this must meantime be deferred. In applying the present method, in all cases where double integrations occur alternative solutions can frequently be obtained by reversing the order of the integrations. Problems relating to heat conduction in bars exposed to loss of heat at the surface must also be left to a later paper.

The method of solving problems by means of wave-trains which we have employed in the case of plane waves is equally applicable to cylindrical and spherical waves. In

\* See Carslaw's 'The Conduction of Heat,' § 77, where original papers are referred to.

† *Ibid.* § 36.

each case there are two positive wave-trains corresponding to the trains given in (2) and two negative wave-trains of the same type. The discussion of fundamental solutions in terms of cylindrical wave-trains would take up considerable space and will therefore be dealt with in a later paper, but the fundamental solutions for spherical waves resemble closely those already dealt with and can be shortly stated. The two wave-trains travelling outwards from the origin 0 are given by

$$e^{-r\sqrt{\frac{k}{2\kappa}}} \frac{1}{r} \cos\left(kt - r\sqrt{\frac{k}{2\kappa}}\right) \quad \text{and} \quad e^{-r\sqrt{\frac{k}{2\kappa}}} \frac{1}{r} \sin\left(kt - r\sqrt{\frac{k}{2\kappa}}\right) \quad \dots \quad (36)$$

and the corresponding negative wave-trains are given by

$$e^{r\sqrt{\frac{k}{2\kappa}}} \frac{1}{r} \cos\left(kt + r\sqrt{\frac{k}{2\kappa}}\right) \quad \text{and} \quad e^{r\sqrt{\frac{k}{2\kappa}}} \frac{1}{r} \sin\left(kt + r\sqrt{\frac{k}{2\kappa}}\right) \quad \dots \quad (37)$$

Suppose that at the origin there is a periodic heat-supply  $q \cos kt$ , the solution which we require must satisfy

$$\text{Lt}_{r=0} \left( -4\pi r^2 K \frac{\partial v}{\partial r} \right) = q \cos kt. \quad \dots \quad (38)$$

Hence we obtain

$$\text{Lt}_{r=0} \left( -4\pi r^2 K \frac{\partial v}{\partial r} \right) = \text{Lt}_{r=0} \left\{ q e^{-r\sqrt{\frac{k}{2\kappa}}} \cos\left(kt - r\sqrt{\frac{k}{2\kappa}}\right) \right\}$$

and

$$v = \frac{q e^{-r\sqrt{\frac{k}{2\kappa}}}}{4\pi K r} \cos\left(kt - r\sqrt{\frac{k}{2\kappa}}\right), \quad \dots \quad (39)$$

and the solution corresponding to the instantaneous generation of a quantity of heat  $q$  at the origin at time  $t=0$  is given by

$$v = \frac{q}{4\pi^2 K r} \int_0^\infty dk e^{-r\sqrt{\frac{k}{2\kappa}}} \cos\left(kt - r\sqrt{\frac{k}{2\kappa}}\right) = \frac{q e^{-\frac{r^2}{4\kappa t}}}{8K \sqrt{\pi^3 \kappa t^3}} \quad \dots \quad (40)$$

Similarly if the periodic heat-supply at the origin be  $q \sin kt$ , we obtain

$$\begin{aligned} v &= \frac{q}{4\pi^2 K r} \int_0^\infty dk e^{-r\sqrt{\frac{k}{2\kappa}}} \sin\left(kt - r\sqrt{\frac{k}{2\kappa}}\right) \\ &= \frac{q}{4\pi^2 K r t} \{1 - 2\alpha e^{-2\alpha^2} (I_c - I_s)\}, \quad (41) \end{aligned}$$

which represents a point source of a different type from that given by (40) above.

If a periodic supply of heat be maintained at the spherical surface  $r=r_1$ , the supply per unit area being  $q \cos kt$ , part of the heat supplied will give rise to waves travelling inwards from the surface and part to waves travelling outwards from the surface. Thus two separate solutions are required,  $v_i$  for the region within the sphere  $r=r_1$ , and  $v_0$  for the region without the sphere, respectively. Consider first the conditions to be fulfilled at the surface  $r=r_1$  only. These conditions are

$$v = v_0 : \text{Lt}_{r=r_1} -4\pi r^2 K \left( \frac{\partial v_0}{\partial r} - \frac{\partial v_i}{\partial r} \right) = 4\pi r_1^2 q \cos kt, \quad (42)$$

and they are fulfilled by the two wave-trains

$$v_i = \frac{qr_1 \sqrt{\kappa}}{2Kr \sqrt{k}} e^{-\frac{(r_1-r)\sqrt{k}}{2\kappa}} \cos \left( kt - (r_1-r) \sqrt{\frac{k}{2\kappa}} - \frac{\pi}{4} \right), \quad (43)$$

$$v_0 = \frac{qr_1 \sqrt{\kappa}}{2Kr \sqrt{k}} e^{-\frac{(r-r_1)\sqrt{k}}{2\kappa}} \cos \left\{ kt - (r-r_1) \sqrt{\frac{k}{2\kappa}} - \frac{\pi}{4} \right\}, \quad (44)$$

each of which supplies the quantity of heat  $\frac{q \cos kt}{2}$  per unit area in its own direction. But the negative train, on arrival at the origin, gives rise to an infinite temperature there. It represents in fact a source or sink of heat at the origin, whereas the only source postulated is at the surface  $r=r_1$ . The negative train in (43) above must therefore be considered to pass through the origin and thereafter to become a positive train represented by

$$- \frac{qr_1 \sqrt{\kappa}}{2Kr \sqrt{k}} e^{-(r+r_1)\sqrt{\frac{k}{2\kappa}}} \cos \left\{ kt - (r+r_1) \sqrt{\frac{k}{2\kappa}} - \frac{\pi}{4} \right\}. \quad (45)$$

This train must be added to both  $v_i$  and  $v_0$ , and the complete solution representing a periodic source  $q \cos kt$  at the surface  $r=r_1$  is

$$v_i = \frac{qr_1 \sqrt{\kappa}}{2Kr \sqrt{k}} \left[ e^{-\frac{(r_1-r)\sqrt{k}}{2\kappa}} \cos \left\{ kt - (r_1-r) \sqrt{\frac{k}{2\kappa}} - \frac{\pi}{4} \right\} - e^{-\frac{(r_1+r)\sqrt{k}}{2\kappa}} \cos \left\{ kt - (r_1+r) \sqrt{\frac{k}{2\kappa}} - \frac{\pi}{4} \right\} \right], \quad (46)$$

$$v_0 = \frac{qr_1 \sqrt{\kappa}}{2Kr \sqrt{k}} \left[ e^{-\frac{(r-r_1)\sqrt{k}}{2\kappa}} \cos \left\{ kt - (r-r_1) \sqrt{\frac{k}{2\kappa}} - \frac{\pi}{4} \right\} - e^{-\frac{(r_1+r)\sqrt{k}}{2\kappa}} \cos \left\{ kt - (r_1+r) \sqrt{\frac{k}{2\kappa}} - \frac{\pi}{4} \right\} \right]. \quad (47)$$



Similar solutions hold for a source supplying  $q \sin kt$  per unit area at  $r=r_1$ .

If the spherical surface  $r=r_1$  is maintained at the temperature  $\theta \cos kt$ , the conditions to be fulfilled at the surface  $r_1$  are now

$$v_i = v_0 = \theta \cos kt; \quad \frac{\partial v_i}{\partial x} + \frac{\partial v_0}{\partial x} = 0 \quad . \quad . \quad . \quad . \quad (48)$$

The latter equation expresses the condition that the flow of heat from the surface outwards is equal to the flow of heat from the surface inwards. Taking first the condition  $v_i = v_0 = \theta \cos kt$ , we choose the two wave-trains represented by

$$v_i = \theta \frac{r_1}{r} e^{-(r_1-r)\sqrt{\frac{k}{2\kappa}}} \cos \left\{ kt - (r_1-r)\sqrt{\frac{k}{2\kappa}} \right\}, \quad (49)$$

$$v_0 = \theta \frac{r_1}{r} e^{-(r-r_1)\sqrt{\frac{k}{2\kappa}}} \cos \left\{ kt - (r-r_1)\sqrt{\frac{k}{2\kappa}} \right\}, \quad (50)$$

of which  $v_i$  represents a wave-train travelling inwards from the surface  $r=r_1$  and  $v_0$  represents a wave-train travelling outwards from the surface  $r=r_1$ . These terms do not, however, fulfil the condition with reference to flow of heat inwards and outwards from the surface  $r=r_1$ . To fulfil the second condition stated above, without violating the first, we require to add an inward travelling wave-train to  $v_i$  and to deduct the corresponding outward travelling wave-train from  $v_0$ . In this way the surface  $r=r_1$  experiences an increase of temperature on one side and an equal decrease of temperature on the other, the net result being a zero change of temperature and a change in the gradients sufficient to secure the fulfilment of the second condition. The conditions at the surface  $r=r_1$  are all fulfilled by the trains

$$v_i = \theta \frac{r_1}{r} e^{-(r_1-r)\sqrt{\frac{k}{2\kappa}}} \cos \left\{ kt - (r_1-r)\sqrt{\frac{k}{2\kappa}} \right\} \\ + \theta \frac{\sqrt{\kappa}}{r\sqrt{k}} e^{-(r_1-r)\sqrt{\frac{k}{2\kappa}}} \cos \left\{ kt - (r_1-r)\sqrt{\frac{k}{2\kappa}} - \frac{\pi}{4} \right\}, \quad (51)$$

$$v_0 = \theta \frac{r_1}{r} e^{-(r-r_1)\sqrt{\frac{k}{2\kappa}}} \cos \left\{ kt - (r-r_1)\sqrt{\frac{k}{2\kappa}} \right\} \\ - \theta \frac{\sqrt{\kappa}}{r\sqrt{k}} e^{-(r-r_1)\sqrt{\frac{k}{2\kappa}}} \cos \left\{ kt - (r-r_1)\sqrt{\frac{k}{2\kappa}} - \frac{\pi}{4} \right\}. \quad (52)$$

Just as in the case previously discussed the two negative wave-trains after passing through the origin become positive wave-trains, so that to obtain the complete solution for the space within the sphere  $r=r_1$  we have to add to  $v_i$  the terms

$$-\theta \frac{r_1}{r} e^{-(r_1+r)\sqrt{\frac{k}{2\kappa}}} \cos \left\{ kt - (r_1+r)\sqrt{\frac{k}{2\kappa}} \right\} \\ - \theta \frac{\sqrt{\kappa}}{r\sqrt{k}} e^{-(r_1+r)\sqrt{\frac{k}{2\kappa}}} \cos \left\{ kt - (r_1+r)\sqrt{\frac{k}{2\kappa}} - \frac{\pi}{4} \right\}. \quad (53)$$

These two positive wave-trains in turn violate the conditions stated above for the surface  $r=r_1$ , and we have therefore to add to  $v_0$  the corresponding terms, namely,

$$\theta \frac{r_1}{r} e^{-(r+r_1)\sqrt{\frac{k}{2\kappa}}} \cos \left\{ kt - (r+r_1)\sqrt{\frac{k}{2\kappa}} \right\} \\ + \theta \frac{\sqrt{\kappa}}{r\sqrt{k}} e^{-(r+r_1)\sqrt{\frac{k}{2\kappa}}} \cos \left\{ kt - (r+r_1)\sqrt{\frac{k}{2\kappa}} - \frac{\pi}{4} \right\}. \quad (54)$$

Thus the four terms contained in  $v_i$  and the four contained in  $v_0$  are accounted for.

If the condition to be fulfilled is that the origin is maintained at the temperature  $\theta \cos kt$  the solution contains one negative train which, on passing through the origin, gives rise to the corresponding positive train. It is

$$v = \frac{\sqrt{\kappa}}{\sqrt{2kr}} \left\{ e^{r\sqrt{\frac{k}{2\kappa}}} \cos \left( kt + r\sqrt{\frac{k}{2\kappa}} \right) \right. \\ \left. - e^{-r\sqrt{\frac{k}{2\kappa}}} \cos \left( kt - r\sqrt{\frac{k}{2\kappa}} \right) \right\}. \quad (55)$$

If at the surface  $r=r_1$  there is an instantaneous supply of heat of amount  $q$  per unit area, the solution is to be obtained by integrating with respect to  $k$  the terms contained in (46) and (47) as before, the result obtained being

$$v_i = \frac{qr_1\sqrt{\kappa}}{2Kr\sqrt{\pi t}} \left[ e^{-\frac{(r_1-r)^2}{4\kappa t}} - e^{-\frac{(r+r_1)^2}{4\kappa t}} \right], \quad \dots \quad (56)$$

$$v_0 = \frac{qr_1\sqrt{\kappa}}{2Kr\sqrt{\pi t}} \left[ e^{-\frac{(r-r_1)^2}{4\kappa t}} - e^{-\frac{(r+r_1)^2}{4\kappa t}} \right], \quad \dots \quad (57)$$

in agreement with the well-known solution for a spherical surface source.

If at the surface  $r=r_1$  the temperature is suddenly brought to  $\theta$  at instant  $t=0$ , the solution obtained by integrating the four terms given for  $v_i$  in (51) and (53), and the four terms for  $v_0$  given in (52) and (54) with respect to  $k$ , is

$$v_i = \frac{\theta \sqrt{\kappa}}{r \sqrt{\pi t}} \left[ e^{-\frac{(r_1-r)^2}{4\kappa t}} - e^{-\frac{(r_1+r)^2}{4\kappa t}} \right] + \frac{\theta r_1(r_1-r)}{2r \sqrt{\pi \kappa t^3}} e^{-\frac{(r_1-r)^2}{4\kappa t}} - \frac{\theta r_1(r_1+r)}{2r \sqrt{\pi \kappa t^3}} e^{-\frac{(r_1+r)^2}{4\kappa t}}, \quad (58)$$

$$v_0 = -\frac{\theta \sqrt{\kappa}}{r \sqrt{\pi t}} \left[ e^{-\frac{(r-r_1)^2}{4\kappa t}} - e^{-\frac{(r+r_1)^2}{4\kappa t}} \right] + \frac{\theta r_1(r-r_1)}{2r \sqrt{\pi \kappa t^3}} e^{-\frac{(r-r_1)^2}{4\kappa t}} + \frac{\theta r_1(r+r_1)}{2r \sqrt{\pi \kappa t^3}} e^{-\frac{(r+r_1)^2}{4\kappa t}}. \quad (59)$$

This again is in agreement with the well-known spherical doublet source solution.

In all the above cases the fundamental condition involves  $\cos kt$ , and a group of similar solutions can be obtained when the cosine is replaced by a sine. All the above solutions refer to a uniform medium.

Suppose now that medium 1 defined by the values  $K_1, \kappa_1$  for conductivity and diffusivity respectively occupies the sphere of radius  $r=a$  and that medium 2 defined by the values  $K_2, \kappa_2$  occupies the volume outside the surface  $r=a$ . The fundamental problem which arises is to determine the reflected and transmitted wave-trains produced when a positive wave-train arrives at the boundary  $r=a$  of mediums 1 and 2. If all heat and temperature sources are within medium 1, only positive wave-trains fall to be considered. As an example we may accordingly consider the case of a periodic heat source  $q \cos kt$  situated at the centre of medium 1. This accordingly requires the wave-train given by equation (39) starting from the origin. When this train arrives at the surface  $r=a$  reflected and transmitted wave-trains are produced, and the most general case which can arise is that in which the reflected and transmitted wave-trains are of both the types referred to in (36). The phases of all wave-trains of the same type must be in agreement at the boundary, hence to fulfil the conditions at the boundary

we take

$$v_1 = \frac{qe^{-r\sqrt{\frac{k}{2\kappa_1}}}}{4\pi K_1 r} \cos \left( kt - r\sqrt{\frac{k}{2\kappa_1}} \right) + \frac{Ae^{\frac{(r-2a)\sqrt{\frac{k}{2\kappa_1}}}}{4\pi K_1 r}} \cos \left\{ kt + (r-2a)\sqrt{\frac{k}{2\kappa_1}} \right\} + \frac{Be^{\frac{(r-2a)\sqrt{\frac{k}{2\kappa_1}}}}{4\pi K_1 r}} \sin \left\{ kt + (r-2a)\sqrt{\frac{k}{2\kappa_1}} \right\}, \quad (60)$$

$$v_2 = \frac{Ce^{-\frac{(r-a')\sqrt{\frac{k}{2\kappa_2}}}}{4\pi K_2 r}} \cos \left\{ kt - (r-a')\sqrt{\frac{k}{2\kappa_2}} \right\} + \frac{De^{-\frac{(r-a')\sqrt{\frac{k}{2\kappa_2}}}}{4\pi K_2 r}} \sin \left\{ kt - (r-a')\sqrt{\frac{k}{2\kappa_2}} \right\}, \quad (61)$$

with  $a' = a \left( 1 - \sqrt{\frac{\kappa_2}{\kappa_1}} \right),$

where the constants A, B, C, D, are to be determined from

$$v_1 = v_2; \quad \text{and} \quad K_1 \frac{\partial v_1}{\partial r} = K_2 \frac{\partial v_2}{\partial r}; \quad \text{at } r = a. \quad (62)$$

The values of these constants are found to be

$$A = q \left[ a^2 \left( K_1^2 \frac{k}{\kappa_1} - K_2^2 \frac{k}{\kappa_2} \right) - (K_1 - K_2)^2 + 2aK_2(K_1 - K_2)\sqrt{\frac{k}{2\kappa_2}} \right] / \Delta,$$

$$B = q \cdot \left( 2aK_1(K_1 - K_2)\sqrt{\frac{k}{2\kappa_1}} \right) / \Delta,$$

$$C = q \left[ 2a^2K_1K_2\frac{k}{\kappa_1} + 2a^2K_2^2\sqrt{\frac{k^2}{\kappa_1\kappa_2}} - 2aK_2(K_1 - K_2)\sqrt{\frac{k}{2\kappa_1}} \right] / \Delta,$$

$$D = \frac{K_2}{K_1} B,$$

where

$$\Delta = \left[ 2a^2 \left( K_1\sqrt{\frac{k}{2\kappa_1}} + K_2\sqrt{\frac{k}{2\kappa_2}} \right)^2 + (K_1 - K_2)^2 - 2a(K_1 - K_2) \left( K_1\sqrt{\frac{k}{2\kappa_1}} + K_2\sqrt{\frac{k}{2\kappa_2}} \right) \right]. \quad (63)$$

Each of the negative wave-trains represented by the A and B terms in (60) above passes through the origin and thereafter becomes a positive train. We have accordingly to add to  $v_1$  the two terms

$$-\frac{Ae^{-\frac{(r+2a)\sqrt{\frac{k}{2\kappa_1}}}{4\pi K_1 r}}}{4\pi K_1 r} \cos \left\{ kt - (r+2a)\sqrt{\frac{k}{2\kappa_1}} \right\} \\ - \frac{Be^{-\frac{(r+2a)\sqrt{\frac{k}{2\kappa_1}}}{4\pi K_1 r}}}{4\pi K_1 r} \sin \left\{ kt - (r+2a)\sqrt{\frac{k}{2\kappa_1}} \right\}. \quad (6\pm)$$

Each of these in turn, on arrival at the boundary  $r=a$ , gives rise to reflected and transmitted wave-trains similar to the reflected and transmitted wave-trains introduced by the original positive train from the origin. The complete solution of the problem therefore consists of an infinite series of terms introduced to fulfil conditions at the boundary  $r=a$  and at the origin alternately.

The case of an inner sphere initially at a uniform temperature will be discussed fully later. All the numerous problems relating to spherical distribution of heat or temperature sources, or to surfaces kept at special temperatures varying with the time, involving the transference of heat from one medium to another, either by conduction of heat or by radiation according to any specified law, can evidently be solved by the method which we have employed in the above problem. The problems which we have dealt with above are given mainly to illustrate the idea that all problems of heat conduction can be solved by treating each problem as a problem in wave-motion. The method of procedure is then the same as in the corresponding optical problem. The application of the above method to important problems of practical interest remains to be made. In this connexion it is of considerable interest to obtain the complete theory of certain convenient experimental methods\* of determining the conductivity of solids and liquids, which are in common use in the laboratory but of which no adequate theory has been given. This may be taken up at a later time. In addition it should be mentioned that the idea that heat conduction and all other forms of diffusion form part of the larger subject of wave-motion may require also to be investigated from the point of view of the rate of transference of energy by waves across any plane in the medium perpendicular to the wave-front and its relation to frequency of the wave-trains which predominate at the plane considered, or even more generally.

\* Methods based on that described by J. H. Gray in Proc. Roy. Soc. London, 1894, have been in use in the laboratory here for some time.



# LXXVIII. *Electrical Filters.*

By A. B. MORICE, *B.Sc.(Eng.), A.M.I.E.E.\**

## SYNOPSIS.

Introduction.

Definition of an electrical filter.

Arrangement and properties of two general types of electrical filter, viz. :—

(a) Double “band-pass” wave filter (Type I.).

(b) “Band-elimination” wave filter (Type II.).

Methods by which Type I. can be changed to a single “band-pass” filter and by which Type II. can be altered to a filter having only one critical frequency.

Properties and computed performance of three types of electrical filter having a single critical frequency, viz. :—

(a) “High-pass” filter (Type III.).

(b) “Low-pass” filter (Type IV.).

(c) Mutual inductance filter (Type V.).

Design and computed performance of an electrical filter to cut out frequencies below a specified value and to operate between input and output terminal apparatus of given impedance.

Some actual applications of electrical filters in telegraph and telephone engineering, as follows :—

(a) Composited working.

(b) Telephonic repeaters.

(c) Thermionic valve oscillator for generating currents of audio-frequency.

(d) Alternating current multiplex telegraphy.

(e) Carrier wave multiplex telephony.

(f) Radio telephony.

(g) Miscellaneous.

Conclusion.

## INTRODUCTION.

IN the different classes of service which have to be provided for by the telegraph and telephone engineer of to-day, the electrical currents employed have a very wide range of frequency. For instance, if reversals are sent by a double-current telegraph set at a speed of 25 words per minute, the fundamental frequency of the current alternations is 10 cycles per second; again, if wireless signals are transmitted through the æther the frequency of the current may be of the order of  $10^6$  cycles per second. Almost all frequencies between these two limits are used in present-day systems of communication by electrical energy.

\* Communicated by the Author. Extracted from a paper given before the Institution of Post Office Electrical Engineers.

*Phil. Mag.* S. 7. Vol. 3. No. 16. *Suppl. April 1927.* 3 F

The efficient utilization of electrical currents having such a large frequency range has presented many research problems for solution. One of these problems was the control of the range of frequency of the currents transmitted in a circuit for any specific purpose. This problem has been tackled successfully by the use of electrical filters.

In view of the increasing importance of electrical filters in connexion with wireless telegraphy and telephony, multiplex high-frequency wire telephony, multiplex alternating-current telegraphy, composited telegraphy and telephony, telephonic repeaters, and also alternating-current measurements, this paper is presented in the hope that a description of their properties and applications may be both interesting and useful.

It is proposed to deal with the subject of electrical filters under the following headings:—

- (A) Definition of an electrical filter.
- (B) Two general types of electrical filter and their properties.
- (C) Three particular types of electrical filter which have been usefully employed, with formulæ for their design.
- (D) Design and computed performance of an electrical filter to cut out frequencies below a specified value and to operate between input and output terminal apparatus of given impedance.
- (E) Some actual applications of electrical filters in telegraph and telephone engineering.
- (F) Conclusion.

#### (A) DEFINITION OF AN ELECTRICAL FILTER.

An electrical filter is an artificial circuit which permits of the transmission of sine-wave voltages and currents of predetermined frequencies with small or negligible attenuation, whilst at the same time suppressing sine-wave voltages and currents of other predetermined frequencies applied to the circuit in the same way. Such a filter can be generally made up of capacity and inductance, the magnitude and arrangement of these being designed in accordance with the principles given in this paper.

#### (B) TWO GENERAL TYPES OF ELECTRICAL FILTER AND THEIR PROPERTIES.

Having defined an electrical filter, we will next proceed to deal with two general types which may be employed and to discuss their properties.

Type I. is shown in fig. 1 (T circuit) and in fig. 2 ( $\pi$  circuit). In this type the impedances in series with the line are composed of inductance and capacity in series, and the impedances shunting the line are composed of inductance and capacity in parallel. Assuming that the impedances

Fig. 1.

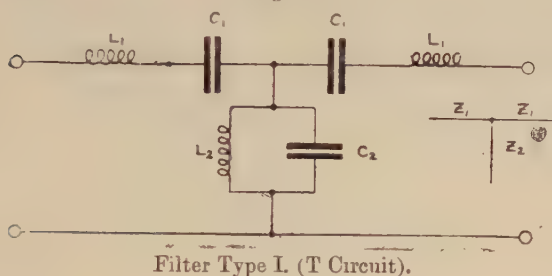
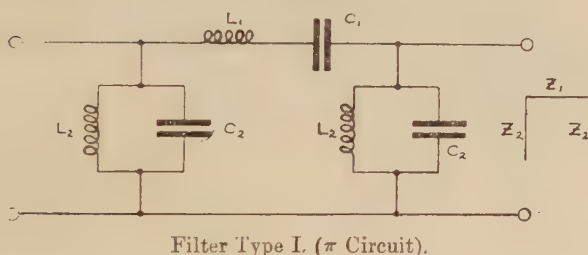
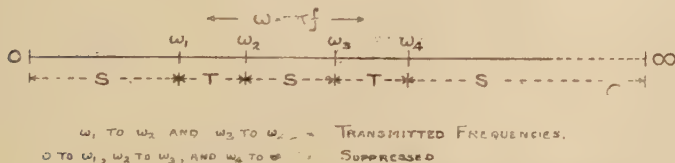


Fig. 2.



are  $Z_1$  and  $Z_2$ , as shown in figs. 1 and 2, that the inductances are resistanceless, and that the condensers have zero leakage, then this type of filter will transmit two bands of frequency without attenuation and suppress all other frequencies, as shown in fig. 3.

Fig. 3.



Transmitted and Suppressed Frequency Bands with Filter Type I.  
(T or  $\pi$  Circuit).

The four critical angular velocities,  $\omega_1$ ,  $\omega_2$ ,  $\omega_3$ , and  $\omega_4$ ,  
3 F 2

which have the same values for the T and the  $\pi$  circuit, are given by the solution of the equations :

$$\frac{Z_1}{Z_2} = 0, \dots \dots \dots (1)$$

$$\frac{Z_1}{Z_2} + 2 = 0. \dots \dots \dots (2)$$

The characteristic impedances  $Z_0$  of the two circuits are :

$$\text{T circuit} \quad Z_0 = \sqrt{Z_1^2 + 2Z_1Z_2}, \dots \dots \dots (3)$$

$$\pi \text{ circuit} \quad Z_0 = \sqrt{\frac{Z_1Z_2^2}{Z_1 + 2Z_2}} \dots \dots \dots (4)$$

The four critical angular velocities\* are related as follows :—

$$\frac{\omega_1}{\omega_2} = \frac{\omega_3}{\omega_4}, \dots \dots \dots (5)$$

and their values are worked out in Appendix I.

Filter Type I. is thus a double “band-pass” wave filter, and there are, apparently, seven ways of reducing it to a single “band-pass” wave filter, namely :—

- (a) If  $L_1C_1 = L_2C_2$ , then  $\omega_2 = \omega_3$  and the two bands become confluent.
- (b) If  $L_1 = 0$ , then one band is relegated to infinity.
- (c) If  $C_2 = 0$ , then the other band is relegated to infinity.
- (d) If  $C_1 = \infty$  (*i. e.*  $C_1$  short-circuited), one band is relegated to zero.
- (e) If  $L_2 = \infty$  (*i. e.*  $L_2$  disconnected), the other band is relegated to zero.
- (f) If  $L_1 = C_2 = 0$ , all frequencies above a specified value are transmitted. (“High-pass” filter.)
- (g) If  $L_2 = C_1 = \infty$ , all frequencies below a specified value are transmitted. (“Low-pass” filter.)

It will be seen that a single-band electrical filter can also be obtained by placing two filters of Type I. in series, in one of which condition (f) is satisfied and in the other of which condition (g) is satisfied. With this arrangement the resultant circuit is either a “band-pass” or a “band-elimination” filter, according as the critical frequency of the filter Type I. (g) is higher or lower than the critical frequency of the filter Type I. (f). The range of the band

\* Angular Velocity =  $2\pi \times$  Frequency.

in each case is the difference between these two critical frequencies.

Filter Type II., which may be termed a "band-elimination" wave filter, is shown in fig. 4 (T circuit) and in fig. 5

Fig. 4.

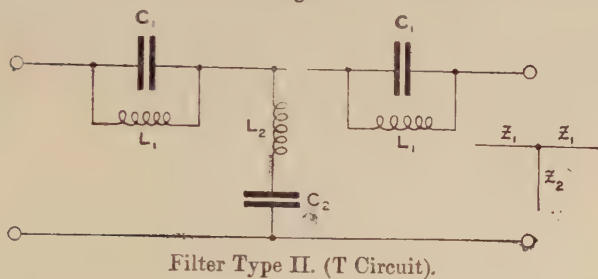
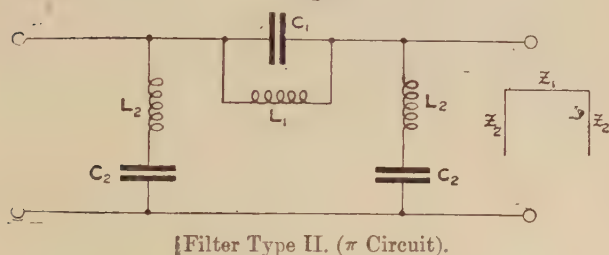
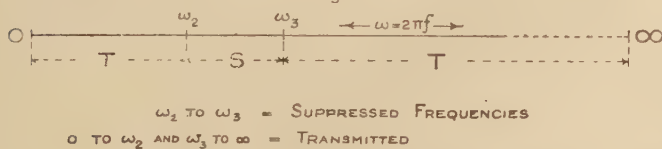


Fig. 5.



( $\pi$  circuit). In this type the impedances in series with the line are composed of inductance and capacity in parallel, and the impedances shunting the line are composed of inductance and capacity in series. Assuming that the impedances are  $Z_1$  and  $Z_2$ , as shown in figs. 4 and 5, that the inductances are resistanceless, and that the condensers have no leakance, then this type of filter will transmit frequencies between

Fig. 6.



Transmitted and Suppressed Frequency Bands with Filter Type II.  
(T or  $\pi$  Circuit).

0 and  $\omega_2$  and between  $\omega_3$  and  $\infty$  as shown in fig. 6, and will suppress the band of frequencies between  $\omega_2$  and  $\omega_3$ . The



critical frequencies  $\omega_2$  and  $\omega_3$  for the filters shown in figs. 4 and 5 are worked out in Appendix II., being given by the solution of equations (1) and (2), and the characteristic impedances of the T and  $\pi$  circuits are given by formulæ (3) and (4) respectively.

This type of filter can be reduced to one having only one critical frequency in four different ways, namely :—

- (a) If  $C_1=0$  or  $L_2=0$ , the filter suppresses all frequencies above a specified value.
- (b) If  $C_2=\infty$  or  $L_1=\infty$ , the filter suppresses all frequencies below a specified value.

It should be pointed out that the properties of these two types of electrical filter only apply when an infinite number of sections, similar to those shown, are connected in series, or, if a finite number of sections is used, when the last section is closed through the characteristic impedance of the filter. This latter impedance is that of a filter containing an infinite number of sections, and when joined at the end of a finite number of filter sections it forms a non-reflective terminal impedance. And further, the suppression of the frequency bands by a filter of either Type I. or II. is only perfect if the inductances and condensers used do not dissipate energy. The effect of resistance in the coils and of leakage in the condensers is to make the suppression and transmission of the frequency bands more or less imperfect; an actual filter will approximate to the ideal by using coils and condensers in which the ratio  $\frac{\text{Resistance}}{\text{Reactance}}$  is kept small. The critical frequencies of the actual filter will, however, be the same as that of the ideal filter.

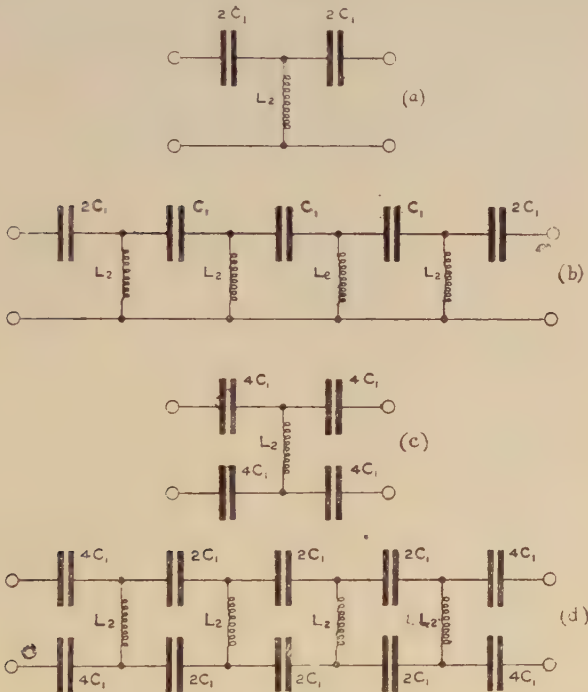
### (C) THREE PARTICULAR TYPES OF ELECTRICAL FILTER WHICH HAVE BEEN USEFULLY EMPLOYED, WITH FORMULÆ FOR THEIR DESIGN.

Having discussed two general types of electrical filter, we will next proceed to deal with three particular types which, for convenience, have been called Types III., IV., and V., and are derived from Types I. and II.

Type III. (T circuit) is shown in fig. 7 (a), (b), (c), and (d). It consists of capacities as series elements and inductances as shunt elements. At (a) is shown one section of a single-wire filter of this type, and four of these sections in series are shown at (b). At (c) is shown one section of a

double-wire filter of this type, and four of these sections in series are shown at *d*. This type of circuit passes without attenuation frequencies higher than a specified value, and

Fig. 7



Electrical Filter Type III. (T Circuit).

attenuates frequencies lower than the specified value, the attenuation increasing rapidly as the frequency falls below this value. Let

$f$  = frequency,

$\omega$  = angular velocity  $= 2\pi f$ ,

$\omega_c$  = critical angular velocity  $= 2\pi f_c$ ,

$\beta$  = attenuation constant per section,

$\alpha$  = wave-length „ „ „

$R_2$  = resistance of inductance  $L_2$ ,

$Z_0$  = characteristic impedance, *i. e.* the impedance by which a line of an infinite number of sections, or of a number of sections with a non-reflective output impedance, can be replaced without changing the current at the sending end.

Then the properties of this type of filter may be expressed as follows :—

(1) *Resistanceless Filter* (i. e.  $R_2=0$ ).

$$\beta = 0 \text{ if } \omega = \text{or} > \frac{1}{2\sqrt{L_2C_1}}, \text{ i. e. } \omega_c = \frac{1}{2\sqrt{L_2C_1}}, \quad (6)$$

$$\beta = \cosh^{-1} \left\{ \frac{1}{2L_2C_1\omega^2} - 1 \right\} \text{ if } \omega < \frac{1}{2\sqrt{L_2C_1}} \quad \dots (7)$$

$$= \cosh^{-1} \left\{ 2\frac{\omega_c^2}{\omega^2} - 1 \right\}, \quad \text{,,} \quad \text{,,} \quad \text{,,} \quad \dots (7A)$$

$$\alpha = \cos^{-1} \left\{ 1 - \frac{1}{2\omega^2C_1L_2} \right\} \text{ if } \omega = \text{or} > \frac{1}{2\sqrt{L_2C_1}} \quad (8)$$

$$= \cos^{-1} \left\{ 1 - 2\frac{\omega_c^2}{\omega^2} \right\}, \quad \text{,,} \quad \text{,,} \quad \text{,,} \quad (8A)$$

$$\alpha = \pi \text{ if } \omega < \frac{1}{2\sqrt{L_2C_1}}, \quad \dots \dots \dots (9)$$

$$Z_0 = \sqrt{\frac{L_2}{C_1} - \frac{1}{4C_1^2\omega^2}} = \sqrt{\left(1 - \frac{\omega_c^2}{\omega^2}\right) \frac{L_2}{C_1}} \quad \dots \dots (10)$$

The variation of the attenuation and wave-length constants with variation of the quantity  $\omega\sqrt{L_2C_1}$  is shown in Table I. In the last column of this table there is compiled the quantity  $e^{-10\beta}$ , which is the ratio of the current amplitude in the tenth section to the current amplitude in the zeroth section; this quantity shows the sharpness with which the line of ten sections cuts off frequencies near the limit of frequencies for which the attenuation is zero. Currents of all angular velocities from  $\omega=\infty$  to  $\omega=\frac{0.5}{\sqrt{L_2C_1}}$  are transmitted unattenuated; while, on the other hand, if  $\omega=\frac{0.497}{\sqrt{L_2C_1}}$  the current in the tenth section is only 11 per cent. of the current in the zeroth section, and if  $\omega=\frac{0.48}{\sqrt{L_2C_1}}$  the current in the tenth section is only  $\frac{1}{10}$  per cent. of the current in the zeroth section.

TABLE I.

## Resistanceless Filter of Type III.

Attenuation Constant  $\beta$  and Wave-length Constant  $\alpha$  per Section for different Angular Velocities  $\omega$  of the Current.

$L_2$  = Shunt Inductance per Section }  
 $C_1$  = Series Capacity                "    "    }

$\omega \sqrt{L_2 C_1}$	$\beta$ .	$\alpha$ radians.	$e^{-10\beta}$ .
0.0	$\infty$	$3.14 = \pi$	0.00000
0.2	3.13	$3.14 = \pi$	0.00000+
0.3	2.20	$3.14 = \pi$	0.00000+
0.4	1.39	$3.14 = \pi$	0.00000+
0.45	0.93	$3.14 = \pi$	0.00009
0.46	0.83	$3.14 = \pi$	0.0002
0.47	0.71	$3.14 = \pi$	0.0008
0.48	0.57	$3.14 = \pi$	0.0032
0.495	0.29	$3.14 = \pi$	0.058
0.497	0.22	$3.14 = \pi$	0.111
0.499	0.13	$3.14 = \pi$	0.273
0.500	0.00	$3.14 = \pi$	1.00
0.501	0.00	3.02	1.00
0.503	0.00	2.92	1.00
0.505	0.00	2.86	1.00
0.6	0.00	1.97	1.00
0.7	0.00	1.59	1.00
0.8	0.00	1.35	1.00
0.9	0.00	1.18	1.00
1.0	0.00	1.05	1.00
2.0	0.00	0.50	1.00
3.0	0.00	0.33	1.00
4.0	0.00	0.25	1.00
$\infty$	0.00	0.00	1.00

The variation of the attenuation and wave-length constants is also shown graphically in fig. 8.

(2) *Filter with inductance  $L_2$  having resistance  $R_2$ .*

In this case we have :

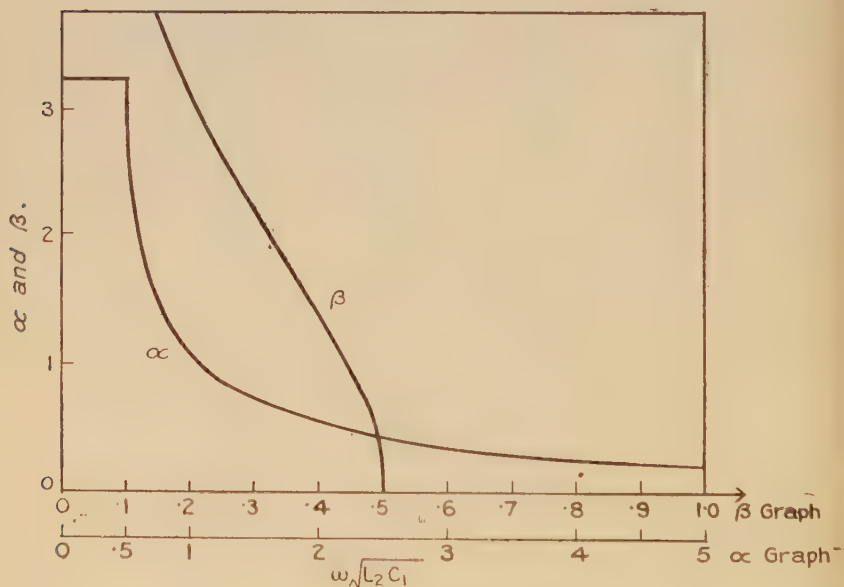
$$\beta = \sinh^{-1} \left\{ \frac{1}{2x \sqrt{2(1+y^2)}} \sqrt{\pm \sqrt{16x^2y^2 + (1-4x)^2} + (1-4x)} \right\}, \quad (11)$$

$$\alpha = \sin^{-1} \left\{ \frac{1}{2x \sqrt{2(1+y^2)}} \sqrt{\pm \sqrt{16x^2y^2 + (1-4x)^2} - (1-4x)} \right\}, \quad (12)$$

$$\text{where } x = L_2 C_1 \omega^2 \text{ and } y = \frac{R_2}{L_2 \omega},$$

$$Z_0 = \sqrt{\frac{L_2}{C_1}} \sqrt{1 - \frac{1}{4L_2 C_1 \omega^2} - \frac{jR_2}{L_2 \omega}} \quad \dots \dots \dots (13)$$

Fig. 8.



Ideal Filter Type III.

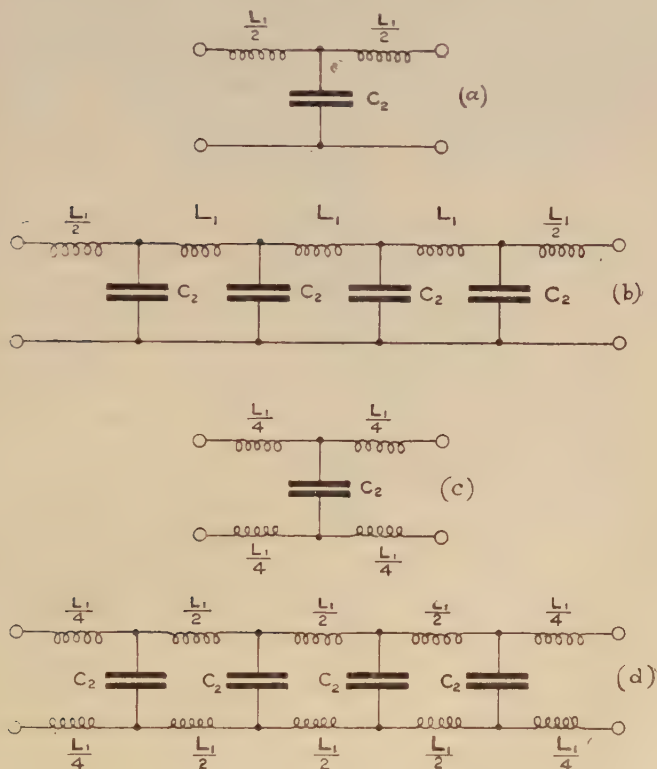
These formulæ enable a study to be made of the filter action of this type under any specified conditions.

Type IV. (T circuit) is shown in fig. 9 (a), (b), (c), and (d). It consists of inductances as series elements, and capacities as shunt elements. At (a) is shown one section of a single-wire filter of this type, and four of these sections in series are shown at (b). At (c) is shown one section of a double-wire filter of this type, and four of these sections in series are shown at (d). This type of circuit passes frequencies lower than the specified value without attenuation, and



attenuates currents of frequencies higher than the specified value, the attenuation rising rapidly as the frequency rises

Fig. 9.



Electrical Filter Type IV. (T Circuit).

above this value. The properties of this type of filter may be expressed as follows:—

(1) *Resistanceless Filter* (i. e.  $R_1=0$ ).

$$\beta = 0 \text{ if } \omega = \text{ or } < \frac{2}{\sqrt{L_1 C_2}}, \text{ i. e. } \omega_c = \frac{2}{\sqrt{L_1 C_2}}, \quad (14)$$

$$\beta = \cosh^{-1} \left\{ \frac{L_1 C_2 \omega^2}{2} - 1 \right\} \text{ if } \omega > \frac{2}{\sqrt{L_1 C_2}} \quad \cdot \cdot \cdot (15)$$

$$= \cosh^{-1} \left\{ 2 \frac{\omega^2}{\omega_c^2} - 1 \right\}, \quad \cdot \cdot \cdot (15A)$$

$$\alpha = \cos^{-1} \left\{ 1 - \frac{\omega^2 L_1 C_2}{2} \right\} \quad \text{if } \omega = \text{ or } < \frac{2}{\sqrt{L_1 C_2}} \quad (16)$$

$$= \cos^{-1} \left\{ 1 - 2 \frac{\omega^2}{\omega_c^2} \right\}, \quad \text{,,} \quad \text{,,} \quad \text{,,} \quad \text{,,} \quad (16A)$$

$$\alpha = \pi \quad \text{if } \omega > \frac{2}{\sqrt{L_1 C_2}}, \quad . \quad . \quad . \quad . \quad . \quad . \quad . \quad (17)$$

$$Z_0 = \sqrt{\frac{L_1}{C_2} - \frac{L_1^2 \omega^2}{4}} = \sqrt{\left(1 - \frac{\omega^2}{\omega_c^2}\right) \frac{L_1}{C_2}} \quad . \quad . \quad . \quad (18)$$

TABLE II.

## Resistanceless Filter of Type IV.

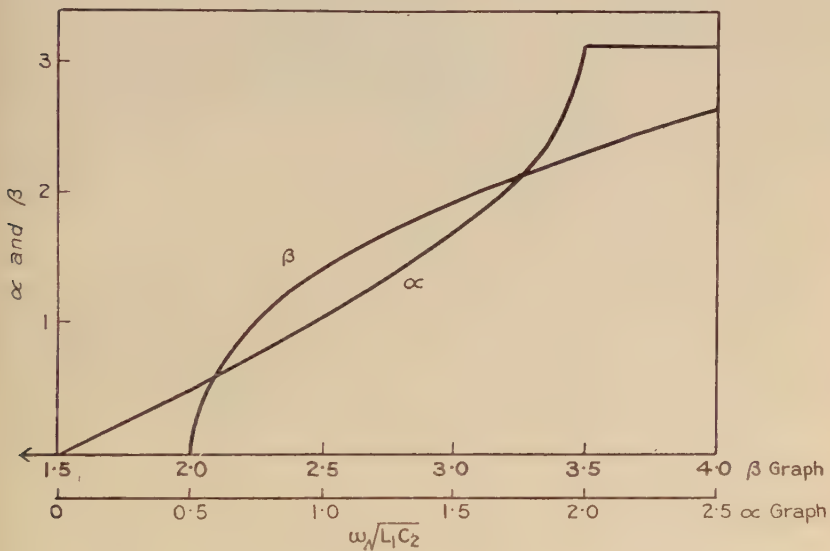
Attenuation Constant  $\beta$  and Wave-length Constant  $\alpha$  per Section for different Angular Velocities  $\omega$  of the Current.

$L_1$  = Series Inductance per Section }  
 $C_2$  = Shunt Capacity " " }

$\omega, \sqrt{L_1 C_2}$	$\beta$	$\alpha$ radians.	$\frac{T}{\sqrt{L_1 C_2}}$	$e^{-10\beta}$
0.00	0.000	0.000	1.000	1.000
0.10	0.000	0.100	1.001	1.000
0.20	0.000	0.200	1.002	1.000
0.30	0.000	0.301	1.004	1.000
0.40	0.000	0.403	1.007	1.000
0.60	0.000	0.609	1.016	1.000
0.80	0.000	0.823	1.03	1.000
1.00	0.000	1.05	1.05	1.000
1.40	0.000	1.55	1.12	1.000
1.80	0.000	2.24	1.24	1.000
2.00	0.000	3.14 = $\pi$	1.57	1.000
2.001	0.064	3.14 = $\pi$	—	0.527
2.002	0.090	3.14 = $\pi$	—	0.406
2.003	0.111	3.14 = $\pi$	—	0.329
2.004	0.128	3.14 = $\pi$	—	0.277
2.005	0.143	3.14 = $\pi$	—	0.239
2.01	0.200	3.14 = $\pi$	—	0.135
2.02	0.283	3.14 = $\pi$	—	0.059
2.04	0.399	3.14 = $\pi$	—	0.0185
2.1	0.630	3.14 = $\pi$	—	0.00185
2.2	0.887	3.14 = $\pi$	—	0.00014
2.5	1.386	3.14 = $\pi$	—	0.00000+
3.0	1.925	3.14 = $\pi$	—	0.00000+
3.5	2.318	3.14 = $\pi$	—	0.00000+
4.0	2.634	3.14 = $\pi$	—	0.00000+

The variation of the attenuation and wave-length constants with variation of the quantity  $\omega \sqrt{L_1 C_2}$  is shown in Table II. Currents of all frequencies from  $\omega \sqrt{L_1 C_2} = 0$  to  $\omega \sqrt{L_1 C_2} = 2$  are transmitted unattenuated. When this value reaches 2.04 it will be seen from the last column of Table II. that the current in the tenth section is 1.8 per cent. of the current in the zeroth section. The variation of the attenuation and wave-length constants given in Table II. is shown graphically in fig. 10.

Fig. 10.



Ideal Filter Type IV.

Tables I. and II. also contain values of the current-lag-angle per section, and in Table II. is given a related quantity T, which is the number of seconds by which the current in any section lags behind the current in the preceding section. The relation between T and  $\alpha$  is

$$\alpha = T\omega, \quad . \quad . \quad . \quad . \quad . \quad (19)$$

and in the table  $\frac{T}{\sqrt{L_1 C_2}}$  has been calculated for convenience, as it is the ratio of the third and first column figures. It

will be seen that for small values of  $\omega\sqrt{L_1C_2}$  the time-lag  $T$  per section is approximately constant.

(2) *Filter with inductance  $L_1$  having resistance  $R_1$ .*

In this case we have :

$$\beta = \sinh^{-1} \left\{ \sqrt{\frac{x}{2}} \right. \\ \left. \sqrt{\pm \sqrt{y^2 + \left\{ 1 - \frac{x}{4}(1+y^2) \right\}^2} - \left\{ 1 - \frac{x}{4}(1+y^2) \right\}} \right\}, \\ \dots \dots (20)$$

$$\alpha = \sin^{-1} \left\{ \sqrt{\frac{x}{2}} \right. \\ \left. \sqrt{\pm \sqrt{y^2 + \left\{ 1 - \frac{x}{4}(1+y^2) \right\}^2} + \left\{ 1 - \frac{x}{4}(1+y^2) \right\}} \right\} \\ \dots \dots (21)$$

where  $x = L_1C_2\omega^2$  and  $y = \frac{R_1}{L_1\omega}$ ,

$$Z_0 = \sqrt{\frac{L_1}{C_2}} \sqrt{1 + \frac{R_1^2C_2}{4L_1} - \frac{L_1C_2\omega^2}{4}} + j \left\{ \frac{R_1C_2\omega}{2} - \frac{R_1}{L_1\omega} \right\}. \\ \dots \dots (22)$$

These formulæ provide a method of studying the action of a filter of this type with any specified values of  $R_1$ ,  $L_1$ , and  $C_2$ .

These two types of electrical filter may also be made up as  $\pi$  circuits.

Type III. ( $\pi$  circuit) is shown in fig. 11 (a), (b), (c), and (d), and these four diagrams correspond to those shown in fig. 7. Neglecting resistance, the critical point of this filter

occurs when  $\omega = \frac{1}{2\sqrt{L_2C_1}}$ , and

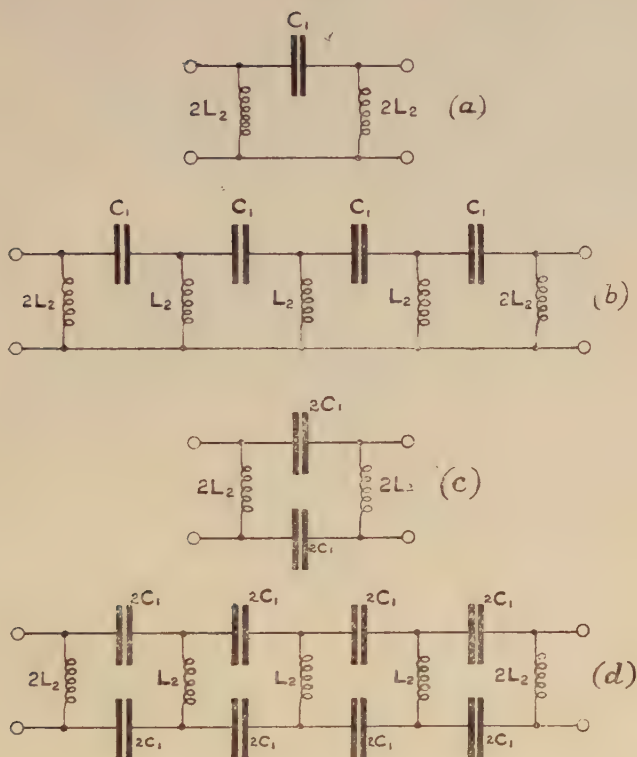
$$\text{if } \omega\sqrt{L_2C_1} = 0, \text{ then } \beta = \infty \text{ and } \alpha = \pi, \dots (23)$$

$$,, \omega\sqrt{L_2C_1} = 0.5, ,, \beta = 0 ,, \alpha = \pi, \dots (24)$$

$$,, \omega\sqrt{L_2C_1} = \infty, ,, \beta = 0 ,, \alpha = 0. \dots (25)$$

$$\text{Also } Z_0 = \frac{2\omega L_2}{\sqrt{4\omega^2 L_2 C_1 - 1}}. \dots \dots (26)$$

Fig. 11.



Electrical Filter Type III. ( $\pi$  Circuit).

Type IV. ( $\pi$  circuit) is shown in fig. 12 (a), (b), (c), and (d), and these four diagrams correspond to those given in fig. 9. Neglecting resistance, the critical point of this filter

occurs when  $\omega = \frac{2}{\sqrt{L_1 C_2}}$ ,

$$\text{if } \omega \sqrt{L_1 C_2} = 0, \text{ then } \beta = 0 \text{ and } \alpha = 0, \quad (27)$$

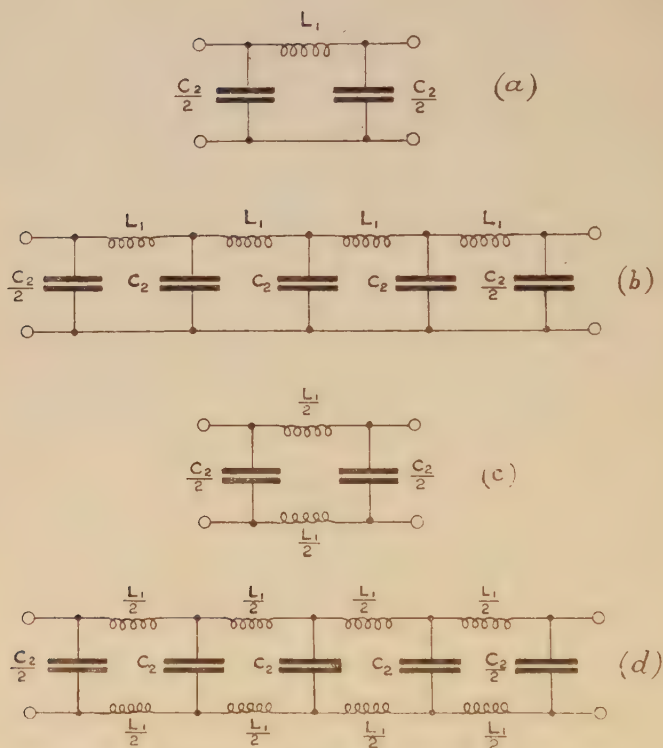
$$,, \omega \sqrt{L_1 C_2} = 2, \quad ,, \beta = 0 \quad ,, \alpha = \pi, \quad (28)$$

$$,, \omega \sqrt{L_1 C_2} = \infty, \quad ,, \beta = \infty \quad ,, \alpha = \pi. \quad (29)$$

$$\text{Als o} \quad Z_0 = \sqrt{\frac{4L_1}{C_2(4 - \omega^2 L_1 C_2)}} \cdot \cdot \cdot \cdot (30)$$



Fig. 12.

Electrical Filter Type IV. ( $\pi$  Circuit).

Type V. is shown in fig. 13 (a), (b), (c), and (d). It is similar to Type IV. (T circuit), but there is mutual inductance  $M$  between the two series inductance coils of each T circuit. The inductance of each coil in fig. 13 (a) is  $\frac{L_1}{2}$  and the capacity of the shunt condenser is  $C_2$ . At (a) is shown one section of a single-wire filter of this type, and four of these sections in series are shown at (b). At (c) is shown one section of a double-wire filter of this type, and four of these sections in series are shown at (d). The properties of this type of filter may be expressed as follows:—

(1) *Resistanceless Filter* (i. e.  $R_1=0$ ).

$$\beta = 0 \text{ if } \omega = \text{ or } < \frac{2}{\sqrt{C_2(L_1-2M)}}, \quad . \quad . \quad (31A)$$

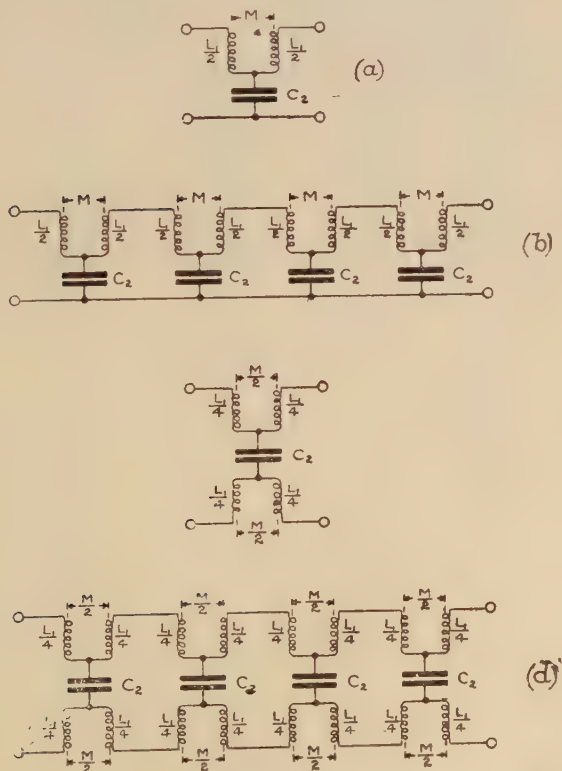
$$\beta = \infty \text{ if } \omega^2 = -\frac{1}{MC_2}, \quad . \quad . \quad . \quad . \quad . \quad (31B)$$

$$\left. \begin{array}{l} \alpha = 0 \text{ if } \omega = 0, \\ \alpha = \pi \text{ if } \omega = \text{ or } > \frac{2}{\sqrt{C_2(L_1-2M)}} \end{array} \right\}, \quad . \quad (32)$$

$$Z_0 = \sqrt{\frac{(L_1+2M)}{C_2} + \frac{(\pm M^2 - L_1^2)\omega^2}{4}}. \quad . \quad . \quad (33)$$

The frequency given in (31B) is generally known as the Campbell cut-off point for this type of filter.

Fig. 13.



Electrical Filter Type V.

It will be seen from (31A) that if  $M = \frac{L_1}{2}$  (*i. e.* no magnetic leakage), then this filter will pass all possible frequencies without attenuation. Such an arrangement is not a good filter, but is useful for its retardation properties when it is desired to transmit, with suitable retardation, all frequencies.

When  $M$  is negative with respect to  $L_1$ , this filter is usually called a negative mutual inductance filter. If

TABLE II A.

## Resistanceless Filter of Type V.

Attenuation Constant  $\beta$  and Wave length Constant  $\alpha$  per Section for different Angular Velocities  $\omega$  of the Current.

$$\left. \begin{array}{l} L_1 = \text{Series Inductance per Section} = 0.310 \text{ henry} \\ M = \text{Mutual " " " } = -0.140 \text{ henry} \\ C_2 = \text{Shunt Capacity " " } = 0.034 \mu\text{f.} \end{array} \right\}.$$

$\omega$ radians per sec.	$\beta$ .	$\alpha$ radians.	$e^{-10\beta}$ .
0	0.000	0.000	1.000
2,000	0.000	0.065	1.000
4,000	0.000	0.133	1.000
6,000	0.000	0.211	1.000
8,000	0.000	0.308	1.000
10,000	0.000	0.445	1.000
12,000	0.000	0.697	1.000
13,000	0.000	0.977	1.000
14,000	0.000	2.084	1.000
14,121	0.000	$3.14 = \pi$	1.000
14,200	1.013	$3.14 = \pi$	0.00004
14,300	1.733	$3.14 = \pi$	0.00000+
14,400	2.656	$3.14 = \pi$	0.00000+
14,450	3.49	$3.14 = \pi$	0.00000+
*14,494	$\infty$	$3.14 = \pi$	0.00000+
14,500	5.61	$3.14 = \pi$	0.00000+
14,600	2.821	$3.14 = \pi$	0.00000+
14,750	2.093	$3.14 = \pi$	0.00000+
15,000	1.616	$3.14 = \pi$	0.00000+
15,500	1.227	$3.14 = \pi$	0.00000+
16,000	1.045	$3.14 = \pi$	0.00003
17,000	0.859	$3.14 = \pi$	0.00019
18,000	0.762	$3.14 = \pi$	0.00049
19,000	0.701	$3.14 = \pi$	0.00090
20,000	0.660	$3.14 = \pi$	0.00136

\* Campbell cut-off point.

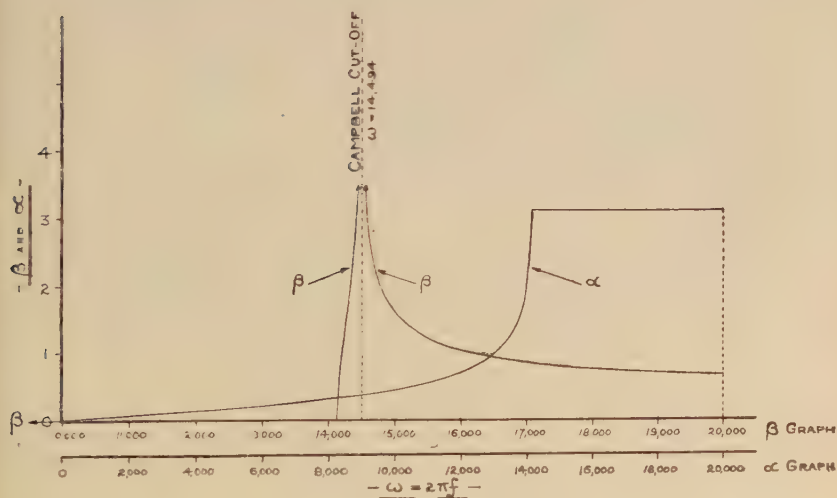
$M = -\frac{L_1}{2}$ , this filter will pass, without attenuation, all frequencies from zero up to  $\omega = \sqrt{\frac{2}{C_2 L_1}}$ .

Table II.A gives calculated values of  $\beta$  and  $\alpha$ , for different values of  $\omega$ , for a resistanceless negative mutual inductance filter having the constants given above this table. The variation of  $\beta$  and  $\alpha$ , as  $\omega$  changes from 0 to 20,000, is shown graphically in fig. 13 A.

Fig. 13 A.

- IDEAL FILTER TYPE V -

$L_1 = 0.310$  HENRY  $M = -0.140$  HENRY  $C_2 = 0.034 \mu.f$



Ideal Filter Type V.

(2) Filter with resistance  $R_1$  per section.

In this case we have:

$$\beta = \sinh^{-1} \left\{ \sqrt{\frac{x}{2}} \right. \\ \left. \sqrt{1 \pm \sqrt{y^2 + \left\{ 1 - \frac{x}{4} (1 + y^2) \right\}^2 - \left\{ 1 - \frac{x}{4} (1 + y^2) \right\}}} \right\},$$

$$\alpha = \sin^{-1} \left\{ \sqrt{\frac{x}{2}} \sqrt{\pm \sqrt{y^2 + \left\{ 1 - \frac{x}{4}(1+y^2) \right\}^2 + \left\{ 1 - \frac{x}{4}(1+y^2) \right\}}} \right\}, \quad (35)$$

where  $x = \frac{(L_1 + 2M)C_2\omega^2}{1 + MC_2\omega^2}$  and  $y = \frac{R_1}{(L_1 + 2M)\omega}$ ,

$$Z_0 = \sqrt{\frac{L_1 + 2M}{C_2} \sqrt{1 + \frac{R_1^2 C_2}{4(L_1 + 2M)} - \frac{(L_1 - 2M)C_2\omega^2}{4} + j \left\{ \frac{R_1 C_2 \omega}{2} - \frac{R_1(1 + MC_2\omega^2)}{(L_1 + 2M)\omega} \right\}}}. \quad (36)$$

One of the important advantages of the negative mutual inductance filter is that its resistance is practically ohmic for audio frequencies, and it can therefore be constructed to give a sharp cut-off if the ohmic resistance is kept small.

(D) DESIGN AND COMPUTED PERFORMANCE OF A FILTER TO CUT OUT FREQUENCIES BELOW A SPECIFIED VALUE AND TO OPERATE BETWEEN INPUT AND OUTPUT TERMINAL APPARATUS OF GIVEN IMPEDANCE.

For this purpose we will select a filter of Type III. (T circuit).

Let  $\omega_0$  = angular velocity below which the filter is to give high attenuation. Then by formula (6) we have :

$$\omega_0 = \frac{1}{2\sqrt{L_2 C_1}}. \quad (37)$$

Next find another formula determined by the impedance of the terminal apparatus. To avoid reflexion the impedance  $Z_a$  of the input apparatus and the impedance  $Z_b$  of the output apparatus shall each equal the characteristic impedance of the filter ; i. e. .

$$Z_a = Z_b = Z_0. \quad (38)$$



Now, the value of  $Z_0$  for this type of line is given in (10), and is a function of the frequency. We cannot in general make  $Z_0 = Z_a$  and  $Z_b$  for all values of the frequency; in this case, however, we require to transmit efficiently the frequencies above  $\omega_0$ ; *i. e.* high frequencies. Hence we assume that

$$Z_0 = \sqrt{\frac{L_2}{C_1}} \quad . \quad . \quad . \quad . \quad . \quad (32)$$

if  $\frac{1}{4C_1^2\omega^2}$  in (10) is negligible in comparison with  $\frac{L_2}{C_1}$ . If this is true, the filter impedance is of the nature of a pure resistance independent of frequency, and the terminal apparatus should be as nearly as possible a pure resistance of value

$$Z_a = Z_b = \sqrt{\frac{L_2}{C_1}} = R \text{ (say)}. \quad . \quad . \quad . \quad (40)$$

Eliminating between (37) and (40), we obtain:

$$L_2 = \frac{R}{2\omega_0} \quad . \quad . \quad . \quad . \quad . \quad (41)$$

and

$$C_1 = \frac{1}{2R\omega_0} \quad . \quad . \quad . \quad . \quad . \quad (42)$$

Equations (41) and (42) give the value of inductance and capacity of the filter to cut off angular velocities above  $\omega_0$  and to operate between input and output apparatus each of impedance  $R$  (reactanceless).

As to the resistance of the inductance coils used in the filter, it is desirable to have this resistance  $R_2$  as low as possible. Let us suppose that

$$\frac{R_2}{L_2} = 2\Delta \text{ (say)}, \quad . \quad . \quad . \quad . \quad . \quad (43)$$

where  $\Delta$  is a constant for any given type of coil.

Using formulæ (11) and (12), we can compute  $\beta$  and  $\alpha$  for various ratios of  $\omega$  to  $\omega_0$ .

Suppose  $2\Delta = 250$  and  $\omega_0 = 5000$ . This means that the coils  $L_2$  have 250 ohms per henry, and that we wish to cut off currents of any frequency below 800 cycles per second.

The results of the calculated filter performance are given in Table III., and are shown graphically on fig. 14.

TABLE III.

## Filter Type III. (T Circuit).

Performance of a Filter computed to cut off all Angular Velocities less than  $\omega_0=5000$ , given  $\frac{R_2}{L_2}=250$ .

$\frac{\omega}{\omega_0}$	$\beta$ .	$\alpha$ radians.	$e^{-10\beta}$ .
0.2	4.56	0.249	0.00000+
0.4	3.13	0.136	0.00000+
0.5	2.63	0.113	0.00000+
0.6	2.19	0.104	0.00000+
0.8	1.39	0.103	0.00000+
0.9	0.938	0.127	0.00008
0.95	0.662	0.164	0.00134
1.0	0.311	0.321	0.0449
1.05	0.144	0.640	0.236
1.1	0.0979	0.868	0.375
1.2	0.0636	1.174	0.530
1.4	0.0364	1.546	0.694
1.6	0.0250	1.351	0.778
2.0	0.0144	1.047	0.865
2.5	0.00873	0.823	0.916
3.0	0.00589	0.680	0.942
4.0	0.00323	0.505	0.967

NOTE.— $x$  in formulæ (11) and (12) =  $L_2 C_1 \omega^2 = \frac{\omega^2}{4\omega_0^2} = \frac{1}{4} \left( \frac{\omega}{\omega_0} \right)^2$ .

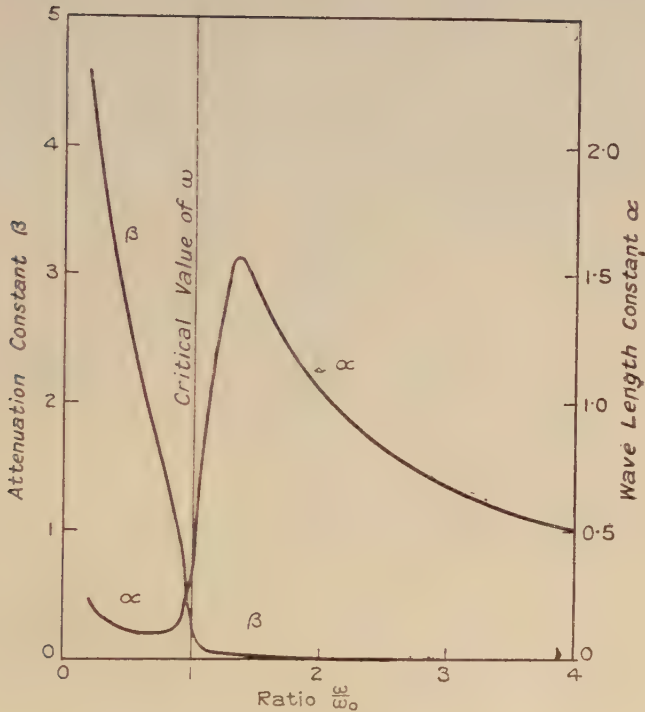
$y$  in formulæ (11) and (12) =  $\frac{R_2}{L_2 \omega} = \frac{2\Delta}{\omega_0} \left( \frac{\omega_0}{\omega} \right)$

(E) SOME ACTUAL APPLICATIONS OF ELECTRICAL FILTERS  
IN TELEGRAPH AND TELEPHONE ENGINEERING.

(a) *Composited working.*

By means of electrical filters it is possible to work telegraph and telephone sets on the same circuit at the same time without mutual interference. One such arrangement of a composited circuit is shown in fig. 15. It is in effect two frequency filters, and by this means two telegraph circuits and one telephone circuit are obtained on one pair of wires. The filters A and B may be designed to permit frequencies from zero to about 50 cycles per second to pass with small attenuation, and to suppress currents of a higher

Fig. 14.



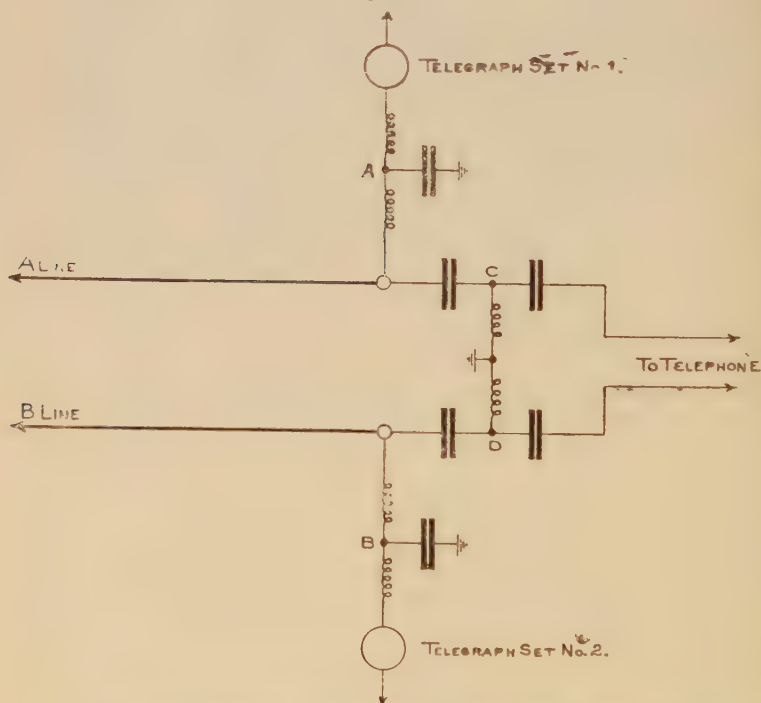
Filter Type III.

frequency. These filters will therefore allow Wheatstone reversals up to about 125 words per minute to pass to line. The filters C and D may be arranged to pass all frequencies of, say, 100 cycles per second and higher, and to suppress all frequencies below this figure. In this way the telephone circuit is protected from interference by the telegraph signals, and the telegraph sets are protected from any interference by telephone ringing or speech currents. It should be mentioned that the impedances of all these filters must be such that they introduce as little transmission loss as possible to the actual telegraph and telephone working and signalling currents.

It may be of interest to give, at this juncture, a brief description of some recent experiments which have been

made on the application of electrical filters to composited working. The object of these experiments was, by the aid of filters, to provide a simple and satisfactory method of hand-speed duplex telegraph working on each wire (A and B) of a telephone loop circuit without any appreciable over-hearing in the telephone circuit, the ordinary Post Office "B" relay being used as the receiving instrument for the telegraph signals. It was not found necessary to use the filters corresponding to C and D in fig. 15. These were

Fig. 15.

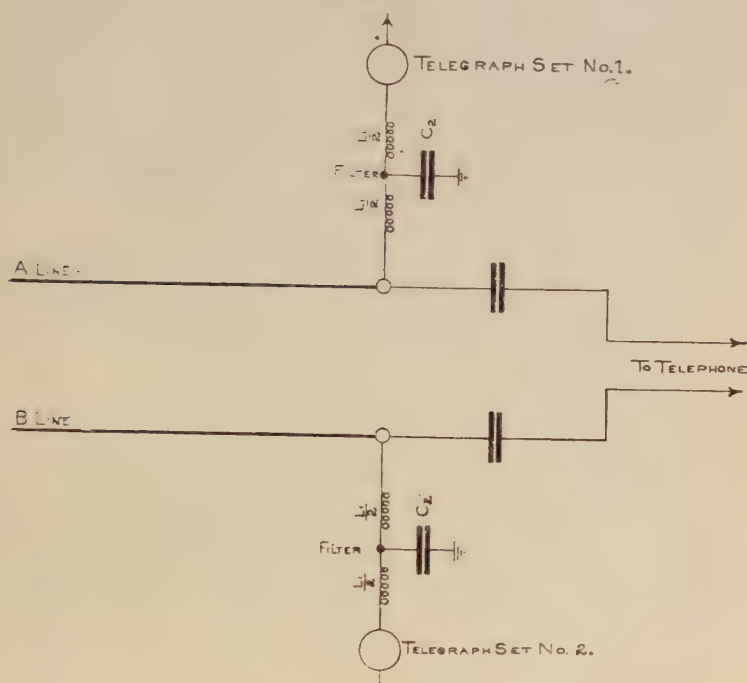


Application of Electrical Filters to Composited Circuit.

replaced by condensers, which offered a high impedance to low-frequency currents, but a low impedance to currents of audio-frequency, and a diagram of connexions of the method employed is shown in fig. 16. With the type of filter used, if  $\frac{L_1}{2} = 10$  henrys and  $C_2 = 4 \mu.f.$ , the frequency of cut-off works out to be 35.6 cycles per second ; this frequency

corresponds to the number of dots per second sent by a Wheatstone transmitter running at 89 words per minute.

Fig. 16.



Circuit used in recent P.O. Experiments in Compositing Working.

This type and design of filter was decided upon for the following reasons:—

- (1) It should be suitable for key and slow Wheatstone telegraph working, with a reliable margin for key speeds.
- (2) The cut-off frequency of 35.6 cycles per second being well below the lowest audible frequency, a sufficient margin should be allowed for the fact that an actual filter having resistance associated with its inductance does not perfectly cut off all frequencies above the theoretical value.



Suitable inductance coils, having a D.C. resistance of approximately 50 ohms and an inductance of approximately 10 henrys with any current between 2 and 15 m.a., were designed and constructed. An oscillographic investigation showed that a filter of this design was very effective in cutting out from Wheatstone reversals the harmonics which would interfere with the telephone circuit.

For the experiments two filter sections were made up for each telegraph set, and it was arranged that either one or two could be switched into circuit as required. These filters were placed between the Wheatstone Transmitter or Double-Current Key and the "B" relay so that when working differential duplex it was not necessary to provide balancing filter sections in the compensation circuit.

The following summary give the results which have been obtained: in each case the resulting noise introduced into the telephone circuit was considered to be negligible.

(a) *Aerial Loop Telephone Circuit*, equated length  $22\frac{1}{2}$  miles of standard cable. The actual line consisted of 196 miles of 200 lb. aerial line, terminated at one end by 14.25 miles of 150 lb. coil-loaded underground cable, and at the other end by 14.25 miles of 100 lb. coil-loaded underground cable. Two differential duplex telegraph sets, one on each conductor, worked successfully up to 57 words per minute.

(b) *Unloaded Underground Cable Loop Telephone Circuit*, equated length  $24\frac{1}{2}$  miles of standard cable. The actual line consisted of 20 lb. unloaded A.S.P.C. cable. Two differential duplex telegraph sets, one on each conductor, worked successfully up to 70 words per minute.

(c) *Coil-Loaded Underground Cable Loop Telephone Circuits*. The actual lines used were 40 lb. coil-loaded A.S.P.C. cable circuits in the London-Manchester telephone cable. Using a side circuit, equated length 22 miles of standard cable, two differential duplex sets were worked successfully, one on each conductor, up to 35 words per minute. Using a phantom circuit, equated length 19 miles of standard cable, a telegraph speed up to 40 words per minute was obtained with the same system of working.

It is deduced from these results that a satisfactory composited system working at key speed and giving two duplex telegraph channels per telephone loop, within the limits indicated, can now be designed by the aid of electrical filters.

It should be added that telephone signalling was successfully arranged for in these experiments by using current of a frequency of 133 cycles per second.

(b) *Telephonic Repeaters.*

In the case of telephonic repeaters of the type where the line is balanced by means of an artificial impedance, it is advantageous to employ a filter to cut out currents of frequencies outside the range over which this impedance balances the line impedance. A method of connecting the filter in circuit with a telephonic repeater of this type is shown in fig. 17.

Fig. 17.

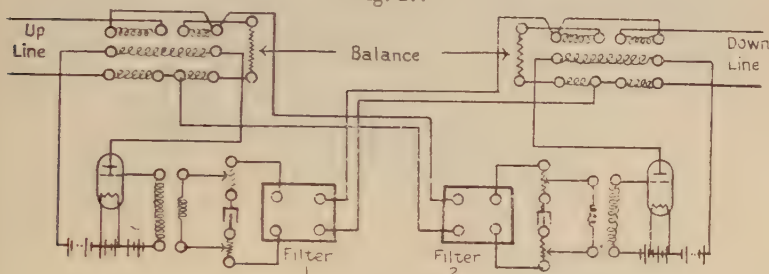


Diagram of Repeater with Filter in Circuit.

To give an example of the operation of a filter under these conditions, we will refer to some experiments made to develop such a filter for use in a telephonic repeater suitable for coil-loaded underground cable circuits. Now, it is possible to design a balancing impedance for such circuits which is fairly accurate over the range of frequencies between 320 cycles per sec. ( $\omega = 2000$ ) and 2200 cycles per sec. ( $\omega = 14,000$ ). The repeater itself falls in efficiency at the low end of this frequency range, so the filters were designed to cut off the high frequencies only. As the attenuation constant of the present type of coil-loaded underground cable circuit rises rapidly at about 2200 cycles per sec., this frequency was therefore taken for the cut-off point of the filters. Electrical filter Type V. (fig. 13 c) was chosen, and as a sharper cut-off is obtained when  $M$  is negative, the series coils were joined up in such a way that they opposed each other magnetically.

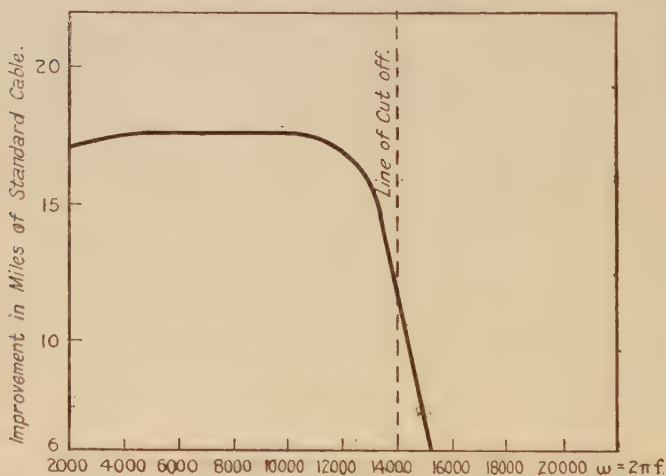
In making the experiments, a double-valve repeater, designed for use on lines of 1300 ohms impedance, fitted with potentiometer values of 650 ohms and  $1 \mu.f.$ , was used and connected in the centre of 40 standard miles of non-reactive artificial cable with a characteristic impedance of 1300 ohms. With a fixed current of 3 m.a. sent into the line, the improvement of the repeater was measured at

angular velocities ranging from  $\omega=2000$  to  $\omega=16,000$  radians per second. After a preliminary investigation, the most suitable type of filter was found to be one having the following constants :

$$\begin{aligned} \frac{L_1}{2} &= 0.155 \text{ henry,} & C_2 &= 0.034 \mu\text{f.,} \\ M &= -0.140 \text{ ,,} & Z_0 &= 650 \text{ ohms.} \end{aligned}$$

A three-section filter was made up and tested as described, and the results are shown in fig. 18, the filter having a calculated cut-off<sub>2</sub> at  $\omega=14,000$  radians per second.

Fig. 18.



Performance of Telephone Repeater with 3-section Negative Mutual Inductance Filter (Type V.) in Circuit. Line Impedance = 1300 ohms.

From fig. 18 it will be seen that the loss at the calculated cut-off point is equivalent to about 5 standard miles. The improvement of the repeater is reduced to zero at about 16,000 radians per second. The loss when tested by speech, due to the introduction of this filter, was found to be negligible.

Two of these filters, impedance 650 ohms, were inserted in an 800-ohm double-valve repeater in a phantom circuit of the London-Manchester Coil-Loaded Telephone Cable. It was found by speech tests that the minimum standard cable equivalent to which the circuit could be reduced, consistent with stability, was from 29 to 19 without the filters and to

12 with the filters. This shows the improvement gained by cutting out frequencies above the ordinary range of speech frequencies, even with a filter whose impedance is not quite correct for the circuit in which it is used.

These experiments show that a filter of three sections, made as described, will, when inserted as shown in a double-valve repeater of the corresponding impedance, cut off satisfactorily currents of the pre-designed frequency without causing any appreciable attenuation over the range of frequencies which the filter is intended to transmit. Also the cutting-off of frequencies above the usual range of speech frequencies results in an appreciable reduction in the standard cable equivalent of a circuit in which a double-valve repeater is inserted.

An alternative position for the filter used in conjunction with a telephone repeater is shown in fig. 19.

Fig. 19.

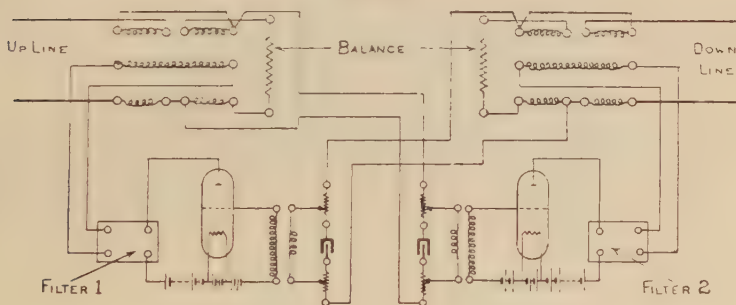


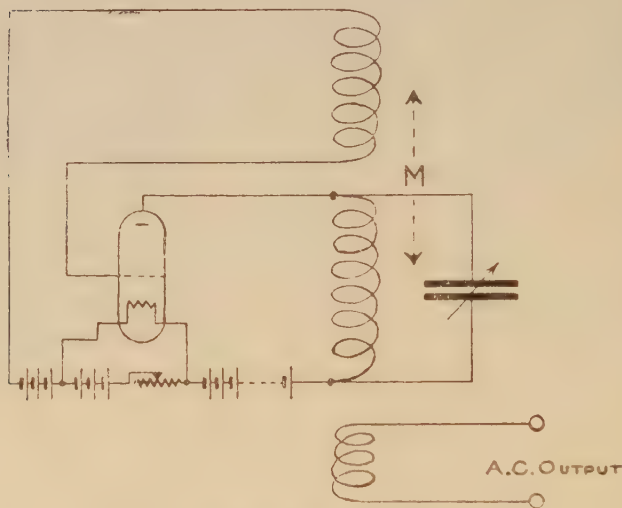
Diagram of Repeater with Filter in Circuit.

### (c) *Thermionic Valve Oscillator.*

In order to provide a source of alternating current of audio-frequency for telephonic measurements, the thermionic valve connected up as an oscillator forms a very convenient and portable generator. When used in this way the apparatus is usually joined up as shown in fig. 20. The working of this generator will be clear from the figure, and by means of an adjustable  $1 \mu.f.$  condenser the oscillator, if suitably designed, can be made to generate alternating current having a range of frequency from  $2\pi f = 1250$  to  $2\pi f = 16,000$ , which will meet all the usual requirements for telephonic measurements. The simple form of oscillator shown in fig. 20 has, however, several defects, one of which is that the alternating current generated contains harmonics. When

using such a source of alternating current for bridge measurements, it is not always possible to obtain silence in the telephone, as in the general case, on balancing out the fundamental frequency, the harmonics still remain unbalanced and cause a noise in the telephone. In some cases this residual noise seriously affects the utility of the test results. The

Fig. 20.



Thermionic Valve Oscillator.

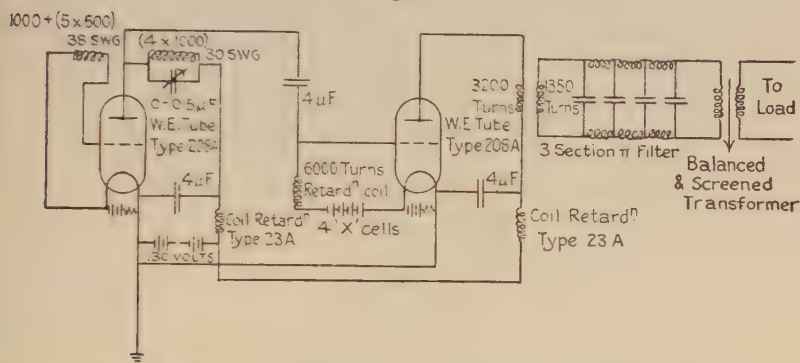
oscillator shown in fig. 21 was designed in order to meet the following main requirements :—

- (1) The frequency range to be from 200 to 2500 periods per second with at least 76 steps.
- (2) The output current available to be at least 15 m.a. through 1000 ohms.
- (3) The output volts to be constant over the frequency range.
- (4) The frequency not to be appreciably affected by the impedance of the load circuit.
- (5) The wave form of the oscillations to be as nearly as possible sinusoidal.



To satisfy this last requirement, it was found after investigation that self-inductance filters (Type IV.,  $\pi$  circuit) of three sections could be used with satisfactory results. To

Fig. 21.



cover the oscillator range, seven filters, each of three sections, were recommended to cover the following ranges :—

Filter I.	$\omega$ from	1250 to 1600,
„ II.	„ „	1600 to 2600,
„ III.	„ „	2600 to 3800,
„ IV.	„ „	3800 to 5500,
„ V.	„ „	5500 to 7800,
„ VI.	„ „	7800 to 11000,
„ VII.	„ „	11000 to 16000.

With these ranges and suitable types of self inductance, the efficiency of transmission throughout the working range varies from 70 to 85 per cent., while the lowest harmonics are attenuated from 0.4 to 4 per cent. of their value before filtration.

† The use of filters in connexion with this type of oscillator makes its range of usefulness considerably greater.

The two curves shown in fig. 22, plotted from actual test results, will show clearly the action of the filters used in the lowest and highest ranges. In these curves :

$I_R$  = Output current through 1000 ohms, filter in circuit.

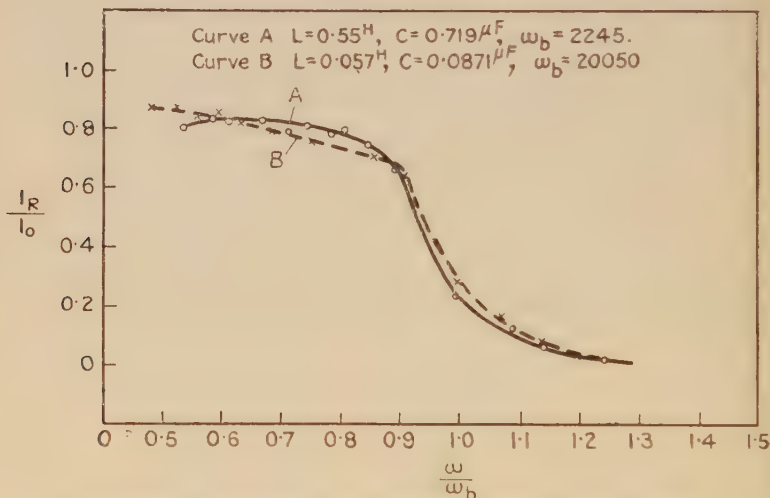
$I_0$  = „ „ „ „ filter out of circuit.

$\omega$  = Angular velocity of output current.

$\omega_0$  = „ „ „ filter cut off (theoretical).

From these curves it will be seen that  $\frac{I_R}{I_0}$  reaches the small value of approximately 0.04 when  $\frac{\omega}{\omega_b} = 1.22$ . If a minimum efficiency for the fundamental frequency is, say, 70 per cent., the highest working point for these filters is where  $\frac{\omega}{\omega_b} = 0.88$ , say. In order to ensure this minimum

Fig. 22.



Performance of 3-section Self-Inductance  $\pi$ -Type Filters using 0.75 inch stampings and 0.28 inch airgap.

efficiency for the fundamental frequencies of a range as well as a satisfactory attenuation of the harmonics of these frequencies, it was found that the seven filters before mentioned are required to cover the stated output frequency range. Further experiments are in hand with the object of reducing the number of filters required.

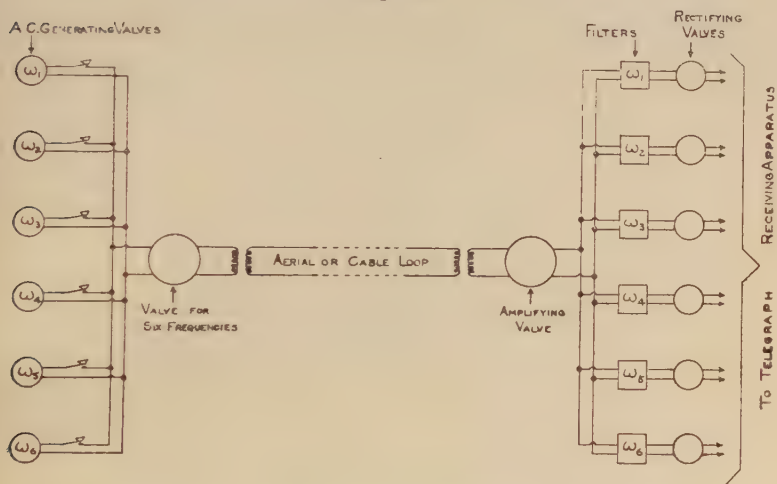
(d) *Alternating-Current Multiplex Telephony* \*.

The problem of using alternating current for sending telegraph signals is not by any means a new problem, but a great deal of consideration has been given to its solution since the development of the thermionic valve. In recent

\* See "Alternating-Current Telegraphy with Tonic Frequencies," by F. Luschen. *Electro-Technische Zeitschrift*, Jan. 4th and 11th, 1923.

years a system of multiplex alternating-current telegraphy has been developed which permits of reliable working. For the transmitters and receivers, thermionic valves are employed as oscillators, amplifiers, and receivers, and these operate with the same potentials as are employed in telephony. It is only proposed in this paper to describe this system in sufficient detail in order to make clear the important function of the electrical filters in making the method a success. In fig. 23 is shown in principle the arrangement of a sextuple

Fig. 23.

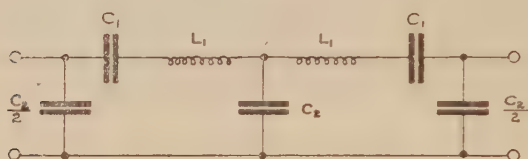


Application of Filters to Alternating-Current Telegraphy.

multiplex telegraph system. Six valves are used as generators of the alternating currents having angular velocities  $\omega_1$ ,  $\omega_2$ ,  $\omega_3$ ,  $\omega_4$ ,  $\omega_5$ , and  $\omega_6$ . The adjustment of each of these frequencies can be easily carried out by a variable capacity or inductance in the valve oscillating circuit. The six telegraph transmitters may be of any of the ordinary types employed, and they send alternating-current signals to the grid of a common transmitting valve. The currents sent by the six transmitters pass together over the line to the receiving end, where they are amplified in a common terminal amplifying valve. The currents now encounter electrical filters, each of which only transmits that frequency for which it is designed. After passing through the filters, the currents are rectified by rectifying valves which make these currents suitable for working the telegraph receiving

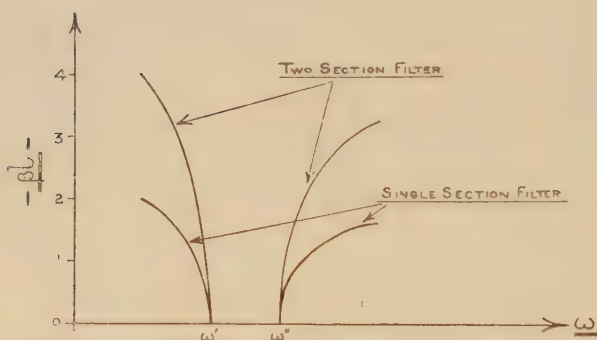
apparatus. The type of filter which has been used is shown in fig. 24, and it contains two sections : the attenuation of one and two sections of this type of filter is shown in fig. 25,

Fig. 24.



Two-section Filter for A.C. Multiplex Telegraphy.

Fig. 25.

Variation of  $\beta l$  with  $\omega$  for Single and Two-section Filter of the Type shown in Fig. 24.

and with two sections it will be seen that the attenuation rises rapidly to over  $\beta l = 3$  for the frequencies which are not allowed to pass.

On an aerial line it has been possible to transmit six telegrams simultaneously, using a frequency range of 20,000 to 30,000 cycles per second. Frequencies higher than these are subjected to so much loss on the lines that too much energy has to be employed, and the stated frequencies therefore are the highest which can be considered for aerial lines. A lower frequency of 3000 to 10,000 cycles per second has also been successfully used on aerial lines for alternating current multiplex telegraphy.

When this method of multiplex telegraphy is used in cables, the alternating current must have a frequency range of about 400 to 1700 cycles per second, as higher frequencies are too greatly attenuated. But it is possible to adopt this

range, and thus the method has been used even with coil-loaded telephone cable circuits. Experiments have shown that reliable working is obtained when six Siemens fast-speed automatic sets worked simultaneously over an underground cable loop having an equated length of  $22\frac{1}{2}$  standard miles. It may be of interest to mention some brief particulars of the design of the filters used in these experiments. The chief difficulty was that, in order to achieve success, six telegrams must be sent by alternating current having a frequency range of approximately 1300 periods per second, whereas with overhead lines a range of 7000 or even 10,000 periods per second is possible. The frequency "band" in the filters was finally calculated, so that, in addition to the nominal frequency, those frequencies above and below which differed from it to the extent of 15 periods per second ( $\omega = 100$  radians per second) were included within the range allowed by the "band." The amplitude of the neighbouring frequencies transmitted by any of the filters was limited to a maximum of  $1/15$ th of the amplitude of the normal frequency allowed to pass.

Without the use of electrical filters, reliable alternating-current multiplex telegraphy has not, as far as the author of this paper knows, been possible; but by their use a system of working has been developed which appears to have possibilities of considerable use in the future.

#### (e) *Carrier-Wave Multiplex Telephony* \*.

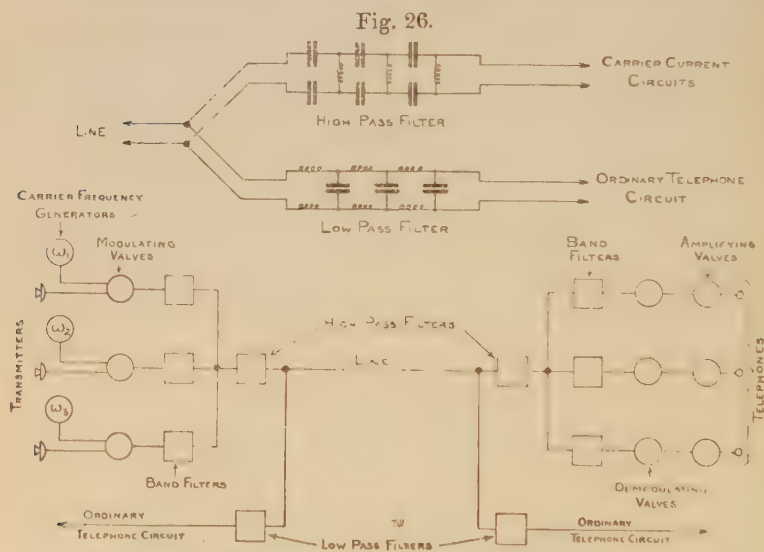
In this system the speech currents are superimposed on an alternating current of higher frequency which acts as a carrier wave for the former currents. The resulting wave is usually termed a "modulated" wave. If we suppose that the frequency of the carrier wave used is 10,000 cycles per sec. and that the speech currents have a frequency varying from 200 to 2000 cycles per sec., then the modulated wave will contain two frequency bands, viz. 10,200 to 12,000 and 9800 to 8000 cycles per sec. These are known as upper and lower side bands, and speech can be transmitted and received by using either side band. This is important, as it halves the range of frequency to be assigned to each communication channel.

Fig. 26 shows in diagrammatic form the arrangement of three one-way channels working on one line; for convenience in drawing, each line in this diagram represents a two-wire circuit. Each channel uses a carrier wave of a different frequency generated by a thermionic valve, and this current

\* See "Carrier Current Telephony and Telegraphy," by E. H. Colpitts and O. B. Blackwell. *Journal of the American I. E. E.* vol. xl. (1921).



is modulated by speech currents from a transmitter. This modulated current passes through a band filter, then through a high-pass filter to the line. At the receiving end the modulated wave passes through the corresponding band filter, thence to a demodulating valve and an amplifying valve, before reaching the telephone receiver. Each band filter at the sending end is designed so that only the range of frequency assigned to the particular channel can reach the line, and the corresponding band filter at the receiving end only allows this same frequency range to be received by the demodulating valve. In this way mutual interference between



Application of Filters to Carrier Current Multiplex Telephony.

the channels is prevented. With ideal apparatus the carrier frequencies must have at least a difference of 2000 cycles per sec., and the ideal band filter would therefore transmit efficiently a frequency range of 2000 cycles per sec. and would entirely suppress all frequencies outside of this range. Because it is physically impossible to secure such an ideal band filter, a greater separation is arranged than that made necessary by the width of the transmitted band. It has been found that for carrier-wave operation at moderate frequencies, the nearest known approach to an ideal selective circuit is obtained by the use of an electrical filter. The type which has been used to great advantage in carrier-wave telephony

is Type I. ( $\pi$  circuit), in which  $L_1$  is zero. This filter transmits a band of frequencies, and it has been termed a "band-pass" filter. The attenuation of this filter is uniform within the transmitted range of frequency, and hence the distortion is negligible; the actual attenuation loss of the transmitted currents can be compensated by amplification. If a simple tuned circuit is used in place of a band filter, it either introduces prohibitive distortion of speech or, if made sufficiently non-selective to avoid this distortion, the carrier channels would need to be widely apart in frequency. In fact, the development of the band filter was of vital importance in order to make a success of carrier-wave multiplex telephony. Suitable filters have been constructed using mica condensers for the capacities, and for the inductances toroidal coils having a finely-divided iron core (sometimes called "dust-core" coils).

The attenuation curve of the filter outside its efficient transmission band determines the necessary frequency separation between the side bands of adjacent channels, and therefore to a large degree the number of channels which may be operated in any given total frequency range. For example, if channel A is operating through a given filter, then the frequency band for channel B must be chosen so that the filter attenuation in channel A of currents of the frequencies used in channel B is at least as great as some value fixed by the cross-talk requirements of the telephone system.

With regard to the separation of frequency of adjacent channels, it has been found practicable to design filters which permit of satisfactory operation with a range of 1000 cycles per sec. between adjacent channels; *i. e.* about 3000 cycles between adjacent carrier frequencies.

In addition to separating the various carrier channels from each other, it has been found convenient from the operating standpoint to separate the carrier frequencies as a group from the frequencies used for ordinary telegraphy and telephony. This is done by the "high-pass" and "low-pass" filters shown in fig. 26. The former filter transmits all frequencies above, say, 3000 cycles per sec., and suppresses all frequencies below this value; the latter filter passes all frequencies below, say, 3000 cycles per sec., and suppresses all frequencies above that value. Further, the high-pass filter is designed to offer a high impedance to currents of ordinary telephone frequencies and to have an impedance equal to that of the line for currents within the carrier range. Similarly, the low-pass filter is designed to offer a high impedance to

currents of carrier frequencies and to have an impedance equal to that of the line for currents of ordinary telephone frequencies. From the attenuation characteristics of these high- and low-pass filters, it is interesting to find that a sharp discrimination is obtained even for frequencies quite close to the cut-off point of 3000 cycles per sec. For example, if 2700 cycles is selected (*i. e.* near the upper limit of the voice range) the transmission equivalent for the low-pass filter is 1 S.M., and approximately 45 S.M. for the high-pass filter ; also, if 3200 cycles per sec. is selected, the transmission equivalent for the high-pass filter is less than 1 S.M., and is approximately 45 S.M. for the low-pass filter. These differences correspond roughly to a ratio of energies greater than 10,000 to 1.

Transmission in two directions on a line by means of carrier-wave multiplex telephony is arranged on the same principles that are used in ordinary two-way telephonic repeaters ; but as this problem does not really affect the question of filter operation, it is not included here.

#### (f) *Radio-Telephony.*

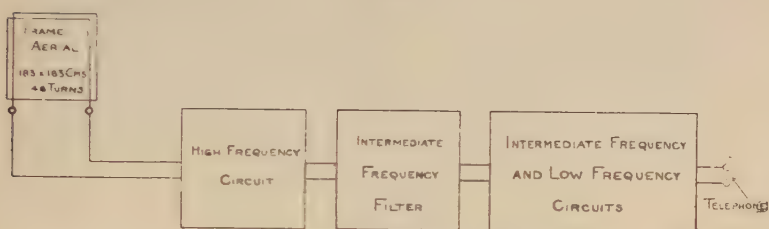
To give a practical example of the use of electrical filters in radio-telephony, a brief description is given of the transoceanic experiments carried out in 1923 by the American Telephone and Telegraph Company in co-operation with the Radio Corporation of America\*. At a pre-arranged time telephonic messages were sent out from New York, and at New Southgate, London, they were received clearly and with uniform intensity over a period of about two hours.

At the wireless transmitting station at Rocky Point a carrier current of 55,500 cycles per second was used, and this current was modulated by means of speech currents producing two side bands. One of these bands, having a frequency range of 55,800 to 58,500 cycles per second, was selected by means of a band filter and transmitted. At the receiving end, if a current of the original carrier frequency of 55,500 cycles per second is supplied to the detector it will remodulate or "beat" with the received side band and a difference-frequency band of 300 to 3000 cycles per second, *i. e.* the voice-frequency band, will result. The arrangement actually used, however, was not quite so simple as this. It is shown diagrammatically in fig. 27. Reception was carried out in two steps, the received band

\* See "Transatlantic Radio Telephony," by H. D. Arnold and L. Espenschied. *Journal of the American I. E. E.* vol xlii.

being stepped down to a lower frequency before final detection. The stepping-down action was accomplished in the high-frequency circuit by combining with the received band a locally-generated beating current of 90,000 cycles per second. In the output of this detector the difference-frequency band of 34,200 to 31,500 cycles per second was

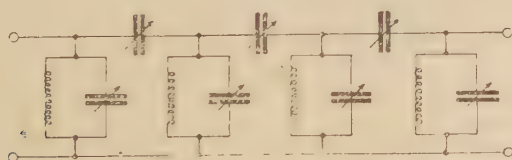
Fig. 27.



Receiving Circuit in Rocky Point-London Radio Tests, Feb. 1923.

selected by an intermediate frequency or band filter and passed through an amplifier (4-valve stages provided) to the low-frequency detector. This detector was supplied with a current of 34,500 cycles per second, which, beating with the selected band, gave as output the original voice-frequency band. The type of filter which was used was Type I. ( $\pi$  circuit), in which  $L_1$  was made zero and the capacities  $C_1$  and  $C_2$  were made adjustable. It is shown in fig. 28.

Fig. 28.



Filter Circuit used in Rocky Point-London Radio Telephony Tests Feb. 1923.

The object of thus stepping-down the received frequency band was to secure a high degree of selectivity together with flexibility in tuning. The high selectivity was obtained by the use of a band filter, and was further improved by applying the filter after rather than before the frequency had been stepped down. To illustrate this improvement, assume there was present an interfering signal of 60,000 cycles per second, *i. e.* 1500 cycles per second off from the

edge of the received telephone band. This is a frequency difference of about  $2\frac{1}{2}$  per cent.; but after each of the received band frequencies is subtracted from 90,000 the corresponding difference of 1500 cycles per second becomes almost 5 per cent. Consequently the filter was able to effect a sharper discrimination between the received and interfering signals. Further, the filter was not required to be of variable frequency, since by adjusting the frequency of the beating oscillator in the high-frequency circuit the filter could be readily applied to work anywhere in a wide range of received frequencies. The receiving method outlined therefore enabled the filter circuit and also the intermediate-frequency and low-frequency circuits to be designed for maximum efficiency at fixed frequency values without sacrificing the flexibility of the receiving set.

#### (g) *Other Applications.*

In an alternating-current Wheatstone bridge for measuring impedance, if the supply wave is not free from harmonics, a filter is sometimes interposed between the telephone receiver and the bridge. This filter is employed to suppress the harmonics, and thus to enable silence to be obtained when the bridge is balanced for the fundamental frequency, even if the source of A.C. supply is not of pure sine-wave form.

A filter can be usefully employed to smooth the anode-voltage supply to a thermionic valve when that supply is obtained from a direct-current generator or from rectified alternating current. This filter, when used in a valve circuit for low-frequency magnification, will usually remove a good deal of the hissing or rustling noise which is sometimes heard with two or three stages of magnification.

In wireless reception, in order to obtain marked selectivity, filters are often employed. The function of these is to make it possible to receive signals of any given frequency (wave-length) and at the same time to cut off signals of any other frequency (wave-length), even if very close in value to the one it is desired to receive.

#### (F) CONCLUSION.

In conclusion, it should be mentioned that the utilization of electrical filters appears to be of increasing importance to the telegraph and telephone engineer. In this paper the author has endeavoured to outline the fundamental properties and method of design of some useful types of such



filters, as well as to indicate some of their practical applications. The author ventures to hope that this outline has been presented in a clear, useful, and interesting manner, and also that the information contained in this paper will be of considerable assistance to engineers, especially to those who design and use electrical filters.

# APPENDIX.

## I. Evaluation of the four critical frequencies for electrical filter, Type I.

In this case

$$Z_1 = j\omega L_1 - \frac{j}{\omega C_1} = j \left[ \frac{\omega^2 L_1 C_1 - 1}{\omega C_1} \right]$$

and

$$Z_2 = \frac{j\omega L_2 \times \frac{-j}{\omega C_2}}{j\omega L_2 - \frac{j}{\omega C_2}} = \frac{-j \frac{L_2}{C_2}}{\frac{\omega^2 L_2 C_1 - 1}{\omega C_2}} = -j \frac{\omega L_2}{\omega^2 L_2 C_2 - 1}.$$

$$\therefore \frac{Z_1}{Z_2} = \frac{-(\omega^2 L_1 C_1 - 1)(\omega^2 L_2 C_2 - 1)}{\omega^2 L_2 C_1}.$$

From equation (1), page 804, we have

$$\frac{-(\omega^2 L_1 C_1 - 1)(\omega^2 L_2 C_2 - 1)}{\omega^2 L_2 C_1} = 0.$$

$$\therefore \omega_2 = \sqrt{\frac{1}{L_1 C_1}} \text{ and } \omega_3 = \sqrt{\frac{1}{L_2 C_2}}.$$

From equation (3), page 804, we have

$$\begin{aligned} 2 - \frac{(\omega^2 L_1 C_1)(\omega^2 L_2 C_2 - 1)}{\omega^2 L_2 C_1} &= 0, \\ \omega^4 L_1 C_1 L_2 C_2 - \omega^2 (L_1 C_1 + L_2 C_2 + 2L_2 C_1) + 1 &= 0, \\ (L_1 C_1 + L_2 C_2 + 2L_2 C_1) & \\ \omega^2 = \frac{\pm \sqrt{(L_1 C_1 + L_2 C_2 + 2L_2 C_1)^2 - 4L_1 C_1 L_2 C_2}}{2L_1 C_1 L_2 C_2}, & \end{aligned}$$

$$\omega = \sqrt{\frac{(L_1 C_1 + L_2 C_2 + 2L_2 C_1)}{2L_1 C_1 L_2 C_2} \pm \sqrt{\frac{(L_1 C_1 + L_2 C_2 + 2L_2 C_1)^2 - 4L_1 C_1 L_2 C_2}{2L_1 C_1 L_2 C_2}}},$$

or

$$\begin{aligned} \omega &= \sqrt{\frac{1}{2L_1 C_2}} \times \\ &\sqrt{\left(\frac{L_1}{L_2} + \frac{C_2}{C_1} + 2\right) \pm \sqrt{\left(\frac{L_1}{L_2} + \frac{C_2}{C_1} + 2\right)^2 - 4\frac{L_1 C_2}{L_2 C_1}}}, \end{aligned}$$

from which we have

$$\omega_1 = \sqrt{\frac{1}{2L_1C_2}} \times \sqrt{\left(\frac{L_1}{L_2} + \frac{C_2}{C_1} + 2\right) - \sqrt{\left(\frac{L_1}{L_2} + \frac{C_2}{C_1} + 2\right)^2 - 4\frac{L_1C_2}{L_2C_1}}}$$

and

$$\omega_4 = \sqrt{\frac{1}{2L_1C_2}} \times \sqrt{\left(\frac{L_1}{L_2} + \frac{C_2}{C_1} + 2\right) + \sqrt{\left(\frac{L_1}{L_2} + \frac{C_2}{C_1} + 2\right)^2 - 4\frac{L_1C_2}{L_2C_1}}}.$$

NOTE.— $\omega_1 = 2\pi f_1$ ,  $\omega_2 = 2\pi f_2$ ,  $\omega_3 = 2\pi f_3$ ,  $\omega_4 = 2\pi f_4$ .

## II. Evaluation of the four critical frequencies for electrical filter, Type II.

In this case

$$Z_1 = \frac{j\omega L_1}{1 - \omega^2 L_1 C_1}$$

and

$$Z_2 = j \left[ \frac{\omega^2 L_2 C_2 - 1}{\omega C_2} \right].$$

$\therefore$

$$\frac{Z_1}{Z_2} = \frac{j\omega L_1}{1 - \omega^2 L_1 C_1} \times \frac{\omega C_2}{j(\omega^2 L_2 C_2 - 1)} = \frac{\omega^2 L_1 C_2}{(1 - \omega^2 L_1 C_1)(\omega^2 L_2 C_2 - 1)}.$$

From equation (1), page 804, we have

$$\frac{\omega^2 L_1 C_2}{(1 - \omega^2 L_1 C_1)(\omega^2 L_2 C_2 - 1)} = 0.$$

$\therefore$

$$\omega_1 = 0 \text{ and } \omega_4 = \infty.$$

From equation (2), page 804, we have

$$2(1 - \omega^2 L_1 C_1)(\omega^2 L_2 C_2 - 1) + \omega^2 L_1 C_2 = 0,$$

$$2\left[1 - \omega^2(L_1 C_1 + L_2 C_2) + \omega^2 L_1 L_2 C_1 C_2\right] - \omega^2 L_1 C_2 = 0,$$

$$\omega^4 L_1 L_2 C_1 C_2 - \omega^2 \left( L_1 C_1 + L_2 C_2 + \frac{L_1 C_2}{2} \right) + 1 = 0,$$

$$\left( L_1 C_1 + L_2 C_2 + \frac{L_1 C_2}{2} \right)$$

$$\omega^2 = \frac{\pm \sqrt{\left( L_1 C_1 + L_2 C_2 + \frac{L_1 C_2}{2} \right)^2 - 4 L_1 L_2 C_1 C_2}}{2 L_1 L_2 C_1 C_2}.$$

or

$$\omega = \sqrt{\frac{1}{2L_1C_2}} \times \sqrt{\left(\frac{L_1}{L_2} + \frac{C_2}{C_1} + \frac{1}{2}\right) \pm \sqrt{\left(\frac{L_1}{L_2} + \frac{C_2}{C_1} + \frac{1}{2}\right)^2 - 4\frac{L_1C_2}{L_2C_1}}},$$

from which we have

$$\omega_2 = \frac{1}{\sqrt{2L_1C_2}} \times \sqrt{\left(\frac{L_1}{L_2} + \frac{C_2}{C_1} + \frac{1}{2}\right) - \sqrt{\left(\frac{L_1}{L_2} + \frac{C_2}{C_1} + \frac{1}{2}\right)^2 - 4\frac{L_1C_2}{L_2C_1}}}$$

and

$$\omega_3 = \frac{1}{\sqrt{2L_1C_2}} \times \sqrt{\left(\frac{L_1}{L_2} + \frac{C_2}{C_1} + \frac{1}{2}\right) + \sqrt{\left(\frac{L_1}{L_2} + \frac{C_2}{C_1} + \frac{1}{2}\right)^2 - 4\frac{L_1C_2}{L_2C_1}}}.$$

NOTE.— $\omega_1 = 2\pi f_1$ ,  $\omega_2 = 2\pi f_2$ ,  $\omega_3 = 2\pi f_3$ ,  $\omega_4 = 2\pi f_4$ .

LXXIX. *The Flash Arc Spectrum of Cæsium.* By F. H. NEWMAN, D.Sc., A.R.C.S., Professor of Physics, University College of the South-West of England, Exeter\*.

[Plates XIII. & XIV.]

### 1. Introduction.

IN previous papers† it has been shown that an intermittent arc passing between electrodes of alkali metals gives rise to spectra in which the first spark spectrum lines are relatively brighter than the arc lines. The structure of these spark spectra being similar to that of the inert gas arc types, it follows that they are produced by complete removal of the valence electron and displacement of one electron from the outermost completed shell. This double ionization may occur in various ways. In the first place both electrons may be removed by a single impact, but this process is probable only at small current densities and can be excluded in the case of any heavy discharge. Secondly, the electron from

\* Communicated by the Author.

† Phil. Mag. vol. ii. p. 1042 (1926); vol. iii. p. 229 (1927).

the outermost completed shell may be removed, and this process may be followed by ejection of the valence electron by means of another collision before the atom resumes its normal state. Thirdly, successive collisions in the reverse order may occur, and the probability of the second and third methods of excitation taking place will increase as the square of the current. These modes of excitation will be favoured, accordingly, in the arc. The fourth excitation process, which is probably the predominant one in the flash arc, is through removal of one electron and displacement of the other to a greater energy orbit by single or successive impacts. The critical potentials necessary for this double ionization decrease considerably as the current density increases. Hence at low gas pressures conditions are favourable for an appreciable number of the electrons in the interrupted arc to attain energy equivalent to that necessary for the production of the spark lines.

In the case of caesium, which has been investigated in the present work, the conditions necessary for the excitation of spark lines have been determined by Mohler \*. Making use of the fact that there is a large thermionic emission from metals exposed to caesium, he used a large cathode surface in a two-electrode discharge tube. The outer electrode sheath was made negative, while wires running the length of the tube near its axis served as the anode. He found that under these conditions spark lines appeared at about 14 volts impacting energy at high current densities. With low density currents the lines were faintly visible at 20 volts and were of about the same intensity at 21 volts. The relative intensity of the spark lines, as compared with the arc lines, increased rapidly up to 28 volts, but between 28 and 32 volts there was no appreciable increase. Within the range 32-40 volts and between 40 and 80 volts all the spark lines were relatively enhanced, and from these results he concluded that the first spark spectrum of caesium was excited at 21.5 volts with small currents and, approximately, at 8 volts lower with high currents. There was no definite evidence of stages in this excitation of the lines. Those which appeared at the lowest voltages were the strongest lines.

In more recent work Mohler †, using a tube containing two thermionic units electrically shielded from each other, found that photo-ionization of caesium vapour was produced

\* Bureau of Standards Scientific Papers, No. 505 (1925).

† Phys. Rev. xxviii. p. 46 (1926).

at a critical potential  $13.0 \pm .5$  volts, and the second spectrum should appear at this energy with high currents.

Sommer \* investigated the spark spectra of the metal by passing a high voltage discharge through a mixture of helium and cæsium. He tabulates 361 spark lines in the range  $\lambda$  7300–3200. Dunoyer † used the induction discharge and gives the wave-lengths of 330 lines.

The first and second spark spectra of cæsium, which have widely different excitation potentials, appear in nearly the same relative intensity in the thermionic discharge at 80 volts and in the disruptive discharge. This fact indicates that the effective voltage of the latter is about 80 volts. On the other hand, Dunoyer finds that the high voltage lines are of much greater intensity, so that the effective voltage in his type of discharge must be greater than that in the other methods. Both Sommer and Dunoyer note that the relative intensity of the spark lines, as compared with the arc lines, is much greater than Mohler obtained in his work; but this difference can be ascribed to the very much greater instantaneous current density in the high-voltage type of discharge.

Mohler concludes from his results that if the impacting electrons have energy equivalent to 13.5–14 volts this energy is sufficient to remove a single electron from the outermost completed shell of the cæsium atom. At high current densities, if the metastable atom is then bombarded with a second electron, the valence electron is removed, and under these conditions energy equivalent to 14 volts or even 13 volts is sufficient to doubly ionize the atom. At low vapour pressure and high current density it is to be expected, therefore, that spark lines should make their appearance in the arc, and in the interrupted arc their relative brightness, compared with the arc lines, should be high.

## 2. Experiments.

An apparatus similar to that which had been used with the other alkali metals was employed in the experiments with cæsium. Two of the electrodes consisted of cæsium metal packed into glass tubes, through which passed iron rods by means of which a potential of 100 volts could be applied across the cæsium electrodes, which in the experiment were 1 cm. apart. A third iron electrode in the tube enabled a momentary electric discharge to be passed, this discharge

\* *Journ. d. Phys.* vol. iii. p. 261 (1922).

† *Ann. d. Phys.* vol. lxxv. p. 165 (1924).



being necessary to start the arc. The latter, once made, could be struck and quenched intermittently, and the radiation, showing the characteristic violet colour, was photographed by means of a quartz spectrograph. The residual gas pressure was maintained below  $10^{-4}$  mm. The chief lines were measured and, with the exception of the arc lines, are given in Table I. As shown in spectrogram *b* (Plate XIII.), the flash arc spectrum is entirely different from that given by the ordinary persistent arc. After a few flashes most of the caesium had vaporized, but enough remained on the end of the iron electrode to give the characteristic caesium radiation. No trace of iron lines appeared in the spectrograms.

TABLE I.  
The Flash Arc Spectrum of Cæsium.

Wave-length. $\lambda$ Å.U.	Intensity.	Wave-length. $\lambda$ Å.U.	Intensity.
6648	3	4974	8
6536	1	4954	8
6496	1	4879	5
6425	0	4869	9
6159	0	4829	7
6129	2	4788	4
6078	1	4764	7
5986	0	4732	4
5926	4	4662	1
5845	2	4646	3
5833	5	4622	1
5816	0	4616	5
5664	1	4604	9
5635	0	4573	0
5600	0	4539	2
5567	7	4527	9
5508	0	4502	8
5466	0	4437	0
5424	5	4406	8
5376	5	4386	0
5354	6	4374	1
5308	0	4364	8
5274	2	4336	3
5250	4	4307	3
5228	8	4301	3
5212	3	4289	10
5102	2	4277	10
5086	2	4266	8
5061	3	4235	6
5053	3	4214	3
5044	4	4188	3

TABLE I. (*continued*).

Wave-length $\lambda$ Å.U.	Intensity.	Wave-length $\lambda$ Å.U.	Intensity.
4174	0	3067.9	1
4153	0	3067.0	2
4133	0	2977.6	2
4120	0	2938.9	2
4069	7	2931.6	4
4044	0	2922.0	0
4040	6	2915.1	0
4024	0	2894.2	1
4007	1	2869.0	0
3978	3	2859.6	1
3974	4	2846.0	2
3966	3	2838.1	0
3960	5	2817.0	3
3926	0	2811.1	0
3898	1	2788.9	1
3865	4	2776.8	1
3806	4	2707.0	1
3786	2	2701.3	4
3735	0	2652.1	1
3704	0	2643.0	1
3700	0	2634.9	1
3663	1	2631.0	3
3643	0	2610.1	1
3632	0	2600.4	3
3608	1	2597.3	3
3599	1	2573.0	1
3415	1	2568.5	1
3411.8	0	2551.4	1
3407.0	0	2544.0	6
3358.1	0	2533.2	0
3350.3	1	2525.7	1
3349.1	1	2485.7	1
3316.9	0	2477.8	3
3272.2	2	2455.6	3
3269.0	3	2393.1	4
3267.2	2	2379.2	2
3211.0	0	2376.0	2
3202.1	0	2340.3	0
3153.0	0	2332.3	3
3150.0	0	2316.0	1
3102.2	0	2286.4	1
3092.9	2	2274.0	1
3081.0	1	2267.8	2
3070.0	1		

Practically all of these lines are among those measured by

Dunoyer, with the exception of the following:— $\lambda$  6648, 6078, 5845, 5664, 5102, 5081, 4622, and some very faint lines. Another interesting fact is that most of the lines in the less refrangible part of the induction spectra, and also all those given by Mohler as excited at 24 volts energy occur in the flash arc spectrum. The lines in the latter can be separated into two groups. The first one extends from  $\lambda$  5400– $\lambda$  3780, approximately, and the other from  $\lambda$  3700– $\lambda$  2268, the lines in the first group being by far the more intense. The spectral centre of the first group is at  $\lambda$  4350, and this group contains practically all of the first spark spectrum lines. The second group contains many lines of a second spark spectrum, which Mohler has found is excited between 40 and 80 volts. The two groups are analogous to the two different types of xenon arc spectra—the red\* and what is known as the blue spectrum, although the latter consists probably of first, second, and third spark spectra†. The red spectrum, the true arc one, arises from the neutral atom, the structure of which is very similar to that of a singly ionized cæsium atom. The faintness of the lines in the second group in the flash arc spectrum is explained by the relatively small impacting energy possessed by the electrons in the arc discharge.

In a second series of experiments the cæsium metal was replaced by the chloride and the flash arc spectrum photographed. The result is shown in spectrogram *c* (Plate XIII.). The more prominent spark lines of cæsium are present, those situated in the visible region being by far the most intense.

Observations upon the other alkali metals had shown, previously, that each flash arc spectrum could be separated into two groups of lines with the further characteristic that the group containing the lines of longer wave-length, *i. e.* the group corresponding to the red spectrum of the analogous inert gas, was by far the more prominent. Moreover, these “red” groups in the different vapours show a regular displacement from one metal to another in the order of the atomic weights. To exhibit this, the author photographed the flash arc spectra of the four alkalis. The similarity of the spectra and the progression in the position of the spectral centre of the red group is shown in Plate XIV. The correspondence between the groups is very striking, although the relation between individual lines is not clear.

In conclusion, the author wishes to express his thanks to the Royal Society for a Government Grant which enabled this research to be undertaken.

\* See Sommer, *Zeits. f. Phys.* vol. xiii. p. 85 (1923).

† See Bloch and Déjardin, *Ann. d. Phys.* vol. ii. p. 461 (1924).

LXXX. *Dispersion of an Electron Beam.*

By E. E. WATSON, M.Sc. (*McGill University*)\*.

IF an electron beam is used as an indicating device it is desirable that the recording end should be as small as possible. For example, in the cathode ray oscillograph the lines traced on the photographic plate by the beam of cathode rays must be narrow and sharp, but the energy of the electrons striking the plate must be high enough to produce a developable image. This is a difficult condition to fulfil, for a beam of electrons is naturally divergent, owing to the mutual repulsive force between each electron and its neighbours. The following analysis shows how the beam may be adjusted so that it shall work at maximum efficiency.

Consider an electron beam of radius  $r$ , formed by the liberation from a circular aperture of  $n$  electrons per second, moving with a velocity  $v$ . It is assumed that the electrons emerge from the aperture moving parallel to its axis. Let  $y$  be the radius of the beam at a distance  $x$  along the axis, and let  $R \equiv \frac{y}{r}$ .

There are  $\frac{n}{v}$  electrons in unit length of the beam, so that the radial electrostatic field  $E$  at the surface of the beam is given by

$$\int_c E ds = 4\pi \frac{ne}{v},$$

whence 
$$E = \frac{2ne}{yv} \text{ e.s.u.}$$

$\therefore$  Radial electrostatic force on a single surface electron

$$= Ee \text{ e.s.u.}$$

$$= \frac{2ne^2}{yv} \cdot c^2 \text{ e.m.u.}$$

The electromagnetic field  $H$

$$= \frac{2I}{y} = \frac{2ne}{y} \text{ e.m.u.}$$

$\therefore$  Radial electromagnetic force on a single surface electron

$$= -Hev$$

$$= -\frac{2ne^2v}{y} \text{ e.m.u.}$$

\* Communicated by Prof. A. S. Eve, F.R.S.

∴ Total radial force  $Y$  on a surface electron, given by the sum of the electrostatic and electromagnetic forces, is

$$Y = \frac{2ne^2(c^2 - v^2)}{v} \cdot \frac{1}{y}$$

$$= \frac{k}{y}, \quad \text{where } k \equiv \frac{2ne^2(c^2 - v^2)}{v}.$$

Hence the Equation of Energy for an electron on the surface of the beam is

$$\frac{1}{2}m\dot{y}^2 = \int_r^y \frac{k}{y} dy$$

$$= k \log \frac{y}{r},$$

$$\sqrt{\frac{m}{2k}} \cdot \frac{dy}{\sqrt{\log \frac{y}{r}}} = dt.$$

Integrating this,

$$t = \sqrt{\frac{m}{2k}} \cdot \int_r^y \frac{dy}{\sqrt{\log \frac{y}{r}}},$$

where  $t$  is the time taken for the radius of the beam to expand from  $r$  to  $y$ .

$$\text{Now } y = R \cdot r, \quad \therefore t = \sqrt{\frac{m}{2k}} \cdot r \cdot \int_1^R \frac{dR}{\sqrt{\log R}},$$

$$x = vt = \sqrt{\frac{mr^2}{2k}} \cdot v \int_1^R \frac{dR}{\sqrt{\log R}}.$$

$$\text{But } m = m_0 \left(1 - \frac{v^2}{c^2}\right)^{-1/2}$$

$$\text{and } k = 2ne^2 \left(1 - \frac{v^2}{c^2}\right) \frac{c^2}{v},$$

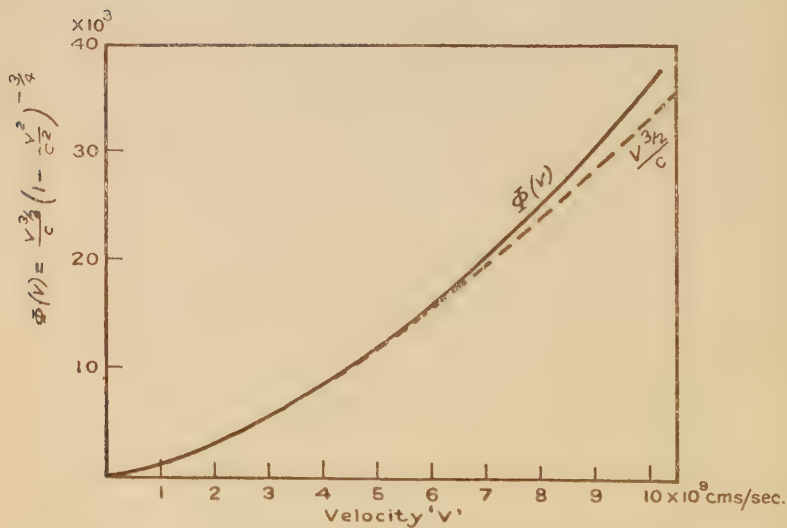
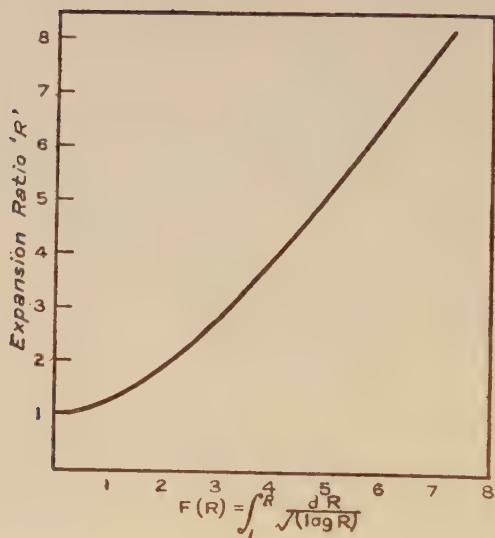
$$\therefore \frac{m}{k} = \frac{m_0}{2ne^2} \left(1 - \frac{v^2}{c^2}\right)^{-3/2} \frac{v}{c^2},$$

$$x = \frac{m_0 v^2}{4ne^2} \left(1 - \frac{v^2}{c^2}\right)^{-3/4} \frac{v^{3/2}}{c} \int_1^R \frac{dR}{\sqrt{\log R}}.$$





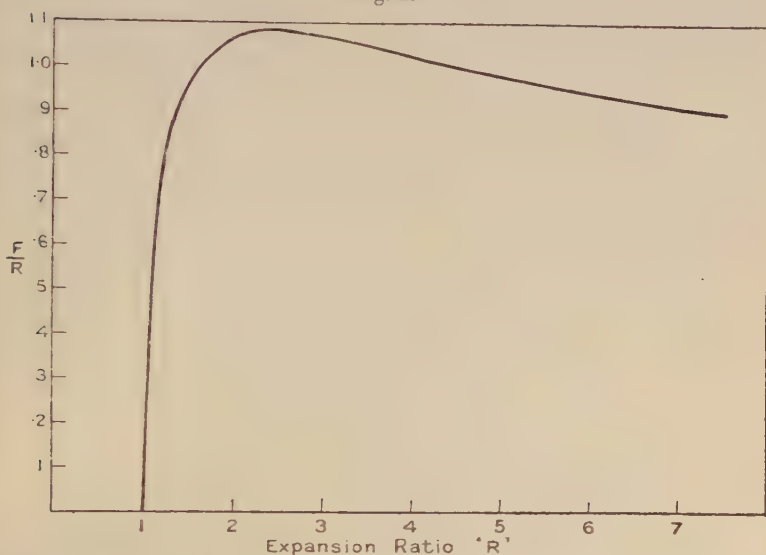
Fig. 1.



(3) The remaining variable  $\frac{F^2}{R^2}$  should be made to have its maximum value. As is shown by the accompanying

graph (fig. 2),  $\frac{F^2}{R^2}$  is a maximum when  $R \doteq 2.4$  or  $F \doteq 2.6$ .

Fig. 2.



Now  $F = ar \frac{\sqrt{J}}{\Phi}$ , so that  $F$  may be given its optimum value

by adjusting the current density  $J$ . Hence we have only to adjust the electron emission until the spot formed by the end of the beam is 2.4 times the diameter of the pinhole aperture limiting the initial size of the beam.

(4) The diameter of this pinhole is given by dividing the maximum allowable diameter of the "spot" by 2.4.

The design of any instrument using a cathode ray beam as an indicator should be governed by (1), (2) and (4) above, while the optimum working conditions of such an instrument are given by (1) and (3).

The Macdonald Physics Building,  
McGill University,  
August 23rd, 1926.

LXXXI. *Variation of Logarithmic Decrement with Amplitude and Viscosity of certain Metals.*—IV. (concluding). By G. SUBRAHMANIAM, M.A., A.Inst.P.\*

**T**HIS is the fourth and concluding paper of a series, the first three of which have already appeared in this journal†. The present paper deals with a study of the behaviour of wires made of three more metallic elements, namely, magnesium, zinc, and cadmium.

As these metals could not be drawn into wires without considerable difficulty, I could not procure them easily. Dr. Walter Rosenhain, F.R.S., of the National Physical Laboratory, Teddington, has kindly had made for me two gauges of cadmium wire by Messrs. Henry Wiggin & Sons, Ltd., of Birmingham. Messrs. John G. Griffin & Sons, Ltd., of London, have specially made for me magnesium and zinc wires. I thank Dr. Rosenhain for the interest he has taken in this work, and also the manufacturers for kindly providing me with these wires, free of all cost.

The experimental arrangements are quite similar to those already described, in detail, in my first communication. Each of the test-wires is subjected to the usual preliminary treatment. The zinc and magnesium wires are kept stretched by half the maximum load which they can carry for the given dimensions and are allowed to remain undisturbed for a few days. In the case of cadmium wires which are relatively softer, bars of variable moments of inertia weighing a few grms. and just sufficient to keep the wires straight are attached. To bring each of the wires to a state of maximum torsional elasticity it is kept continuously vibrating over a small range, for about ten to twelve hours. It is then taken to the vacuum chamber and successive swings are read off, by the usual telescope and scale method. When, however, the amplitude has fallen to about a cm. of the scale, readings are taken with the help of the tele-microscope kept focussed on the vertical pointer behind the mirror, as previously explained.

#### EXPERIMENTAL RESULTS.

In all these experiments the scale is, as before, held at a constant distance of 74 cm. so that an amplitude of 1 cm. is equivalent to a twist of about 0.39 of a degree. The maximum twist to which the magnesium and zinc wires are

\* Communicated by Prof. W. Rosenhain, F.R.S.

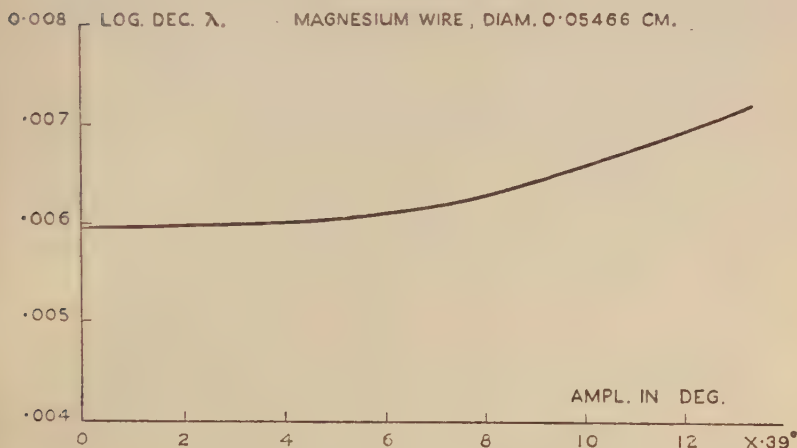
† Phil. Mag., April 1925, pp. 711-724; Oct. 1925, pp. 716-722; May 1926, pp. 1074-1081.

subject is about  $5^\circ$ . Owing to the shift of zero in the case of cadmium wires, the total twist is never allowed to exceed about 20 min. of arc.

Results of these experiments are plotted on graph paper. As the curves indicate the readings sufficiently accurately, tables of values are omitted from the paper.

(1) *Magnesium wire* (Graph 1).

Graph 1.



A single length of 96.2 cm. of magnesium wire, diam. 0.05466 cm. is used. The log. dec. has a constant value 0.005962, so long as the twist per unit length does not exceed  $0.39$  of a min. Thereafter it is found to increase, more or less linearly, with amplitude. As the total twist is increased to about  $5^\circ$ , which, as has been mentioned above, is the maximum used in these experiments, the log. dec. increases to about 0.00731, *i.e.*, by 23 per cent. of its constant value.

The log. dec. and amplitude curve for this metal suggests an equation of the form :

$$\lambda_a = \lambda_0 + f(a - m) ;$$

where  $\lambda_a$  is the log. dec. for amplitude ' $a$ ,'  $\lambda_0$  that when the amplitude is zero, ' $m$ ' the limiting amplitude, and  $f(a - m)$  a linear function. For all values of ' $a$ ' less than or equal to ' $m$ ,'  $f(a - m) = 0$ , so that  $\lambda_a = \lambda_0$ .

(2) *Zinc wire* (Graph 2).

The diameter of the zinc wire used is 0.0918 cm. and the experiment is conducted with two different lengths. In both these cases the log. dec. does not tend to a constant

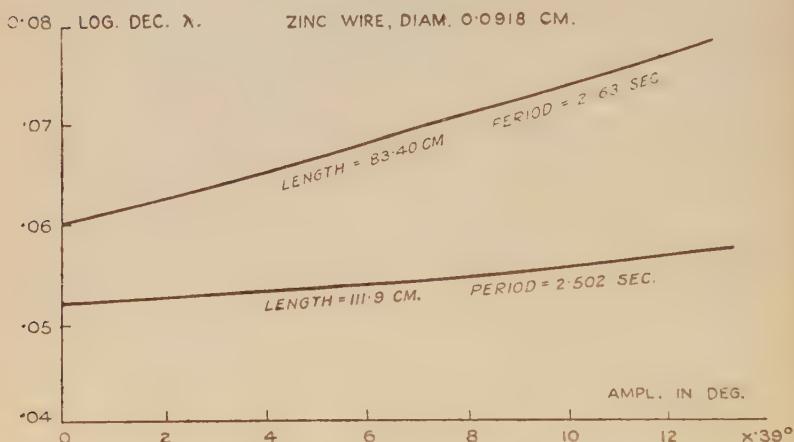


value, but is found to decrease with decreasing amplitude, almost linearly, so that

$$\lambda_a = \lambda_0 + f(a),$$

where  $f(a)$  is a linear function depending, as is seen from the curves, on the length of the wire as well.

Graph 2.



The log. decrements extrapolated for zero twist are 0.05241 and 0.06011, when the lengths of the wire are 11.9 and 83.4 cm. respectively.

### (3) *Cadmium wires.*

Two different thicknesses of cadmium wire are used. With regard to these wires no detailed investigation is found practicable, as the total twist never exceeded about 20 min. Owing to the rapid subsidence of vibrations, the log. dec. for each of the wires is found by noting three successive half swings to the same side of zero with the help of the tele-microscope.

For purposes of calculating the viscosity coefficients, the log. dec. as extrapolated for zero twist is substituted in the equation :

$$\eta = \frac{8I\lambda_0}{\pi \cdot TR^4}.$$

From a reference to the tables of values in this series it is seen that the coefficient of viscosity of different materials, so far examined, is in almost all cases of the order of  $10^8$  poises, and is the same as that obtained by Kei Iokibe and

Table of values. Temp.  $25^{\circ}\cdot4-26^{\circ}\cdot9$  C.

Metal.	I. gm. cm <sup>2</sup> .	l. cm.	R. cm.	T sec.	$\lambda_0$ .	$\eta$ poises.
Magnesium .	1136	96·2	0·02733	5·806	0·005962	$5\cdot119 \times 10^8$
Zinc .....	3563	111·9	·04590	2·502	·05241	47·92 „
Zinc .....	3563	83·4	·04590	2·163	·06011	47·39 „
Cadmium ...	607·4	113·6	·04212	1·713	·2203	71·78 „
Cadmium ...	153·1	126·8	·03460	1·348	·2871	73·45 „

Sukeaki Sakai \*. Of the available data on this point, the value  $6-60 \times 10^{17}$  for the absolute viscosity of steel by Barus†,  $10^{12}$  for different lead and tin alloys by Albert Ernest Dunstan‡, and  $10^{14}-10^{16}$  for lead by Boris Weinberg§ seem to be enormously large, while  $10^7$  for copper by Voigt|| seems to be low. In marked disagreement with these values, Quimby's¶ results are of the order  $10^3$ .

Maharaja's College,  
Vizianagaram.

LXXXII. *On the Temperature Coefficient of Contact Electromotive Force.* By J. J. MCHENRY, M.Sc., M.A.\*\*

INTRODUCTION.

PROFESSOR ANDERSON has described experiments in a copper-zinc uranium oxide cell, in which he measured the contact electromotive force between copper and zinc at different temperatures††. Professor Anderson used tarnished metal electrodes—that is, he allowed the cell to stand until its e.m.f. decreased from ·72 volt at room temperature to ·34 volt. This change took place in about three months, and the e.m.f. of the cell then remained constant when the temperature was constant. The change of electromotive force with temperature could then be studied, and was unaffected by the rapid diminution of the

\* Phil. Mag., Sept. 1921, pp. 397-418.

† Phil. Mag. (5) xxix. 1890, p. 337.

‡ Phil. Mag., Jan. 1909, pp. 192-201.

§ Phys. Soc. Proc. London, xix. pp. 472-74.

|| *Wied. Ann.* xlvii. p. 671 (1892).

¶ Phys. Rev., March 1925.

\*\* Communicated by Prof. Alexander Anderson, M.A.

†† "On a Copper-Zinc Uranium-Oxide Cell and the Theory of Contact Electromotive Forces," Proc. Phys. Soc. Lond. vol. xxiv. pt. ii. Feb. 15th, 1912.

electromotive force which takes place in ordinary air when clean metal electrodes are used.

The contact e.m.f. between tarnished zinc and copper was found to be a linear function of the temperature from  $13^{\circ}\text{C.}$  to  $150^{\circ}\text{C.}$ , and could be represented by the equation  $E = 0.27 + .002t$ , where  $E$  represents the electromotive force of the cell in volts, and  $t$  the temperature in degrees centigrade. The temperature coefficient  $\frac{dE}{dt}$  was .002 volt/degree C.  $E$  evidently vanishes at  $-135^{\circ}\text{C.}$  The equation could also be written

$$E = -0.276 + T \frac{dE}{dt}$$

after the equation of Helmholtz for a reversible chemical cell, where  $T$  is the absolute temperature. This equation shows that the cell has a forward electromotive force  $T \frac{dE}{dt}$  volts and a back e.m.f. of .276 volt,  $T \frac{dE}{dt}$  being .546 volt at  $0^{\circ}\text{C.}$ , and representing the heat absorbed by the cell from its surroundings per unit quantity of electricity.

Prof. Anderson concludes that the cell is a heat cell, and that, during the working of the cell, part of the heat is changed into potential energy of some kind, probably at the surfaces. The cell then differs greatly from the ordinary cells, such as the Daniell cell, in which potential energy in the form of chemical energy is used up and the term  $T \frac{dE}{dt}$  is relatively unimportant.

In the following paper experiments are described in which the temperature coefficient  $\frac{dE}{dt}$  was measured when clean metals were used as electrodes and the rapid tarnishing, which usually takes place with clean metals, prevented, or at least very much reduced, by including a drying agent, usually  $\text{CaCl}_2$ , in the cell.

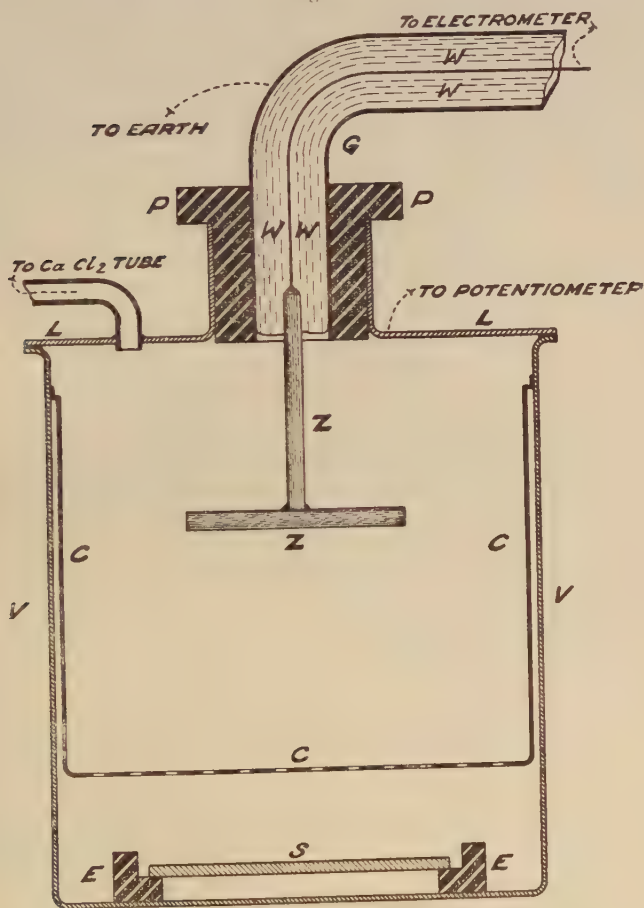
A zinc-copper cell whose e.m.f. would have dropped to .3 volt after three months in ordinary air still gave an e.m.f. of .69 volt six months after being sealed up with a vessel of calcium chloride inside.

#### *Experimental Arrangements.*

The cell used is shown on fig. 1, and consisted of an outer copper vessel  $V$ . On the bottom of the vessel rested three ebonite supports ( $E$ ) carrying a source of  $\alpha$ -rays. Above

this is a second copper vessel C, perforated to allow the passage of  $\alpha$ -rays. This vessel was soldered to V and made of pure electrolytic copper. The vessel V was closed with a lid L cemented with wax to V, and joined to it by a copper wire. Through the lid passed an ebonite plug P and a

Fig. 1.

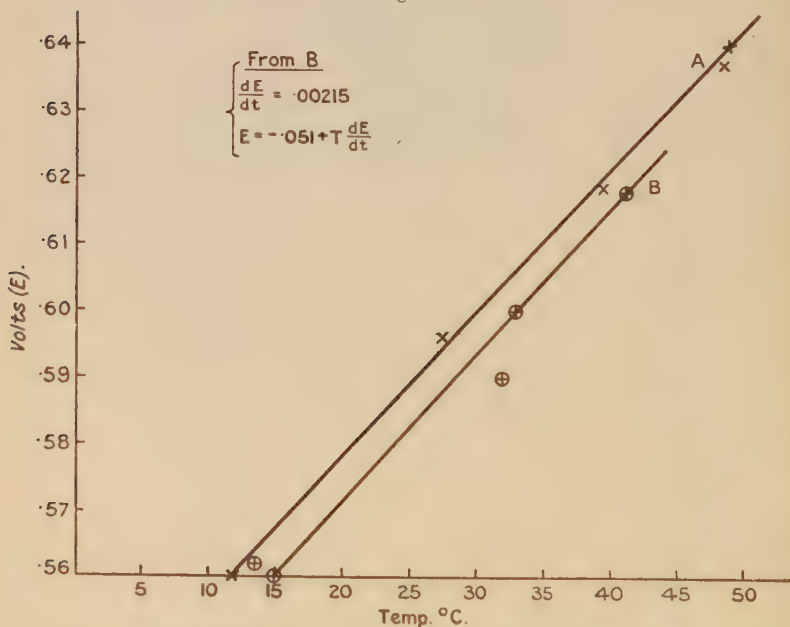


copper guard-ring. The guard-ring was filled with paraffin-wax which held the zinc rod and plate Z in position. The top of the zinc rod was soldered to a copper wire, which passed through the guard-ring to a quadrant electrometer. A calcium chloride tube was kept in communication with the vessel as shown, and no air could enter except through it. In some of the experiments an additional vessel of

calcium chloride was placed below C near the  $\alpha$ -ray source S.

The temperature of the cell was varied by immersing it in a vessel of water, so that the lid L was immersed. A thermometer was placed in the water, which was kept at constant temperature by a small gas flame held underneath. The potential of the copper plate was varied by means of a potentiometer by steps of  $\cdot 0001$  volt, though readings were generally taken to  $\cdot 001$  volt only. When the zinc plate and electrometer were insulated, the electrometer-needle was deflected and brought back again to zero by adjusting

Fig. 2.



the potential of the copper plate by means of the potentiometer. This method is the null method used by Prof. Anderson and Dr. Bowen\*.

With this arrangement and with metal surfaces cleaned before the cell was sealed up, the electromotive force  $E$  of the cell remained constant during the experiments, each of which lasted several hours.  $E$  increased linearly with the temperature and decreased through the same values when the temperature was reduced. These results are shown in Table I. and plotted as a graph in fig. 2.

\* Anderson and Bowen, "On the Measurement of Contact Differences of Potential," Proc. Phys. Soc. London, vol. xxiii. pt. v. (1911).



TABLE I.

Date of Experiment.	Temperature 0° C.	Contact e.m.f. (volts).	Observations.
Feb. 9th, 1926.	14.4	.642	Metals cleaned before sealing up.
Feb. 10th .....	15 32 41.2 33.0 13.4	.560 .590 .618 .600 .562	Shown in Graph B, fig. 2.
Feb. 11th. ....	11.7 27.6 39.4 48.4 49	.560 .596 .619 .637 .640	Shown in Graph A, fig. 2.

In the experiment of Feb. 10th, the contact electromotive  $E$  is represented by the equation

$$E = -.051 + T \frac{dE}{dt},$$

where  $\frac{dE}{dt} = .00215$  volt per degree centigrade. The back e.m.f., which was .276 volt with tarnished metals, decreases to .051 volt with the cleaner metals used in these experiments.

The contact e.m.f.  $E$ , would vanish at  $-.249^{\circ}$  C. or  $24^{\circ}$  above absolute zero.

The contact electromotive force is nearly proportional to the absolute temperature. It seems probable that if the metals were perfectly clean, the contact e.m.f. would be proportional to the absolute temperature and the value of  $E$  for any absolute temperature  $T$  would then be  $T \frac{dE}{dt}$ . This

would give for clean zinc and copper a contact e.m.f. of .616 volt at  $14^{\circ}$  C. The contact e.m.f. at  $14^{\circ}.4$  C. measured when the cell was freshly sealed was found to be .642 volt. It may be noted that the zinc plate used in the experiment was made of commercial zinc and may not have been quite pure.

Further experiments were performed with slightly modified apparatus. The results in the case of copper and zinc do not differ greatly from those already given, except that in the case of clean metals there is generally a small forward electromotive force. The results given for aluminium and tin are averages. The results with aluminium were

## 862 *Temperature Coefficient of Contact Electromotive Force.*

irregular, perhaps because the aluminium could not be soldered and the connexion with the electrometer may have been faulty. With tin the results were regular and over many days no appreciable permanent change was noted, but the graph of  $E$  against  $t$  was not a straight line, but a loop, and the values of  $E$  for descending temperatures were greater than those for ascending temperatures. A mean value of  $\frac{dE}{dt}$  was taken from the graph on the ascending

and descending branches of the curve. It is possible that the Cu vessel, which was 1 cm. thick, may have been at a higher temperature than the tin plate when the cell was being heated, and at a lower temperature when the cell was being cooled. The results of these additional experiments are shown in Table II.

TABLE II.

Metals	$\frac{dE}{dt}$	$E$ .	$E$ measured at room temperature.
Zn-Cu	·002 5	$T \frac{dE}{dt} + \cdot 08$	·692
Zn-Cu	·00222	$T \frac{dE}{dt} + \cdot 002$	·635 at 16° C.
Zn-Cu	·00195	$T \frac{dE}{dt} + \cdot 136$	·694 at 13·2° C.
Zn-Cu	·002	$T \frac{dE}{dt} + \cdot 118$	·664 at 0° C.
Zn-Cu	·0017	$T \frac{dE}{dt} + \cdot 169$	·63 at 0° C.
Cu-Al	·00267	$T \frac{dE}{dt} - \cdot 149$	·62 during experiment.
		or ·769 at 15° C.	When cleaned ·828.
Cu-Sn	·00116	$T \frac{dE}{dt} + \cdot 032$	·323 at 6° C.
	·00114	$T \frac{dE}{dt} + \cdot 022$	·342 at 8° C.

### *Discussion of Results.*

The mean value of  $\frac{dE}{dt}$  for copper-zinc is ·002 volt per degree centigrade. At 15° C. the value of  $T \frac{dE}{dt}$  is then ·576 volt, and this represents the true contact difference of potential between copper and zinc at room temperature. The value when measured in air immediately after cleaning is usually ·70 to ·76 volt, but part of this high value is due to electro-chemical processes, when the passage of electricity

through the cell is attended by occlusion of gases or chemical combination. A phenomenon very similar occurs in the measurement of the surface tension of mercury \*. When a mercury drop is produced in a vacuum the surface tension is constant and equal to 436.3 dynes per cm. When formed in a gas the initial surface tension is much bigger, 532 dynes per cm., and decreases rapidly to a value not very different from that obtained in a vacuum. The surface energy of mercury is sometimes supposed to be the same as the energy in an electrical double layer at the surface †. The intrinsic potential is due to the same double layer, and the contact potential difference between two metals is the same as the difference between their intrinsic potentials. The initial decrease in the surface tension may be due to the same cause as the initial decrease in the contact potential differences.

#### ABSTRACT.

The contact electromotive force  $E$ , between clean copper and zinc is found to be a linear function of the temperature according to the equation  $E = q + T \frac{dE}{dT}$ , where  $q$  is very small and sometimes positive sometimes negative.

It is suggested that the contact e.m.f. is proportional to the absolute temperature for absolutely clean metals.

Measurements were made also with copper-aluminium and copper-tin cells, and though the results obtained were not so steady as in the case of copper-zinc, they confirm the above result. Further experiments are intended with pure metals.

University College,  
Galway.

### LXXXIII. *The Surface Tension of Solids.*

*To the Editors of 'The Philosophical Magazine.'*

GENTLEMEN,—

IN Dr. Antonoff's interesting paper "On Surface Tension of Solids" (Phil. Mag. ser. 7, i. p. 1258) it is supposed that the surface tension of the solid is equal to that of a liquid which neither rises nor falls in a capillary tube of that solid. Dr. Antonoff, in the summary, expresses a slight doubt whether this quantity is really the surface tension of the solid, or a constant related to it. It can be shown that the quantity is not the surface tension of the solid, but the "work of adhesion" of the liquid to the solid.

\* Bibesco, *Ann. de Physique*, iii., Mai-Juin 1925.

† Frenkel, *Phil. Mag.*, April 1917.

The proof that the quantity is the work of adhesion is as follows:—Combining Dupré's equation  $W + \gamma_{SL} = \gamma_{SA} + \gamma_{LA}$  ( $W$  being the work required to separate the liquid from the solid, perpendicularly, per square centimetre of contact,  $\gamma_{LA}$ ,  $\gamma_{SL}$ ,  $\gamma_{SA}$  the surface tensions of the interfaces liquid-air, solid-liquid, and solid-air respectively) with the equation for a liquid resting at an equilibrium angle of contact  $\theta$  on the solid,  $\gamma_{SA} = \gamma_{SL} + \gamma_{LA} \cos \theta$ , the relation

$$W = \gamma_{LA} (1 + \cos \theta) \quad . . . . . (1)$$

is obtained. Equation (1) was known to Thomas Young, and has received occasional reference, but seems much less well known than it deserves, for it elucidates the physical meaning of contact angles as the result of the relative intensities of the adhesion of the liquid to the solid and of the liquid to itself. If there is no adhesion, the contact angle becomes  $180^\circ$ ; if the adhesion increases, the contact angle diminishes, until when the adhesion becomes equal to the work of cohesion ( $2\gamma_{LA}$ ) of the liquid for itself, the contact angle vanishes.

Dr. Antonoff's condition of the liquid neither rising nor falling in the tube is a contact angle of  $90^\circ$ , so that  $W = \gamma_{LA}$ .

It is possible that, as the surface tension of water is diminished by the addition of such a substance as isobutyric acid, there is much less alteration in the value of  $W$  than in  $\gamma_{LA}$ . The amount of solute required to make the contact angle  $90^\circ$  may be very nearly the same as that required to reduce the surface tension of water to the value of  $W$  for pure water adhering to the solid. We know little about the effect of dissolved substances on  $W$ .

The surface tension  $\gamma_L$ , being the work necessary to form one square centimetre of fresh surface, is a measure of the work required to drag molecules from the interior to the surface—that is, of the inward pull on the surface molecules. The work of adhesion is a measure of the outward pull of the liquid molecules on the solid. I do not see any reason for expecting a relationship between these quantities; but it is of such importance to find a trustworthy method for determining the surface tension of solids that I hope your readers will be able to detect a relation.

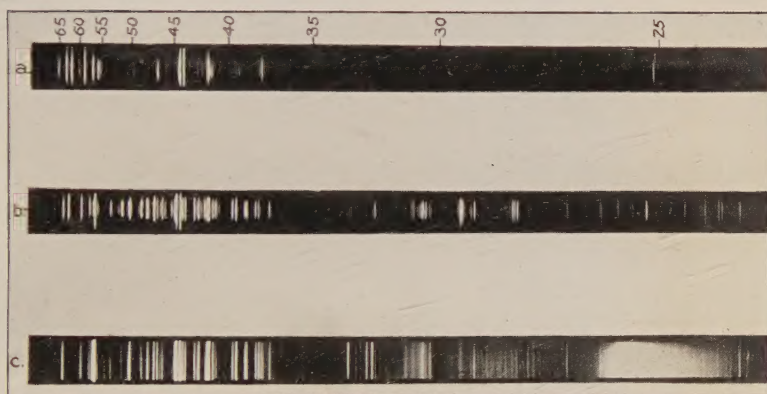
Yours faithfully,

N. K. ADAM.

The University, Sheffield,  
Feb. 4th, 1927.

[The Editors do not hold themselves responsible for the views expressed by their correspondents.]

Flash Arc Spectrum of Cæsium.

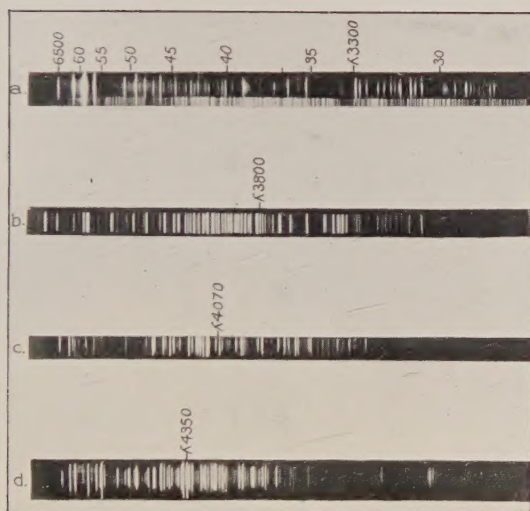


- a.* Cæsium Arc Spectrum.
- b.* Cæsium Flash Arc Spectrum.
- c.* Flash Arc Spectrum of Cæsium Chloride.





Flash Arc Spectra of Alkali metals showing spectral  
centre of spark lines developed.



*a.* Sodium. *b.* Potassium. *c.* Rubidium. *d.* Cæsium.

